ISSN 2663-9084 (Print)
ISSN 2663-9092 (Online)

Ukrainian Neurosurgical Journal

Vol. 32, N1, 2026

Is a scholarly Open Access journal
Founded in April 1995. Quarterly.
State Registration Certificate KV No 23771-13611PR dated 14 February 2019

The journal is on the List of Scientific Professional Editions of Ukraine, where results of thesis research for earning academic degrees of doctor and candidate of sciences and PhD may be published (Order of the Ministry of Education and Science of Ukraine No. 1721 dated 10 December 2024)
The journal is included in the Scopus scientometric database.

Journal publishes peer-reviewed works.

Founders
Romodanov Neurosurgery Institute
Ukrainian Association of Neurosurgeons
National Academy of Medical Sciences of Ukraine

Publisher
Romodanov Neurosurgery Institute

Contact
32 Platona Mayborody st., Kyiv, 04050, Ukraine
tel. +380 44 483-91-98
fax +380 44 489-35-61
E-mail: unj.office@gmail.com
http://theunj.org

The journal went to press 09 March 2026
Format 60 × 841/8. Offset Paper No.1
Order No. 26-10

Circulation 300 copies

Polygraphic services
FOP Golosuy IE
Certificate AA No. 9221702
86 Kyrylivska st., Kyiv, 04080, Ukraine
Tel. +380 44 239-19-85

The master layout of the journal was approved and recommended for publication and distribution via the Internet at the joint meeting of the Editorial Board of the Ukrainian Neurosurgical Journal and the Academic Council of Romodanov Neurosurgery Institute (Meeting Minutes N. 2 dated 27 February 2026)

On the cover

Figures from the article by Irakli B. Goginava, Giorgi Murvelashvili, Mikheil A. Shavgulidze, Mariia V. Riezunenko, Giorgi L. Giorgidze "Bifid median nerve: case report", стор. 126-128

Content

Review article

Original article

Case report

Review article

Ukrainian Neurosurgical Journal. 2026;32(1):3-9
doi: 10.25305/unj.339193

Injury of the visual analyzer in blast trauma: mechanisms, diagnosis, treatment

Oleksandr S. Solonovych [1], Lidia L. Chebotariova [2], Natalia V. Medvedovska [3], Vira A. Vasyuta [4], Anastasiia S. Solonovych [5], Oksana I. Mytsak [1], Yesenia I. Severenchuk [6], Maria S. Kyslitska [4]

[1] Department of Functional Diagnostics, Romodanov Neurosurgery Institute, Kyiv, Ukraine
[2] Department of Neurophysiology, Romodanov Neurosurgery Institute, Kyiv, Ukraine
[3] Acting Chief Scientific Secretary of the Presidium of the National Academy of Medical Sciences of Ukraine, Kyiv, Ukraine
[4] Scientific and Organizational Department, Romodanov Neurosurgery Institute, Kyiv, Ukraine
[5] Diagnostic Consultancy Outpatient Department, Heart Institute, Kyiv, Ukraine
[6] Outpatient Clinic, Romodanov Neurosurgery Institute, Kyiv, Ukraine

Received: 13 September 2025
Accepted: 14 October 2025

Address for correspondence:
Oleksandr S. Solonovych, Department of Functional Diagnostics, Romodanov Neurosurgery Institute, 32 Platon Maiborody st., Kyiv, 04050, Ukraine, e-mail: medsolon@ukr.net

Blast trauma is one of the most challenging problems in modern ophthalmology and neurology, as it is often accompanied by severe injuries of the visual system. According to various authors, ocular involvement accounts for up to 28% of all blast-related injuries. Traumatic brain injury (TBI), which frequently coexists with blast trauma, is complicated by ophthalmic disorders in 84% of cases. This highlights the exceptional vulnerability of the eye to blast-related factors — shock wave, thermal effects, and fragments.

The most common injuries include open globe trauma, intraocular foreign bodies, globe rupture, retinal detachment, and traumatic optic neuropathy. Secondary factors (shrapnel, building debris, soil, metal) markedly increase the risk of severe complications such as endophthalmitis, post-traumatic glaucoma, and retinal neovascularization, which often lead to disability.

Diagnosis requires a comprehensive approach involving ophthalmological methods (ophthalmoscopy, ultrasound, optical coherence tomography), neurophysiological techniques (visual evoked potentials, electroretinography), and neuroimaging (CT/MRI of the orbits and brain). Their combination enables detection of both local ocular damage and central visual pathway impairment.

Treatment includes emergency surgery (globe repair, removal of foreign bodies, vitreoretinal interventions), infection prophylaxis (systemic and local antibiotic therapy), as well as anti-inflammatory and immunomodulatory therapy. Timely prevention of sympathetic ophthalmia is of particular importance. Further rehabilitation involves restorative and functional methods aimed at preserving residual vision and improving patient adaptation.

Thus, blast-related injury of the visual analyzer is characterized by multifactorial mechanisms and a high risk of permanent vision loss. Optimal diagnosis and treatment are possible only through a comprehensive multidisciplinary approach with an emphasis on early intervention and long-term rehabilitation.

Keywords: *blast trauma; visual analyzer; visual analyzer contusion; traumatic optic neuropathy; diagnosis; rehabilitation*

Introduction

In the context of contemporary armed conflicts, the number of patients with blast traumas (BT) accompanied by damage to the organ of vision has been steadily increasing. Given the extraordinary diversity, combined effects, and complexity of blast injury mechanisms, ocular trauma resulting from explosive injuries represents one of the most severe and challenging problems in modern ophthalmology and neurology [1]. Studies have demonstrated that a substantial proportion of blast-related injuries to the visual analyzer are associated with persistent visual impairment or complete vision loss [2]. According to various authors, blast-related ocular injuries account for approximately 28% of the total number of injuries caused by blast wave exposure [3, 4]. During Operations Enduring Freedom (OEF) and Operation Iraqi Freedom (OIF), 10–15% of combat-related injuries involved ocular damage [5]. Traumatic brain injuries (TBI) are frequently accompanied by visual system complications, with a reported incidence of up to 84% [6]. These findings indicate a high vulnerability of the visual analyzer to both direct and indirect effects of blast waves, fragments, and thermal factors.

Explosive devices widely used in modern warfare and terrorist attacks often result in severe damage to the visual analyzer. The most typical injuries associated with such trauma include open globe injury, intraocular foreign bodies, globe rupture, as well as complications such as retinal detachment and traumatic optic neuropathy [7].

Secondary blast factors—such as shrapnel, building debris, soil particles, and metal fragments—pose a particular threat, as they penetrate the structures of the eyeball at high velocity. Even small intraocular foreign bodies may lead to serious complications, including

endophthalmitis, post-traumatic glaucoma, and retinal neovascularization, resulting in a high rate of patient disability [8, 9].

Issues related to timely diagnosis, surgical management, and rehabilitation of patients with blast-related ocular injuries have become increasingly relevant in modern armed conflicts. Early and high-quality diagnosis of visual impairments is critically important for preventing long-term disability in affected patients.

Mechanisms of visual analyzer injury in blast trauma

The eyeball is an exceptionally vulnerable anatomical structure when exposed to blast-related factors, owing to its spherical shape, high fluid content, rich vascularization, and the delicate architecture of its internal tissues [10]. Its exposed anatomical position and the absence of rigid bony protection render the organ of vision particularly susceptible to the mechanical, thermal, and barometric effects of blast waves. Even brief exposure to overpressure or fragment-related injury may result in profound structural damage, ranging from contusion to complete globe rupture [11, 12].

Explosive devices cause four principal types of BT, which differ in their mechanisms of action and in their effects on the visual analyzer [13].

Primary BT results from the impact of the shock wave, which generates excessive overpressure propagating through media of varying densities. Organs containing air—such as the lungs, intestines, and tympanic membrane—are the most vulnerable [14]. In the visual system, the shock wave may induce globe contusion, retinal detachment, intraocular hemorrhage, and traumatic optic neuropathy. The shock wave leads to an abrupt rise in intraocular pressure (IOP), posing a significant threat to the integrity of the ocular coats. Peak intraocular pressure during a blast may reach 0.29 MPa (≈ 2175 mmHg) as early as 1.63 ms after shock wave exposure, which is more than twice the normal physiological IOP (~ 15 mmHg) in healthy eyes [15]. Additional factors determining the pattern and severity of blast-related ocular injury include peak overpressure, the duration of blast wave exposure (pressure impulse), distance from the explosion epicenter, head orientation, and gaze direction at the moment of the explosion (i.e., whether the eyes were directed toward the source of the shock wave). These parameters substantially influence intraocular pressure elevation, the degree of globe deformation, and the likelihood of optic nerve and retinal damage [16, 17].

Secondary BT represents the most common mechanism of ocular trauma [18]. It is caused by direct impact of fragments from the explosive device itself or exogenous debris propelled by the blast wave, including shrapnel, glass, metal, and soil particles. Such fragments may result in open penetrating globe injuries and rupture of the cornea or sclera [19]. Damage to superficial ocular structures is also possible, manifesting as closed globe injuries, including superficial foreign bodies, lamellar (partial-thickness) lacerations, or non-penetrating blunt trauma with or without globe rupture. These injuries are frequently associated with combined craniofacial and abdominal trauma [20, 21]. From a physiological standpoint, the primary blast wave reaches the eye significantly earlier than the fragments it carries; however, once fragments strike the eyeball, the intensity and severity of injury increase sharply. Thus, secondary injuries are "secondary" not only in terms of their underlying mechanism but also in the sequence of their occurrence. They rarely occur in isolation and are almost always accompanied by primary blast injuries, resulting in complex and combined trauma patterns of varying severity [22].

Tertiary BT occurs when the "blast wind" propels the injured individual against solid surfaces or objects [23]. This mechanism results in blunt trauma, including closed globe injuries, orbital fractures, compressive injury to the optic nerve, and damage to the extraocular nerves and muscles. Characteristic manifestations include orbital trauma (bone fractures), globe compression, optic nerve injury at the level of the optic canal (traumatic optic neuropathy), ptosis, and paralysis of the extraocular muscles due to cranial nerve damage [24].

Quaternary BT encompasses additional pathophysiological effects not directly related to the blast wave or fragment impact. These include exposure to high temperatures, intense light (flash), and toxic substances. Such injuries comprise thermal burns of the eyelids, cornea, conjunctiva, and facial tissues caused by extreme heat; photochemical retinal damage ("flash blindness"); and chemical burns of the eyes resulting from explosive materials [25, 26]. Quaternary injuries may also be associated with respiratory tract damage, falling debris, leading to craniofacial trauma, including skull base fractures and orbital involvement [27].

A study by Ying-Ying Zou *et al*. (2013) demonstrated that blast wave exposure induces pathological changes in the retina, accompanied by increased expression of proteins involved in inflammation, edema, and apoptotic processes, including vascular endothelial growth factor, aquaporin-4, and glutamate synthetase etc. These changes were detected immediately after blast wave exposure and persisted for up to two weeks. The most pronounced alterations were observed in astrocytes and Müller cells, indicating their critical role in the retinal pathophysiological processes triggered by blast injury [28].

Combined injuries are of particular clinical significance. Numerous studies have demonstrated a close association between blast-related ocular trauma and systemic injuries. In the study by Erdurman *et al*., the incidence of combined injuries was 69.0%; Weichel *et al*. reported 66.0%, while Kalayci *et al*. reported 60.7% [9, 13, 20]. The most common associated injuries involve the maxillofacial region, musculoskeletal system, and thorax. In cases of concussion, visual manifestations are frequently observed due to the extensive integration of the visual system within the cerebral cortex.

Blast trauma is often accompanied by TBI, which may affect higher levels of the visual analyzer, including the optic nerve, optic chiasm, optic tracts, and the visual cortex of the occipital lobe [29]. Such injuries may result in partial or complete vision loss, homonymous hemianopia, visual agnosia, and other visual dysfunctions. TBI is frequently the consequence of diffuse axonal injury caused by rapid acceleration, deceleration, or rotational movements of the head. These mechanical forces lead to abrupt neuronal dysfunction

with massive release of accumulated neurotransmitters, resulting in excessive activation of postsynaptic membranes. This process initiates a pathophysiological cascade characterized by increased energy demand, metabolic crisis, and impaired glucose metabolism in neurons [30, 31].

Acute symptomatology typically persists for 7–10 days and is transient in nature, with gradual functional recovery over several weeks. However, in a subset of patients, residual or persistent symptoms may remain for months or even years [32]. The most common manifestations of post-concussive syndrome include headache, migraine, cognitive impairment, reduced concentration, and prolonged reaction time. In some cases, these conditions may be associated with delayed and long-term neurodegenerative processes [33].

In blast-related injury to the visual analyzer, damage is frequently bilateral. According to the literature, binocular involvement in BT occurs in 3.33–72.91% of cases, whereas in "conventional" causes of ocular injury (domestic, sports-related, or occupational trauma), the incidence of bilateral involvement is only 0–2.13% [2, 13].

Diagnosis

Assessment of the visual analyzer in patients who have sustained BT is a complex multidisciplinary task requiring the involvement of not only an ophthalmologist but also a neuro-ophthalmologist, neurologist, otolaryngologist, neurophysiologist, and, in some cases, a neurosurgeon. The primary objectives include identifying ocular and optic nerve disorders, detecting damage to the central components of the visual analyzer (cortical visual areas), and determining the extent and nature of injury (mechanical, ischemic, compressive, contusive, or combined).

Careful collection of medical history is of critical importance. The evaluation should include a detailed analysis of the circumstances of the explosion, such as distance from the epicenter, intensity of exposure, duration of blast impact, and use of personal protective equipment. Particular attention should be paid to a history of loss of consciousness and to patient-reported symptoms, including decreased visual acuity, diplopia, ocular pain, and tearing [34].

In addition, prior ophthalmic history and the presence of concomitant systemic diseases that may affect visual function or hinder recovery should be assessed.

Clinical examination includes evaluation of the eyelids and conjunctiva, identification of foreign bodies, hematomas, hemorrhages, and orbital deformities. Despite the possible absence of overt external ocular or adnexal injuries in patients with BT, comprehensive ophthalmological examination remains essential. This should include assessment of visual acuity (visometry), tonometry (measurement of intraocular pressure), evaluation of pupillary responses (including relative afferent pupillary defect), analysis of extraocular motility, and slit-lamp examination to detect traumatic lesions of the cornea, anterior chamber, and lens [35].

Cockerham *et al*. emphasize the importance of assessing not only visual acuity using high-contrast charts but also spatial contrast sensitivity and visual fields [36]. Retinal or central nervous system damage may not reduce standard visual acuity yet may be associated with abnormalities in visual fields, contrast sensitivity, or color perception [34].

Perimetry is a method used to examine and evaluate the visual field, defined as the area visible to an individual with a fixed gaze and stationary head position. It is a key test for glaucoma diagnosis as well as for assessing the condition of the optic nerve and retina [37]. The main types of perimetry include kinetic perimetry, which employs a moving light stimulus, and static perimetry, in which stationary stimuli of varying intensities are presented. Standard automated perimetry (SAP) is currently the most widely used technique, utilizing automated static testing to achieve more standardized and reproducible results [38].

Imaging studies may be useful for clarifying the nature and extent of injury. Computed tomography (CT) and magnetic resonance imaging (MRI) of the orbit allow visualization of the optic nerve and optic canal and enable assessment of orbital fractures, bone fragments, or optic nerve sheath hematoma [39].

Ophthalmic imaging modalities, such as ophthalmoscopy and optical coherence tomography (OCT), can detect subtle but clinically significant changes, including optic disc edema or thinning of the retinal nerve fiber layer, as well as the presence of hemorrhages, tears, or retinal detachment, etc [40].

Optical coherence tomography is a modern noninvasive diagnostic technique in ophthalmology that uses the properties of coherent light to obtain high-resolution three-dimensional images of intraocular structures, including the retina, optic nerve, and cornea. This method enables detection of pathological conditions such as degenerative processes, glaucoma, optic nerve disorders, and minute tissue alterations, making OCT a versatile diagnostic tool in ophthalmic practice [41].

The operation of an optical coherence tomograph is based on the principle of light interferometry. Light interference refers to the spatial redistribution of radiant energy resulting from the superposition of two or more light waves.

On OCT images, retinal layers are differentiated according to their reflectivity. A standard color scale is used for image reconstruction: highly reflective structures are displayed in red and white tones, whereas weakly reflective structures appear in dark colors (black, blue, or dark green) [42, 43].

Retinal thickness is defined as the distance from the inner retinal surface to the level of the retinal pigment epithelium (RPE). However, an important methodological consideration should be noted: some OCT devices measure thickness to the inner boundary of the RPE, whereas others measure to its outer boundary. Consequently, discrepancies may arise, complicating comparisons of retinal thickness obtained using different OCT systems [44].

To obtain tomographic images of the optic nerve head, both longitudinal and circular linear scanning are employed. OCT allows assessment of optic disc diameter, excavation size and depth, cup-to-disc ratio (area-based as well as horizontal and vertical meridians), and retinal nerve fiber layer thickness in the peripapillary region [45].

An important technical feature of optical coherence tomography is the use of an infrared light beam with an

average wavelength of approximately 830 nm, which enables layer-by-layer retinal imaging, quantitative assessment of retinal thickness, and evaluation of the extent and distribution of pathological changes [43].

Functional magnetic resonance imaging (fMRI) is a neuroimaging technique that enables assessment of brain functional activity based on changes in cerebral blood flow (blood oxygen level–dependent, BOLD, signal). In studies of the visual analyzer, fMRI is used to map the visual cortex, analyze functional organization and neuroplasticity following traumatic injury, and investigate cortical responses to visual stimuli [46]. This method is particularly valuable in comprehensive diagnostics, as it complements structural neuroimaging data and allows correlations between morphological alterations and functional activity to be established [47].

In addition to clinical ophthalmological examination and neuroimaging techniques, neurophysiological methods are also employed in the diagnosis of visual analyzer injury. The most widely used include visual evoked potentials (VEPs), which provide an objective assessment of visual signal conduction along the visual pathways from the retina to the cerebral cortex, and electroretinography, which is used to evaluate retinal function and electrophysiological activity [48]. These methods have considerable potential for comprehensive diagnosis and patient monitoring and will be discussed in greater detail in subsequent publications.

The principal diagnostic methods for assessing visual analyzer injury in BT are presented in ***Table 1***.

Therapeutic Approaches and Rehabilitation

Treatment of visual analyzer injury is often complex and prolonged. Depending on the nature of the injury, patients may require different therapeutic modalities, including conservative management, pharmacological therapy, surgical intervention, or a combination thereof. Primary care consists of applying a sterile dressing and transporting the patient to a medical facility as rapidly as possible. Hospitalization is frequently required, with multiple surgical procedures aimed at preserving globe integrity and restoring visual function. Appropriate surgical techniques are selected on an individual basis according to the clinical scenario [49]. At the initial stage, the most common interventions include globe repair, enucleation with implantation of an ocular prosthesis, and removal of intraocular and orbital foreign bodies. The second stage (planned procedures) may involve enucleation and orbital reconstruction, pars plana vitrectomy, including potential use of silicone oil to maintain globe configuration and normal intraocular pressure [50, 51]. Following surgery, patients with significant retinal fibrosis or scarring are at increased risk of tractional retinal detachment or may experience difficulty in achieving retinal reattachment, necessitating prolonged retention of silicone oil within the eye.

Proliferative vitreoretinopathy is a process of intraocular scarring characterized by the growth and contraction of cellular membranes within the vitreous cavity, on both surfaces of the retina, as well as intraretinal fibrosis [52, 53]. It typically develops after retinal breaks, allowing retinal pigment epithelial cells to migrate into the vitreous space. Currently, no pharmacological agents have been proven to prevent or modulate the development of proliferative vitreoretinopathy. Vitrectomy remains the only effective treatment; however, there is no consensus regarding patient selection or the optimal timing of surgical intervention [54, 55].

Table 1. Instrumental diagnostic methods for visual analyzer injury in blast trauma

Method	Level of injury assessed	Typical findings in BT
Ophtalmoscopy	Retina, optic disc	Hemorrhages, retinal detachment, secondary optic nerve atrophy
Optical Coherence Tomography (OCT)	Retinal nerve fiber layer, ganglion cell layer	Thinning of the retinal nerve fiber layer, signs of optic nerve atrophy
Perimetry	Function of visual pathways from the retina to the cortex	Scotomas, visual field defects (asymmetric, often with non-classical topography)
ERG	Function of photoreceptors and inner retinal layers	Reduced amplitudes or localized response defects in contusion-related retinopathy
VEP, (conventional)	Conduction from the retina to the cortex (optic nerve, chiasm, optic tracts)	Reduced P100 amplitude, prolonged latency, interhemispheric asymmetry, absence of response in severe injury
mfVEP	Local assessment of conduction within different sectors of the visual field	Focal defects corresponding to localized nerve fiber damage (partial involvement of the optic nerve, chiasm, or optic tract)
CT/MRI of the orbits and brain	Orbits, optic nerves, chiasm, optic tracts, occipital cortex	Orbital fractures, hematomas, optic nerve compression or rupture, diffuse axonal injury
fMRI	Occipital cortex	Reduced or absent activation of the primary visual cortex during stimulation of the affected eye

Note. ERG — electroretinography; mfVEP — multifocal visual evoked potentials.

In addition, many patients require oculoplastic, corneal, or glaucoma surgery, while a smaller proportion need consultation with a uveitis specialist, underscoring the importance of a multidisciplinary approach.

One of the most serious complications is sympathetic ophthalmia, a granulomatous autoimmune uveitis that occurs in 0.06–0.19% of cases and may lead to vision loss in the contralateral eye [56]. Historically, severely injured eyes were believed to require enucleation within two weeks after trauma to prevent sympathetic ophthalmia; however, neither the timing nor the effectiveness of this practice has been supported by robust evidence. Prompt initiation of corticosteroid therapy or immunosuppressive agents (cyclosporine, azathioprine) in cases of sympathetic ophthalmia can significantly improve treatment outcomes [57].

Therefore, available evidence supports the principle that even in cases of severe open globe injury, every effort should be made to preserve and reconstruct the eye whenever clinically feasible.

Endophthalmitis ranks second after open globe trauma and affects approximately 16.5% of patients. In this context, systemic antibiotic prophylaxis has limited evidence of efficacy, whereas intravitreal antibiotic injections, although used less frequently, are supported by stronger evidence [58, 59].

Prognosis

The prognosis of blast-related visual analyzer injury remains variable and depends on multiple factors, including the severity of the primary injury, involvement of the optic nerve, timeliness and effectiveness of therapeutic interventions, individual compensatory capacity, and response to treatment. In some patients, substantial recovery of visual function is possible, whereas others experience persistent and disabling visual impairment. Importantly, prognosis improves significantly with early diagnosis and initiation of treatment within the first hours to days following injury.

Conclusions

Combat-related blast trauma (BT) is a leading cause of combined damage to the visual analyzer. The pathophysiological mechanisms of such trauma are complex and multifactorial, and the absence of visible ocular damage does not preclude injury. Assessment of the visual analyzer in patients after BT requires a comprehensive approach, including the evaluation of both structural and functional characteristics of the eye and visual pathways. Blast injury may result in direct mechanical damage to the eye as well as secondary changes caused by the effects of the shock wave, exposure to high temperatures, infrared radiation, toxic substances, and other factors.

The examination of these patients should be comprehensive and multidisciplinary, involving an ophthalmologist, neurologist, neurosurgeon, and, when necessary, a plastic surgeon. Careful collection of the history of the blast event, when feasible, enables initial risk stratification and helps in selecting optimal diagnostic tools. Blast-related ocular injuries may present with a wide spectrum of symptoms, ranging from minimal discomfort to severe pain or complete loss of vision.

A basic ophthalmological examination (visometry, tonometry, pupillary reactions, slit-lamp examination, assessment of ocular motility, and perimetry) is mandatory even in the absence of obvious external injuries. It is essential to perform not only an initial but also a dynamic assessment, as a number of pathological changes (e.g., optic nerve atrophy) may become apparent in the delayed period.

Neuroimaging and neurophysiological methods play an important role in the comprehensive diagnosis and monitoring of patients with visual analyzer injuries. These techniques allow not only for the precise determination of the localization and nature of structural damage, but also for objective assessment of the functional state of the visual pathways and retina, which is crucial for determining prognosis and selecting an appropriate treatment strategy.

To improve long-term outcomes, regular ophthalmological and neurophysiological monitoring is required, along with active patient involvement in visual rehabilitation programs, training in compensatory strategies, and the use of a multidisciplinary approach. Even in cases with unfavorable functional recovery, comprehensive support and rehabilitation can significantly improve patients' quality of life.

Disclosure

Conflict of Interest

The authors declare no conflict of interest.

Funding

The study received no external funding.

References

1. Krasnovid TA, Aslanova VS, Bondar NI. Main aspects of traumatic eye injures during wars and military conflicts. Arch Ukr Ophthalmol. 2020;8(1):78-85. Ukrainian. doi: 10.22141/2309-8147.8.1.2020.200741
2. Zhang Y, Kang X, Wu Q, Zheng Z, Ying J, Zhang MN. Explosive eye injuries: characteristics, traumatic mechanisms, and prognostic factors for poor visual outcomes. Mil Med Res. 2023 Jan 12;10(1):3. doi: 10.1186/s40779-022-00438-4
3. Morley MG, Nguyen JK, Heier JS, Shingleton BJ, Pasternak JF, Bower KS. Blast eye injuries: a review for first responders. Disaster Med Public Health Prep. 2010 Jun;4(2):154-60. doi: 10.1001/dmp.v4n2.hra10003
4. McMaster D, Clare G. Incidence of ocular blast injuries in modern conflict. Eye (Lond). 2021 Dec;35(12):3451-3452. doi: 10.1038/s41433-020-01359-z
5. Harvey MM, Justin GA, Brooks DI, Ryan DS, Weichel ED, Colyer MH. Ocular Trauma in Operation Iraqi Freedom and Operation Enduring Freedom from 2001 to 2011: A Bayesian Network Analysis. Ophthalmic Epidemiol. 2021 Aug;28(4):312-321. doi: 10.1080/09286586.2020.1828494
6. Rauchman SH, Albert J, Pinkhasov A, Reiss AB. Mild-to-Moderate Traumatic Brain Injury: A Review with Focus on the Visual System. Neurol Int. 2022 May 30;14(2):453-470. doi: 10.3390/neurolint14020038
7. Sukkarieh G, Lahoud C, Ghorayeb R, Abi Karam M, Succarieh Y, Saleh M, Jalkh A. Characteristics of open eye injuries in the Beirut Port explosion. Injury. 2021 Sep;52(9):2601-2605. doi: 10.1016/j.injury.2021.07.031
8. Notghi B, Bhardwaj R, Bailoor S, Thompson KA, Weaver AA, Stitzel JD, Nguyen TD. Biomechanical Evaluations of Ocular Injury Risk for Blast Loading. J Biomech Eng. 2017 Aug 1;139(8). doi: 10.1115/1.4037072
9. Erdurman FC, Hurmeric V, Gokce G, Durukan AH, Sobaci G, Altinsoy HI. Ocular injuries from improvised explosive devices. Eye (Lond). 2011 Nov;25(11):1491-8. doi: 10.1038/eye.2011.212
10. Alam M, Iqbal M, Khan A, Khan SA. Ocular injuries in blast

victims. J Pak Med Assoc. 2012 Feb;62(2):138-42.
11. Karimi A, Razaghi R, Girkin CA, Downs JC. Ocular biomechanics due to ground blast reinforcement. Comput Methods Programs Biomed. 2021 Nov;211:106425. doi: 10.1016/j.cmpb.2021.106425
12. Goncharova NA, Kovtun MI, Pastukh IV, Pavlyuchenko OS, Muzhychuk OP. Damage to the visual analyzer in military personnel with concussion (clinical cases). EMERGENCY MEDICINE.2024;20(4):288-298. Ukrainian. doi: 10.22141/2224-0586.20.4.2024.1717
13. Kalayci M, Er S, Tahtabasi M. Bomb Explosion: Ocular Effects of Primary, Secondary and Tertiary Mechanisms. Clin Ophthalmol. 2020 Apr 28;14:1145-1151. doi: 10.2147/OPTH.S253438
14. Rex TS, Reilly MA, Sponsel WE. Elucidating the effects of primary blast on the eye. Clin Exp Ophthalmol. 2015 Apr;43(3):197-9. doi: 10.1111/ceo.12502
15. Razaghi R, Biglari H, Karimi A. Finite element modeling of the eyeglass-related traumatic ocular injuries due to high explosive detonation. Eng Fail Anal. 2020;117:104835. doi: 10.1016/j.engfailanal.2020.104835
16. Sherwood D, Sponsel WE, Lund BJ, Gray W, Watson R, Groth SL, Thoe K, Glickman RD, Reilly MA. Anatomical manifestations of primary blast ocular trauma observed in a postmortem porcine model. Invest Ophthalmol Vis Sci. 2014 Feb 24;55(2):1124-32. doi: 10.1167/iovs.13-13295
17. Monsour M, Ebedes D, Borlongan CV. A review of the pathology and treatment of TBI and PTSD. Exp Neurol. 2022;351:114009. doi: 10.1016/j.expneurol.2022.114009
18. Justin GA, Baker KM, Brooks DI, Ryan DS, Weichel ED, Colyer MH. Intraocular Foreign Body Trauma in Operation Iraqi Freedom and Operation Enduring Freedom: 2001 to 2011. Ophthalmology. 2018 Nov;125(11):1675-1682. doi: 10.1016/j.ophtha.2018.06.006
19. Gundogan FC, Akay F, Yolcu U, Uzun S, Ilhan A, Toyran S, Eyi E, Diner O. Ocular blast injuries related to explosive military ammunition. J R Army Med Corps. 2016 Feb;162(1):39-43. doi: 10.1136/jramc-2015-000408
20. Weichel ED, Colyer MH. Combat ocular trauma and systemic injury. Curr Opin Ophthalmol. 2008 Nov;19(6):519-25. doi: 10.1097/ICU.0b013e3283140e98
21. Kulkarni AR, Aggarwal SP, Kulkarni RR, Deshpande MD, Walimbe PB, Labhsetwar AS. Ocular manifestations of head injury: a clinical study. Eye (Lond). 2005 Dec;19(12):1257-63. doi: 10.1038/sj.eye.6701753
22. Hassan Naqvi SA, Malik S, Zulfiqaruddin S, Anwar SB, Nayyar S. Etiology and severity of various forms of ocular war injuries in patients presenting at an Army Hospital in Pakistan. Pak J Med Sci. 2016 Nov-Dec;32(6):1543-1546. doi: 10.12669/pjms.326.11158
23. Belmonte-Grau M, Garrido-Ceca G, Marticorena-Álvarez P. Ocular trauma in an urban Spanish population: epidemiology and visual outcome. Int J Ophthalmol. 2021 Sep 18;14(9):1327-1333. doi: 10.18240/ijo.2021.09.06
24. Rasiah PK, Hardenburger J, Dong H, Hardin R, Locke A, Jenkins JL, Artis E, Caskey C, Millis B, Jansen ED, Rex TS, Mahadevan-Jansen A. Subcellular and macrostructural immediate responders to airblast traumatic brain injury. Sci Rep. 2025 Aug 4;15(1):28454. doi: 10.1038/s41598-025-13288-6
25. Kheir WJ, Awwad ST, Bou Ghannam A, Khalil AA, Ibrahim P, Rachid E, El Salloukh NA, Yehia M, Torbey J, El Zein L, Jabbur NS, Noureddin B, Alameddine RM. Ophthalmic Injuries After the Port of Beirut Blast-One of Largest Nonnuclear Explosions in History. JAMA Ophthalmol. 2021 Sep 1;139(9):937-943. doi: 10.1001/jamaophthalmol.2021.2742
26. Lee I, Davis B, Purt B, DesRosiers T. Ocular Trauma and Traumatic Brain Injury on the Battlefield: A Systematic Review After 20 Years of Fighting the Global War on Terror. Mil Med. 2023 Aug 29;188(9-10):2916-2923. doi: 10.1093/milmed/usac226
27. Rana V, Patra VK, Bandopadhayay S, Raj B, Sharma VK, Gupta A, Mishra SK, Kumar P. Combat ocular trauma in counterinsurgency operations. Indian J Ophthalmol. 2023 Dec 1;71(12):3615-3619. doi: 10.4103/IJO.IJO_609_23
28. Zou YY, Kan EM, Lu J, Ng KC, Tan MH, Yao L, Ling EA. Primary blast injury-induced lesions in the retina of adult rats. J Neuroinflammation. 2013 Jul 2;10:79. doi: 10.1186/1742-2094-10-79
29. Taran S, Pelosi P, Robba C. Optimizing oxygen delivery to the injured brain. Curr Opin Crit Care. 2022 Apr 1;28(2):145-156. doi: 10.1097/MCC.0000000000000913
30. Armstrong RA. Visual problems associated with traumatic brain injury. Clin Exp Optom. 2018 Nov;101(6):716-726. doi: 10.1111/cxo.12670
31. Alvarez TL, Kim EH, Vicci VR, Dhar SK, Biswal BB, Barrett AM. Concurrent vision dysfunctions in convergence insufficiency with traumatic brain injury. Optom Vis Sci. 2012 Dec;89(12):1740-51. doi: 10.1097/OPX.0b013e3182772dce
32. Bailey MD, Gambert S, Gruber-Baldini A, Guralnik J, Kozar R, Qato DM, Shardell M, Albrecht JS. Traumatic Brain Injury and Risk of Long-Term Nursing Home Entry among Older Adults: An Analysis of Medicare Administrative Claims Data. J Neurotrauma. 2023 Jan;40(1-2):86-93. doi: 10.1089/neu.2022.0003
33. Dwyer B, Katz DI. Postconcussion syndrome. Handb Clin Neurol. 2018;158:163-178. doi: 10.1016/B978-0-444-63954-7.00017-3
34. Pattnaik S, Panda BB, Swain SC. Spectrum of Ocular Findings in Closed Head Injuries, Correlation With Severity of Neurological Involvement, and Treatment Outcome: A Hospital-Based Cross-Sectional Study. Cureus. 2021 Jul 20;13(7):e16515. doi: 10.7759/cureus.16515
35. Adhan IK, Gunton KB. Optimal Diagnostic Strategies for Concussion-Related Vision Disorders: A Review. Eye Brain. 2025 May 12;17:27-36. doi: 10.2147/EB.S492854
36. Cockerham GC, Goodrich GL, Weichel ED, Orcutt JC, Rizzo JF, Bower KS, Schuchard RA. Eye and visual function in traumatic brain injury. J Rehabil Res Dev. 2009;46(6):811-8. doi: 10.1682/jrrd.2008.08.0109
37. Ruia S, Tripathy K. Humphrey Visual Field. 2025 Jan 20. In: StatPearls [Internet]. Treasure Island (FL): StatPearls Publishing; 2025 Jan–.
38. Rai BB, Sabeti F, Carle CF, Maddess T. Visual Field Tests: A Narrative Review of Different Perimetric Methods. J Clin Med. 2024 Apr 23;13(9):2458. doi: 10.3390/jcm13092458
39. Chaudhary R, Upendran M, Campion N, Yeung A, Blanch R, Morgan-Warren P, Gibb I, Nelson T, Scott R. The role of computerised tomography in predicting visual outcome in ocular trauma patients. Eye (Lond). 2015 Jul;29(7):867-71. doi: 10.1038/eye.2015.39
40. Costello F. Optical Coherence Tomography in Neuro-ophthalmology. Neurol Clin. 2017 Feb;35(1):153-163. doi: 10.1016/j.ncl.2016.08.012
41. Zeppieri M, Marsili S, Enaholo ES, Shuaibu AO, Uwagboe N, Salati C, Spadea L, Musa M. Optical Coherence Tomography (OCT): A Brief Look at the Uses and Technological Evolution of Ophthalmology. Medicina (Kaunas). 2023 Dec 3;59(12):2114. doi: 10.3390/medicina59122114
42. Ko TH, Fujimoto JG, Duker JS, Paunescu LA, Drexler W, Baumal CR, Puliafito CA, Reichel E, Rogers AH, Schuman JS. Comparison of ultrahigh- and standard-resolution optical coherence tomography for imaging macular hole pathology and repair. Ophthalmology. 2004 Nov;111(11):2033-43. doi: 10.1016/j.ophtha.2004.05.021
43. Al-Mujaini A, Wali UK, Azeem S. Optical coherence tomography: clinical applications in medical practice. Oman Med J. 2013 Mar;28(2):86-91. doi: 10.5001/omj.2013.24
44. Nam KT, Yun C, Seo M, Ahn S, Oh J. Comparison of retinal thickness measurements among four different optical coherence tomography devices. Sci Rep. 2024 Feb 12;14(1):3560. doi: 10.1038/s41598-024-54109-6
45. Wollstein G, Ishikawa H, Wang J, Beaton SA, Schuman JS. Optical coherence tomography longitudinal evaluation of retinal nerve fiber layer thickness in glaucoma. Arch Ophthalmol. 2005 Apr;123(4):464-70. doi:10.1001/archopht.123.4.464
46. Arruabarrena C, Montejano-Milner R, de Aragón F, Allendes G, Teus MA. Resultados del tratamiento de los pacientes con DMAE exudativa durante la pandemia por COVID-19 [Results of the treatment of patients with exudative AMD during the COVID-19 pandemic]. Arch Soc Esp Oftalmol. 2022 Apr;97(4):184-190. Spanish. doi: 10.1016/j.oftal.2021.02.012
47. Sujanthan S, Shmuel A, Mendola JD. Resting-state functional MRI of the visual system for characterization

of optic neuropathy. Front Hum Neurosci. 2022 Oct 18;16:943618. doi: 10.3389/fnhum.2022.943618
48. Mahroo OA. Visual electrophysiology and "the potential of the potentials". Eye (Lond). 2023 Aug;37(12):2399-2408. doi: 10.1038/s41433-023-02491-2
49. Liu Y, Feng K, Jiang H, Hu F, Gao J, Zhang W, Zhang W, Huang B, Brant R, Zhang C, Yan H. Characteristics and treatments of ocular blast injury in Tianjin explosion in China. BMC Ophthalmol. 2020 May 6;20(1):185. doi: 10.1186/s12886-020-01448-3
50. Lytvynchuk LM, Ponomarov M, Reyna EC, Stieger K, Andrassi-Darida M. Multi-Stage Reconstructive Surgery of the Eyeball with No Light Perception After Severe Open Globe Injury. *Clin Ophthalmol.* 2025;19:847-856. doi:10.2147/OPTH.S474942
51. Aylward GW. Vitreous management in penetrating trauma: primary repair and secondary intervention. *Eye (Lond)*. 2008 Oct;22(10):1366-1369. doi:10.1038/eye.2008.74
52. Jin Y, Chen H, Xu X, Hu Y, Wang C, Ma Z. TRAUMATIC PROLIFERATIVE VITREORETINOPATHY: Clinical and Histopathological Observations. Retina. 2017 Jul;37(7):1236-1245. doi: 10.1097/IAE.0000000000001350
53. Orban M, Schranz PJ, Oppegard N, Kruse F, Ulbig M, Hansen LL. Timing and outcomes of vitreoretinal surgery after open-globe injury. *Eye (Lond).* 2016;30(1):101-8. doi:10.1038/eye.2015.170
54. McMaster D, Halliday S, Hussain SF, Kempapidis T, Bush LS, Colyer M, McClellan SF, Miller S, Justin G, Agrawal R, Hoskin AK, Cavuoto K, Leong J, Rousselot Ascarza AM, Woreta FA, Cason J, Miller K, Caldwell MC, Gensheimer W, Williamson TH, Dhawahir-Scala F, Shah P, Coombes A, Sundar G, Mazzoli R, Woodcock M, Watson SL, Kuhn F, Gomes RSM, Blanch RJ. Early versus delayed timing of vitrectomy after open-globe injury. Cochrane Database Syst Rev. 2024 Nov 29;11(11):CD016086. doi: 10.1002/14651858.CD016086
55. Yu H, Li J, Yu Y, Li G, Li D, Guan M, Lu L, Liu T, Luo Y, Shen L, Wu Q, Liu B, Feng S, Yuan L. Optimal timing of vitrectomy for severe mechanical ocular trauma: A retrospective observational study. Sci Rep. 2019 Nov 29;9(1):18016. doi: 10.1038/s41598-019-54472-9
56. Patterson TJ, Kedzierski A, McKinney D, Ritson J, McLean C, Gu W, Colyer M, McClellan SF, Miller SC, Justin GA, Hoskin AK, Cavuoto K, Leong J, Rousselot Ascarza A, Woreta FA, Miller KE, Caldwell MC, Gensheimer WG, Williamson T, Dhawahir-Scala F, Shah P, Coombes A, Sundar G, Mazzoli RA, Woodcock M, Watson SL, Kuhn F, Halliday S, Gomes RSM, Agrawal R, Blanch RJ. The Risk of Sympathetic Ophthalmia Associated with Open-Globe Injury Management Strategies: A Meta-analysis. Ophthalmology. 2024 May;131(5):557-567. doi: 10.1016/j.ophtha.2023.12.006
57. Paulbuddhe V, Addya S, Gurnani B, Singh D, Tripathy K, Chawla R. Sympathetic Ophthalmia: Where Do We Currently Stand on Treatment Strategies? Clin Ophthalmol. 2021 Oct 20;15:4201-4218. doi: 10.2147/OPTH.S289688
58. Blanch RJ, McMaster D, Patterson TJ. Management of open globe injury: a narrative review. Eye (Lond). 2024 Nov;38(16):3047-3051. doi: 10.1038/s41433-024-03246-3
59. Van Swol JM, Myers WK, Beall JA, Atteya MM, Blice JP. Post-traumatic endophthalmitis prophylaxis: a systematic review and meta-analysis. J Ophthalmic Inflamm Infect. 2022 Nov 18;12(1):39. doi: 10.1186/s12348-022-00317-y

Review article

Ukrainian Neurosurgical Journal. 2026;32(1):10-16
doi: 10.25305/unj.342189

Post-concussion syndrome: Part 2. Clinical characteristics, diagnosis, and treatment

Vadym V. Biloshytsky [1,2], Yurii V. Zavaliy [3], Alisa V. Pachevska [4], Illia V. Biloshytskyi [5]

[1] Scientific and Organizational Department, Romodanov Neurosurgery Institute, Kyiv, Ukraine
[2] Pain Management Center SPRAVNO, Kyiv, Ukraine
[3] Department of Neurosurgery, National Military Medical Clinical Center "Main Military Clinical Hospital", Kyiv, Ukraine
[4] Department of Pediatric Stomatology, National Pirogov Memorial Medical University, Vinnytsia, Ukraine
[5] Educational and Scientific Institute of Medicine, Bogomolets National Medical University, Kyiv, Ukraine

Received: 26 October 2025
Accepted: 21 November 2025

Address for correspondence:
Vadym V. Biloshytsky, Pain Management Center SPRAVNO, Mezhyhirska St., 28, Kyiv, 04071, Ukraine, e-mail: dr.biloshytsky@spravno.clinic

This paper presents current data on the clinical features, diagnosis, and treatment of post-concussion syndrome (PCS) that develops after mild blast-related traumatic brain injury (mbTBI). It is emphasized that PCS is one of the most common long-term consequences of mbTBI among military personnel exposed to blast waves, which determines the clinical and social relevance of this problem. The diagnostic criteria for PCS according to the International Statistical Classification of Diseases, 10th Revision (ICD-10), and the Diagnostic and statistical manual of mental disorders, fourth edition (DSM-IV), are described, as well as the difficulty of differentiating PCS from post-traumatic stress disorder, which frequently co-occurs with PCS in combat veterans. The following symptom groups are identified: cognitive, psychoemotional, somatosensory, autonomic, and vestibular. Particular emphasis is placed on the importance of using neurophysiological methods—quantitative electroencephalography and P300 event-related potentials—to objectify the diagnosis of PCS. The therapeutic approach should be multidisciplinary and personalized, incorporating physical rehabilitation, cognitive-behavioral therapy, sleep hygiene, and pharmacological management (antidepressants, analgesics, botulinum toxin therapy, and hyperbaric oxygen therapy). Research findings indicate the importance of early physical activity.

Keywords: *post-concussion syndrome; mild blast-related traumatic brain injury; cognitive impairment; post-traumatic stress disorder; neurorehabilitation.*

Post-concussion syndrome: clinical features, diagnosis, and differential diagnosis

A blast wave may cause mild, moderate, or severe traumatic brain injury (TBI). The clinical manifestations of mild blast-related TBI (mbTBI) in the acute phase are variable and include headache, fatigue, tinnitus, irritability, as well as neuropsychiatric and cognitive disturbances. Many injured military personnel who sustained mbTBI during military operations in Afghanistan and Iraq exhibited disorders of higher nervous activity and behavior, characterized by memory and cognitive impairments (reduced attention and concentration, slowed cognitive processing, speech changes), irritability, anxiety, and fatigue. Emotional changes, including mood lability, anxiety, depression, and personality alterations, are frequently observed concurrently [1, 2].

Complete recovery after mbTBI may occur within several days or weeks; however, many symptoms persist for a prolonged period. Unlike patients with moderate or severe TBI, individuals diagnosed with mbTBI typically have no visible structural brain damage and remain conscious, presenting with characteristic symptoms such as headache, confusion, dizziness, memory impairment, and behavioral changes. These disturbances may persist long after the injury or become permanent, leading to significant functional impairment. The chronic nature of cognitive deficits may be related to the fact that blast-related TBI increases the risk of delayed development of neurodegenerative diseases, including Alzheimer's disease and chronic traumatic encephalopathy [1, 3–5].

Patients with a history of multiple mbTBIs may experience more severe and persistent symptoms. Such injuries can cause immediate and, in some cases, prolonged neuronal damage and dysfunction, axonal stretching and injury, and alterations in neuronal plasticity. Thus, mbTBI may represent not a single "event" but rather a progressive pathological "process" of brain injury sustained by secondary molecular mechanisms, including neuroinflammation, oxidative damage, excitotoxicity, and other processes [4,6]. The clinical manifestations of mbTBI should not be regarded as purely "functional" due to the limited number of abnormalities detected by conventional neuroimaging. The underlying pathology involves both structural and functional damage of varying severity, independent of the type or apparent severity of injury. These changes often remain undetectable using routine imaging techniques such as computed tomography or magnetic resonance imaging (CT/MRI) [7].

The possibility of long-term persistence of neurological and cognitive deficits after mild TBI served

as the basis for identifying a distinct nosological entity—postconcussion syndrome (PCS).

The diagnostic criteria for PCS were developed by the World Health Organization and further elaborated in the Diagnostic and statistical manual of mental disorders, fourth edition (DSM-IV). According to the International statistical classification of diseases and related health problems, Tenth Revision (ICD-10), a diagnosis of PCS may be established when a TBI is sufficiently severe to cause loss of consciousness and is subsequently (within 4 weeks after the injury) accompanied by the development of at least three of the following features: 1) complaints of unpleasant sensations (dizziness, general malaise, excessive fatigue, or noise intolerance) and headache; 2) emotional changes (irritability, emotional lability, or depression and/or anxiety of varying severity); 3) subjective complaints of difficulties with concentration and the performance of mental tasks, as well as memory problems in the absence of clear objective evidence; 4) insomnia; 5) reduced tolerance to alcohol; and 6) preoccupation with these symptoms and fear of persistent brain damage, potentially progressing to hypochondriacal concerns and adoption of the sick role [8].

According to DSM-IV, the diagnostic criteria for PCS include: A) a history of TBI resulting in a "significant cerebral concussion"; B) deficits in cognitive functioning, specifically attention and/or memory; C) the presence of at least three of eight symptoms (fatigue, sleep disturbance, headache, dizziness, irritability, affective disturbances, personality change, apathy) that emerge after the injury and persist for ≥3 months; D) onset or worsening of symptoms following the injury; E) interference with social or role functioning; and F) exclusion of dementia due to head trauma and other disorders that better account for the symptoms. Criteria C and D define a symptom threshold requiring that the onset or exacerbation of symptoms be temporally related to the injury, differ from pre-existing symptoms, and be of sufficient duration [8,9]. It has been noted that the symptoms listed in both ICD-10 and DSM-IV occur more frequently in patients with traumatic brain injury than in those with extracranial injuries. The ICD-10 criteria encompass a broader range of symptoms than the DSM-IV criteria; however, the latter are more specific to traumatic brain injury [9].

According to V. Renga (2021) [7], the clinical manifestations of PCS can be grouped into five categories:

1) cognitive impairments: memory deficits; difficulties with attention and concentration; speech disturbances; executive function disorders; fine motor impairment;

2) psychological disturbances: depression, anxiety, irritability, personality changes, fatigue, derealization;

3) somatosensory and vestibulocochlear dysfunction: headache, nausea and vomiting, hypersensitivity to light and sound, hyperalgesia, tinnitus;

4) visual symptoms and oculomotor dysfunction: photophobia, blurred vision, convergence insufficiency, diplopia, Horner syndrome;

5) autonomic symptoms: fluctuations in heart rate and blood pressure, sweating disorders, pupillary abnormalities, impaired thermoregulation, sexual dysfunction, and sleep disturbances with reduced sleep efficiency.

The pathophysiological mechanisms underlying the delayed onset and prolonged persistence of PCS symptoms have been addressed in several literature reviews [6–8,10–13]. As noted above, the primary cause of pathological changes is damage to neuronal axons and small blood vessels, referred to as diffuse axonal injury with molecular consequences. In mild TBI, diffuse axonal injury most commonly involves the frontal and frontotemporal regions of the brain. One of the most significant consequences is disruption of functional brain networks. The human brain contains more than 100 billion neurons interconnected by trillions of synaptic connections. Neuroimaging studies (functional MRI with BOLD sequences, positron emission tomography, arterial spin labeling [ASL]) demonstrate disturbances of these functional networks following mild TBI. Such alterations persist for a prolonged period after the injury. According to functional near-infrared spectroscopy data, neurovascular coupling becomes inefficient even in the presence of normal or increased cerebral blood flow, indicating a functional mismatch between perfusion and the metabolic demands of neuronal cells. In addition to intracranial damage, the development of PCS may also be influenced by whiplash injury involving the cervical nerve roots, vestibular system, and cervical musculature. These extracranial effects contribute to headache, dizziness, visual disturbances, and balance problems. Intracranial, extracranial, and functional components of PCS pathogenesis are not mutually exclusive; they often overlap and are difficult to distinguish. The combination of these components shapes the clinical presentation of PCS and determines its individual characteristics.

Headache develops as a result of activation of the trigeminothalamic system. Activation of the trigeminal nerve begins with stimulation of the orofacial skin or cervical muscles. Whiplash injuries may initiate this process through mechanisms of convergence of sensory afferents within the trigeminocervical nucleus. In particular, stimulation of the greater occipital nerves (originating from the cervical roots) increases the excitability of nociceptive afferents of the dura mater, thereby activating the trigeminal pain system [7, 12, 13].

The vestibular system contributes to stabilization of the neck and trunk via vestibulocollic and vestibulospinal reflexes. Vestibular stem and peripheral disturbances lead to impaired cervical muscle tone and disruption of spinal balance mechanisms. Alterations of the vestibulo-ocular reflex may compromise visual target stabilization, resulting in blurred vision. Cervicovestibular dysfunction underlies the majority of symptoms associated with PCS. Cervical proprioceptors are synchronized with vestibulo-ocular and optokinetic reflexes to maintain gaze fixation on a visual target during head movements. Increased tension of the cervical muscles due to irritation of the cervical roots restricts the range of active neck movements and disrupts convergence mechanisms, leading to diplopia, dizziness, and postural instability [7, 12].

In PCS, dysfunction of higher central autonomic regulatory centers of the brain, as well as the peripheral autonomic nervous system, is also observed. Sympathetic innervation of the head and neck arises

from the superior, middle, and inferior cervical ganglia. The stellate ganglion gives rise to branches innervating the heart and cerebral vessels. Its involvement may result in impaired vascular regulation, leading to tachycardia and fluctuations in arterial blood pressure. In addition, disruption of central autonomic regulation also contributes to changes in heart rate and blood pressure. Ipsilateral partial Horner's syndrome is a typical sign of cervical injury. Conversely, sympathetic hyperactivity may also occur, manifesting as mydriasis, facial flushing, and hyperhidrosis [7].

A characteristic feature of mbTBI observed during recent military conflicts is the frequent coexistence of PCS and post-traumatic stress disorder (PTSD). More than one third of U.S. veterans from recent wars diagnosed with PCS following mbTBI also suffer from PTSD or depression [14, 15].

In the fifth edition of the diagnostic and statistical manual of mental disorders (DSM-5), PTSD is described as a psychiatric disorder that develops following direct or indirect exposure to life events that may result in serious injury, sexual violence, or death. PTSD comprises four symptom clusters: 1) various phenomena of re-experiencing, including recurrent, intrusive, and involuntary thoughts or images; distressing dreams; dissociative reactions such as flashbacks, during which the individual feels or acts as if the traumatic event were recurring, often involving all five sensory modalities; as well as marked emotional and physiological reactivity to external environmental or internal psychological cues associated with the traumatic experience; 2) avoidance, manifested by efforts to avoid trauma-related reminders, both internal (e.g., thoughts or memories) and external (e.g., places, conversations, films, and television programs), leading to social withdrawal and isolation; 3) negative alterations in cognition and mood, including cognitive distortions, memory deficits (inability to recall aspects of the traumatic experience), and persistent negative emotional states, as a result of which individuals with PTSD commonly experience fear, anger, guilt, or shame; hold negative beliefs and expectations about themselves (e.g., low self-esteem, self-blame, a sense of impending death) or about the world (e.g., believing that no one can be trusted or that no one is safe); exhibit diminished interest in activities, emotional detachment from others, and difficulty experiencing positive emotions; 4) marked alterations in arousal and reactivity of the central and autonomic nervous systems, manifested by irritability, verbal and/or physical outbursts of anger, reckless and/or self-destructive behavior, hypervigilance, exaggerated startle response, impaired concentration, and insomnia [16].

Epidemiological studies indicate that PTSD is a common problem among combat veterans. Between 4% and 33% of military personnel who served in Iraq and/or Afghanistan are affected by this disorder [17]. In a study conducted in the United Kingdom among active service members, 21.9% reported symptoms of mental disorders, probable PTSD was identified in 6.2%, and 10.0% reported alcohol misuse [18]. According to other data, while the prevalence of probable PTSD among active British military personnel was 4.8%, it reached 17.0% among former service members who had participated in combat operations [19]. Greater combat exposure is associated with more severe PTSD symptoms, which hinder adaptation to civilian life and adversely affect family relationships [20, 21].

When PCS and PTSD coexist, diagnostic evaluation becomes more challenging, as clinically distinguishing between these two conditions is often difficult due to substantial symptom overlap [22]. The symptoms listed in the diagnostic criteria are not specific to PCS alone; they are also observed in non-injured populations and in other non-traumatic conditions, such as depression, anxiety disorders, and chronic pain [23, 24]. In some cases, TBI and PTSD may coexist as a result of the independent effects of physical trauma and psychological stressors [22].

It has been noted that, in the absence of objective diagnostic assessments, particularly during the chronic phase of TBI, the validity of PCS as a diagnostic entity is questioned by many specialists [13]. Notably, observations indicate that the frequency of reported symptoms increases when individuals are involved in legal proceedings [25]. It has been suggested that the apparent epidemic of PCS among Western military personnel during the wars in Iraq and Afghanistan may represent an artifact resulting from a lowered diagnostic "threshold" for mbTBI, including the consideration of minor transient alterations in consciousness. Studies have shown that PCS symptomatology can be attributed solely to blast exposure only in cases involving a clear loss of consciousness, which was reported by a minority of veterans of these conflicts. A 2014 report by the U.S. Institute of Medicine concluded that there is scientific evidence indicating that, in affected individuals, most shared symptoms are better explained by comorbid PTSD rather than by the consequences of mbTBI alone [22,26].

Conversely, complaints of cognitive and behavioral impairments often do not emerge immediately after the injury but rather 1–3 months thereafter. This delay may lead to their misinterpretation as being caused not by TBI but by affective disorders [27,28].

Despite its apparent simplicity, the diagnosis of PCS remains a subject of debate for several reasons, including insufficient symptom specificity, the influence of premorbid status on injury outcomes, "recall bias", and the impact of psychosocial factors [13]. "Recall bias", also referred to as the "good old days" phenomenon, occurs both in healthy individuals and in various pathological conditions. It reflects a tendency to underestimate the severity and extent of prior symptoms, particularly during the premorbid period [29]. A study involving children and adolescents with PCS during the post-traumatic period demonstrated that patients and their parents, when retrospectively assessing premorbid symptomatology one month after injury, underestimated its severity by approximately 80%. This level of underestimation persisted until the end of follow-up (three months post-injury) [30]. These findings indicate that the "good old days" phenomenon may lead to underestimation of premorbid symptoms and overestimation of PCS severity. Investigation of this phenomenon and the development of methods to mitigate "recall bias" may help reduce patients' anxiety regarding the severity of their condition and promote a more accurate subjective perception of TBI severity and its impact on quality of life [13, 31].

The diagnosis of PCS following mbTBI may also be complicated by additional factors. Clinicians may find it difficult to accurately assess the true severity of TBI due to limited information about the circumstances of the injury, which may rely on the injured individual's subjective recollection months or even years after the event(s). Furthermore, the absence of certain objective characteristics of the injury circumstances may compromise the accuracy of "blast self-assessment," particularly regarding distance from the explosion and the severity of concussive forces—data that are often missing from primary medical records. The lack of reliable information on injury characteristics complicates determination of cognitive recovery trajectories and rehabilitation planning. Typically, the presence and severity of PCS are assessed based on the current state of neuropsychological and cognitive functioning using screening scales, which are not necessarily specific to TBI and may instead reflect the severity of comorbid PTSD or depression [10, 32].

Thus, the symptom complexes of PCS and PTSD are largely similar and may substantially "overlap" within an individual patient. In patients with PCS, the likelihood of comorbid PTSD is high due to its considerable prevalence among combatants. The presence of PTSD significantly complicates the diagnosis of PCS because of the similarity of clinical manifestations. However, TBI represents an organic injury to neural tissue, whereas PTSD is a psychological response to a stressor and is not accompanied by structural changes. This fundamental distinction necessitates different therapeutic approaches to these conditions. While the treatment of PTSD primarily focuses on normalization of stress responses through psychological and pharmacological interventions, the management of TBI must account for structural and molecular-biological alterations in order to prevent their impact on the severity and duration of neurological deficits [22, 33].

An important objective is to improve the diagnosis of PCS following mbTBI by refining objective criteria for structural and functional disturbances of the central nervous system. This would enhance prognostic assessment of mbTBI in injured individuals and facilitate optimization of treatment strategies, including personalized approaches aimed at preventing the development of persistent neurological deficits. Neurophysiological investigations hold substantial potential for the objective verification of PCS following mbTBI. According to previously published results of our study, quantitative electroencephalography (qEEG) in patients with PCS reveals alterations in the frequency and topography of the α-rhythm, reduced α amplitude, frequency–spatial inversion, and signs of dysfunction of nonspecific brain structures; spectral analysis demonstrates decreased α power, increased β power, and elevated activity in the θ- and δ-frequency bands. These characteristics may persist into the long-term period after mbTBI and should therefore be taken into account in the differential diagnosis with PTSD [34]. The analysis of event-related cognitive potentials (P300) has shown that these parameters are statistically significantly associated with the severity of cognitive impairment and may serve as an effective tool for objective assessment of the degree of cognitive dysfunction in patients with PCS [35].

Treatment of post-concussion syndrome resulting from mild blast-related traumatic brain injury

The management of PCS differs from therapeutic approaches used in the acute and subacute phases of mild TBI. Rather than emphasizing rest and inactivity, the primary goals are to improve overall functioning, restore daily activities, and facilitate a return to normal life. This is achieved gradually, with active involvement of the patient and their social environment. Once the clinician has a clear understanding of the clinical presentation, attention should be focused on one or two of the most problematic symptoms, as other symptoms often regress during the course of treatment. Patients with persistent dizziness, balance disturbances, or ongoing visual complaints should be referred to appropriate specialists. Peripheral vestibular dysfunction should initially be managed with specialized physical therapy. Migraine-associated dizziness may be treated with preventive migraine therapies. Convergence insufficiency and persistent reading dysfunction may respond to oculomotor neurorehabilitation. The most common problems typically include sleep disturbances, headaches, as well as cognitive and mood disorders [13].

Rest and sleep. According to polysomnographic data, sleep disturbances in PCS are characterized by reduced sleep efficiency, prolonged sleep latency, and an increased number of nocturnal awakenings. Their development correlates with structural changes observed on magnetic resonance imaging, psychological disorders (particularly anxiety), and decreased melatonin production [7,36]. Adequate sleep and rest are of crucial importance for both the prevention and treatment of PCS. Rest should include both physical and cognitive components; however, prolonged rest is not recommended. Routine daily activities are necessary to maintain basic functioning. The optimal duration of rest varies between individuals. For physically active persons, complete cessation of activity may be unnatural; in such cases, maintaining a certain level of daily activity may be beneficial. Individual characteristics related to age, physical condition, and psychological factors should be taken into account.

Brain recovery depends on sufficient sleep. Sleep quality and rest are particularly important, as deeper stages of sleep promote the reorganization of neural connections. Waking up feeling refreshed is an indicator of good sleep quality. In patients with PCS, sleep quality is often impaired. Adjunctive measures such as melatonin supplementation, sleep music, or white noise may be helpful. Cyclobenzaprine provides a dual effect by relaxing muscles and improving sleep. It is especially important for patients with PCS to fall asleep at the same time each night, as this may help stabilize disrupted circadian rhythms [7, 13]. For the management of sleep disturbances, amitriptyline may be used; it can also be beneficial for headache treatment, short courses of non-benzodiazepine hypnotics (e.g., zopiclone) and cognitive-behavioral therapy may also be considered [13].

Physical therapy. It has been noted that restriction of physical activity after mild TBI leads to delayed recovery and greater severity of symptoms within the spectrum of post-concussion syndrome (PCS) [38]. Prolonged physical inactivity may exacerbate the development of secondary symptoms, such as depression, anxiety, and fatigue [39]. In contrast, early rather than delayed initiation of moderate physical exercise improves clinical outcomes in patients with PCS [40]. Improvements have been demonstrated in patients who received physical therapy compared with those who did not [12]. In the study by [39], the PCS treatment program included physical therapy in the form of jogging, cycling, joint and soft tissue repositioning or mobilization procedures, as well as vestibular and oculomotor rehabilitation techniques. Physical therapy contributed to a greater regression of post-traumatic symptoms. The authors note that the absence of spontaneous recovery after mild TBI may be partly attributable to concomitant injuries of the spine and other body regions caused by the traumatic physical force.

The cornerstone of PCS therapy is physical therapy targeting the vestibular system and the cervical spine. Vestibular therapy includes exercises aimed at training the vestibular apparatus through oculomotor exercises, as well as head and trunk exercises designed to improve balance and visual stability. Visual and oculomotor therapy may help restore smooth pursuit eye movements and fixation. A normal range of cervical motion is essential for balance reflexes that prevent falls. Most patients with PCS exhibit components of cervicogenic dizziness and balance impairment. Therefore, cervical physical therapy should be an integral part of PCS rehabilitation. Manual therapy and relaxation of the cervical musculature using therapeutic exercises, massage, warm compresses, and topical applications may also be beneficial. Severe vestibular dysfunction, particularly in the acute phase, can be difficult to manage because of pronounced dizziness and nausea. In such cases, the use of vestibular sedative agents, such as benzodiazepines, flunarizine, or betahistine, may be considered. Gabapentin and amitriptyline may also help reduce sensitization phenomena, while cyclobenzaprine is useful for muscle relaxation. All of these medications also have sedative effects [7].

Behavioral interventions. Recovery involves relearning previously acquired skills. Adherence to a structured daily routine represents the most important behavioral modification for restoring normal brain function. Waking and going to sleep at consistent times may help entrain the brain to a regular schedule. In the evening, the use of stimulants, including caffeine and alcohol, as well as substances that depress the central nervous system, should be avoided. It is important to avoid public gatherings, excessive social media engagement, loud sounds, and rock music. Screen time involving television, computers, or mobile phones should be reduced. Beneficial activities include quiet walks in nature at dawn or sunset, listening to calming instrumental music, and reading printed books [7].

Hyperbaric oxygen therapy. This modality involves placing the patient in a chamber in which the pressure of pure oxygen is gradually increased to levels 1.5–3.0 times higher than normal atmospheric pressure. The mechanism of action is thought to involve stimulation of angiogenesis, potentially leading to increased cerebral perfusion. Enhanced blood supply to brain regions that have become ischemic or hypoxic due to vascular injury may accelerate recovery processes. A study evaluating the neurotherapeutic effects of hyperbaric oxygen therapy in PCS using cerebral perfusion imaging and clinical assessment of cognitive function demonstrated positive outcomes. Patients showed significant improvements in cognitive domains such as information processing, processing speed, and visuospatial processing. In addition, cerebral blood flow and cerebral blood volume increased in brain regions responsible for visual, sensorimotor, memory, and attentional functions [41].

Pharmacotherapy. Headache management. Treatment of pain syndromes, including headache, typically begins with the administration of anti-inflammatory and analgesic agents such as acetylsalicylic acid, ibuprofen, and paracetamol. Due to the similarity between post-traumatic headache and migraine, migraine-specific medications, such as triptans, are often prescribed. However, frequent use of large quantities of medications increases the risk of medication-overuse headache. To prevent this condition, preventive therapy with antidepressants, β-blockers, anticonvulsants, and agents for neuropathic pain is recommended. More invasive procedures, including botulinum toxin therapy and nerve blocks, may also be effective. Botulinum toxin therapy is an effective modality approved by the U.S. FDA for the treatment of chronic migraine. The neuromuscular blocker botulinum toxin type A is believed to inhibit peripheral signal transmission to the central nervous system, thereby preventing central sensitization and reducing pain perception in both migraine and post-traumatic headache. A common cause of headache in PCS is irritation of the cervical nerve roots. Irritation of the occipital nerves resulting from whiplash injury often leads to migraine attacks, dizziness, and cervical muscle spasm. Occipital nerve blocks may help interrupt the headache pathway between the cervical nerve roots and the spinal trigeminal nucleus [7, 12, 42, 43].

Antidepressants – are among the most commonly prescribed medications for the symptomatic treatment of post-concussion syndrome (PCS). Patients with depression exhibit deficits in cerebral monoaminergic neurotransmitters (norepinephrine, serotonin, and/or dopamine). The balance and levels of these neurotransmitters play a crucial role in many behavioral symptoms, including mood, fatigue, and psychomotor activity. The etiology of comorbid depression in patients with PCS is associated with post-traumatic chemical imbalance of these neurotransmitters in the brain. Certain selective serotonin reuptake inhibitors have been widely used in the management of PCS. Correction of post-traumatic depression and anxiety has been achieved with sertraline at daily doses of 25–100 mg and fluoxetine at daily doses of 20–60 mg [12]. Cannabinoids have also been considered a potentially effective option for the treatment of PCS symptoms [44].

Cognitive rehabilitation. Cognitive rehabilitation begins with a baseline assessment using a battery of tests, such as the Montreal Cognitive Assessment. In cases of chronic persistent cognitive difficulties with

symptoms resembling attention-deficit/hyperactivity disorder, central nervous system stimulants, including methylphenidate, may be considered. However, methylphenidate should not be prescribed in patients at risk of dependence or seizures, or in those with sleep disturbances. Donepezil has been evaluated for short-term memory impairments associated with PCS. Daytime sleep-related problems may be addressed with modafinil. Cognitive-behavioral therapy is beneficial for mood disorders associated with PCS. Breathing and meditation exercises help improve autonomic regulation and enhance attention, serving as an anchor around which recovery processes may occur [7].

Thus, the therapeutic range for PCS includes a broad range of non-pharmacological and pharmacological interventions. The selection of treatment modalities is determined by the individual clinical characteristics of the patient, with clinical presentation often being highly variable. This underscores the need for an individualized approach to management and, in many clinical situations, for the adoption of personalized clinical decision-making.

Disclosure of Information

Conflict of Interest

The authors declare no conflict of interest.

Funding

This study received no external funding.

References

1. Karr JE, Areshenkoff CN, Duggan EC, Garcia-Barrera MA. Blast-related mild traumatic brain injury: a Bayesian random-effects meta-analysis on the cognitive outcomes of concussion among military personnel. Neuropsychol Rev. 2014 Dec;24(4):428-44. doi: 10.1007/s11065-014-9271-8
2. Lindberg MA, Moy Martin EM, Marion DW. Military Traumatic Brain Injury: The History, Impact, and Future. J Neurotrauma. 2022 Sep;39(17-18):1133-1145. doi: 10.1089/neu.2022.0103
3. Veitch DP, Friedl KE, Weiner MW. Military risk factors for cognitive decline, dementia and Alzheimer's disease. Curr Alzheimer Res. 2013 Nov;10(9):907-30. doi: 10.2174/15672050113109990142
4. Lucke-Wold B, Nolan R, Nwafor D, Nguyen L, Cheyuo C, Turner R, Rosen C, Marsh R. Post-Traumatic Stress Disorder Delineating the Progression and Underlying Mechanisms Following Blast Traumatic Brain Injury. J Neurosci Neuropharmacol. 2018;4(1):118.
5. Dieter JN, Engel SD. Traumatic Brain Injury and Posttraumatic Stress Disorder: Comorbid Consequences of War. Neurosci Insights. 2019 Dec 31;14:1179069519892933. doi: 10.1177/1179069519892933
6. Kaplan GB, Leite-Morris KA, Wang L, Rumbika KK, Heinrichs SC, Zeng X, Wu L, Arena DT, Teng YD. Pathophysiological Bases of Comorbidity: Traumatic Brain Injury and Post-Traumatic Stress Disorder. J Neurotrauma. 2018 Jan 15;35(2):210-225. doi: 10.1089/neu.2016.4953
7. Renga V. Clinical Evaluation and Treatment of Patients with Postconcussion Syndrome. Neurol Res Int. 2021 May 29;2021:5567695. doi: 10.1155/2021/5567695
8. Dwyer B, Katz DI. Postconcussion syndrome. Handb Clin Neurol. 2018;158:163-178. doi: 10.1016/B978-0-444-63954-7.00017-3
9. Boake C, McCauley SR, Levin HS, Pedroza C, Contant CF, Song JX, Brown SA, Goodman H, Brundage SI, Diaz-Marchan PJ. Diagnostic criteria for postconcussional syndrome after mild to moderate traumatic brain injury. J Neuropsychiatry Clin Neurosci. 2005 Summer;17(3):350-6. doi: 10.1176/jnp.17.3.350
10. Kobeissy F, Mondello S, Tümer N, Toklu HZ, Whidden MA, Kirichenko N, Zhang Z, Prima V, Yassin W, Anagli J, Chandra N, Svetlov S, Wang KK. Assessing neuro-systemic & behavioral components in the pathophysiology of blast-related brain injury. Front Neurol. 2013 Nov 21;4:186. doi: 10.3389/fneur.2013.00186
11. Elder GA, Ehrlich ME, Gandy S. Relationship of traumatic brain injury to chronic mental health problems and dementia in military veterans. Neurosci Lett. 2019 Aug 10;707:134294. doi: 10.1016/j.neulet.2019.134294
12. Kim K, Priefer R. Evaluation of current post-concussion protocols. Biomed Pharmacother. 2020 Sep;129:110406. doi: 10.1016/j.biopha.2020.110406
13. Barlow KM. Postconcussion Syndrome: A Review. J Child Neurol. 2016 Jan;31(1):57-67. doi: 10.1177/0883073814543305
14. Hoge CW, McGurk D, Thomas JL, Cox AL, Engel CC, Castro CA. Mild traumatic brain injury in U.S. Soldiers returning from Iraq. N Engl J Med. 2008 Jan 31;358(5):453-63. doi: 10.1056/NEJMoa072972
15. Vasterling JJ, Verfaellie M, Sullivan KD. Mild traumatic brain injury and posttraumatic stress disorder in returning veterans: perspectives from cognitive neuroscience. Clin Psychol Rev. 2009 Dec;29(8):674-84. doi: 10.1016/j.cpr.2009.08.004
16. American Psychiatric Association. Diagnostic and Statistical Manual of Mental Disorders. 5th ed. Arlington, VA: American Psychiatric Publishing; 2013. doi: 10.1176/appi.books.9780890425596
17. Gates MA, Holowka DW, Vasterling JJ, Keane TM, Marx BP, Rosen RC. Posttraumatic stress disorder in veterans and military personnel: epidemiology, screening, and case recognition. Psychol Serv. 2012 Nov;9(4):361-382. doi: 10.1037/a0027649
18. Stevelink SAM, Jones M, Hull L, Pernet D, MacCrimmon S, Goodwin L, MacManus D, Murphy D, Jones N, Greenberg N, Rona RJ, Fear NT, Wessely S. Mental health outcomes at the end of the British involvement in the Iraq and Afghanistan conflicts: a cohort study. Br J Psychiatry. 2018 Dec;213(6):690-697. doi: 10.1192/bjp.2018.175
19. Jones E. PTSD in an era of uncertainty and challenge. Int Rev Psychiatry. 2019 Feb;31(1):1-2. doi: 10.1080/09540261.2019.1603663
20. Foy DW, Sipprelle RC, Rueger DB, Carroll EM. Etiology of posttraumatic stress disorder in Vietnam veterans: analysis of premilitary, military, and combat exposure influences. J Consult Clin Psychol. 1984 Feb;52(1):79-87. doi: 10.1037//0022-006x.52.1.79
21. Taft CT, Schumm JA, Panuzio J, Proctor SP. An examination of family adjustment among Operation Desert Storm veterans. J Consult Clin Psychol. 2008 Aug;76(4):648-56. doi: 10.1037/a0012576
22. Elder GA. Update on TBI and Cognitive Impairment in Military Veterans. Curr Neurol Neurosci Rep. 2015 Oct;15(10):68. doi: 10.1007/s11910-015-0591-8
23. Iverson GL, Lange RT. Examination of "postconcussion-like" symptoms in a healthy sample. Appl Neuropsychol. 2003;10(3):137-44. doi: 10.1207/S15324826AN1003_02
24. Fear NT, Jones E, Groom M, Greenberg N, Hull L, Hodgetts TJ, Wessely S. Symptoms of post-concussional syndrome are non-specifically related to mild traumatic brain injury in UK Armed Forces personnel on return from deployment in Iraq: an analysis of self-reported data. Psychol Med. 2009 Aug;39(8):1379-87. doi: 10.1017/S0033291708004595
25. Lees-Haley PR, Fox DD, Courtney JC. A comparison of complaints by mild brain injury claimants and other claimants describing subjective experiences immediately following their injury. Arch Clin Neuropsychol. 2001 Oct;16(7):689-95.
26. Elder GA, Stone JR, Ahlers ST. Effects of low-level blast exposure on the nervous system: is there really a controversy? Front Neurol. 2014 Dec 19;5:269. doi: 10.3389/fneur.2014.00269
27. Dikmen S, Machamer J, Fann JR, Temkin NR. Rates of symptom reporting following traumatic brain injury. J Int Neuropsychol Soc. 2010 May;16(3):401-11. doi: 10.1017/S1355617710000196
28. Meares S, Shores EA, Taylor AJ, Batchelor J, Bryant RA, Baguley IJ, Chapman J, Gurka J, Marosszeky JE. The prospective course of postconcussion syndrome: the role of mild traumatic brain injury. Neuropsychology. 2011 Jul;25(4):454-65. doi: 10.1037/a0022580

29. Gunstad J, Suhr JA. "Expectation as etiology" versus "the good old days": postconcussion syndrome symptom reporting in athletes, headache sufferers, and depressed individuals. J Int Neuropsychol Soc. 2001 Mar;7(3):323-33. doi: 10.1017/s1355617701733061
30. Brooks BL, Kadoura B, Turley B, Crawford S, Mikrogianakis A, Barlow KM. Perception of recovery after pediatric mild traumatic brain injury is influenced by the "good old days" bias: tangible implications for clinical practice and outcomes research. Arch Clin Neuropsychol. 2014 Mar;29(2):186-93. doi: 10.1093/arclin/act083
31. Iverson GL, Brooks BL, Ashton VL, Lange RT. Interview versus questionnaire symptom reporting in people with the postconcussion syndrome. J Head Trauma Rehabil. 2010 Jan-Feb;25(1):23-30. doi: 10.1097/HTR.0b013e3181b4b6ab
32. Nelson NW, Hoelzle JB, McGuire KA, Ferrier-Auerbach AG, Charlesworth MJ, Sponheim SR. Neuropsychological evaluation of blast-related concussion: illustrating the challenges and complexities through OEF/OIF case studies. Brain Inj. 2011;25(5):511-25. doi: 10.3109/02699052.2011.558040
33. Elder GA, Mitsis EM, Ahlers ST, Cristian A. Blast-induced mild traumatic brain injury. Psychiatr Clin North Am. 2010 Dec;33(4):757-81. doi: 10.1016/j.psc.2010.08.001
34. Tretiakova AI, Zavaliy YV. Evaluation of Doppler and electroencephalographic changes in patients with postconcussion syndrome due to mild blast traumatic brain injury. Ukrainian Neurosurgical Journal. 2022;28(2):31–36. doi: 10.25305/unj.254486
35. Zavaliy YV, Solonovych OS, Biloshitsky VV, Tretiakova AI, Chebotariova LL, Suliy LM. Cognitive evoked potentials in the diagnosis of post-concussion syndrome due to blast mild traumatic brain injury. Ukrainian Neurosurgical Journal. 2021;27(4):3–9. doi: 10.25305/unj.236138
36. Datta SG, Pillai SV, Rao SL, Kovoor JM, Chandramouli BA. Post-concussion syndrome: Correlation of neuropsychological deficits, structural lesions on magnetic resonance imaging and symptoms. Neurol India. 2009 Sep-Oct;57(5):594-8. doi: 10.4103/0028-3886.57810
37. Shekleton JA, Parcell DL, Redman JR, Phipps-Nelson J, Ponsford JL, Rajaratnam SM. Sleep disturbance and melatonin levels following traumatic brain injury. Neurology. 2010 May 25;74(21):1732-8. doi: 10.1212/WNL.0b013e3181e0438b
38. Harmon KG, Drezner JA, Gammons M, Guskiewicz KM, Halstead M, Herring SA, Kutcher JS, Pana A, Putukian M, Roberts WO. American Medical Society for Sports Medicine position statement: concussion in sport. Br J Sports Med. 2013 Jan;47(1):15-26. doi: 10.1136/bjsports-2012-091941
39. Grabowski P, Wilson J, Walker A, Enz D, Wang S. Multimodal impairment-based physical therapy for the treatment of patients with post-concussion syndrome: A retrospective analysis on safety and feasibility. Phys Ther Sport. 2017 Jan;23:22-30. doi: 10.1016/j.ptsp.2016.06.001
40. Thomas DG, Apps JN, Hoffmann RG, McCrea M, Hammeke T. Benefits of strict rest after acute concussion: a randomized controlled trial. Pediatrics. 2015 Feb;135(2):213-23. doi: 10.1542/peds.2014-0966
41. Tal S, Hadanny A, Sasson E, Suzin G, Efrati S. Hyperbaric Oxygen Therapy Can Induce Angiogenesis and Regeneration of Nerve Fibers in Traumatic Brain Injury Patients. Front Hum Neurosci. 2017 Oct 19;11:508. doi: 10.3389/fnhum.2017.00508
42. Lippert-Grüner M. Botulinum toxin in the treatment of post-traumatic headache - case study. Neurol Neurochir Pol. 2012 Nov-Dec;46(6):591-4. doi: 10.5114/ninp.2012.32109
43. Yerry JA, Kuehn D, Finkel AG. Onabotulinum toxin a for the treatment of headache in service members with a history of mild traumatic brain injury: a cohort study. Headache. 2015 Mar;55(3):395-406. doi: 10.1111/head.12495
44. Schurman LD, Lichtman AH. Endocannabinoids: A Promising Impact for Traumatic Brain Injury. Front Pharmacol. 2017 Feb 17;8:69. doi: 10.3389/fphar.2017.00069

Original article

Ukrainian Neurosurgical Journal. 2026;32(1):17-23
doi: 10.25305/unj.339192

A stage-based approach to pain syndrome management in patients with warfare injuries to the peripheral nerves of the extremities

Andrii S. Lysak [1], Anna Y. Kyrpychova [1], Anna V. Loboda [2]

[1] Department of reconstructive microsurgery and orthopaedic surgery, Main Medical Clinical Centre of the Ministry of Internal Affairs of Ukraine, Kyiv, Ukraine

[2] Department of anesthesiology and intensive care, Main Medical Clinical Center of the Ministry of Internal Affairs of Ukraine, Kyiv, Ukraine

Received: 12 September 2025
Accepted: 03 October 2025

Address for correspondence*: Andrii S. Lysak, Department of reconstructive microsurgery and orthopaedic surgery, Main Medical Clinical Centre of the Ministry of Internal Affairs of Ukraine, Berdychivska Street, 1, Kyiv, 04116, Ukraine, e-mail: dr.andrew.lysak@gmail.com*

Objective: To develop a stage-based treatment algorithm for pain syndrome in patients with warfare injuries to the peripheral nerves of the extremities and to determine the optimal timing for surgical intervention on peripheral nerves through analysis of the literature and our own clinical data.

Materials and methods: Pain management outcomes were analyzed in 1,053 patients with peripheral nerve injuries sustained during warfare. All patients underwent clinical and ultrasonographic examination, and pain intensity was assessed using the Visual Analogue Scale (VAS). Patients were divided into two treatment groups: primary conservative treatment and primary surgical treatment. The primary conservative treatment group included 265 patients who were managed using conservative methods (pharmacotherapy, nerve hydrodissection, administration of steroid anti-inflammatory agents, platelet-rich plasma injections, or botulinum toxin). The primary surgical treatment group comprised 788 patients with warfare injuries to the peripheral nerves of the extremities who required surgical nerve repair, including patients with painful neuromas after limb amputations. Pain intensity (VAS) was reassessed at 1, 3, 6, and 12 months after treatment.

Results: Conservative treatment demonstrated satisfactory outcomes in cases of mild pain syndrome with maintained positive dynamics during the first month from treatment initiation. Surgical treatment of warfare injuries to peripheral nerves resulted in a stable and predictable effect in the majority of cases. However, in the long-term follow-up period, some patients experienced worsening of regenerative pain during skeletal muscle reinnervation. Patients with painful neuromas represented the most challenging subgroup, as pain in these cases was typically chronic and difficult to manage.

Conclusions: Patients with warfare injuries to the peripheral nerves of the extremities should undergo ultrasound examination. In the absence of nerve compression or irritation and with preserved anatomical continuity, treatment should begin with pharmacotherapy; if necessary, nerve hydrodissection or injection therapy with steroids or botulinum toxin may be performed. In cases of significant compression, nerve disruption, or lack of effect after conservative treatment within 6 weeks, surgical intervention is recommended.

Key words: *pain, nerve, warfare injury, neurolysis, nerve grafting, targeted muscle reinnervation (TMR), regenerative peripheral nerve interface (RPNI).*

The distinctive features of modern warfare, characterized by the deployment of advanced military technologies, the predominance of artillery, and the extensive use of FPV drones, determine the severity and polystructural nature of combat injuries. The rapid increase in high-energy shrapnel and blast injury significantly complicates the provision of medical care, particularly the restoration of anatomical structures and functional capacity of the limbs.

According to the Department of Statistics of the National Military Medical Clinical Center "Main Military Clinical Hospital," between February 2022 and June 2023, combat-related limb injuries accounted for approximately 69% of all injuries, of which 85% were polystructural lesions. Regarding distribution between upper and lower extremities, combat injuries of the lower limbs slightly predominated (55%). Gunshot wounds involving only soft tissues were registered in 65–68% of patients; in two-thirds of these cases, they were accompanied by tissue defects (36–38% small and medium defects; 29–31% large and extensive defects). According to our data, between April 2014 and October 2025, approximately 32% of patients were diagnosed with gunshot injuries to the peripheral nerves of the extremities.

It is known that in cases of gunshot injury to a peripheral nerve, approximately 26% of patients become

disabled due to persistent neuropathic pain and loss of limb function. Reports from the National Health Service of Ukraine indicate that more than 90,000 limb amputations were performed between 2022 and 2024, many of which may have been complicated by the development of phantom limb pain or painful neuromas. According to various authors, among traumatic limb amputations caused by combat injuries, lower limb lesions predominate, with blast injury being the most common etiological factor.

Currently, clinicians have at their disposal a wide range of modalities for pain management, including contemporary multimodal anesthesia approaches, placement of perineural catheters and anesthetic infusion pumps, as well as surgical interventions aimed at reconstructing painful neuromas or implanting neurostimulators. Despite the clinical relevance of the problem and the availability of numerous therapeutic options, there is no universally accepted comprehensive approach to the management of pain syndrome in patients with gunshot injuries to the peripheral nerves of the extremities.

Objective: To develop a stage-based treatment algorithm for pain syndrome in patients with warfare injuries to the peripheral nerves of the extremities and to determine the optimal timing for surgical intervention on peripheral nerves through analysis of the literature and our own clinical data.

Materials and methods

Study participants

The treatment outcomes of pain syndrome in 1,053 patients (1,006 men and 47 women; mean age 34.1 ± 8.2 years) with gunshot injuries to the peripheral nerves between April 2014 and October 2025 were analyzed.

The study was approved by the Bioethics Committee of the Institute of Traumatology and Orthopedics of the National Academy of Medical Sciences of Ukraine (Minutes No. 1 dated January 19, 2026). The research was conducted in accordance with the bioethical principles of the Helsinki Convention of the Council of Europe on Human Rights and Biomedicine, as well as relevant legislation of Ukraine. The patient information sheet clearly outlined all study provisions and measures aimed at ensuring patient health protection, respect for human rights, dignity, and ethical standards. Written informed consent was obtained from all participants.

Inclusion criteria

The inclusion criteria were as follows: gunshot injury to the extremities sustained between April 2014 and October 2025; gunshot injury to the peripheral nerves of the extremities; presence of pain syndrome.

Exclusion criteria

The exclusion criteria included: non-gunshot peripheral nerve injury associated with combat-related limb trauma (e.g., injuries caused by external fixation device pins or tourniquet syndromes); absence of pain syndrome; follow-up period of less than 12 months.

Study design

All patients underwent clinical and ultrasonographic examination (***Fig. 1***). When indicated, radiography or computed tomography of the affected segment was performed. Baseline pain intensity was assessed using the Visual Analogue Scale (VAS): 0 cm — no pain; 1–3 cm — mild pain, occasionally requiring additional correction and generally not interfering with daily activities; 4–6 cm — moderate pain syndrome, potentially requiring additional pharmacological management and causing some discomfort, but tolerable during daytime; 6 cm — severe persistent pain requiring continuous medical treatment, significantly reducing quality of life and, in many cases, serving as an indication for surgical intervention. Depending on diagnostic findings, patients were divided into two groups: those receiving primary conservative treatment and those undergoing primary surgical treatment. Pain intensity according to the VAS was reassessed at 1, 3, 6, and 12 months after treatment. Through telephone follow-up, treatment outcomes were obtained for 683 patients (approximately 64.9%).

The advantages and disadvantages of each treatment modality, as well as their role in the management of pain syndrome in gunshot-related peripheral nerve injuries of the extremities, were analyzed.

Group characteristics

The primary conservative treatment group comprised 265 patients (246 men and 19 women; mean age 35.2 ± 6.5 years). In this cohort, conservative pain management strategies were employed, including medications containing the active substances lornoxicam, pregabalin, and antidepressants from the class of serotonin–norepinephrine reuptake inhibitors. Ultrasound-guided nerve hydrodissection was performed in cases where fibrotic tissue surrounded the nerve but did not preclude its visualization. Additional interventions included the administration of steroidal anti-inflammatory agents, platelet-rich plasma (prepared with a predominance of anti-inflammatory factors), and botulinum toxin. In the absence of a satisfactory response to conservative therapy (40 cases; 15.1%), patients were recommended for appropriate surgical intervention.

The primary surgical treatment group included 788 patients (760 men and 28 women; mean age 33.6 ± 9.0 years):

- 732 patients (704 men and 28 women; mean age 36.2 ± 10.2 years) with gunshot injuries to the peripheral nerves of the extremities requiring surgical repair (***Fig. 2***);

- 56 patients (all men; mean age 30.9 ± 7.8 years) with post-amputation sequelae following gunshot trauma, who developed pain syndrome due to the formation of painful neuromas (***Fig. 3***).

Approximately 53.1% of gunshot-related peripheral nerve injuries were associated with a primary nerve defect and required autoneuroplasty.

Statistical analysis

Statistical analysis was performed using standard descriptive statistical methods. Continuous variables are presented as the arithmetic mean (*M*) and standard deviation (*SD*). Comparisons between baseline (pre-treatment) values and those obtained at one year were conducted using the paired t-test. A p-value < 0.05 was considered statistically significant.

This article contains some figures that are displayed in color online but in black and white in the print edition

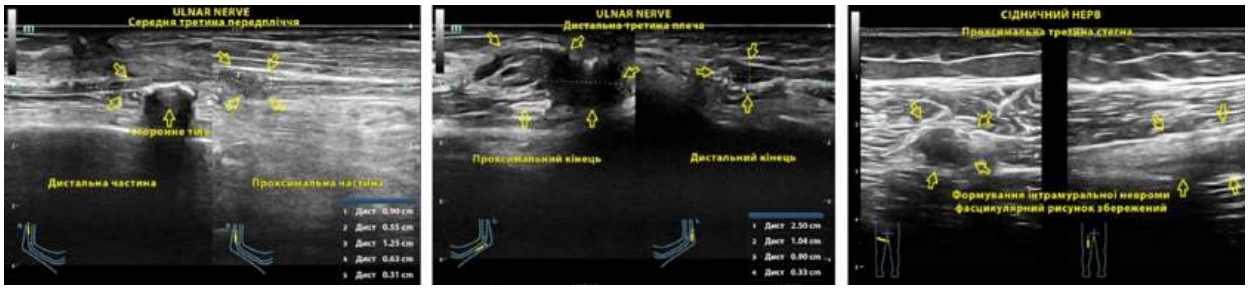

Fig. 1. Ultrasonographic patterns of various types of gunshot injuries to peripheral nerves

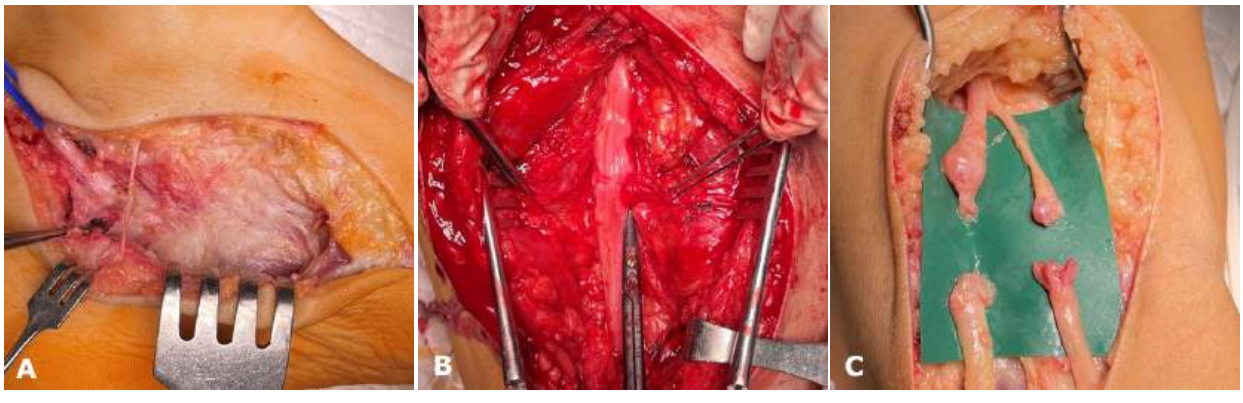

Fig.2. Principal types of gunshot injury to peripheral nerves: (a) nerve compression resulting from fibrotic degeneration of the mesoneurium;(b) formation of a fibrotic band (a zone of peripheral nerve fixation) preventing normal nerve gliding and leading to ischemia;(c) anatomical injury—complete nerve transection with a defect of the nerve tissue

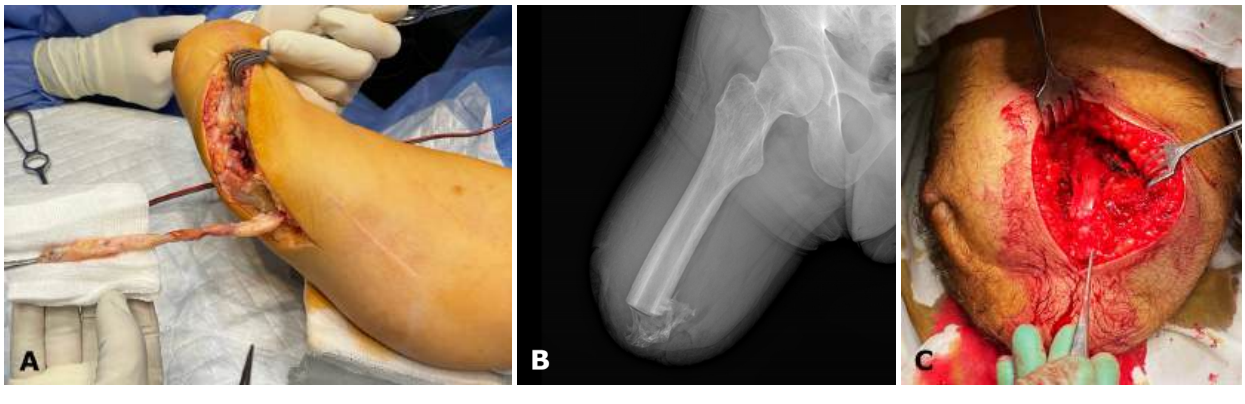

Fig. 3. Key factors contributing to the transformation of a neuroma into a painful neuroma: (a) nerve stump compression (by a ligature or fixation device); (b) nerve irritation (e.g., by a bony exostosis); (c) absence of visible irritation or compression (a possible autoimmune response cannot be excluded)

Results

In patients presenting with pain syndrome following gunshot injuries to peripheral nerves, conservative treatment was proposed as the first-line approach under the following conditions: preserved nerve continuity (according to ultrasonographic findings), absence of significant nerve compression or intraneural structural disruption, and involvement limited to superficial cutaneous branches of peripheral nerves. Management was initiated with pharmacological pain control. In the absence of clinical improvement, ultrasound-guided hydrodissection of the nerve trunk was performed (in cases of compression by fibrotically altered tissues), or injections of platelet-rich plasma (for mild pain syndrome) or a steroidal anti-inflammatory agent (for more pronounced pain syndrome) were administered. If a positive response to platelet-rich plasma or steroidal anti-inflammatory injection was observed but without substantial pain reduction, botulinum toxin injection was performed under conduction anesthesia or general sedation. In our study, platelet-rich plasma injections demonstrated only a modest positive effect.

If peripheral nerve injury was confirmed or if conservative treatment proved ineffective within 6 weeks, surgical intervention was undertaken. The procedures included peripheral nerve neurolysis (33.7% of cases), nerve suturing (10.5%, provided that tension-free approximation was feasible and adjacent joints demonstrated full passive mobility), and peripheral nerve autoneuroplasty (55.8%).

In all patients undergoing peripheral nerve surgery, lipofilling was performed using a mixture of aspirated subcutaneous adipose tissue and red bone marrow to restore the paraneural adipose cuff.

In patients with pain syndrome resulting from the formation of painful neuromas, the following surgical procedures were performed: neuroma resection with transposition of the nerve into deeper tissues (21.4% of cases); regenerative peripheral nerve interface (RPNI) creation (60.7%)—wrapping groups of fascicles of a mixed nerve with small fragments of denervated free skeletal muscle (***Fig. 4***); and targeted muscle reinnervation (TMR) (17.9%)—coaptation of the mixed nerve forming the painful neuroma to a motor nerve innervating the skeletal muscle of the residual limb (***Fig. 5***).

Neuroma resection with transposition reduced pain only during the acute postoperative period; however, recurrence of pain was observed later (up to 6 months), in some cases with increased intensity. Consequently, the majority of these patients required repeat surgical intervention.

In the postoperative period, all patients received multimodal analgesia (placement of a perineural catheter or anesthetic pump), pharmacological therapy with nonsteroidal anti-inflammatory drugs (lornoxicam), and anti-edema therapy (dexamethasone). This approach made it possible to avoid the use of opioid analgesics in the postoperative period.

Discussion

According to the data presented in ***Table 1***, pain reduction following treatment in patients with gunshot injuries to peripheral nerves was statistically significant across all treatment modalities ($p < 0.05$).

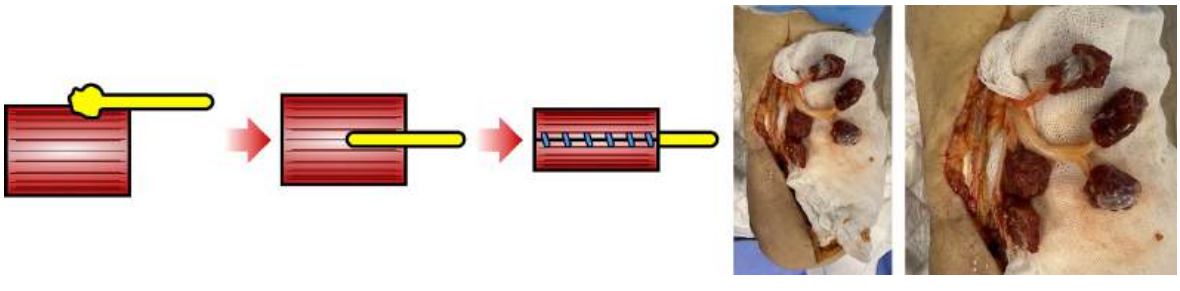

Fig. 4. Formation of a regenerative peripheral nerve interface (RPNI)

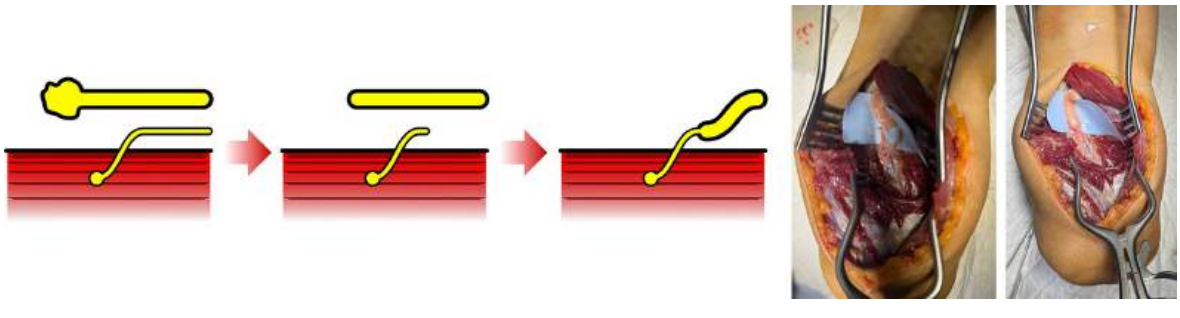

Fig. 5. Targeted muscle reinnervation (TMR)

Table 1. Assessment of pain intensity according to the VAS, depending on the treatment modality, cm

Treatment modality	Before treatment	In 1 month	In 3 months	In 6 months	In 12 months	p-value
Pharmacological therapy, n=99	2,2 ± 0,9	1,6 ± 0,8	1,2 ± 0,7	1,1 ± 0,5	1,1 ± 0,4	< 0,0001
Hydrodissection, n=29	3,9 ± 1,1	1,9 ± 0,2	1,6 ± 1,2	1,8 ± 1,3	1,9 ± 1,1	< 0,0001
Injection therapy, n=44	4,3 ± 1,3	1,1 ± 0,4	1,4 ± 1,1	1,7 ± 1,5	1,6 ± 1,9	< 0,0001
Neurolysis, n=161	5,6 ± 2,1	4,7 ± 1,5	4,2 ± 1,7	2,1 ± 1,1	1,8 ± 1,2	< 0,0001
Nerve reconstruction, n=315	4,2 ± 1,1	1,2 ± 0,6	2,1 ± 0,8	1,6 ± 1,0	2,1 ± 0,9	< 0,0001
Neuroma transposition, n=8	6,3 ± 2,1	1,1 ± 0,4	3,4 ± 2,1	4,6 ± 1,8	2,2 ± 1,5	0,0004
RPNI, n=22	6,7 ± 1,7	1,2 ± 1,4	1,4 ± 1,1	2,1 ± 1,6	2,2 ± 0,9	< 0,0001
TMR, n=7	6,2 ± 1,6	1,1 ± 0,8	1,1 ± 1,2	1,5 ± 0,6	2,1 ± 1,2	0,0003

Conservative management provided satisfactory results in cases of mild pain syndrome, particularly when a positive clinical trend was observed during the first month of treatment (***Fig. 6***). Pharmacological therapy as a standalone modality should be considered the first-line treatment in patients with mild pain intensity (up to 3 cm on the VAS) and as baseline therapy in combination with hydrodissection, injection-based interventions, or during the early postoperative period. Hydrodissection in cases of fibrotic compression of a peripheral nerve significantly alleviated pain in the early postoperative period; however, pain intensity could increase over time, necessitating repeated procedures. Injection therapy demonstrated a good analgesic effect, although gradual exacerbation of pain was observed in some cases, potentially requiring repeated injections or subsequent surgical intervention.

In our study, the use of platelet-rich plasma resulted only in modest and temporary improvement; in 8% of cases, it led to a marked increase in pain intensity, which may be attributed to differences in preparation techniques and a predominance of pro-inflammatory factors. Botulinum toxin injections produced a sustained positive effect; however, recurrence of pain was frequently observed in the long-term follow-up period.

Surgical management of gunshot injuries to peripheral nerves generally produced a stable and predictable outcome in most cases. However, in the long-term follow-up period, an increase in pain intensity may be observed due to the development of regenerative pain associated with reinnervation of skeletal muscles (***Fig. 7***).

Overall, peripheral nerve neurolysis is characterized by a progressive but gradual reduction in pain intensity over a period of up to 6 months following surgery. Peripheral nerve reconstruction (either direct nerve suturing or autoneuroplasty) may lead to a marked reduction in pain during the early postoperative period as a result of neuroma resection. Nevertheless, in the long-term period, regenerative pain originating from reinnervated muscles, as well as neuroma formation at the nerve suture site, may occur. These changes can provoke pain and paresthesia upon mechanical irritation.

The most challenging cohort for treatment comprises patients with painful neuromas, as pain associated with such neuromas is typically chronic and resistant to therapy (***Fig. 8***).

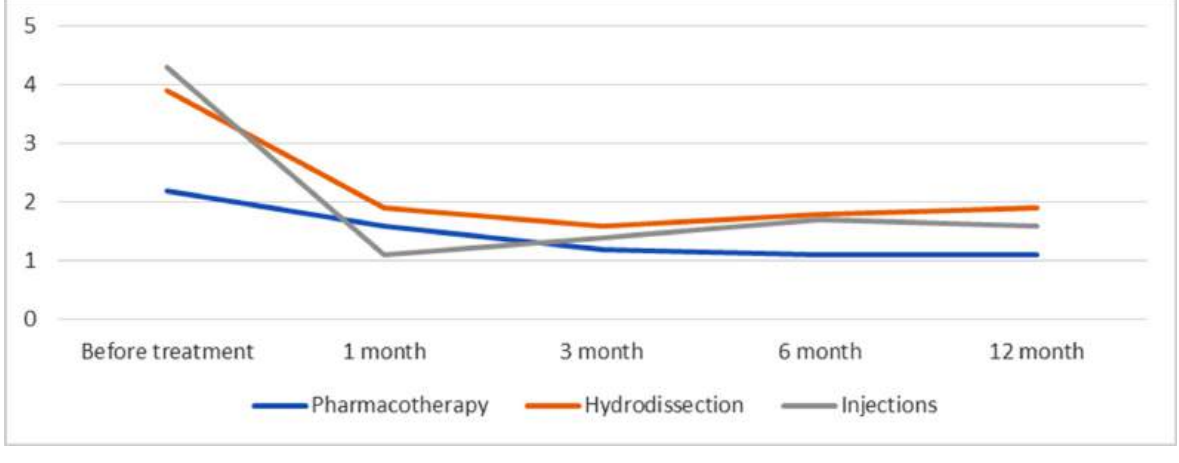

Fig. 6. Dynamics of pain intensity depending on the method of conservative treatment

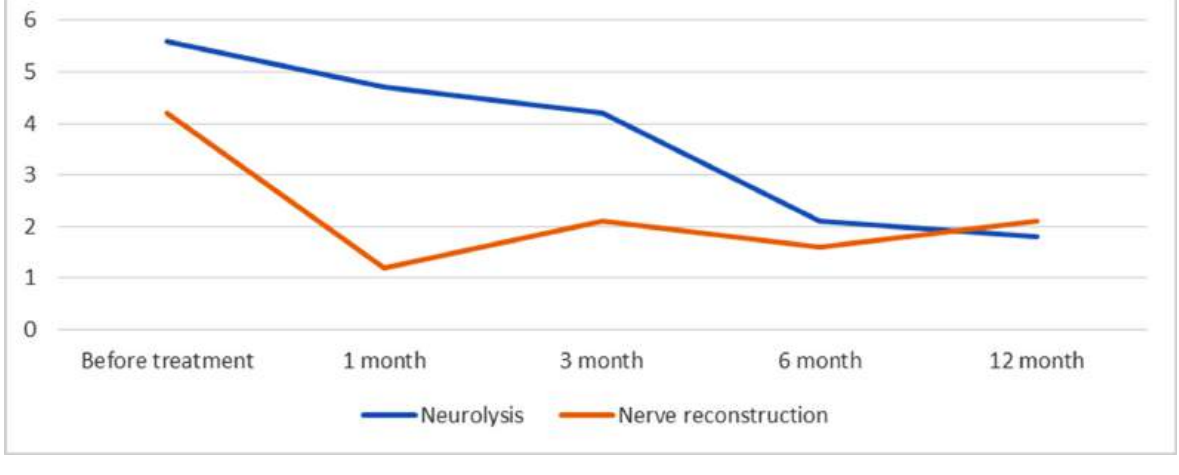

Fig. 7. Dynamics of pain intensity depending on the method of surgical treatment for gunshot injuries to peripheral nerves

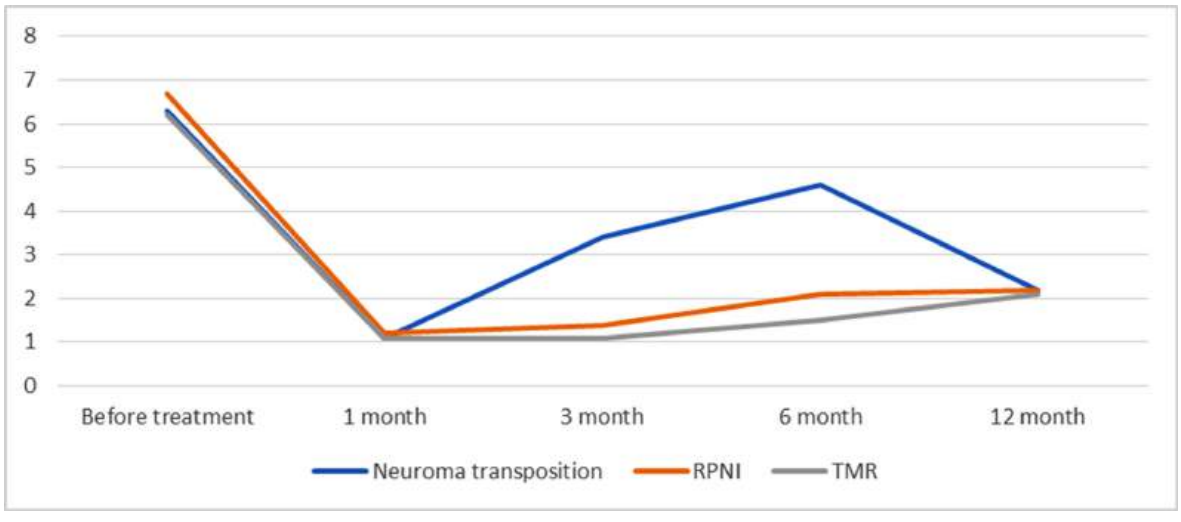

Fig. 8. Dynamics of pain intensity in painful neuromas depending on the method of surgical treatment

In recent years, there has been a global paradigm shift in the management of painful neuromas—from a passive palliative strategy involving neuroma resection or transposition (which frequently results in recurrence, even in the early postoperative period) to an active reconstructive approach, the principal objective of which is encapsulated in the concept: "provide the nerve with a target for reinnervation." In accordance with this principle, contemporary techniques such as the creation of a regenerative peripheral nerve interface and targeted muscle reinnervation have been developed. In the majority of cases (approximately 80.4%), the formation of a painful neuroma results from improperly performed limb amputation and chronic compression or irritation of the neuroma.

When discussing the concept of pain in gunshot injuries to peripheral nerves, it is essential to consider the pathophysiological mechanisms underlying the transformation of nociceptive pain—serving as a protective response to actual or potential tissue damage through stimulation of thermoreceptors, mechanoreceptors, chemoreceptors, and free nerve endings—into neuropathic pain, which is characterized by abnormal neuronal activity secondary to disease, trauma, or dysfunction of the somatosensory nervous system. Prolonged nociceptive stimulation activates both peripheral mechanisms (hyperexcitability of nerve ending membranes, ectopic synaptic discharges, and alterations in gene transcription) and central mechanisms (increased excitability of the nervous system, impaired inhibitory control of excitation, and consequent reorganization of processes and stimuli within the central nervous system). These changes may lead to sensitization of the nervous system and the development of neuropathic pain. Therefore, timely intervention aimed at reducing nociceptive stimulation following injury is crucial to prevent the formation of a neuropathic pain focus. In this context, the concept of timing and a staged therapeutic approach is of paramount importance.

Based on the analysis of our findings and the data reported in the scientific literature, we propose a staged approach to the management of pain syndrome in patients with gunshot injuries to peripheral nerves of the extremities.

Conclusions

1. All patients with gunshot injuries to peripheral nerves of the extremities or with painful neuromas following limb amputation should undergo ultrasonographic examination.

2. In the absence of objective causes of nerve compression or irritation and with preserved anatomical continuity, treatment should begin with optimization of pharmacological therapy; if necessary, hydrodissection of the nerve trunk or injection therapy with steroidal anti-inflammatory agents or botulinum toxin should be performed.

3. In the presence of an objective cause of nerve irritation, significant compression, anatomical disruption, or failure of conservative treatment within 6 weeks, surgical intervention should be recommended.

4. The application of contemporary reconstructive techniques for painful neuromas (RPNI and TMR) provides superior and more durable pain control compared with classical techniques of neuroma resection or transposition.

5. The use of multimodal anesthesia in the early postoperative period—including perineural catheter placement, administration of lornoxicam, and anti-edema therapy (dexamethasone)—makes it possible to minimize the need for opioid analgesics and contributes to interrupting the pathological mechanisms underlying the development of neuropathic pain.

Disclosure

Conflict of interest

The authors declare no conflict of interest.

Ethical approval

All procedures performed in studies involving human participants were conducted in accordance with the ethical standards of the institutional and national research committees and with the 1964 Helsinki Declaration and its later amendments or comparable ethical standards.

Informed consent

Written informed consent was obtained from each patient or a family member prior to surgery.

Funding

The study received no external financial support.

References

1. Lysak A, Gaiovych V, Strafun S, Shypunov V. Ukrainian Orthopedic Trauma Experience in Managing Wartime Injuries of the Upper Extremity. Hand Clin. 2025 Aug;41(3):373-385. doi: 10.1016/j.hcl.2025.03.012
2. Rivera JC, Glebus GP, Cho MS. Disability following combat-sustained nerve injury of the upper limb. Bone Joint J. 2014 Feb;96-B(2):254-8. doi: 10.1302/0301-620X.96B2.31798
3. Guriev S, Lysun D, Kushnir V, Satsyk S, Kurachenko I. Lower extremity amputations due to modern combat operations: clinical and anatomical aspect. TRAUMA. 2018;19(4):5-8. doi: 10.22141/1608-1706.4.19.2018.142099
4. Tsema EV, Khomenko IP, Bespalenko AA, Buryanov OA, Mishalov VG, Kikh AY. Clinico-statistical investigation of the extremity amputation level in wounded persons. Klin. Khirurhiia. 2017;10:324-31. doi: 10.26779/2522-1396.2017.10.51
5. Dones I, Levi V. Spinal Cord Stimulation for Neuropathic Pain: Current Trends and Future Applications. Brain Sci. 2018 Jul 24;8(8):138. doi: 10.3390/brainsci8080138
6. Schestatsky P, Vidor L, Winckler PB, Araújo TG, Caumo W. Promising treatments for neuropathic pain. Arq Neuropsiquiatr. 2014 Nov;72(11):881-8. doi: 10.1590/0004-282x20140157
7. Papenhoff MC, Habig K, Schmitz C, Lundin S, Schreier D, Tineghe J, Dudda M. Complex Regional Pain Syndrome (CRPS) [Complex Regional Pain Syndrome (CRPS) - State of the Art in Diagnostics and Therapy]. Z Orthop Unfall. 2023 Jun;161(3):337-352. German. doi: 10.1055/a-1898-2454
8. Malinowski MN, Jain S, Jassal N, Deer T. Spinal cord stimulation for the treatment of neuropathic pain: expert opinion and 5-year outlook. Expert Rev Med Devices. 2020 Dec;17(12):1293-1302. doi: 10.1080/17434440.2020.1801411
9. Ciaramella A. Psychopharmacology of chronic pain. Handb Clin Neurol. 2019;165:317-337. doi: 10.1016/B978-0-444-64012-3.00019-8
10. List EB, Klieverik V, Martin E, Krijgh DD, Henk Coert J. Prevalence of residual limb pain and neuromas after upper extremity amputation: a systematic review and meta-analysis. J Hand Surg Eur Vol. 2025 Dec;50(11):1440-1447. doi: 10.1177/17531934251345368
11. Morteza Bagi H, Ahmadi S, Tarighat F, Rahbarghazi R, Soleimanpour H. Interplay between exosomes and autophagy machinery in pain management: State of the art. Neurobiol Pain. 2022 Jun 9;12:100095. doi: 10.1016/j.ynpai.2022.100095
12. Issa CJ, Svientek SR, Dehdashtian A, Cederna PS, Kemp SWP. Pathophysiological and Neuroplastic Changes in Postamputation and Neuropathic Pain: Review of the Literature. Plast Reconstr Surg Glob Open. 2022 Sep 28;10(9): e4549. doi: 10.1097/GOX.0000000000004549

UA-XEFO-PUB-032026-085

Original article

Ukrainian Neurosurgical Journal. 2026;32(1):24-39
doi: 10.25305/unj.339535

Endovascular treatment of chronic subdural hematomas

Vadym A. Perepelytsia [1], Yurii V. Cherednychenko [1], Andrii Yu. Miroshnychenko [1], Andrii H. Sirko [2], Rocco A. Armonda [3,4]

[1] Endovascular Center, Mechnikov Dnipropetrovsk Regional Clinical Hospital, Dnipro, Ukraine
[2] Center of Cerebral Neurosurgery, Mechnikov Dnipropetrovsk Regional Clinical Hospital, Dnipro, Ukraine
[3] Neuro-endovascular Surgery & Neurotrauma Department, Georgetown University Hospital, Washington, D.C., USA
[4] Neuro-Critical Care Department, Washington Hospital Center, Washington, D.C., USA

Received: 17 September 2025
Accepted: 06 October 2025

Address for correspondence*:*
Vadym A. Perepelytsia, Endovascular Center, Mechnikov Dnipropetrovsk Regional Clinical Hospital, Soborna Square, 14, Dnipro, 49044, Ukraine, e-mail: neuro.perepelitsa@gmail.com

Objective: To evaluate the effectiveness of middle meningeal artery embolization (MMAe) in patients with chronic subdural hematoma (cSDH) based on the first 19 clinical cases performed at Mechnikov Dnipropetrovsk Regional Clinical Hospital. To clarify the indications for isolated versus combined treatment of cSDH and to assess the feasibility of the transradial approach.

Materials and methods: A retrospective cohort study was conducted based on the analysis of prospectively collected data from patients with chronic subdural hematomas who underwent MMAe at I.I. Mechnikov Dnipropetrovsk Regional Clinical Hospital between March 24, 2022, and November 6, 2024. The study included 19 patients who underwent endovascular intervention, either as a standalone procedure or in combination with open surgery. Demographic data, etiological factors, clinical presentation, CT, MRI, and DSA findings were analyzed. Treatment effectiveness was assessed at 1, 3, and 6 months postoperatively.

Results: According to the type of treatment, patients were divided into 3 groups: isolated MMAe — 13 patients (68.4%); primary MMAe followed by surgical drainage — 3 patients (15.8%); primary surgical evacuation followed by MMAE — 3 patients (15.8%). Traumatic cSDH was diagnosed in 12 patients (63.2%), while spontaneous cSDH occurred in 7 patients (36.8%), including two cases with mycotic aneurysms of cortical Middle Cerebral Artery (MCA) branches, which were managed with endovascular deconstructive exclusion and subsequent MMAe. One patient with chronic anemia underwent isolated MMAe. Among all patients, 5 (26.3%) were on anticoagulant/antiplatelet therapy, and hemodynamically significant carotid stenosis was identified in 3 patients (15.8%). Follow-up imaging (CT, MRI) at 6 months demonstrated clinical improvement in 100% of cases, with complete hematoma resolution in 17 patients (89.5%).

Conclusions: MMAe has proven to be highly effective and safe in the management of cSDH, both as a stand-alone method and as an adjunct to conventional surgery. The transradial approach demonstrated advantages in elderly and high-risk patients, contributing to reduced hospitalization times. Furthermore, the use of Onyx™ ensured deeper penetration and more durable occlusion of pathological vessels compared to polyvinyl alcohol (PVA) particles. These findings are consistent with current global trends and confirm the promising role of MMAe in cSDH treatment.

Keywords: *chronic subdural hematoma; middle meningeal artery embolization; Onyx™; transradial approach; endovascular neurosurgery; minimally invasive treatment; military neurotrauma*

Introduction

Chronic subdural hematoma (cSDH) is one of the most common causes of neurosurgical hospitalization among elderly patients and is characterized by a high recurrence rate following standard surgical treatment. The prevalence of cSDH ranges from 13 to 20 cases per 100,000 population, while among individuals older than 65 years it increases four- to fivefold and may exceed 70 cases per 100,000 population. By 2030, the incidence is expected to rise to 121 cases per 100,000 population, driven by population aging and the widespread use of anticoagulant therapy [1,2]. Standard surgical management (burr-hole drainage or craniotomy with evacuation) is effective; however, recurrence rates of 11–20% have been reported, and the need for repeat interventions reaches approximately 14% [1, 3]. These limitations have stimulated the search for less invasive approaches with more durable therapeutic effects.

One of the most promising strategies is endovascular embolization of the middle meningeal artery (MMA). The proposed mechanism of action involves interruption of the blood supply to the neovascularized outer membrane

of the hematoma, thereby disrupting the cycle of recurrent microhemorrhages and promoting sustained hematoma resorption. Initially described as a "last-resort" therapy for high-risk patients, accumulating evidence now supports the effectiveness of MMAe both as an adjunct to surgical drainage and as a stand-alone treatment modality [4, 5]. The evidence base has been substantially strengthened by several high-quality randomized controlled trials (RCTs) published in recent years, including studies at the New England Journal of Medicine level. In the EMBOLISE trial (>600 patients across 39 centers in the United States), the addition of MMAe to standard care significantly reduced the rate of treatment failure (defined as recurrence or persistence >10 mm, need for reintervention, or major adverse events) without increasing the risk of stroke or 30-day mortality [6]. In the Chinese MAGIC-MT RCT involving patients with non-acute subdural hematomas, the 90-day rate of symptomatic progression was comparable between MMAe and standard treatment; however, treatment efficacy was found to depend on the clinical context (surgical versus conservative management) [7]. Similarly, Fiorella et al. demonstrated a reduction in treatment failure rates with adjunctive embolization in the RCT STEM [8].

Recent consensus statements have emphasized the evolving role of MMAe in the management of cSDH. The ARISE I consensus (2024) highlighted the need for standardized indications and identified priority directions for future research [9]. A European consensus published in Brain & Spine (2024) further clarified the role of MMAe in both primary and recurrent cSDH, while the NICE Interventional Procedures Guidance IPG779 (2023) formally recognized the procedure as a promising strategy for reducing recurrence, although not as a method for immediate mass-effect relief.

A recent systematic review [23] demonstrated a low incidence of serious complications, with only isolated cases of ischemic events or cranial nerve injury, typically associated with hazardous anastomoses. Multicenter data published in 2025 [10, 21] suggest that preoperative MMAe (performed prior to burr-hole drainage) may reduce the risk of reoperation compared with postoperative embolization, although the optimal timing remains to be confirmed in prospective studies.

An expansion of indications for MMAe is currently observed, extending from recurrent and bilateral cSDH to patients receiving anticoagulant or antiplatelet therapy, as well as minimally symptomatic cases. At the same time, editorial reviews in the Journal of NeuroInterventional Surgery emphasize the need for harmonization of patient selection criteria and outcome measures in future trials [10].

In summary, cSDH remains a significant challenge in contemporary neurosurgery. MMAe has demonstrated efficacy both as an adjunct to standard surgical techniques and as an independent therapeutic option in selected patient populations. Data from recent RCTs, meta-analyses, and international consensus statements confirm its ability to reduce recurrence and reintervention rates while maintaining a favorable safety profile. Nevertheless, unresolved issues regarding optimal patient selection, choice of embolic materials, and perioperative timing underscore the need for further multicenter investigations.

Objective. To evaluate the effectiveness of MMAe in patients with chronic subdural hematoma (cSDH) based on the first 19 clinical cases treated at I.I. Mechnikov Dnipropetrovsk Regional Clinical Hospital; to clarify the indications for isolated versus combined treatment of chronic subdural hematomas and to assess the effectiveness of the transradial approach.

Materials and methods

Study participants

This study is based on an analysis of data from 19 patients with cSDH who underwent X-ray endovascular superselective MMAe between March 24, 2022, and November 6, 2024, at the Endovascular Center of the Dnipropetrovsk Regional Clinical Hospital named after I.I. Mechnikov. Before and after the procedure, the selected patients received treatment at the Cerebral Neurosurgery Center and the Vascular Neurosurgery Center of the same institution.

Written informed consent was obtained from all patients in accordance with the Declaration of Helsinki of the World Medical Association on Ethical Principles for Medical Research Involving Human Subjects (1964, as amended), European Union Directive 86/609 concerning the participation of humans in biomedical research, and Order of the Ministry of Health of Ukraine No. 690 dated September 23, 2009, as amended.

Inclusion criteria:

- patient age ≥18 years;
- presence of chronic subdural hematoma (unilateral or bilateral) confirmed by computed tomography/magnetic resonance imaging (CT/MRI);
- performance of X-ray endovascular superselective MMAe as a standalone procedure or in combination with surgical drainage;
- availability of complete clinical and neuroimaging data before treatment and during follow-up (at least 6 months);
- written informed consent to participate in the study.

Exclusion Criteria:

- patient age <18 years;
- absence of confirmed cSDH (acute or subacute subdural hematomas on CT/MRI);
- presence of other intracranial pathology determining the clinical presentation and requiring an alternative treatment strategy (tumors, acute ischemic stroke, intracerebral hemorrhage, etc.);
- incomplete preoperative or postoperative clinical neuroimaging data;
- lack of follow-up.

Group characteristics

Nineteen patients with cSDH who underwent endovascular MMAe as a standalone intervention or in combination with surgical drainage were included in the study. According to the treatment strategy, patients were divided into three groups: isolated MMAe; primary

This article contains some figures that are displayed in color online but in black and white in the print edition

MMAe followed by surgical treatment; and primary surgical treatment followed by MMAe. The mean patient age was 60.2 years, with a predominance of males. Traumatic etiology of cSDH was the most common, whereas spontaneous forms were less frequent and, in some cases, associated with concomitant vascular pathology. The groups were comparable in terms of age, sex distribution, clinical and neurological status, and baseline neuroimaging characteristics, which allowed for a valid analysis of treatment outcomes with consideration of the selected strategy.

Cranial CT was performed using an "Optima CT660" scanner (GE Healthcare, USA), MRI using a "Toshiba Excelart Vantage" 1.5-T scanner (Japan), and cerebral angiography (CAG) using an "Innova IGS 540" system (GE Healthcare, USA). For selective CAG, the contrast agents "Ultravist 370" (Germany) and "Tomohexol 350" (Ukraine) were used.

Based on CT and/or MRI, hematoma density, number of compartments, size (thickness, height, length), volume, localization, and midline shift were assessed before and after surgery. CAG was used to evaluate the presence of concomitant pathology and the anatomical features of MMA branches on the side of the cSDH.

Indications for X-ray endovascular superselective MMAe included hematoma thickness <15 mm and midline shift <5 mm in the absence of pronounced focal neurological symptoms and/or recurrent cSDH. Indications for combined surgical intervention (embolization + drainage or drainage + embolization) were hematoma thickness ≥15 mm, midline shift ≥5 mm, and the presence of focal neurological deficits [1, 3, 11].

All patients were followed postoperatively under dynamic supervision by a neurologist or family physician. Follow-up CT and MRI examinations were performed at 1, 3, and 6 months after surgery in patients with a stable neurological status.

Study design

A single-center retrospective cohort study with analysis of prospectively collected data.

Surgical technique

In all cases, the procedures were performed via a right-sided transradial approach under local anesthesia by the operating team (operator: Yu.V. Cherednychenko; assistant: V.A. Perepelytsia).

In 18 cases (94.7%), Onyx™ 18 (polymeric embolic agent; ethylene–vinyl alcohol copolymer, Medtronic, Irvine, CA, USA) was used for MMAe. In 1 case (5.3%), polyvinyl alcohol (PVA) particles, 250 *μm* (e.g., Contour™, Boston Scientific, USA), were selected as the embolic material.

All procedures were performed using a "GE Innova IGS 540" angiographic system (USA). Through a 6 Fr radial introducer, catheterization of the proximal segment of the external carotid artery on the corresponding side was achieved using a 6 Fr guiding catheter. Through the guiding catheter, a dimethyl sulfoxide–compatible microcatheter was advanced over a 0.014-inch microguidewire to catheterize the distal segments of the MMA via the maxillary artery. After superselective catheterization of the MMA and angiographic confirmation of vascularization of the cSDH capsule sources, the embolic agent was gradually injected under fluoroscopic guidance. During injection, the microcatheter was slowly repositioned proximally until complete occlusion of the pathological vascular network was achieved.

Particular attention was paid to monitoring retrograde reflux of the embolic agent to prevent its migration into non-target vascular territories through "dangerous" anastomoses with the internal carotid and ophthalmic artery systems, as well as intertympanic arterial connections. The proximal limit of embolization was defined by the origins of arterial branches arising from the proximal segment of the MMA (petrosal and cavernous branches), which anastomose with the internal carotid artery system via the inferolateral trunk and the meningohypophyseal trunk, as well as the medial branch anastomosing with the ophthalmic artery system. Therefore, for effective embolization, a distal-to-proximal embolization technique was employed, starting from the distal segments of the frontoparietal and petrosquamous branches and progressing proximally to the designated "dangerous" point. The mean procedure duration was 30 minutes.

The entire procedure was accompanied by control series of digital subtraction angiography performed at key stages of the intervention to verify catheter positioning and embolic agent distribution. Vessel catheterization and navigation were conducted using a navigation projection mode, ensuring high-precision positioning of microinstruments.

Statistical analysis

Data processing and analysis were performed using the software packages Statistica 10 (StatSoft® Inc., USA, license No. STA862D175437Q) and MedCalc v.20.218, free trial version (MedCalc SoftwareLtd.,Ostend,Belgium;https://www.medcalc.org/download.php, 2023).

Results

The mean age of patients in our study was lower compared with that reported in the literature—60.2 years [39;85]. The cohort included 12 (63.2%) men and 7 (36.8%) women.

The most common symptoms were headache (94.7%) and dizziness (84.2%). Monoparesis/hemiparesis was detected in 4 (21.1%) cases. Generalized seizures were observed in 2 (10.5%) patients, and speech disorders were identified in 2 (10.5%) cases (dysarthria in 1 patient and sensorimotor aphasia in 1 patient). Two (10.5%) patients presented with impaired consciousness (GCS-12). No asymptomatic cases of chronic subdural hematoma (cSDH) were recorded in our study.

Chronic subdural hematoma was detected by MRI in 7 (36.8%) patients and by CT in 12 (63.2%) patients; of these, 7 (36.8%) subsequently underwent additional MRI evaluation. In all cases, selective digital subtraction cerebral angiography was used for preoperative assessment. Left-sided cSDH was diagnosed in 7 (36.8%) cases, right-sided in 5 (26.3%), and bilateral cSDH in the remaining patients. The majority of hematomas (89.5%) were hemispheric, while 2 (10.5%) were localized in the frontal region. Multiloculated cSDH was identified in 4 (21.1%) cases.

According to T1-weighted brain MRI, the most common signal intensity pattern of cSDH was hyperintensity, observed in 8 (42.1%) patients. Hypointense signal was detected in 3 (15.8%) cases, and heterogeneous signal intensity was also observed in 3 (15.8%) cases.

The mean size of cSDH in our study, expressed as width/length/height, was 14.05/150.23/89.71 mm, with a mean hematoma thickness of 14.05 mm. The mean cSDH volume was 99.9 cm³ (±53 cm³). The smallest hematoma measured 3/65/58 mm with a volume of 11.3 cm³, while the largest measured 30/170/81 mm with a volume of 413.1 cm³. Hematoma thickness was <15 mm in 16 (61.5%) cases and ≥15 mm in 10 (38.5%) cases (including 7 patients with bilateral cSDH). The mean midline shift was 4.16 mm; it was <5 mm in 14 (73.7%) patients and ≥5 mm in 5 (26.3%) patients.

A traumatic etiology of cSDH was documented in 12 (63.2%) cases, including a 41-year-old serviceman who sustained an injury during active combat (clinical case No. 1). Spontaneous subdural hematomas were less frequent. Among 7 (36.8%) such cases, mycotic aneurysms of the cortical (M4) segments of the middle cerebral artery caused ipsilateral cSDH in 2 (10.5%) patients (clinical case No. 2).

In one operated patient with concomitant chronic anemia, only MMAe was performed without surgical drainage. Five (26.3%) patients were receiving antiplatelet/anticoagulant therapy, and hemodynamically significant stenosis of the major cerebral arteries was identified in 3 (15.8%) cases. No intraoperative or postoperative complications were recorded in our study.

According to the treatment modality, patients were divided into the following groups:

- MMAe — 13 (68.4%) cases;
- Primary MMAe followed by surgical drainage — 3 (15.8%) cases;
- Primary surgical treatment followed by MMAe— 3 (15.8%) cases.

Based on follow-up neuroimaging (CT/MRI) performed 6 months after intervention, all patients demonstrated positive dynamics, with complete resolution of cSDH observed in 17 (89.5%) cases.

Clinical Case No. 1

A 41-year-old male military serviceman presented to the I.I. Mechnikov Dnipropetrovsk Regional Clinical Hospital with complaints of headache and dizziness. He had sustained a traumatic brain injury during combat operations on March 9, 2024 (75 days prior to surgery).

Non-contrast brain CT revealed bilateral chronic subdural hematomas (cSDH) in the frontal regions. The hematoma dimensions (thickness/length/height) were 8/48/48 mm on the left and 9/132/51 mm on the right. No displacement of the midline structures of the brain was detected (***Fig. 1***).

For further evaluation, transradial selective digital subtraction cerebral angiography was performed. No vascular pathology was identified.

Single-session procedures were performed on May 23, 2024: bilateral X-ray endovascular MMAe using the Onyx™ embolic agent ***(Figs. 2 and 3).***

The postoperative course was uneventful. The neurological status remained unchanged, and no complications were observed. The patient was discharged from the hospital on postoperative day 2. Follow-up brain CT performed 1 month after surgery ***(Fig. 4)*** demonstrated complete resolution of bilateral frontal cSDH. At follow-up examination, regression of global cerebral symptoms was noted.

Clinical Case No. 2

A 52-year-old man presented to the I.I. Mechnikov Dnipropetrovsk Regional Clinical Hospital with complaints of headache and dizziness that had developed abruptly approximately 1.5 months earlier.

Brain MRI revealed a right-sided hemispheric chronic cSDH with dimensions (thickness/length/height) of 10/166/124 mm and a 4-mm midline shift to the left (***Fig. 5***).

Given the spontaneous onset of symptoms, further diagnostic evaluation was performed using transradial selective digital subtraction cerebral angiography. A mycotic aneurysm of the M4 segment of the right middle cerebral artery was identified (***Fig. 6***).

As a first stage, X-ray endovascular deconstructive embolization of the mycotic aneurysm of the M_4-segment of the right middle cerebral artery using detachable microcoils was performed on October 3, 2024 (***Fig. 7***).

In the same session, X-ray endovascular embolization of the right MMA using the Onyx™ embolic agent was performed on October 3, 2024 (***Fig. 8***).

The postoperative course was uneventful. Neurological status remained unchanged. No complications were observed. The patient was discharged from the hospital on postoperative day 2.

Follow-up brain MRI was performed 3 months after surgery (***Fig. 9***). Complete resolution of the chronic subdural hematoma was observed, with restoration of the normal position of the midline brain structures. On T2-weighted images, a focus of ischemic stroke was visualized in the right frontal lobe within the vascular territory of the excluded branch of the right middle cerebral artery together with the aneurysm. At follow-up examination, no focal neurological deficits were present, and headache and dizziness had resolved.

Clinical Case No. 3

A 45-year-old man presented to I.I. Mechnikov Dnipropetrovsk Regional Clinical Hospital with complaints of headache and dizziness that had been progressively worsening over the preceding 2 weeks. The medical history revealed a domestic head injury sustained on January 5, 2024 (76 days prior to surgery).

Brain MRI demonstrated a right-sided hemispheric multiloculated cSDH with dimensions (thickness/length/height) of 27/165/87 mm and a 5-mm midline shift to the left (***Fig. 10***).

For further diagnostic evaluation, the patient underwent transradial selective digital subtraction cerebral angiography. No vascular pathology was identified.

X-ray endovascular embolization of the right MMA using the Onyx™ embolic agent was performed on March 21, 2024 (***Fig. 11***).

The postoperative course was uneventful. Neurological status remained unchanged, and no complications were observed. The patient was discharged from the hospital on postoperative day 2.

Follow-up brain MRI performed 6 months after surgery (***Fig. 12***) demonstrated complete resolution of the chronic subdural hematoma with restoration of the normal position of the midline brain structures. At follow-up examination, regression of global cerebral symptoms was noted.

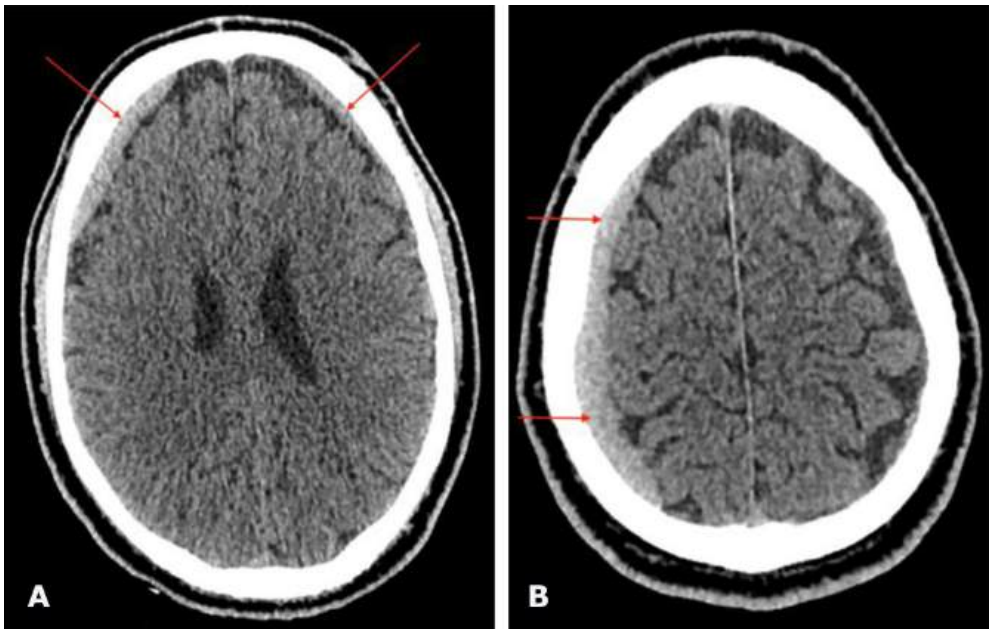

Fig. 1. Preoperative brain CT: A, B—axial projections demonstrating bilateral frontal cSDH (indicated by red arrows)

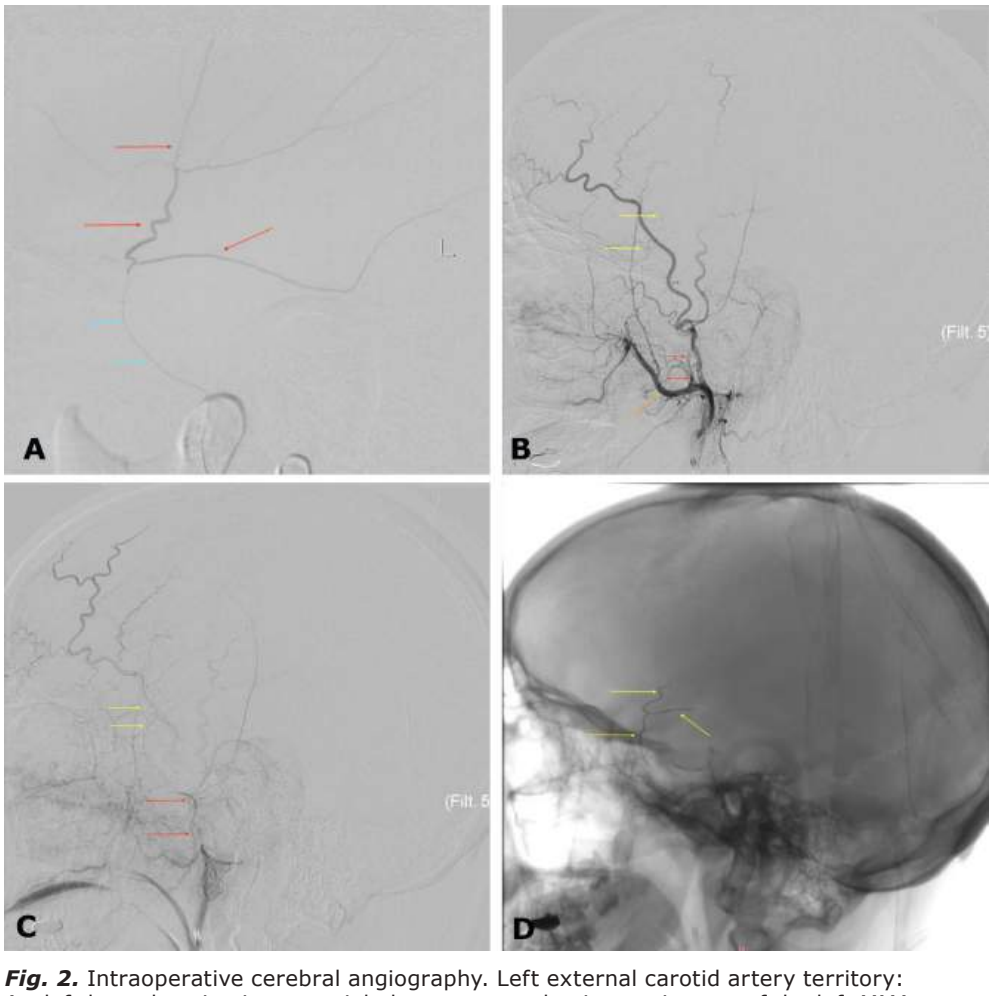

Fig. 2. Intraoperative cerebral angiography. Left external carotid artery territory: A - left lateral projection, arterial phase, superselective angiogram of the left MMA; B - left lateral projection, arterial phase, post-embolization state of the left MMA; C - left lateral projection, late arterial phase, post-embolization state of the left MMA; D - left lateral projection without digital subtraction. The left MMA and its branches are indicated by a red arrow, the left maxillary artery by an orange arrow, and the radiopaque cast of the left MMA after Onyx™ embolization by a yellow arrow

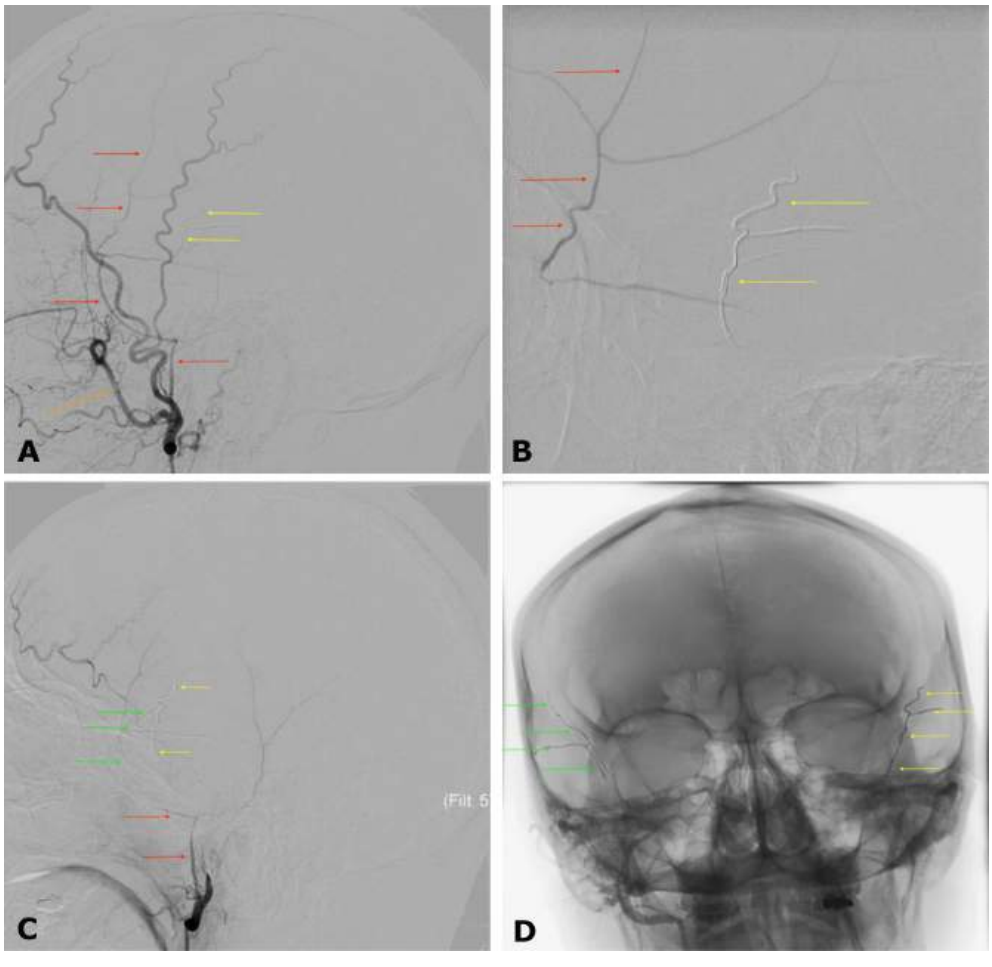

Fig. 3. Intraoperative cerebral angiography. Right external carotid artery territory: A – left lateral projection, arterial phase; B – left lateral projection, arterial phase, superselective angiogram of the right MMA; C – left lateral projection, late arterial phase, post-embolization state of the right MMA; D – anteroposterior projection without digital subtraction demonstrating the post-embolization state of both MMAs. The right MMA and its branches are indicated by a red arrow, the right maxillary artery by an orange arrow, the radiopaque cast of the right MMA after Onyx™ embolization by a green arrow, and the radiopaque cast of the left MMA after Onyx™ embolization by a yellow arrow

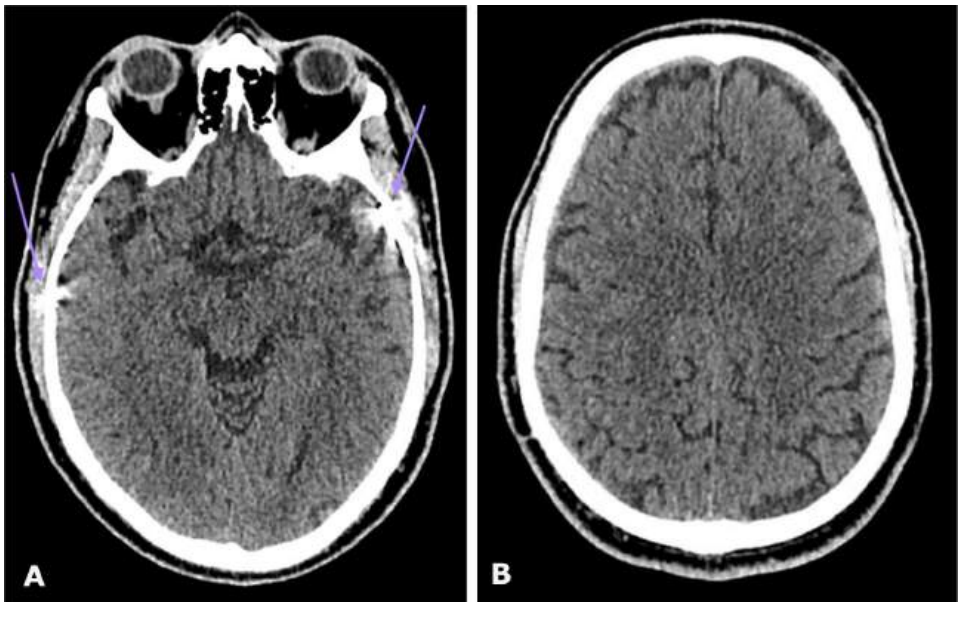

Fig. 4. Postoperative brain CT: A, B – axial projections. Purple arrows indicate the radiopaque embolic agent Onyx™ within the projections of the left and right MMAs

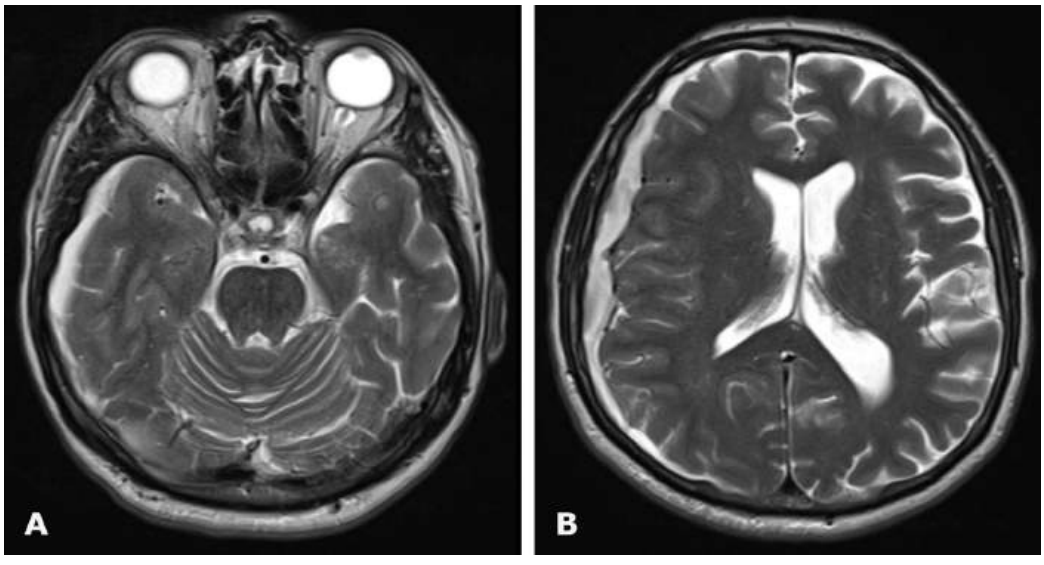

Fig. 5. Preoperative brain MRI, T2-weighted images: A, B – axial projections demonstrating a right-sided hemispheric cSDH

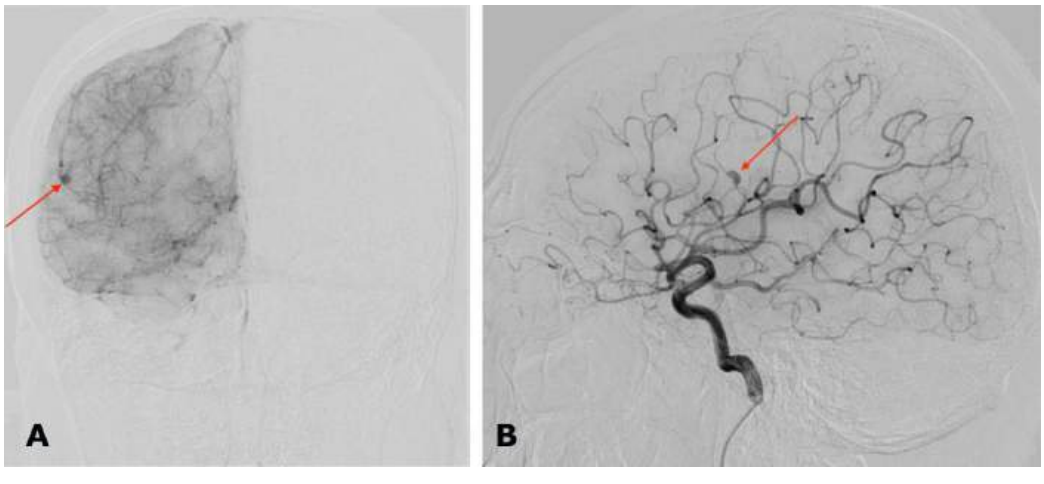

Fig. 6. Preoperative cerebral angiography. Right internal carotid artery territory: A – anteroposterior projection, late arterial phase; B – left lateral projection, arterial phase The red arrow indicates a mycotic aneurysm of the M4-segment of the right middle cerebral artery

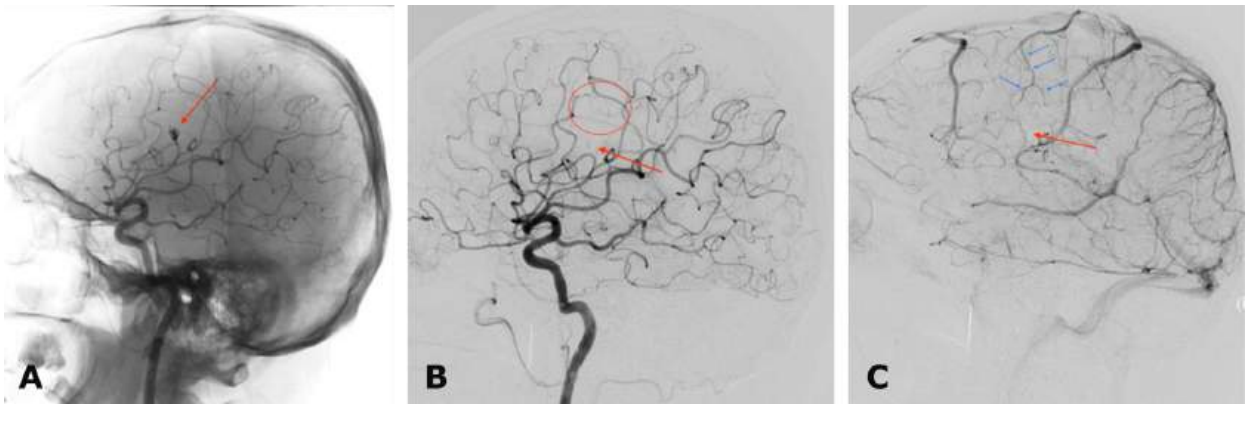

Fig. 7. Postoperative cerebral angiography. Right internal carotid artery territory: A – angiogram in the left lateral projection without digital subtraction; B – subtraction angiogram in the left lateral projection, arterial phase; C – subtraction angiogram in the left lateral projection, late arterial phase. The red arrow indicates the excluded aneurysm of the M4-segment of the right middle cerebral artery; the red circle denotes the avascular area after deconstructive exclusion of the arterial aneurysm; blue arrows indicate compensatory arterial blood flow within the territory of the excluded aneurysm

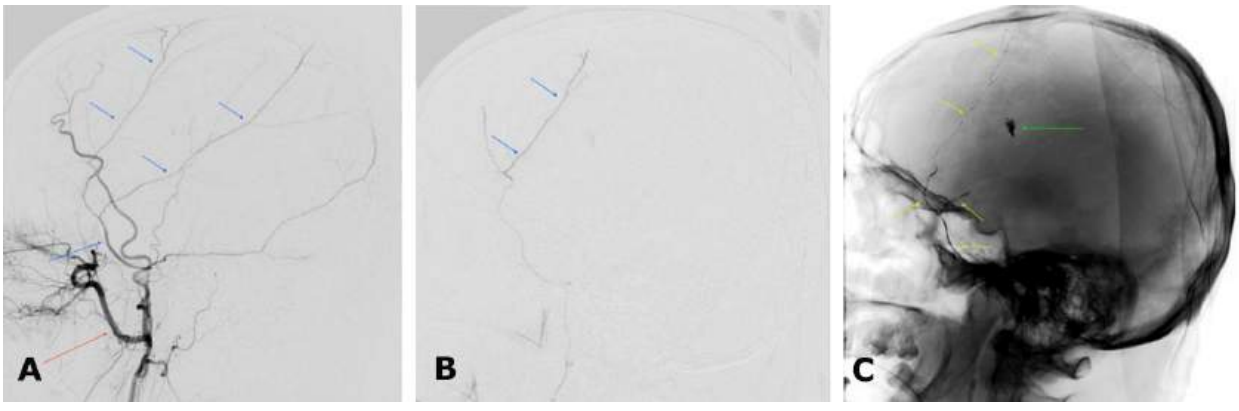

Fig. 8. Postoperative cerebral angiography. Right external carotid artery territory: A – subtraction angiogram in the left lateral projection; B – superselective subtraction angiogram of the MMA in the left lateral projection; C – angiogram in the left lateral projection without digital subtraction. The red arrow indicates the maxillary artery; blue arrows indicate the MMA and its branches; the yellow arrow denotes the contrast-enhanced embolization zone of the MMA; the green arrow indicates microcoils in the projection of the mycotic aneurysm

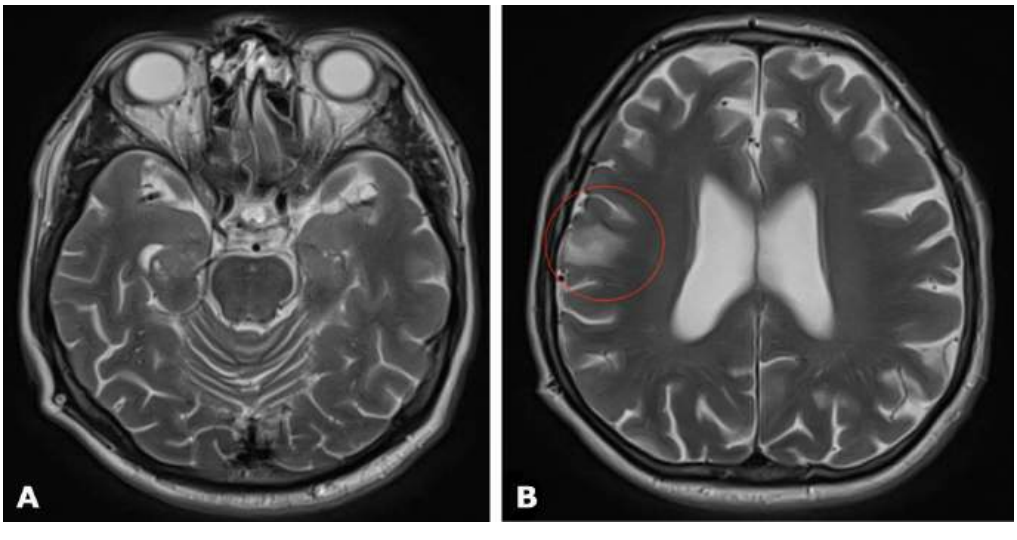

Fig. 9. Postoperative (3-months) brain MRI, T2-weighted images: A, B – axial projections. The red circle indicates a focus of ischemic stroke in the right frontal lobe measuring 19 × 13 mm

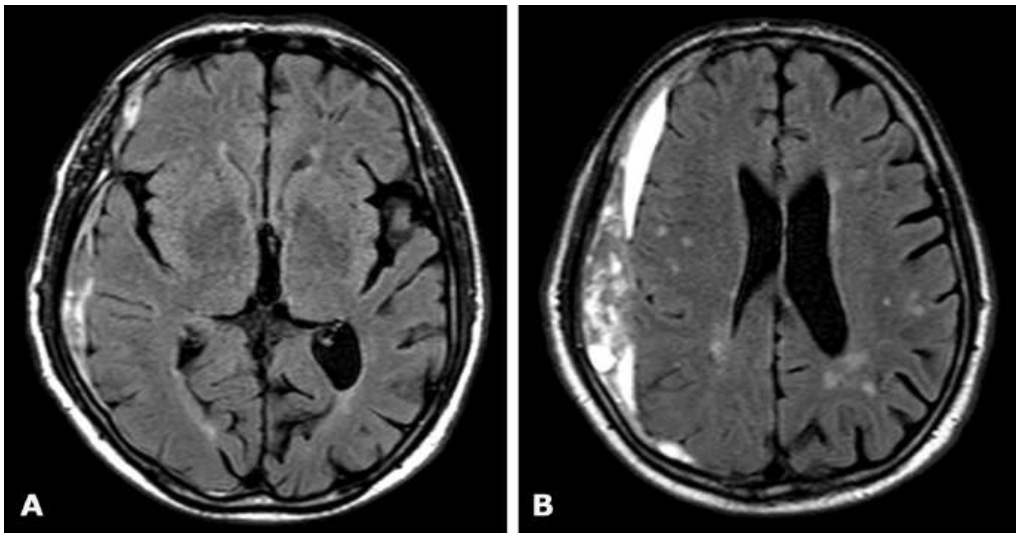

Fig. 10. Preoperative brain MRI, T2 FLAIR sequence: A, B – axial projections demonstrating a right-sided hemispheric multiloculated cSDH

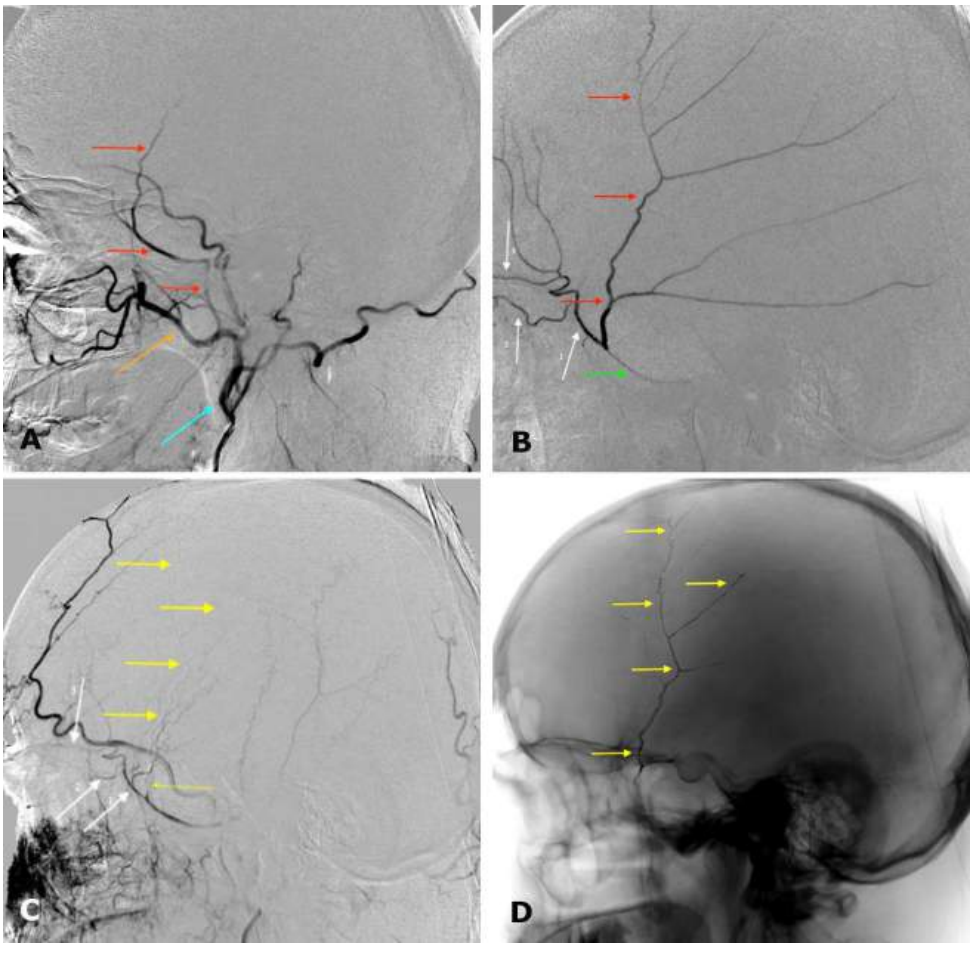

Fig. 11. Intraoperative cerebral angiography. Right external carotid artery territory: A – left lateral projection, arterial phase; B – left lateral projection, arterial phase, superselective angiogram of the right MMA; C – left lateral projection, arterial phase, post-embolization state of the right MMA; D – angiogram in the left lateral projection without digital subtraction. The right MMA and its branches are indicated by a red arrow; the right maxillary artery by an orange arrow; the right external carotid artery by a light blue arrow; the microcatheter positioned within the right MMA by a green arrow; the radiopaque cast of the right MMA after Onyx™ embolization by a yellow arrow; and the hazardous anastomotic branches of the MMA by white arrows: 1—medial; 2—sphenoidal; 3—ramus meningolacrimalis

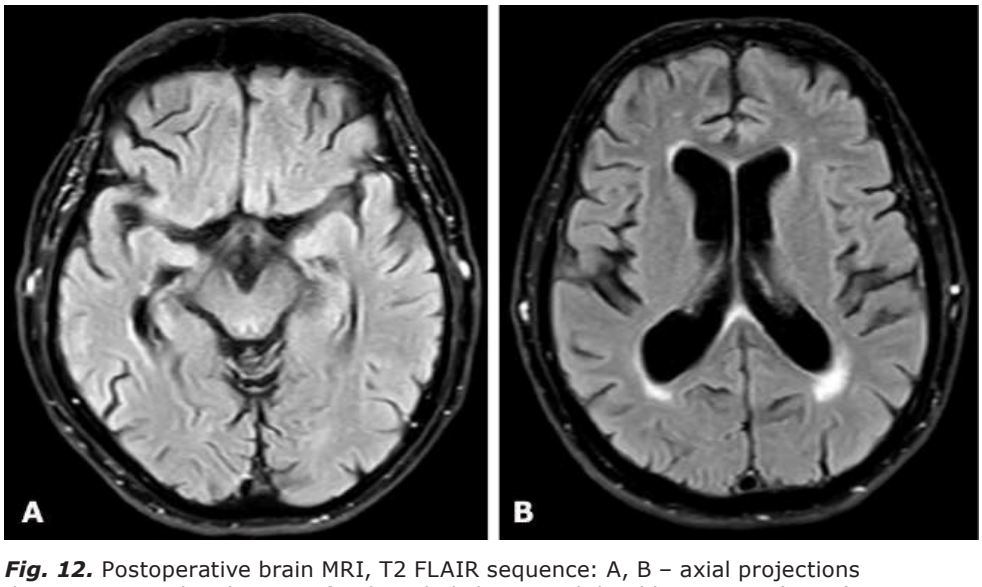

Fig. 12. Postoperative brain MRI, T2 FLAIR sequence: A, B – axial projections demonstrating the absence of right-sided chronic subdural hematoma (cSDH)

Clinical Case No. 4

A 74-year-old man was transported by an emergency medical team to the emergency and diagnostic department of I.I. Mechnikov Dnipropetrovsk Regional Clinical Hospital with depressed consciousness to the level of deep obtundation (Glasgow Coma Scale score of 12), severe right-sided hemiparesis (grade 2), and elements of sensorimotor aphasia. The medical history revealed a domestic head injury sustained on May 1, 2024 (41 days prior to surgery).

Non-contrast brain CT demonstrated a left-sided hemispheric multiloculated cSDH with dimensions (thickness/length/height) of 17/145/104 mm and an 8-mm midline shift to the right (***Fig. 13***).

Given the CT findings and the severity of the patient's condition, emergency surgery was performed for life-saving indications: osteoplastic craniotomy in the left parietal region, evacuation of the left-sided multiloculated cSDH, and inflow–outflow drainage of the left subdural space on June 11, 2024 (***Fig. 14***).

Considering the patient's comorbid condition (atrial fibrillation), for which anticoagulant therapy had been administered, X-ray endovascular embolization of the left MMA was performed on June 11, 2024, to prevent cSDH recurrence (***Fig. 15***).

The postoperative course was uneventful, with gradual improvement in neurological status. No complications were observed. The patient was discharged from the hospital on postoperative day 10.

Given the stability of the patient's condition, follow-up brain MRI was performed 6 months after surgery (***Fig. 16***). Complete resolution of the left-sided cSDH was demonstrated, indicating the absence of recurrence, along with restoration of the normal position of the midline brain structures. At follow-up examination, the patient was in satisfactory condition without focal neurological deficits.

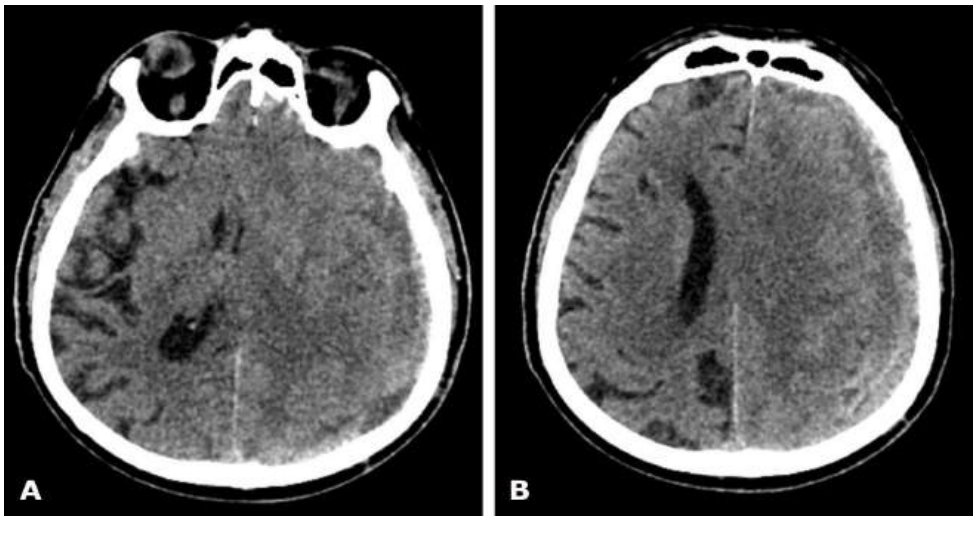

Fig. 13. Preoperative brain CT: A, B – axial projections demonstrating a left-sided hemispheric multiloculated cSDH with marked compression and edema of the left cerebral hemisphere

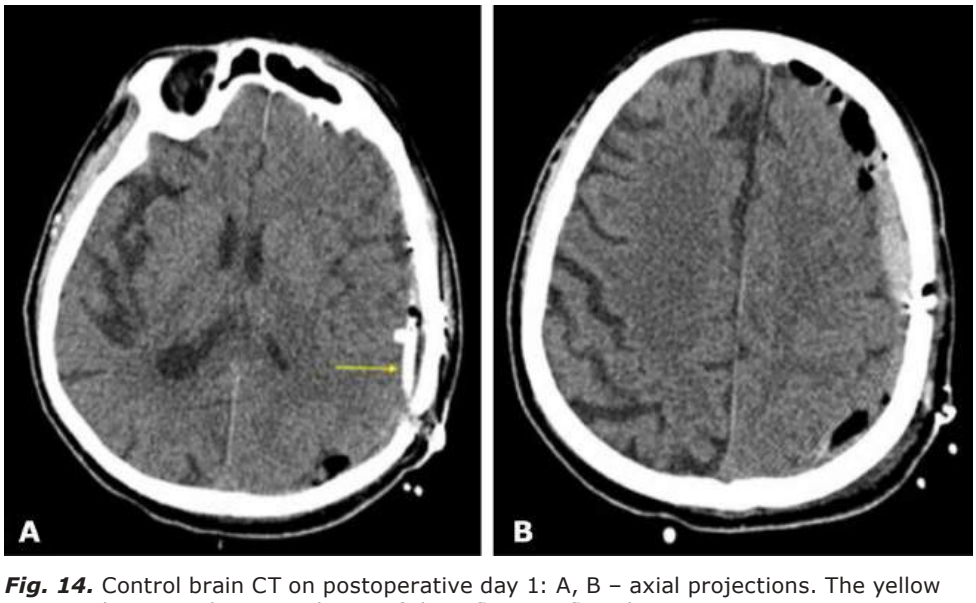

Fig. 14. Control brain CT on postoperative day 1: A, B – axial projections. The yellow arrow indicates radiopaque drains of the inflow–outflow drainage system

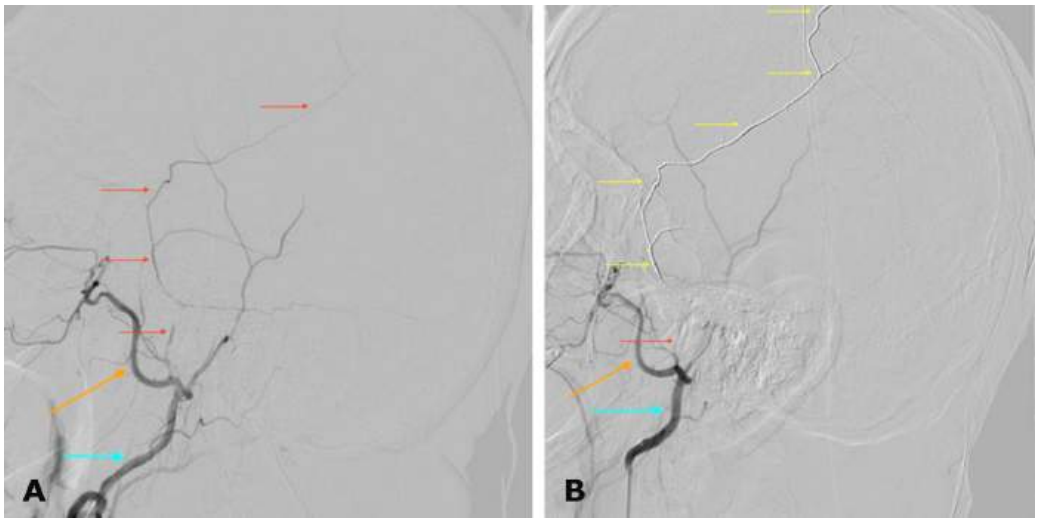

Fig. 15. Intraoperative cerebral angiography. Left external carotid artery territory: A – left lateral projection, arterial phase before MMAe; B – left lateral projection, arterial phase after MMAe. The left MMA and its branches are indicated by a red arrow; the left maxillary artery by an orange arrow; the left external carotid artery by a light blue arrow; and the radiopaque cast of the left MMA after Onyx™ embolization by a yellow arrow

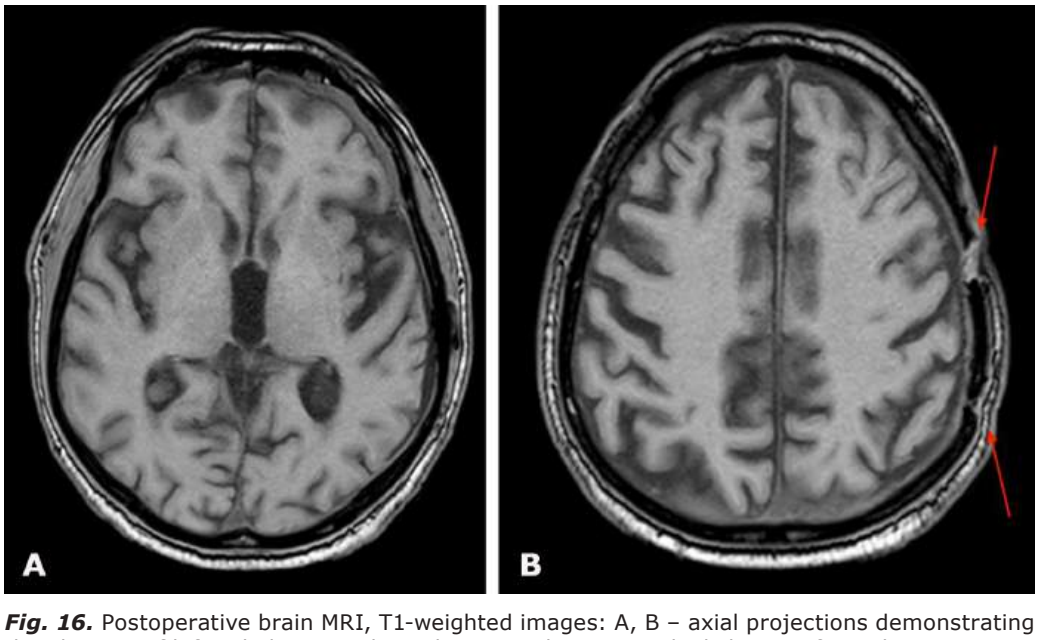

Fig. 16. Postoperative brain MRI, T1-weighted images: A, B – axial projections demonstrating the absence of left-sided cSDH. The red arrow indicates residual changes from the previous craniotomy

Discussion

There are no definitive data in the scientific literature regarding the frequency of use or the advantages of transradial versus transfemoral access for MMAe. Some authors [5,12] report that transfemoral access is used in the majority of cases, as it is considered technically convenient and has traditionally been employed in neuroendovascular interventions. In our study, however, a transradial approach was used exclusively in all patients and demonstrated a high safety profile, particularly in elderly patients or those at increased risk of hemorrhagic complications. This approach allowed a reduction in intraoperative risks and a substantial decrease in hospital length of stay. The mean duration of hospitalization was (5.1 ± 2.6) days.

In most studies [5, 13–15], polyvinyl particles (150–250 μm) were used as the primary embolic agent. This is largely explained by their significantly lower cost compared with Onyx™; moreover, in some countries Onyx™ is not available. In addition, polyvinyl embolic material has a simpler technique of use and does not require a dimethyl sulfoxide–compatible microcatheter. Therefore, in many neuroendovascular centers, polyvinyl embolization is considered the gold standard. However, more recent publications [16–18] demonstrate an increasing use of Onyx™, particularly

in complex cases or in the presence of high risk. At the Endovascular Center of I.I. Mechnikov Dnipropetrovsk Regional Clinical Hospital, Onyx™ 18 was used for MMAe in 18 patients (94.7%). Owing to its liquid form and slow polymerization, this embolic agent is capable of penetrating small and pathologically altered branches supplying the hematoma membrane, thereby providing more radical obliteration. This property is especially relevant in recurrent and/or multiloculated cSDH. In contrast to polyvinyl particles, which may migrate or be partially washed out over time, the polymer embolic agent forms a monolithic cast that maintains durable occlusion of distal meningeal arterial branches. This reduces the likelihood of distal arterial bed reperfusion via collateral flow from other meningeal arteries and, consequently, increases the effectiveness of vascular blockade of the outer layer of the cSDH capsule.

In addition, Onyx™ contains radiopaque components (tungsten or tantalum powder), allowing real-time fluoroscopic monitoring of its injection, as well as the direction of penetration or reflux. This feature is particularly important for preventing intraoperative risks associated with occlusion of "dangerous" anastomoses with the internal carotid and ophthalmic artery territories, as well as blood supply to the myelin sheaths of cranial nerves (***Figs. 11B,C and 17***).

The middle meningeal artery has numerous anastomoses with branches of the internal carotid, ophthalmic, occipital, and ascending pharyngeal arteries. Knowledge of the topography and variability of these anastomoses is crucial for the safe performance of embolization, reduction of neurological complication risk, and improvement of treatment efficacy in cSDH.

In addition to anatomically determined hazardous anastomoses, potential complications related to the access technique and the choice of embolic material should be considered. The transradial approach demonstrated greater safety compared with the transfemoral approach due to a lower risk of local complications, including pulsatile hematomas and pseudoaneurysms at the puncture site, as well as avoidance of the most dangerous complication—retroperitoneal hematoma. The use of soft neuroguidewires and small-diameter microcatheters minimizes the risk of arterial wall perforation, thereby preventing undesirable intracranial hemorrhage or hematoma formation. The use of polyvinyl alcohol particles requires larger-diameter microcatheters, which increases the likelihood of mechanical vessel injury when navigating distal segments. When working from proximal segments, the risk of non-target embolization with small polyvinyl particles increases, whereas the use of larger-diameter particles reduces procedural efficacy due to insufficient penetration into distal portions of the vascular bed.

Thus, the Ukrainian patient series not only confirms the effectiveness of the transradial approach and Onyx™ but also complements contemporary international data regarding the selection of the optimal embolic agent.

Our results are consistent with data from recent randomized trials (EMBOLISE, MAGIC-MT, STEM), which demonstrate a significant reduction in the risk of treatment failure with MMAe [4, 7, 8]. This study is unique in that it demonstrates the feasibility of widespread MMAe in a resource-limited setting, the safety of the transradial approach, and the use of Onyx™ as the primary embolic agent.

The present study is among the first in Ukraine to systematically describe the outcomes of endovascular MMAe for cSDH. The first procedure was performed on March 24, 2022. The experience of I.I. Mechnikov Dnipropetrovsk Regional Clinical Hospital demonstrates that the implementation of modern minimally invasive techniques that improve treatment efficacy and reduce recurrence rates is feasible even under wartime conditions.

Mandatory preoperative selective digital subtraction angiography of all cerebral vascular territories enabled the identification of concomitant pathologies and, in selected cases, the underlying cause of cSDH, which influenced subsequent surgical strategy.

In both patients with spontaneous subdural hematomas in whom mycotic aneurysms of the cortical (M4) segments of the middle cerebral arteries were identified, the surgical strategy included single-session embolization of the mycotic aneurysm as the first stage, followed by MMAe as the second stage. In three other cases, preoperative cerebral angiography revealed severe hemodynamically significant internal carotid artery stenoses in elderly patients. Surgical management in these patients involved a two-stage approach: MMAe as the first stage, followed 1–3 months after clinical stabilization and favorable neuroimaging findings by X-ray endovascular angioplasty with stent implantation and initiation of dual antiplatelet therapy.

Recent literature [5, 20] reports high efficacy of MMAe as a standalone treatment in patients with coagulation disorders or those receiving anticoagulant or antiplatelet therapy. In our study, no patients with overt coagulopathy were included; however, five patients with abnormal coagulation parameters (international normalized ratio >1.2, prothrombin index <90%) receiving anticoagulant or antiplatelet therapy were treated. In two of these patients, MMAe alone was performed.

In 13 patients who underwent embolization alone, the MMA met the following criteria: hematoma thickness <15 mm, midline shift <5 mm, and absence of pronounced neurological symptoms. Only one patient with a multiloculated cSDH had a hematoma thickness of 27 mm and a 5 mm midline shift, taking into account the stable clinical course of the disease (clinical case No. 3).

The group that underwent primary MMAe followed by subsequent drainage included three high-risk patients (cSDH in the setting of anticoagulant/antiplatelet therapy, hematoma thickness ≥15 mm, midline shift ≥5 mm) who nevertheless demonstrated relatively stable neurological status. In these cases, MMAe was performed initially not only to reduce the risk of recurrence but also to devascularize the hematoma capsule and to prevent intraoperative and postoperative hemorrhagic complications during the second stage of surgical treatment.

In three patients, surgical evacuation of cSDH was performed as the first stage for vital indications. Two of these patients had large multiloculated hematomas (thickness >15 mm) with midline shift >5 mm and pronounced focal neurological deficits (clinical case No. 4). The third patient was a military serviceman with a

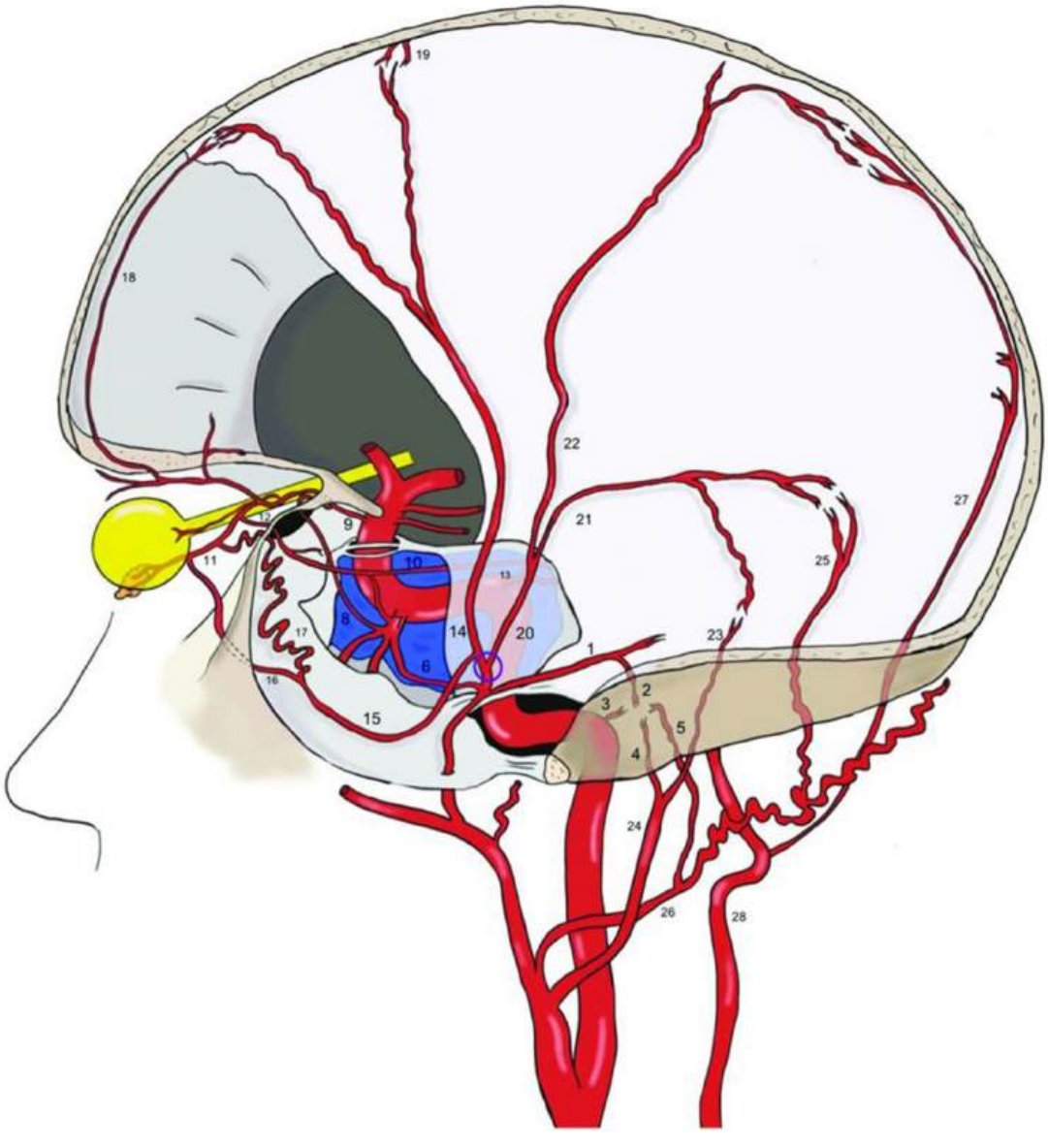

Fig. 17. Schematic illustration of MMA anastomoses [19]. Before its bifurcation (marked by a purple circle), the petrosal branch (1), from which the superior tympanic artery (2) arises, anastomoses within the middle ear with the caroticotympanic artery (3, from the internal carotid artery), as well as with the inferior tympanic artery (4, from the ascending pharyngeal artery) and the posterior tympanic artery (5, from the occipital artery). On the opposite side, the cavernous branch of the MMA (6) anastomoses with the inferolateral trunk (7) and the meningohypophyseal trunk (13). The inferolateral trunk is connected to the ophthalmic artery (9) via its deep recurrent branch (8). The inferolateral trunk, the MMA, and the ophthalmic artery are also interconnected through the marginal tentorial artery (10), whose origin may vary: from the lacrimal artery (11), via the superficial recurrent branch of the ophthalmic artery (12), or from the meningohypophyseal trunk (13). After bifurcation of the MMA in the pterional region, its frontal branch (14) gives rise to a medial branch (15), which may intracranially divide into the meningolacrimal branch (ramus meningolacrimalis) (16) and the medial sphenoidal artery (17). Both branches connect with the lacrimal artery, although the meningolacrimal artery arises more distally than the sphenoidal branch. Anastomoses with the ophthalmic artery and the inferolateral trunk are the most dangerous during transcatheter MMAe due to the risk of embolization of these arteries. The frontal branch of the MMA reaches the convexity surface along the coronal suture and anastomoses with the anterior falcine artery (18, a branch of the ophthalmic artery—the anterior ethmoidal artery) and with branches of the contralateral MMA (19). The posterior branch of the MMA (20) divides into the petrosquamous branch (21) and the parieto-occipital branch (22). The former anastomoses with the jugular branch (23) of the ascending pharyngeal artery (24) and with the mastoid branch (25) of the occipital artery (26). The latter is connected with the posterior meningeal artery (27), arising from the vertebral artery (28) in the border zones

history of blast injury sustained in 2015 and recurrent cSDH, which had been surgically evacuated twice (in 2015 and 2022). During the most recent recurrence in 2024, MMAe was performed after surgical evacuation of the hematoma (23 May 2024). One-year follow-up revealed no recurrence.

Significant limitations of our study include the small sample size (19 patients), which limits statistical power; the single-center and prospective design, which may reduce the level of evidence and limit the generalizability of the findings. Another limitation is the absence of a control group for comparison of MMAe with conventional surgical treatment modalities, which precludes definitive conclusions regarding the superiority of this strategy over "classical" approaches.

The follow-up period was up to 6 months, which, although consistent with current follow-up protocols [3], does not exclude the possibility of late recurrences. In addition, we predominantly used a single embolic agent—Onyx™ 18—thus precluding comparison with polyvinyl particles, which are considered standard in many international series [13, 14].

The economic aspect of Onyx™ use was not sufficiently addressed in our study. This represents an important consideration for healthcare systems, particularly in resource-limited settings, where polyvinyl embolic agents are often used as a cost-effective alternative.

The obtained results confirm the effectiveness and safety of MMAe; however, they require further validation. Prospective multicenter studies with larger patient cohorts are necessary to confirm these findings and enable their extrapolation to different clinical populations.

A second research direction involves comparison of Onyx™ (polymeric embolic agent) and polyvinyl particles as embolization materials in terms of efficacy, complication profiles, and cost-effectiveness, which would allow the development of optimal clinical recommendations.

A third important area is the investigation of long-term outcomes (>12 months), including recurrence rates, cognitive outcomes, and quality of life after treatment.

Current evidence suggests that preoperative MMAe may reduce the risk of repeat interventions as well as intraoperative and postoperative complications, particularly in patients at high risk of bleeding. However, most available data are derived from retrospective cohort studies; therefore, randomized controlled trials are required to compare preoperative and postoperative embolization using standardized endpoints (recurrence, reintervention, quality of life, and cognitive outcomes) [8, 21].

A major challenge remains the lack of unified patient selection criteria. The interdisciplinary ARISE I consensus proposed the creation of registries and the standardization of core outcomes for research. Future studies should separately analyze patients with primary and recurrent cSDH and identify high-risk subgroups, including patients receiving anticoagulant or antiplatelet therapy and those with marked frailty [9, 22]. Particular attention should be paid to antithrombotic management. Patients receiving anticoagulant or antiplatelet therapy represent a complex population in whom the balance between bleeding risk and thromboembolic complications is critical. Available data suggest that MMAe allows for earlier and safer resumption of antithrombotic therapy; however, prospective studies are needed to confirm the safety of early reinstatement of anticoagulant/antiplatelet treatment [8, 23].

Patient-centered outcomes should be a major focus of contemporary research. These include not only recurrence and reoperation rates but also restoration of autonomy, cognitive function, rehospitalization rates, and quality of life. Such metrics are increasingly being incorporated into the latest multidisciplinary guidelines, reflecting a global trend in modern neurosurgery [8,24].

Further development of this field in Ukraine should include the establishment of national clinical protocols adapted to the realities of the domestic healthcare system. A separate research direction may involve analysis of the role of MMAe in the treatment of neurotrauma resulting from military actions, which is particularly relevant under current conditions.

Our results are consistent with contemporary literature, confirming that MMAe may be considered an effective alternative or adjunct to traditional surgical treatment. This topic remains highly relevant in modern neurosurgery, as optimal management strategies for cSDH, including the role of MMAe, continue to be actively debated. Despite the encouraging results of our study, confirmation in larger patient cohorts is required to draw definitive conclusions. Further investigation will enable the development of clear clinical algorithms and improve treatment effectiveness. We are actively working in this direction and plan to continue our research to expand the scientific evidence base.

The authors express their sincere gratitude to Professor Rocco Armonda for his long-standing support and humanitarian assistance, including the provision of microinstruments, Onyx™ embolization material, and microcoils, which made it possible to implement modern endovascular treatment techniques at I.I. Mechnikov Dnipropetrovsk Regional Clinical Hospital. This support enabled the treatment of both military personnel with combat-related injuries and civilian patients with severe neurosurgical conditions.

Special thanks are extended to the organization Razom for Ukraine for its substantial assistance in supplying the hospital with essential consumables required for high-technology interventions. Collaboration with international colleagues and charitable organizations is an extremely important factor in the development of neurosurgery in Ukraine, particularly in the context of full-scale war.

We believe that such initiatives contribute not only to the advancement of clinical practice but also to the integration of Ukrainian neurosurgery into the global medical community, creating a foundation for further scientific research and the implementation of innovative treatment methods.

Conclusions

1. MMA embolization is an effective and safe treatment modality for cSDH: favorable clinical and radiological outcomes were observed in all patients, with complete hematoma resolution achieved in 89.5% at 6-month follow-up. No intraoperative or postoperative complications were recorded in the cohort of 19 patients.

2. The transradial approach demonstrated a high safety profile, particularly in elderly patients, and contributed to reduced length of hospital stay. Patients receiving antiplatelet and/or anticoagulant therapy were also treated successfully without an increased risk of recurrence or complications.

3. The embolic agent Onyx™ 18 demonstrated advantages over polyvinyl particles due to deeper penetration and sustained occlusion of pathological vessels.

4. Combined treatment strategies (MMA embolization followed by drainage or vice versa) were effective in complex cases (hematoma thickness >15 mm, multiloculated hematomas, midline shift >5 mm). MMA embolization may be used as a standalone treatment in cases of small hematomas without significant mass effect or pronounced neurological deficits.

5. Preoperative selective digital subtraction CAG enabled the detection of concomitant vascular pathology (mycotic aneurysms, stenosis of major cerebral arteries), which directly influenced treatment strategy.

6. The presented clinical cases (combat-related trauma, mycotic aneurysm, recurrent cSDH) demonstrate the versatility and adaptability of the technique, and the obtained results are consistent with contemporary international studies (Levitt, 2024; Fiorella, 2025; Gajjar, 2025; Papageorgiou, 2025), confirming global trends in the management of cSDH.

Disclosure

Conflict of Interest

The authors declare no conflicts of interest.

Ethical Approval

All procedures involving human participants were conducted in accordance with the ethical standards of the institutional and national research committees and with the 1964 Declaration of Helsinki and its later amendments or comparable ethical standards.

Informed Consent

Written informed consent was obtained from each patient or a legally authorized representative prior to the procedure.

Funding

This research received no external funding.

References

1. Findlay MC, Holdaway M, Gautam D, Bauer SZ, Gandhoke G, Grandhi R. Cost-minimizing thresholds and recurrence rates in surgical evacuation with adjunctive middle meningeal artery embolization versus evacuation alone. J Neurosurg. 2024 Dec 13;142(5):1457-1464. doi: 10.3171/2024.7.JNS24200
2. Mureb MC, Kondziolka D, Shapiro M, Raz E, Nossek E, Haynes J, Farkas J, Riina HA, Tanweer O. DynaCT Enhancement of Subdural Membranes After Middle Meningeal Artery Embolization: Insights into Pathophysiology. World Neurosurg. 2020 Jul;139:e265-e270. doi: 10.1016/j.wneu.2020.03.188
3. Papageorgiou NM, Palaiodimou L, Melanis K, Theodorou A, Stefanou MI, Tsalouchidou PE, Vlotinou P, Stavrinou LC, Boviatsis E, Magoufis G, Themistocleous M, Sarraj A, Sharma VK, Goyal N, Tsivgoulis G. Embolization of Middle Meningeal Artery in Patients with Chronic Subdural Hematoma: A Systematic Review and Meta-Analysis of Randomized-Controlled Clinical Trials. J Clin Med. 2025 Apr 22;14(9):2862. doi: 10.3390/jcm14092862
4. Levitt MR, Hirsch JA, Chen M. Middle meningeal artery embolization for chronic subdural hematoma: an effective treatment with a bright future. J Neurointerv Surg. 2024 Mar 14;16(4):329-330. doi: 10.1136/jnis-2024-021602
5. Rai AT, Link PS, Lakhani DA. Rising tide of middle meningeal artery embolization for chronic subdural hematomas: current volumes and future growth compared with cerebral aneurysm and stroke interventions. J Neurointerv Surg. 2025 Feb 25:jnis-2025-023109. doi: 10.1136/jnis-2025-023109
6. Davies JM, Knopman J, Mokin M, Hassan AE, Harbaugh RE, Khalessi A, Fiehler J, Gross BA, Grandhi R, Tarpley J, Sivakumar W. Adjunctive middle meningeal artery embolization for subdural hematoma. New England Journal of Medicine. 2024 Nov 21;391(20):1890-900. doi: 10.1056/nejmoa2313472
7. Liu J, Ni W, Zuo Q, Yang H, Peng Y, Lin Z, Li Z, Wang J, Zhen Y, Luo J, Lin Y, Chen J, Hua X, Lu H, Zhong M, Liu M, Zhang J, Wang Y, Wan J, Li Y, Li T, Mao G, Zhao W, Gao L, Li C, Chen E, Cheng X, Zhang P, Wang Z, Chen L, Zhang Y, Tian B, Shen F, Lei Y, Wu Y, Li Y, Duan G, Xu L, Lv N, Yu J, Xu X, Du Z, Zhang H, Hu J, Li Z, Yuan Q, Zhou Y, Wu G, Zhang L, Gao C, Dai D, Wu X, Zhang Y, Jiang H, Zhao R, Su J, Xu Y, Ospel JM, Majoie CBLM, Goyal M, Li Q, Yang P, Gu Y, Mao Y; MAGIC-MT Investigators. Middle Meningeal Artery Embolization for Nonacute Subdural Hematoma. N Engl J Med. 2024 Nov 21;391(20):1901-1912. doi: 10.1056/NEJMoa2401201
8. Fiorella D, Monteith SJ, Hanel R, Atchie B, Boo S, McTaggart RA, Zauner A, Tjoumakaris S, Barbier C, Benitez R, Spelle L, Pierot L, Hirsch JA, Froehler M, Arthur AS; STEM Investigators. Embolization of the Middle Meningeal Artery for Chronic Subdural Hematoma. N Engl J Med. 2025 Feb 27;392(9):855-864. doi: 10.1056/NEJMoa2409845
9. Kan P, Fiorella D, Dabus G, Samaniego EA, Lanzino G, Siddiqui AH, Chen H, Khalessi AA, Pereira VM, Fifi JT, Bain MD, Colby GP, Wakhloo AK, Arthur AS; ARISE I Academic Industry Roundtable. ARISE I Consensus Statement on the Management of Chronic Subdural Hematoma. Stroke. 2024 May;55(5):1438-1448. doi: 10.1161/STROKEAHA.123.044129
10. Gajjar AA, Naqvi A, Chen JY, Custozzo A, Boulos AS, Dalfino JC, Field NC, Paul AR. 2024 middle meningeal artery embolization trials: A comprehensive review of past, recent, and ongoing trials. Interv Neuroradiol. 2025 Apr 4:15910199251329970. doi: 10.1177/15910199251329970
11. Sila D, Casnati FL, Vojtková M, Kirsch P, Rath S, Charvát F. Middle Meningeal Artery Embolization versus Surgery in Patients with Chronic Subdural Hematoma-No More Fence Sitting? Neurol Int. 2023 Dec 6;15(4):1480-1488. doi: 10.3390/neurolint15040096
12. Wang Y, Zhou Y, Cui G, Xiong H, Wang DL. Transradial versus transfemoral access for posterior circulation endovascular intervention: A systematic review and meta-analysis. Clin Neurol Neurosurg. 2023 Nov;234:108006. doi: 10.1016/j.clineuro.2023.108006
13. Ban SP, Hwang G, Byoun HS, Kim T, Lee SU, Bang JS, Han JH, Kim CY, Kwon OK, Oh CW. Middle Meningeal Artery Embolization for Chronic Subdural Hematoma. Radiology. 2018 Mar;286(3):992-999. doi: 10.1148/radiol.2017170053
14. Mishra R, Deora H, Florez-Perdomo WA, Moscote-Salazar LR, Garcia-Ballestas E, Rahman MM, Shrivastava A, Raj S, Chavda V, Montemurro N, Agrawal A. Clinical and Radiological Characteristics for Recurrence of Chronic Subdural Hematoma: A Systematic Review and Meta-Analysis. Neurol Int. 2022 Aug 26;14(3):683-695. doi: 10.3390/neurolint14030057
15. Abdollahifard S, Farrokhi A, Yousefi O, Valibeygi A, Azami P, Mowla A. Particle embolic agents for embolization of middle meningeal artery in the treatment of chronic subdural hematoma: A systematic review and meta-analysis. Interv Neuroradiol. 2024 Feb;30(1):94-104. doi: 10.1177/15910199221125977
16. Ellens NR, Schartz D, Kohli G, Rahmani R, Akkipeddi SMK, Mattingly TK, Bhalla T, Bender MT. Safety and efficacy comparison of embolic agents for middle meningeal artery embolization for chronic subdural hematoma. J Cerebrovasc Endovasc Neurosurg. 2024 Mar;26(1):11-22. doi: 10.7461/jcen.2023.E2023.04.002
17. Sioutas GS, Vivanco-Suarez J, Shekhtman O, Matache

IM, Salem MM, Burkhardt JK, Srinivasan VM, Jankowitz BT. Liquid embolic agents for middle meningeal artery embolization in chronic subdural hematoma: Institutional experience with systematic review and meta-analysis. Interv Neuroradiol. 2023 Jun 15:15910199231183132. doi: 10.1177/15910199231183132

18. Shehabeldin M, Amllay A, Jabre R, Chen CJ, Schunemann V, Herial NA, Gooch MR, Mackenzie L, Choe H, Tjoumakaris S, Rosenwasser RH, Jabbour P, Kozak O. Onyx Versus Particles for Middle Meningeal Artery Embolization in Chronic Subdural Hematoma. Neurosurgery. 2023 May 1;92(5):979-985. doi: 10.1227/neu.0000000000002307
19. Bonasia S, Smajda S, Ciccio G, Robert T. Middle Meningeal Artery: Anatomy and Variations. AJNR Am J Neuroradiol. 2020 Oct;41(10):1777-1785. doi: 10.3174/ajnr.A6739
20. Hamou HA, Clusmann H, Schulz JB, Wiesmann M, Altiok E, Höllig A. Chronic Subdural Hematoma. Dtsch Arztebl Int. 2022 Mar 25;119(12):208-213. doi: 10.3238/arztebl.m2022.0144
21. Sioutas GS, Salem MM, Kuybu O, Salih M, Khalife J, Carroll K, Duckworth EA, Vaishnav D, Essibayi MA, Hoang AN, Baker CM, Mendez Ruiz AA, Abecassis Z, Salah WK, Ruiz Rodriguez JF, Charcos I, Cortez GM, Narayanan S, Haim O, Tanweer O, Hanel R, Kan P, Tonetti DA, Nogueira RG, Jovin TG, Altschul DJ, Lang MJ, Srinivasan VM, Jankowitz BT, Thomas AJ, Levitt MR, Ogilvy CS, Gross BA, Burkhardt JK, Grandhi R. Order and Timing of Middle Meningeal Artery Embolization as a Perioperative Adjunct to Surgical Evacuation for Chronic Subdural Hematomas: A Multicenter Study. Radiology. 2025 Apr;315(1):e241571. doi: 10.1148/radiol.241571
22. Bartek J, Biondi A, Bonhomme V, Castellan L, Catapano G, Cenzato M, Di Nuzzo G, De Robertis E, Giordano F, Iaccarino C, Kulcsar Z, Möhlenbruch MA, Raabe A, Rickard F, Romero CS, Schubert T, D S, Sicignano C, Muto M. Multidisciplinary consensus-based statement on the current role of middle meningeal artery embolization (MMAE) in chronic SubDural hematoma (cSDH). Brain Spine. 2024 Nov 19;4:104143. doi: 10.1016/j.bas.2024.104143
23. Shafi M, Badikol SR, Gerstl JVE, Nawabi NLA, Sukumaran M, Kappel AD, Feroze AH, Smith TR, Mekary RA, Aziz-Sultan MA. Complications of Middle Meningeal Artery Embolization: A Systematic Review and Meta-Analysis. World Neurosurg. 2025 Feb;194:123541. doi: 10.1016/j.wneu.2024.11.124
24. Stubbs DJ, Davies BM, Edlmann E, Ansari A, Bashford TH, Braude P, Bulters DO, Camp SJ, Carr G, Coles JP, de Monteverde-Robb D, Dhesi J, Dinsmore J, Evans NR, Foster E, Fox E, Froom I, Gillespie C, Gray N, Grieve K, Hartley P, Lecky F, Kolias A, Jeeves J, Joannides A, Minett T, Moppett I, Nathanson MH, Newcombe VFJ, Outtrim JG, Owen N, Petermann L, Ralhan S, Shipway D, Sinha R, Thomas W, Whitfield PC, Wilson SR, Zolnourian A, Dixon-Woods M, Menon DK, Hutchinson PJ; Improving Care In Elderly Neurosurgery Initiative (ICENI) Working Group. Clinical practice guidelines for the care of patients with a chronic subdural haematoma: multidisciplinary recommendations from presentation to recovery. Br J Neurosurg. 2024 Nov 11:1-10. doi: 10.1080/02688697.2024.2413445
25. National Institute for Health and Care Excellence (UK). IPG 779. Middle meningeal artery embolisation for chronic subdural haematomas. Interventional procedures guidance. 2023 December 14. https://www.nice.org.uk/guidance/ipg779?utm_source=chatgpt.com
26. Carpenter A, Rock M, Dowlati E, Miller C, Mai JC, Liu AH, Armonda RA, Felbaum DR. Middle meningeal artery embolization with subdural evacuating port system for primary management of chronic subdural hematomas. Neurosurg Rev. 2022 Feb;45(1):439-449. doi: 10.1007/s10143-021-01553-x

Original article

Ukrainian Neurosurgical Journal. 2026;32(1):40-51
doi: 10.25305/unj.339584

Transforaminal lumbar interbody fusion in spondylolisthesis: a prospective evaluation of clinical, radiological, and functional outcomes in a Central Indian cohort

Neeraj Prasad [1], Manish Kumar Nirala [2], Manisha Gupta [3], Abhishek Kumar [4]

[1] Department of Neurosurgery, Government Superspeciality Hospital, Chhattisgarh Institute of Medical Science, Koni, Bilaspur, India
[2] Department of Neurosurgery, Artemis Hospital, Gurgoan, India
[3] Department of Neurology, Government Superspeciality Hospital, Chhattisgarh Institute of Medical Science, Koni, Bilaspur, India
[4] *Department of Cardiology, Government Superspeciality Hospital, Chhattisgarh Institute of Medical Science, Koni, Bilaspur, India*

Received: 24 September 2025
Accepted: 06 October 2025

Address for correspondence: *Dr Neeraj Prasad, Assistant Professor, Department of Neurosurgery, Superspeciality Hospital, Koni, Bilaspur, Chhattisgarh, 495009, India, email: neeraj12prasad12@gmail.com*

Background: Spondylolisthesis, or anterior vertebral displacement, is a complex spinal disorder characterized by diverse symptoms and various treatment approaches. Transforaminal Lumbar Interbody Fusion (TLIF) is increasingly preferred over Posterior Lumbar Interbody Fusion (PLIF); however regional data in India are limited.

Objective: This prospective study evaluated clinical, radiological, and functional outcomes after TLIF in lumbar spondylolisthesis patients treated at a tertiary center in central India.

Methods: Fifty adult patients with Grade II–IV lumbar spondylolisthesis underwent TLIF. Assessments included pain (Visual Analogue Scale, VAS), disability (Oswestry Disability Index, ODI), neurological status, slip angle correction, fusion rates, and complications pre- and postoperatively. Statistical significance was set at $p < 0.05$.

Results: Locations L4–L5 (56%) and L5–S1 (44%) were the affected levels. The mean preoperative VAS and ODI scores were 7.4±1.0 and 74±10%. At 6 months follow-up, VAS decreased by 71.6% to 2.1, and ODI by 88% to 9.5% ($p < 0.001$). Neurological recovery included full motor deficit resolution and 92% sensory improvement. The mean slip angle correction was 14.6±5.3°, and the fusion success rate was 92%. Complications were minimal, including 4% wound infection and 4% transient neurological deficits, with no implant failures.

Conclusion: TLIF shows excellent short-term results, offering substantial pain relief, functional and neurological recovery, and high fusion rates in Indian patients with moderate-to-severe spondylolisthesis. Further studies with larger sample sizes and longer follow-up periods are warranted to validate these findings.

Keywords: *spondylolisthesis; spinal instability; TLIF; ODI; VAS*

Introduction

Spondylolisthesis, characterized by the anterior displacement of a vertebra over the one beneath it, is a common spinal pathology with complex etiology and management considerations. Often resulting from spondylolysis, its classifications—such as that proposed by Marchetti and Bartolozzi—distinguish developmental from acquired forms, helping to understand its natural history, risk of progression, and treatment implications [1].

The widely used Meyerding classification grades severity by measuring the degree of vertebral slippage on lateral radiographs, guiding clinical decision-making [1]. Although it is readily identified on imaging, there remains considerable uncertainty about its pathogenesis and optimal treatment. Its prevalence ranges from 5–6% in the general population to as high as 12% among adolescents engaged in vigorous physical activity such as gymnastics and weightlifting, emphasizing mechanical stress as a key factor [2]. Genetic predisposition is also significant, with familial clustering rates ranging from 27% to 69%, as well as associations with congenital anomalies, such as sacral spina bifida, affecting up to 42% of cases [3].

The most frequently involved segments are L4 and L5, vital for lumbo-sacral stability and load-bearing. Long-term follow-up studies indicate that spondylolisthesis is often benign; however, progression with neurological deficits and chronic pain may occur, correlating with higher Meyerding grades, disc degeneration, and sacral morphology.

Diagnostic accuracy has improved with modalities including oblique radiographs, which reveal the classic "Scotty dog" sign, computed tomography (CT) and single-photon emission computed tomography (SPECT) scans, which enhance the detection of pars interarticularis defects, and MRI, which assesses neural compression and soft tissue damage [4].

Clinically, pain patterns vary by age, with postural and gait abnormalities more common in children due to hamstring tightness, while whereas adults often present with back pain and sciatica, frequently dominated by neurogenic claudication.

Advances in imaging—particularly MRI and dynamic radiographs—have enhanced the evaluation of segmental instability, a critical factor in guiding treatment decisions.

The North American Spine Society (NASS) promotes "advancing spine evidence synthesis" through a rigorous, multidisciplinary approach to developing evidence-based clinical guidelines [5]. The guidelines conclude that low back pain should be diagnosed mainly using patient history and physical examination, with advanced tests reserved for severe or suspicious cases. First-line treatment should focus on non-pharmacological approaches such as exercise and education, while medications or interventions should only be used when clearly needed, with careful consideration of risks and benefits. Individualized care is emphasized to improve patient outcomes and avoid unnecessary interventions. More recently, integration of artificial intelligence in diagnostic imaging has further enhanced sensitivity and accuracy [6].

Despite clear surgical indications in selected patients, controversies persist concerning the optimal surgical technique. Among available techniques, Transforaminal Lumbar Interbody Fusion (TLIF) has gained prominence as the preferred surgical approach, owing to its ability to provide circumferential fusion through a unilateral posterior corridor while minimizing dural and neural retraction, perioperative blood loss, and procedure duration compared to Posterior Lumbar Interbody Fusion (PLIF) [7]. It achieves better restoration of disc height, indirect foraminal decompression, and sagittal alignment correction [7].

Advances in TLIF—particularly with the advent of minimally invasive and expandable cage technologies—have improved fusion rates, functional recovery, and reduced perioperative morbidity [7]. However, there is a paucity of prospective, region-specific data in countries like India, where epidemiological patterns, patient comorbidities, and healthcare accessibility differ significantly from those in Western cohorts. This gap hampers evidence-based surgical planning and decision-making tailored to local needs.

The current study addresses this by systematically correlating clinicoradiological features with outcomes following TLIF, aiming to generate robust evidence for optimizing surgical management in the Indian context, particularly within the tribal belt of central India. Such research is crucial for improving patient-centered outcomes, informing shared decision-making, and enabling efficient allocation of healthcare resources against a backdrop of increasing disability due to spondylolisthesis worldwide.

Materials and methods

Study design and setting

This prospective, observational, single-institution study was conducted in the Department of Neurosurgery at a tertiary care center located in the tribal belt of central India. The study duration was one year. The study protocol was reviewed and approved by the Institutional Ethics Committee. Written informed consent was obtained from all participants or their legal guardians before their inclusion in the study. The study adhered to the ethical principles outlined in the Declaration of Helsinki (2013 revision), ensuring respect for patient rights, safety, and well-being throughout the research process [8].

Inclusion criteria

All consecutive adult patients presenting with lower back pain suggestive of spinal instability were screened. Patients demonstrating both clinical features and radiological evidence of lumbar spondylolisthesis were prospectively enrolled. Patients were included if they met the following criteria:

1. Adults aged ≥18 years.
2. Presentation compatible with clinical features such as chronic low back pain with or without radiculopathy, neurogenic claudication, restricted lumbar spine mobility or segmental instability, neurological deficits including weakness, sensory impairment, or altered reflexes, and positive findings on instability or stretching tests such as the straight leg raising test, femoral stretch test, or instability catch sign.
3. Radiologically confirmed lumbar spondylolisthesis identified on standing lumbosacral X-rays (anteroposterior, lateral, flexion–extension views) and/or lumbar MRI.
4. Single-level spondylolisthesis was included.

Exclusion criteria

Patients were excluded under the following conditions:

1. Presence of scoliosis, abnormal lordosis, or congenital deformities other than spondylolisthesis.
2. Prolapsed intervertebral disc (PIVD) without evidence of spondylolisthesis.
3. Inflammatory spinal disorders (e.g., rheumatoid arthritis, ankylosing spondylitis, seronegative spondyloarthropathies).
4. Patients with previous lumbar spine surgery.
5. Active or recent spinal infections (tuberculous spondylitis, bacterial spondylodiscitis).
6. Spinal tumors or secondary metastatic disease.
7. Severe systemic comorbidities precluding surgery, such as uncontrolled diabetes mellitus, advanced cardiac disease, severe pulmonary compromise, or coagulopathy.
8. Pregnant or lactating women.
9. Patients unwilling or unable to provide informed consent or comply with scheduled follow-up visits.

Preoperative evaluation and data collection

For all included patients, detailed demographic data—including age, sex, residence, occupational history, and contact details—were systematically recorded. A comprehensive medical history was obtained, focusing on presenting symptoms, duration of illness, prior treatments, comorbidities, and both personal and family history. Clinical evaluation involved a thorough general physical examination and detailed neurological assessment, with attention to motor power, sensory perception, reflexes, gait, and spinal flexibility; findings such as instability, radiculopathy, and neurogenic claudication were specifically documented. Preoperative baseline laboratory investigations comprised complete blood count, renal and liver function tests, fasting

This article contains some figures that are displayed in color online but in black and white in the print edition.

or random blood sugar, serum electrolytes, calcium, rheumatoid factor, and C-reactive protein. The following radiological investigations were performed on a need basis:

- Plain X-rays (lumbosacral spine): Standing anteroposterior, lateral, oblique, and flexion–extension views were used to assess alignment, slip degree, slip angle, dynamic instability, scoliosis, and sagittal balance.

- Computed Tomography (CT) (when indicated): Used selectively for detailed bony anatomy in cases of high-grade slips or complex anomalies.

- Magnetic Resonance Imaging (MRI): Performed for all patients to evaluate neural compression, degree of canal stenosis, foraminal narrowing, facet joint morphology, disc degeneration, juxtafacet cysts, and ligamentum flavum hypertrophy. Signal changes on T2-weighted images were noted to assess neural element compromise and loss of cerebrospinal fluid (CSF) signal.

Key spinopelvic parameters include pelvic incidence (PI), pelvic tilt (PT), sacral slope (SS), and lumbar lordosis (LL). These are essential for assessing sagittal balance and spinal alignment [9]. PI, typically ranging from 30° to 80° (average 50°–55°), reflects pelvic anatomy and remains stable post-skeletal maturity; abnormal values may indicate structural imbalances. PT, generally between 10° and 15° (range 5° to 30°), measures pelvic orientation; elevated PT is often seen in spinal deformities. SS assesses the sacrum's inclination, normally 30° to 50°, with deviations indicating potential mechanical issues. LL, the inward curvature of the lower back, usually spans 40°–60° but can range from 20° to 80°; hypo- or hyper lordosis may be related to various pathologies (***Fig. 1***). Abnormalities in these parameters are associated with spinal malalignment, pain risk, and degenerative conditions.

Surgical intervention

Each patient underwent a thorough pre-anesthetic evaluation and fitness assessment. All patients in the study underwent open TLIF surgery. Additionally, reduction was performed in all high-grade spondylolisthesis cases to restore alignment. Operative steps included a midline posterior incision with subperiosteal exposure of the relevant spinal levels, followed by decompression of neural elements through laminotomy and foraminotomy as needed. The intervertebral disc space was then prepared with thorough disc removal, after which interbody fusion was performed using appropriately sized cages combined with autologous or local bone graft. Pedicle screw fixation with rods was employed to achieve spinal stabilization (***Fig. 2***). Adequate hemostasis was achieved, and the wound was closed in layers, with the placement of a suction drain as indicated. Intraoperative parameters, including blood loss, duration of surgery, complications, and the level of fusion, were carefully documented.

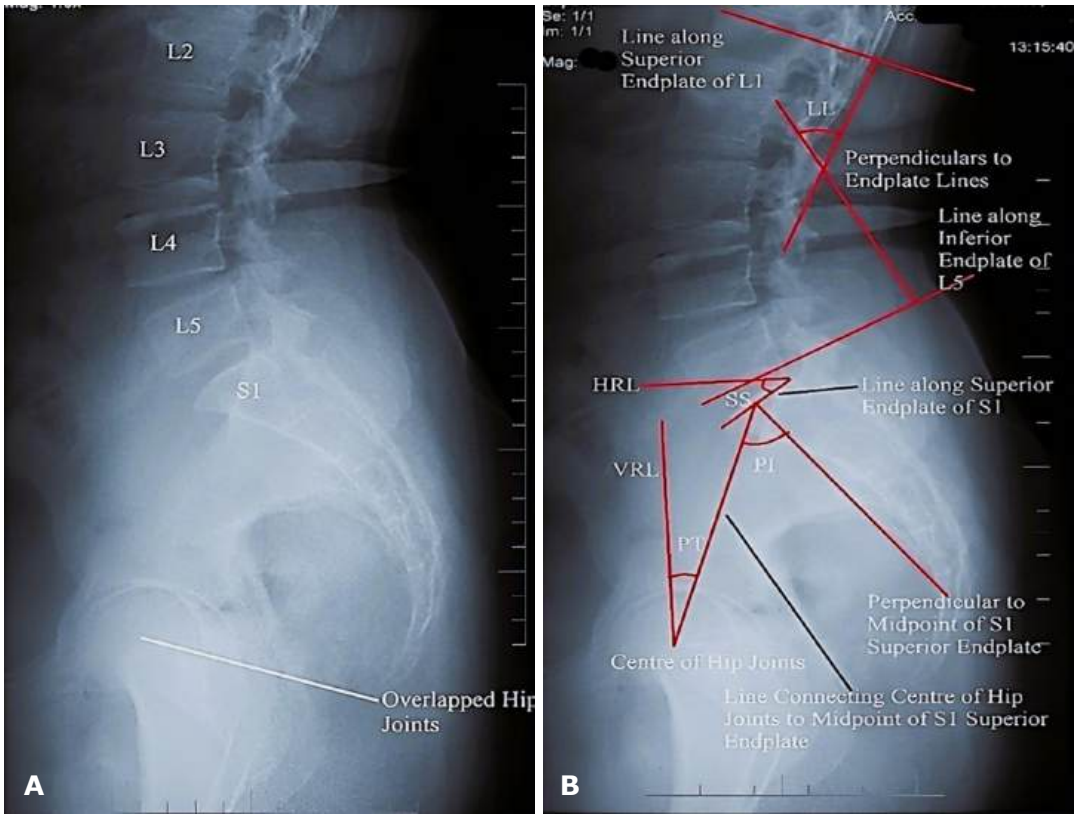

Fig. 1. Standing lateral radiograph of lumbosacral spine. Panel (A): Native image showing vertebral levels (L2–S1) and overlapped hip joints. Panel (B): Same image annotated to demonstrate measurement techniques for spinopelvic parameters. Red lines indicate the superior endplate of L1, the inferior endplate of L5, and the superior endplate of S1. Perpendiculars to endplate lines are shown to illustrate lumbar lordosis (LL), sacral slope (SS), pelvic incidence (PI), pelvic tilt (PT), and vertical reference line (VRL).

Fig. 2. A case study of grade 4 spondylolisthesis. Panel A – MRI of the lumbosacral spine (T2-weighted sagittal images) demonstrates lumbar spondylolisthesis with associated prolapsed intervertebral disc at the L4-L5 level. Panel B – Intraoperative photograph displaying laminotomy (solid white arrow) and placement of a pedicle screw rod construct (solid white star). Panel C – Plain X-rays of the lumbosacral spine (AP and lateral views, preoperative images) show loss of alignment due to spondylolisthesis. Panel D – Postoperative plain X-rays (AP and lateral views) illustrate the pedicle screws, rods, and interbody cage in situ, confirming realignment and stabilization

Postoperative care and follow-up

Patients were mobilized early with lumbar support. Postoperative radiographs were performed to confirm implant placement (***Fig. 2***). Analgesia, physiotherapy, and gradual rehabilitation were provided. Patients were discharged after achieving ambulation with adequate pain relief. Follow-up evaluations were carried out at 1 month, 3 months, and 6 months. Both outpatient visits and telephonic consultations were utilized when in-person visits were not possible.

Outcome measures

Primary outcome measures included postoperative pain, assessed using VAS; functional disability, evaluated with ODI; neurological recovery encompassing motor strength, sensory function, and reflexes; and the average duration of hospital stay [10]. Secondary outcome measures comprised radiographic assessment of vertebral displacement correction, measurement of slip angle reduction, and evaluation of surgical complications, including wound infections, implant-related issues, and any neurological deterioration.

Data analysis

All collected data were entered into a structured database and analyzed using SPSS version 26.0. Continuous variables were expressed as mean±standard deviation (SD), while categorical variables were presented as frequencies and percentages. Paired *t*-tests were used to compare preoperative and postoperative continuous variables, such as VAS and ODI scores. Chi-square tests were employed for the analysis of categorical data. A *p*-value of less than 0.05 was considered statistically significant.

Results

The demographics and baseline characteristics of the study population are shown in (***Table 1***).

The study cohort comprised 50 patients with a mean age of 58±6.9 years (range 41–83), including 44% males and 56% females. The average BMI was 25.4±3.2 (22.5–31.1), with 72% of participants engaging in mixed occupational activity and 28% being sedentary. Comorbidities included hypertension (32%), diabetes (24%), and cardiovascular disease (20%). The mean duration of symptoms was 5.2±1.1 months. Pain was predominantly radicular (72%), with 48% reporting mechanical pain. Prior conservative treatments were physiotherapy (52%), medications (100%), and injections (36%). Lumbar levels L4–L5 and L5–S1 were affected in 56% and 44% respectively. No patients had Grade I spondylolisthesis; 52% had Grade II, 28% Grade III, and 20% Grade IV. In the study population, isthmic spondylolisthesis accounted for 62% (31 cases), whereas degenerative spondylolisthesis comprised 38% (19 cases). Preoperative VAS averaged 7.4±1.0, and ODI was 54±12%. Baseline neurological deficits were noted in 8% of patients as motor and in all patients as sensory. Imaging revealed canal stenosis in 28%, foraminal stenosis in 76%, and facet arthropathy in 12%. Dynamic X-rays showed instability in 92% of patients. The surgical and radiographic outcomes of the study are shown in (***Table 2***).

Table 1. Patient demographics and baseline characteristics (n=50) of the study population

Characteristic	Value / Number (%)	Range / Mean±SD
Age (years)	–	58±6.9 (41–83)
Gender (male/female)	22 (44%) / 28 (56%)	–
Body Mass Index (BMI)	–	25.4±3.2 (22.5–31.1)
Occupational status	Mixed: 36 (72%) Sedentary: 14 (28%)	–
Comorbidities	Hypertension: 16 (32%) Diabetes: 12 (24%) CVD: 10 (20%)	–
Duration of symptoms (months)	–	5.2±1.1 (1–9)
Pain characteristics	Mechanical: 24 (48%) Radicular: 36 (72%)	–
Previous conservative treatment	Physiotherapy: 26 (52%) Medications: 50 (100%) Injections: 18 (36%)	–
Spine levels affected	L4–L5: 28 (56%) L5–S1: 22 (44%)	–
Grade of spondylolisthesis (Meyerding)	Grade I: 0 (0%) Grade II: 26 (52%) Grade III: 14 (28%) Grade IV: 10 (20%)	–
Types of spondylolisthesis	Isthmic: 31 (62%) Degenerative: 19 (38%) Dysplastic: 0 (0%)	
Preoperative VAS score	–	7.4±1.0 (6–9)
Preoperative ODI (%)	–	54±12 (40–80)
Baseline neurological deficit	Motor: 24(8%) Sensory: 50 (100%)	–
Imaging findings	Canal stenosis: 14 (28%) Foraminal stenosis: 36 (76%) Facet arthropathy: 6 (12%)	–
Instability on dynamic X-rays	Yes: 46 (92%) No: 4 (8%)	–

Table 2. Radiographic outcomes and surgical complications in the study population

Parameter	Mean±SD / Number of patients (n=50)	Range	Percentage (%)	Notes
Slip angle reduction (degrees)	14.6±5.3	9–30	–	Significant correction
Fusion rate at 6 months	46 patients / 50	–	92%	2 cases of non-union (pseudoarthrosis)
Wound infection (n, %)	2	–	4%	Superficial, resolved with treatment
Implant-related complications (n, %)	0 (0%)	–	0%	None reported
Neurological deterioration (n, %)	1	–	2%	Transient deficit, recovered
Cardiac complication	1	–	2%	Developed heart failure with atrial fibrillation, managed medically
Reoperation rate (n, %)	0 (0%)	–	0%	None
Average hospital stay (days)	12.5±2.1	5–18	–	Standard postoperative stay
Intraoperative blood loss (mL)	610±85.4	410–930	–	Moderate blood loss
Operative time (minutes)	175.2±24.8	140–220	–	Within the expected range

Surgical intervention resulted in a mean reduction of 14.6±5.3 degrees in slip angle (range, 9–30 degrees). Fusion was successful in 92% (46/50) of patients at 6 months. Complications were minimal, with 4% experiencing wound infection (2 patients), 0% having implant-related issues, and 2% presenting with transient neurological deterioration (1 patient). No reoperations were needed. Average hospital stay was 12.5±2.1 days, intraoperative blood loss averaged 610±85.4 mL, and operative time was 175.2±24.8 minutes. At the 6-month follow-up, spinopelvic parameter assessment revealed that pelvic incidence remained stable (55.4°±7.8° pre-operatively vs. 55.2°±7.5°), indicating no significant change. In contrast, pelvic tilt demonstrated a significant reduction, while sacral slope and lumbar lordosis also showed significant postoperative improvements (***Table 3***). These findings suggest better sagittal alignment and restoration of lumbar curvature following TLIF surgery.

Pre- and post-operative pain assessment is shown in (***Fig. 3***).

The mean VAS scores showed a progressive decrease from 7.4±1.0 preoperatively (median 7, range 5–9) to 4.2±1.3 at 1-month post-op (median 4, range 2–7), reflecting a 43.2% improvement with 44% of patients achieving ≥50% pain reduction (p=0.015). At 3 months, the mean VAS further declined to 3.3±1.2 (median 3, range 1–5), with a 55.4% improvement and 64% of patients with ≥50% improvement (p=0.009). Significant pain relief continued at 6 months, with a mean VAS of 2.1±0.8 (median 2, range 1–4), representing a 71.6% reduction and 84% attaining ≥50% improvement (p < 0.001) (***Table 4***).

The functional outcome of the study is shown in (***Fig. 4***). The mean ODI scores decreased from a preoperative value of 74±10% (median 75, range 55–90) to 62.5±6.8% at 1 month (median 60, range 45–78), reflecting a 16% improvement with 28% of patients achieving ≥30% improvement (p=0.08). At 3 months, mean ODI further improved to 36.5±4.2% (median 35, range 22–53), representing a 51% reduction and 72% of patients with ≥30% improvement (p=0.005). By 6 months, the mean ODI declined markedly to 9.5±1.6% (median 9, range 3–18), showing an 88% improvement with 96% of patients achieving ≥30% improvement (p < 0.001) (***Table 5***).

The neurological outcomes demonstrated significant recovery over time (***Fig. 5***).

Table 3. Pre- and post-operative assessment of spinopelvic parameters using paired t-test

Parameter	Pre-op	Follow-up (6 months)	t-value	*p*-value
Pelvic incidence (PI)	55.4°±7.8°	55.2°±7.5	-0.13	0.8972
Pelvic tilt (PT)	21.3°±7.4°	17.2°±5.1°	-3.23	0.0017
Sacral slope (SS)	33.6°±9.5°	37.8°±8.3°	2.35	0.0211
Lumbar lordosis (LL)	46.5°±12.4°	51.4°±11.2°	2.07	0.0410

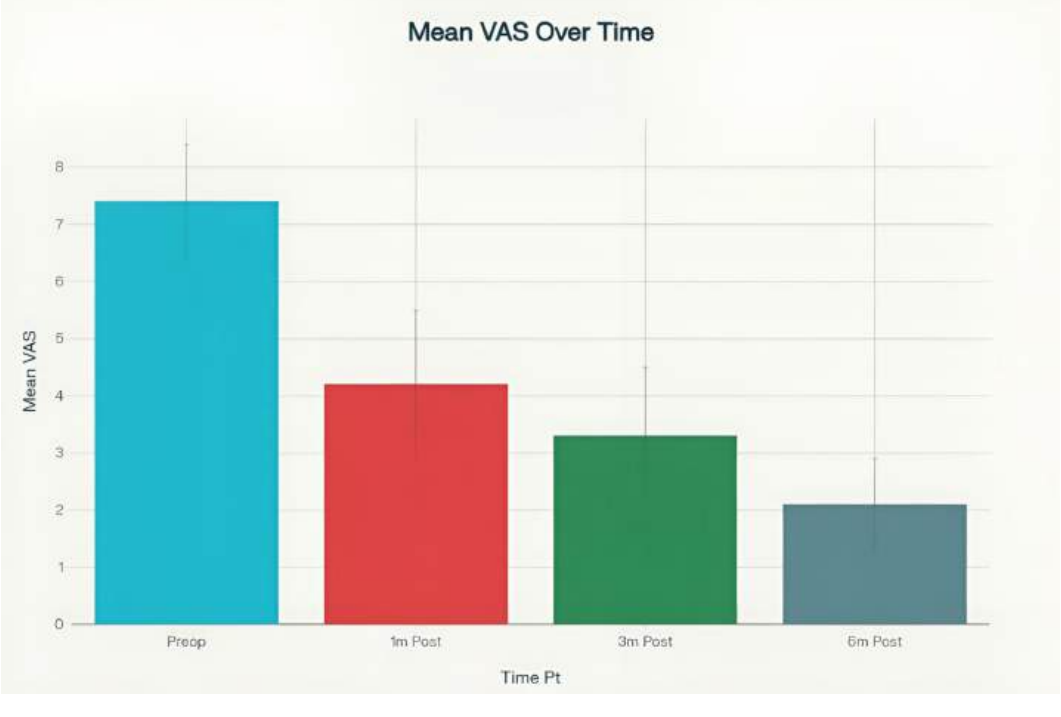

Fig. 3. Mean Visual Analogue Scale of patients during pre-op and follow-up

Table 4. Pre-operative and post-operative pain assessment using VAS

Time point	Mean VAS±SD	Median VAS	Range	% Improvement from Baseline	Number of patients with ≥50 % Improvement (%)	*p*-value (vs Pre-op)
Preoperative	7.4±1.0	7	6–9	–	–	–
1 Month post-op	4.2±1.3	4	2–7	43.2%	22 (44%)	0.015
3 Months post-op	3.3±1.2	3	1–6	55.4%	32 (64%)	0.009
6 Months post-op	2.1±0.8	2	1–4	71.6%	42 (84%)	<0.001

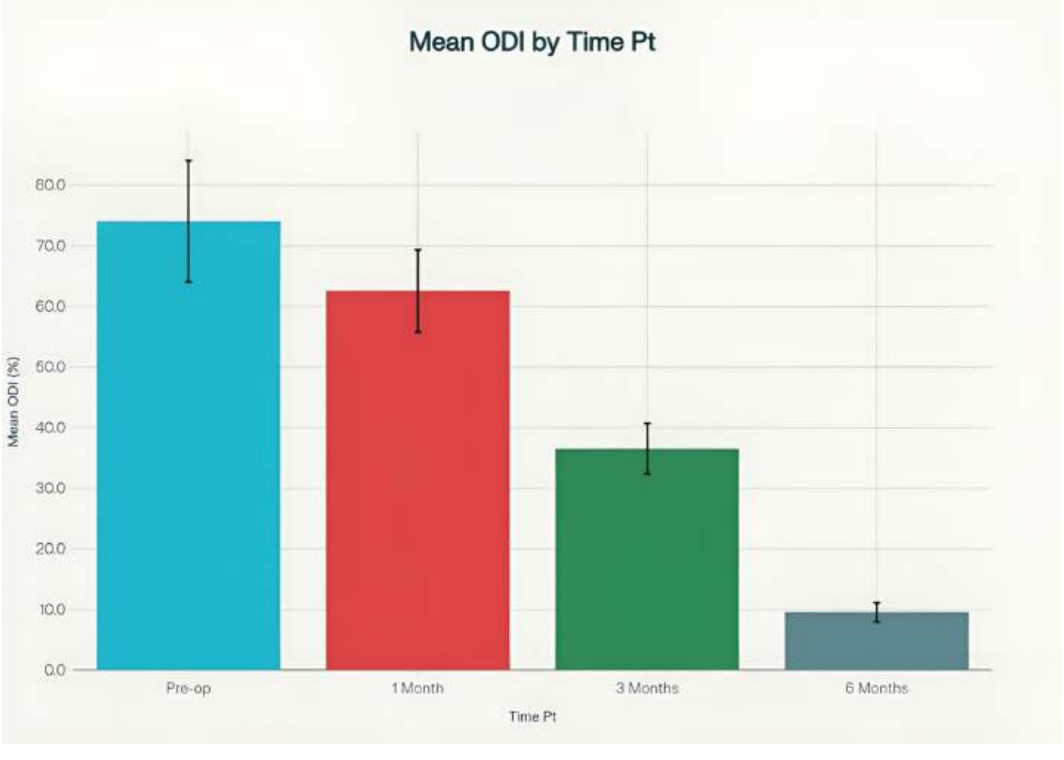

Fig. 4. Mean Oswestry Disability Index (ODI) during pre-op and follow-up

Table 5. Functional disability assessed by ODI during pre-op and follow-up.

Time Point	Mean ODI (%) (Mean±SD)	Median (%)	Range	% Improvement from Baseline	≥30% Improvement (n, %)	*p*-value
Pre-op	74±10	75	55–90	–	–	–
1 Month	62.5±6.8	60	45–78	16%	14 (28%)	0.08
3 Months	36.5±4.2	35	22–53	51%	36 (72%)	0.005
6 Months	9.5±1.6	9	3–18	88%	48 (96%)	<0.001

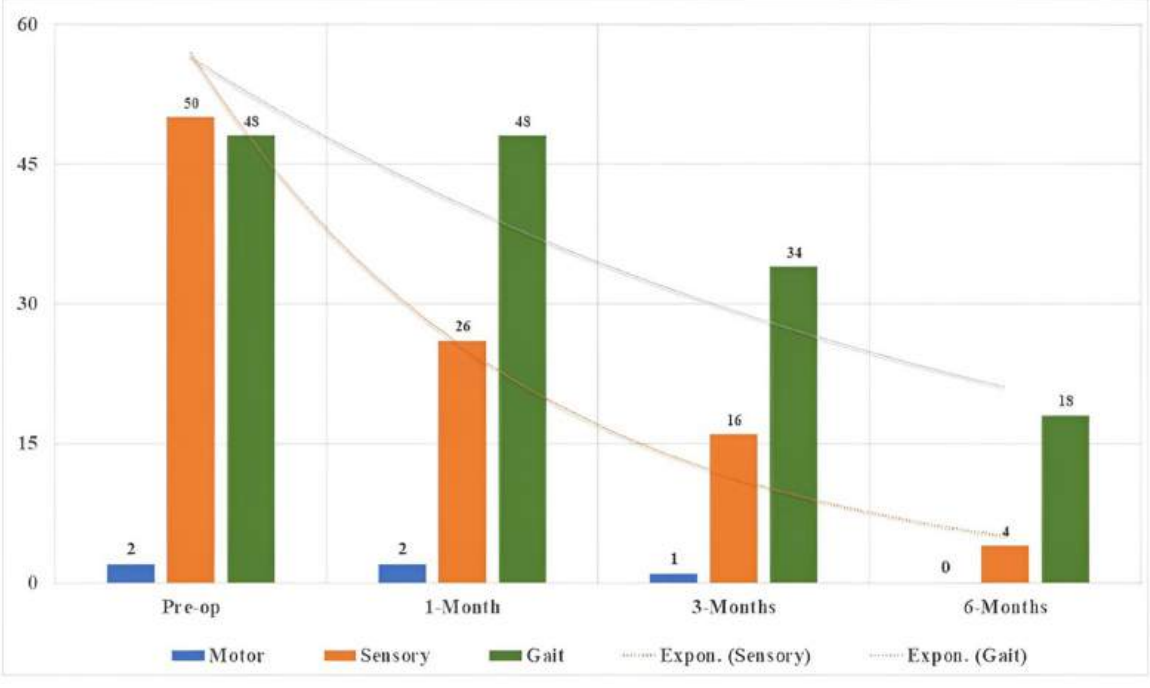

Fig. 5. Neurological recovery histogram at 1,3, and 6 months

A motor deficit was present in 4% of patients preoperatively and persisted immediately and at 1 month postoperatively but resolved completely by 6 months, representing 100% resolution (p=0.04). The sensory deficit was universal preoperatively (100%) and reduced to 52% immediately post-op, 32% at 1 month, and 8% at 6 months, reflecting a 92% overall improvement (p < 0.001). Gait disturbance affected 96% preoperatively and immediately post-op, improved to 68% at 1 month, and further to 36% at 6 months, demonstrating a 62.5% improvement (p=0.001) (***Table 6***).

The correlation analysis of demographic, clinical, and radiographic variables with study outcomes is shown in ***Table 7***. The analysis of study variables showed that older patients (>70 years) and those with obesity had higher disability and pain scores, with obesity significantly affecting both ODI (9.90±1.52 vs. 8.85±1.74, p=0.029) and VAS (2.05±0.69 vs. 2.30±0.82, p=0.001) outcomes. The L4-L5 spinal level was associated with greater disability (ODI 10.06±1.84) compared to L5-S1 (8.79±1.63, p=0.014). Higher grades of spondylolisthesis correlated with worse outcomes, with grade 4 showing the highest ODI (11.27±1.55, p < 0.001). No significant outcome differences were noted based on sex or hypertension.

Discussion

This prospective study evaluated the short-term clinical, radiological, and functional outcomes of TLIF in patients with spondylolisthesis, with an emphasis on pain relief, functional recovery, and fusion success. Our results demonstrate that TLIF provides effective correction of deformity, promotes high fusion rates, and achieves substantial improvements in pain scores, disability indices, and neurological function, with a low complication profile.

The demographic profile of the cohort—mean age 58 years, female predominance (56%), high prevalence of comorbidities (hypertension 32%, diabetes 24%), and a relatively high rates of grade II–IV slips—reflects the typical clinical scenario of Indian patients presenting for spinal surgery. Compared with international cohorts, where many surgical series focus on lower-grade slips and younger patients, our series included a greater proportion of advanced Meyerding grades (48% grade III–IV) [11]. This may highlight a delay in diagnosis and surgical referral in our setting, likely influenced by socioeconomic and healthcare access disparities.

The pre- and post-operative assessment of spinopelvic parameters demonstrated significant changes in PT, SS, and LL at 6 months follow-up, while PI remained stable with no significant difference (p=0.8972). Specifically, PT decreased significantly from 21.3°±7.4° to 17.2°±5.1° (t=-3.23, *p*=0.0017), indicating improved pelvic alignment post-surgery. SS and LL showed a significant increase, suggesting enhanced lumbar curvature contributing to sagittal balance restoration. These findings are consistent with prior studies. Shafiei *et al*. reported that abnormalities in standing pelvic tilt are significantly associated with poorer functional outcomes after total hip arthroplasty, and improvement in PT correlates with better recovery [12]. Similarly, Williams et al. found that PT and LL improved significantly post-lumbar fusion surgery, consistent with the paired t-test findings observed in the present study [13]. These studies collectively confirm that surgical realignment positively impacts the key sagittal parameters PT, SS, and LL, while PI remains a fixed anatomical parameter unaffected by surgery.

Table 6. Neurological recovery outcomes during follow-up

Neurological Parameter	Preoperative (n, %)	Immediate post-op (n, %)	1-Month post-op (n, %)	6-Month post-op (n, %)	Improvement (%)	*p*-value
Motor deficit	2 (4%)	2 (4%)	2 (4%)	0 (0%)	100% resolution	0.04
Sensory deficit	50 (100%)	26 (52%)	16 (32%)	4 (8%)	92% improvement	<0.001
Gait disturbance	48 (96%)	48 (96%)	34 (68%)	18 (36%)	62.5% improvement	0.001

Table 7. Correlation of various demographic, clinical, and radiographical parameters of the study population with study outcomes

Variables	Subclass	Outcome (ODI) Mean±SD	T value / F value (ODI)	P value (ODI)	Outcome (VAS) Mean±SD	T value / F value (VAS)	P value (VAS)
Sex	Male (n=22)	9.79±1.45	1.37157	0.17658	1.83±0.72	1.92345	0.05500
	Female (n=28)	9.27±1.23			2.23±0.78		
Age	<50 Yrs (n=27)	9.00±1.67	4.67581	0.01406	1.97±0.88	2.15790	0.12600
	51-70 Yrs (n=18)	9.95±1.31			2.12±0.74		
	>70 Yrs (n=5)	10.96±1.90			2.31±0.80		
Obesity	Present (n=31)	9.90±1.52	2.24392	0.02949	2.05±0.69	3.33521	0.00110
	Absent (n=19)	8.85±1.74			2.30±0.82		
HTN	Present (n=16)	10.15±1.38	1.76022	0.08474	2.26±0.77	1.15840	0.24560
	Absent (n=34)	9.19±2.00			2.08±0.83		
DM	Present (n=12)	10.00±1.41	0.99836	0.32311	1.85±0.82	3.23211	0.00160
	Absent (n=38)	9.38±1.58			2.21±0.78		
CVD	Present (n=10)	10.02±1.72	1.33140	0.18935	2.49±0.72	2.00822	0.05220
	Absent (n=40)	9.37±1.29			2.03±0.87		
Location	L4-L5 (n=28)	10.06±1.84	2.54546	0.01418	2.19±0.65	1.92830	0.05810
	L5-S1 (n=22)	8.79±1.63			2.00±0.90		
Grade of spondylolisthesis	Grade 2 (n=26)	8.59±1.47	9.79907	0.00028	1.89±0.95	9.36251	0.00150
	Grade 3 (n=14)	9.93±2.10			2.09±0.72		
	Grade 4 (n=10)	11.27±1.55			2.43±0.78		

Postoperative VAS scores demonstrated a significant and sustained decline from 7.4 preoperatively to 2.1 at 6 months, with 84% of patients reporting ≥50% pain relief. Similarly, ODI improved by 88% at final follow-up, with almost all patients (96%) achieving a clinically meaningful improvement. These outcomes are consistent with previous reports demonstrating the efficacy of TLIF for spondylolisthesis. For instance, Hartmann *et al*. have reported VAS backache pain reduction of 69.6 % at 12 weeks post-TLIF, comparable to our 71.6% VAS reduction at 6 months [14]. Also, the ODI scores in this study improved by 53.8% comparable to our study comparable to our study (51% reduction) [14].

The early disability improvement lag at 1 month, followed by sharp gains at 3 and 6 months, may reflect the time required for postoperative rehabilitation and gradual fusion-related stability. Integrating high-intensity interval training (HIIT) into rehabilitation protocols can accelerate these functional gains, as HIIT has been shown to significantly boost cardiovascular fitness, quality of life, and postoperative recovery in patients—suggesting a promising strategy to optimize outcomes in surgical populations [15]. The mean correction in slip angle (14.6 degrees) and the high 6-month fusion rate (92%) confirm TLIF's biomechanical advantages in restoring sagittal balance and promoting stability. Our fusion rate aligns with previously published pooled values of 84.7-94.3% in TLIF series and compares favorably to PLIF, where fusion is often slightly lower and implant-related complications are higher due to bilateral retraction [16]. Notably, our series achieved this with minimal complications and no implant failures, supporting TLIF as a reliable technique for correcting multi-grade spondylolisthesis. Compared to other studies, where at least one complication rates range from approximately 20%—including dural tears, nerve injuries, and pseudoarthrosis—our outcomes were at the lower end, possibly reflecting careful case selection and adherence to surgical protocols [17-18].

Neural decompression is a key advantage of TLIF, where cage placement restores disc height and foramina. In our study, 76% had foraminal stenosis, yet the majority showed neurological recovery. Neurological deterioration was transient in one patient, and there was a single cardiac complication involving heart failure with atrial fibrillation [19-21]. It was managed medically, in line with modern perioperative risk assessments that highlight cardiac morbidity as rare but significant in this and similar populations [3, 22]. Average hospital stays (12.5±2.1 days), intraoperative blood loss (610±85.4 mL), and operative time (175.2±24.8 minutes) were consistent with results from large comparative studies, supporting TLIF's status as an effective technique for spondylolisthesis with a favourable safety and recovery profile that matches current evidence-based guidelines and outcomes research [18].

In the evaluation of neurological outcomes, significant improvements were observed across motor, sensory, and gait parameters over six months. Motor deficits resolved completely by six months (p=0.04). Sensory deficits were initially present in 100% of patients but improved dramatically to 8% at six months, reflecting a 92% improvement with high statistical significance. Gait disturbance was noted in 96% preoperatively, decreasing to 36% by six months, indicating a 62.5% improvement (p=0.001). These findings align well with published data by Balasubramanian *et al*. showing that TLIF effectively decompresses neural elements, promotes nerve root recovery, and facilitates substantial functional neurological recovery, with most deficits improving gradually over months postoperatively without persistent major deficits [23].

Studies have also emphasized that the unilateral posterior approach preserves posterior soft tissues, aiding neurological recovery, and that early motor improvements portend good clinical outcomes [24]. Although some sensory symptoms may persist longer, a profound reduction over time indicates successful nerve decompression and stabilization achieved by TLIF. These neurological outcome trends are supported by both retrospective and prospective clinical series investigating TLIF in the treatment of spondylolisthesis [25]. However, our cohort adds valuable data specific to the Indian context, where higher preoperative disability, advanced slip grades, and delayed presentation are common.

The correlation of various demographic, clinical, and radiographic parameters with study outcomes, measured by ODI and VAS, reveals significant associations, particularly with age, obesity, location of pathology, and grade of spondylolisthesis. Patients >70 years had higher disability scores. Obesity was significantly correlated with worse outcomes in both ODI (p=0.02949) and VAS (p=0.00110), consistent with recent findings by Garcia *et al*., who reported that higher BMI negatively affects recovery and results in elevated pain and disability scores postoperatively [26]. Spondylolisthesis grade also showed a highly significant correlation with both ODI (p=0.00028) and VAS (p=0.00150), with higher grades associated with worse disability and pain, echoing the observations by Nedelea *et al*. regarding functional impairment increasing with severity of spondylolisthesis [27]. The location at L5-S1 was associated with significantly higher ODI compared to L5-S1 (p=0.00848). Sex and hypertension showed no significant correlation with outcomes in this cohort. Diabetes mellitus was significantly correlated with VAS scores (p=0.00160), which aligns with recent data highlighting altered pain perception in diabetic patients [28]. These findings underscore the need for individualized patient assessment incorporating these variables to optimize treatment strategies and prognostication in spinal disorders.

Study strengths and limitations

This study possesses many strengths including its prospective design, which ensures systematic and unbiased data collection; comprehensive evaluation of multiple clinical, radiographic, and functional outcomes such as pain (VAS), disability (ODI), neurological recovery, and fusion rates, providing a holistic picture of TLIF efficacy; and its focus on an Indian patient cohort, filling an important regional data gap and addressing demographic and healthcare nuances. Additionally, the detailed reporting of neurological and functional improvements with statistically significant results, strengthens the clinical relevance of the findings. However, the study has few limitations such as a relatively small sample size of 50 patients, potentially limiting the power to detect rare complications and

reducing generalizability; a short-term follow-up period of six months, which is insufficient to assess long-term fusion success and late complications. Furthermore, its single-center nature, absence of a control or comparison group, and limited detail on rehabilitation protocols may influence functional recovery outcomes and prevent standardization of postoperative care. Despite these limitations the study provides important contribution to Indian spine surgery literature while identifying areas for further research to confirm and expand these findings in larger, multi-center, randomized trials with extended follow-up.

Conclusion

This prospective study highlights that TLIF is an effective and safe surgical option for managing spondylolisthesis in an Indian patient cohort, demonstrating significant postoperative improvements in pain, disability, neurological recovery, and sagittal spinal alignment. Key findings include a significant reduction in pelvic tilt, increased sacral slope and lumbar lordosis, and high fusion rates with minimal complications. Clinical outcomes were influenced by patient- and disease-related factors including age, obesity, diabetes, anatomical level, and grade of spondylolisthesis, emphasizing the need for individualized patient assessment. These results contribute valuable region-specific data to support tailored surgical planning and improve functional and neurological outcomes in patients with varying degrees of spondylolisthesis. However, larger, multi-center studies with longer follow-up are warranted to validate these findings, assess the long-term durability of fusion, and optimize perioperative care protocols tailored to regional patient populations.

Disclosure

Conflict of Interest

None

Funding

No funding is available

Approval of Institutional Ethics Review Board

GMC/KRB/IEC/2023/28 dated 02.05.2023

Authors' Contributions

Neeraj Prasad designed the study, acquired the data, and supervised the work; Manish Kumar Nirala contributed to data collection, methodology, and manuscript revision; Abhishek Kumar performed statistical analysis, data interpretation, and literature review; Manisha Gupta assisted with data validation, figures, editing, and final approval. All authors reviewed and approved the final manuscript.

References

1. Xu C, Wu Y, Bao B, Liu X, Zhang Y, Li R, Yang T, Tang J. Deep Learning-Based Diagnosis of Lumbar Spondylolisthesis Using X-Ray Imaging. Diagnostics (Basel). 2025 Aug 12;15(16):2015. doi: 10.3390/diagnostics15162015
2. Al-Witri A, Li Y. Prevalence of occult spina bifida in isthmic versus degenerative spondylolisthesis: retrospective radiographic review of consecutive surgical patients. J Spine Surg. 2025 Jun 27;11(2):227-233. doi: 10.21037/jss-24-151
3. Walker CT, Bonney PA, Martirosyan NL, Theodore N. Genetics Underlying an Individualized Approach to Adult Spinal Disorders. Front Surg. 2016 Nov 22;3:61. doi: 10.3389/fsurg.2016.00061
4. Zukotynski K, Curtis C, Grant FD, Micheli L, Treves ST. The value of SPECT in the detection of stress injury to the pars interarticularis in patients with low back pain. J Orthop Surg Res. 2010 Mar 3;5:13. doi: 10.1186/1749-799X-5-13
5. Kreiner DS, Matz P, Bono CM, Cho CH, Easa JE, Ghiselli G, et al. Guideline summary review: an evidence-based clinical guideline for the diagnosis and treatment of low back pain. Spine J. 2020 Jul;20(7):998-1024. doi: 10.1016/j.spinee.2020.04.006
6. .Kumar A, Gupta M, Varshney A, Kumari S, Sahu RN. Artificial Intelligence in Cardiac Healthcare: Advancements in Managing Coronary Artery Disease and Acute Coronary Syndrome. Disease and Health Research: New Insights Vol 10. 2024 Nov 23:91-115. doi: 10.9734/bpi/dhrni/v10/3057
7. Nedelea DG, Vulpe DE, Gherghiceanu F, Capitanu BS, Dragosloveanu S, Stoica IC. Surgical and non-surgical management of spondylolisthesis: a comprehensive review. J Med Life. 2025 Mar;18(3):196-207. doi: 10.25122/jml-2025-0039
8. Ehni HJ, Wiesing U. The Declaration of Helsinki in bioethics literature since the last revision in 2013. Bioethics. 2024 May;38(4):335-343. doi: 10.1111/bioe.13270
9. Cho Y, Jo DJ, Hyun SJ, Park JH, Yang NR. From the Spinopelvic Parameters to Global Alignment and Proportion Scores in Adult Spinal Deformity. Neurospine. 2023 Jun;20(2):467-477. doi: 10.14245/ns.2346374.187
10. Adhikari P, Çetin E, Çetinkaya M, Nabi V, Yüksel S, Vila Casademunt A, Obeid I, Sanchez Perez-Grueso F, Acaroğlu E; European Spine Study Group (ESSG). Ability of Visual Analogue Scale to predict Oswestry Disability Index improvement and surgical treatment decision in patients with adult spinal deformity. Brain Spine. 2022 Aug 28;2:100934. doi: 10.1016/j.bas.2022.100934
11. Zhang Q, Yuan Z, Zhou M, Liu H, Xu Y, Ren Y. A comparison of posterior lumbar interbody fusion and transforaminal lumbar interbody fusion: a literature review and meta-analysis. BMC Musculoskelet Disord. 2014 Nov 5;15:367. doi: 10.1186/1471-2474-15-367
12. Shafiei SH, Plaskos C, Bromwich L, Baré JV, McMahon S, Shimmin A. Impact of preoperative spinopelvic risk factors on functional outcomes after total hip arthroplasty: a retrospective cohort study. Bone Joint J. 2025 Aug 1;107-B(8):777-783. doi: 10.1302/0301-620X.107B8.BJJ-2024-1441.R1
13. Williams GP, Giraldo JP, Zhou JJ, Sawa AGU, Lee JJ, Abbatematteo JM, Kelly BP, Turner JD, Snyder LA, Uribe JS. Prediction of Postoperative Segmental Lordosis at L5 to S1 After Single-Level Anterior Lumbar Interbody Fusion. Int J Spine Surg. 2025 Apr 11:8751. doi: 10.14444/8751
14. Hartmann S, Lang A, Lener S, Abramovic A, Grassner L, Thomé C. Minimally invasive versus open transforaminal lumbar interbody fusion: a prospective, controlled observational study of short-term outcome. Neurosurg Rev. 2022 Oct;45(5):3417-3426. doi: 10.1007/s10143-022-01845-w
15. Kumar A, Gupta M, Kohat AK, Agrawal A, Varshney A, Chugh A, Koshy DI, Gurjar R, Kumar P. Impact of High-Intensity Interval Training (HIIT) on Patient Recovery After Myocardial Infarction and Stroke: A Fast Track to Fitness. Cureus. 2024 Nov 18;16(11):e73910. doi: 10.7759/cureus.73910
16. Levin JM, Tanenbaum JE, Steinmetz MP, Mroz TE, Overley SC. Posterolateral fusion (PLF) versus transforaminal lumbar interbody fusion (TLIF) for spondylolisthesis: a systematic review and meta-analysis. Spine J. 2018 Jun;18(6):1088-1098. doi: 10.1016/j.spinee.2018.01.028
17. Poppenborg P, Liljenqvist U, Gosheger G, Schulze Boevingloh A, Lampe L, Schmeil S, Schulte TL, Lange T. Complications in TLIF spondylodesis-do they influence the outcome for patients? A prospective two-center study. Eur Spine J. 2021 May;30(5):1320-1328. doi: 10.1007/s00586-020-06689-w
18. Chen X, Lin GX, Rui G, Chen CM, Kotheeranurak V, Wu HJ, Zhang HL. Comparison of Perioperative and Postoperative Outcomes of Minimally Invasive and Open TLIF in Obese Patients: A Systematic Review and MetaAnalysis. J Pain Res. 2022 Jan 6;15:41-52. doi: 10.2147/JPR.S329162
19. Kumar DA, Muneer DK, Qureshi DN. Relationship between

high sensitivity troponin I and clinical outcomes in non-acute coronary syndrome (non-ACS) acute heart failure patients - a one-year follow-up study. Indian Heart J. 2024 Mar-Apr;76(2):139-145. doi: 10.1016/j.ihj.2024.04.003
20. Kumar A, Gupta M, Varshney A, Kumar R. Flecainide fallout: a rare case report of refractory ventricular tachycardia and updated management strategies. Eur Heart J Case Rep. 2025 Jul 29;9(8):ytaf368. doi: 10.1093/ehjcr/ytaf368
21. Kumar A, Gupta M, Kumar M, Varshney A. High-Sensitivity Cardiac Troponin Assays in Acute Heart Failure, Moving Beyond Myocardial Infarction. Cardiol Rev. 2024 Nov 27. doi: 10.1097/CRD.0000000000000732
22. Sharma AY, Tiwari B, Ekka S, Kumar A, Jangir M, Peswani M, Agrawal S. Postoperative Clinical Outcomes of Transurethral Resection of the Prostate (TURP) Combined With Otis Urethrotomy in High-Risk Patients With Coronary Artery Disease (Post-Angioplasty): Insights From a Prospective Observational Cohort. Cureus. 2025 Sep 1;17(9):e91439. doi: 10.7759/cureus.91439
23. Balasubramanian VA, Douraiswami B, Subramani S. Outcome of transforaminal lumbar interbody fusion in spondylolisthesis-A clinico-radiological correlation. J Orthop. 2018 Feb 24;15(2):359-362. doi: 10.1016/j.jor.2018.02.017
24. Murrad K, Al Harbi Y, Alsabbagh LM, Alwehaibi K, Al Salhi R, Awwad W. Clinical Outcomes of the Transforaminal Lumbar Interbody Fusion Technique Among Patients With Low Back Pain Showing Type 1 Modic Changes on MRI. Cureus. 2024 Jun 5;16(6):e61745. doi: 10.7759/cureus.61745
25. Shahzad H, Lee M, Epitropoulous F, Bhatti N, Singh VK, Kavuri V, Yu E. Comparing trends and outcomes of minimally invasive transforaminal lumbar interbody fusion (TLIF) procedures: A retrospective analysis. J Orthop. 2024 Jul 25;59:82-85. doi: 10.1016/j.jor.2024.07.010
26. Garcia R, Odland K, Sembrano J. Effects of Body Mass Index on Spondylolisthesis Surgery and Associated Patient-Reported Outcomes: A Retrospective Review. Int J Spine Surg. 2025 Sep 2;19(4):375-382. doi: 10.14444/8752
27. Nedelea DG, Vulpe DE, Dragosloveanu S, Stoica IC. Primary Versus Iatrogenic Spondylolisthesis: A Multi-Dimensional Comparison of Outcomes. J Clin Med. 2025 Mar 23;14(7):2193. doi: 10.3390/jcm14072193
28. Zhang J, Liu Y, Zeng Y, Yuan L, Li W. Correlations between spinopelvic parameters and health-related quality of life in degenerative lumbar scoliosis patients before and after long -level fusion surgery. BMC Musculoskelet Disord. 2025 Jan 25;26(1):84. doi: 10.1186/s12891-025-08336-1

Original article

Ukrainian Neurosurgical Journal. 2026;32(1):52-59
doi: 10.25305/unj.338724

Factors contributing to surgical complexity in giant parasagittal and falcine meningiomas: a case-based review

Tommy A. Nazwar [1], Nasim Amar [2], Farhad Bal'afif [1], Donny W. Wardhana [1], Fachriy Bal'afif [1]

[1] Division of Neurosurgery, Department of Surgery, Faculty of Medicine, Brawijaya University-Saiful Anwar General Hospital, Malang, East Java, Indonesia
[2] Faculty of Medicine, Brawijaya University-Saiful Anwar General Hospital, Indonesia

Received: 07 September 2025
Accepted: 16 October 2025

Address for correspondence: *Tommy A. Nazwar, Division of Neurosurgery, Department of Surgery, Brawijaya University/ Saiful Anwar General Hospital, GPT II Building, 2nd Floor, Malang, East Java, 65112, Indonesia, email: tommy@ub.ac.id*

Introduction: Giant parasagittal and falcine meningiomas are surgically challenging due to their frequent involvement of the superior sagittal sinus (SSS), proximity to eloquent cortex, and complex venous anatomy. Although these tumors carry a high operative risk, detailed analyses of surgical difficulty remain limited in the literature.

Objective: This narrative review of published case reports and series aims to delineate the key determinants of surgical complexity in giant parasagittal and falcine meningiomas, including tumor size, sinus involvement, anatomical constraints, and intraoperative decision-making while emphasizing the balance between surgical radicality and patient safety.

Methods: A narrative review and multicase synthesis were performed, analyzing 22 published reports (19 case reports and 3 case series) describing the microsurgical management of giant parasagittal and falcine meningiomas. Studies were included based on the PICOS framework, focusing on tumors ≥5 cm with original surgical and outcome data. Extracted variables included demographics, tumor size, location, SSS involvement, histology, surgical technique, and clinical outcomes**.**

Results: A total of 36 patients were identified. Most tumors were parasagittal (52.8%), involved the middle third of the SSS (38.9%), and demonstrated SSS invasion (78.6%), with complete occlusion in 64.3% of cases. Gross total resection was achieved in 75.7% of cases. Pediatric patients (11.1%) were more frequently associated with high-grade histology and intraoperative complications. Tumors involving the middle third of the SSS and those with parasagittal location were consistently associated with increased technical difficulty, venous bleeding, and postoperative deficits. Overall, 72.2% of patients experienced favorable recovery, while 11.1% had poor outcomes, including tumor recurrence or death.

Conclusion: Surgical management of giant parasagittal and falcine meningiomas is technically demanding, particularly in pediatric cases and when tumors involve the parasagittal region or the middle third of the SSS. Careful preoperative venous evaluation and individualized strategies are crucial for optimizing the resection while minimizing complications.

Keywords: *parasagittal meningioma; falcine meningioma; giant meningioma; surgical complexity*

Introduction

Parasagittal and falcine meningiomas are among the most frequently encountered intracranial tumors, ranking second only to convexity meningiomas in terms of location [1, 2]. Arising from the arachnoid cap cells, often near the arachnoid villi along the falx cerebri or superior sagittal sinus (SSS), these tumors are associated with significant surgical morbidity and account for approximately 2.6–6.7% of meningioma-related deaths [3]. Although they are generally histologically benign, their proximity to essential venous structures and cortical regions poses considerable surgical challenges [4].

Parasagittal meningiomas, which are defined by their involvement with the wall or lumen of the SSS, represent approximately 20-30% of all intracranial meningiomas [5]. Surgical complexity is amplified in giant tumors, commonly defined as those measuring more than 5 cm in diameter [6]. These large tumors often compress or invade the SSS, impair venous drainage, and distort adjacent brain tissue, elevating the risks of venous infarction, cerebral edema, and neurological deficits [4, 7, 8]. The challenges are particularly pronounced when the lesion involves the middle or posterior thirds of the sinus or is situated near eloquent brain areas, such as the sensorimotor

or supplementary motor cortex [1, 9, 10]. Similarly, parafalcine meningiomas, typically located parafalcine meningiomas, typically located deep within the interhemispheric fissure, pose challenges due to limited surgical exposure and proximity to critical structures [5, 11].

While gross total resection (GTR) offers the best chance of minimizing recurrence, its feasibility is often constrained by the need to preserve vital venous and cortical anatomy [11, 12]. Despite the growing awareness of the complexities associated with parasagittal and falcine meningiomas, giant variants remain underrepresented in the literature, particularly in terms of detailed, case-level surgical evaluations [8, 13]. Additionally, there remains limited consensus on optimal strategies for managing tumors with partial or complete SSS occlusion [6]. These gaps underscore the need for a focused synthesis of case-level data on surgical complexity, venous sinus management, and outcomes in giant parasagittal and falcine meningiomas.

Objective

This narrative review of published case reports and series aims to delineate key determinants of surgical complexity in giant parasagittal and falcine meningiomas including tumor size, degree of sinus invasion or occlusion, venous and cortical anatomical constraints, and intraoperative decision making. The review also aims to relate these factors to the extent of resection, perioperative complications, and overall clinical outcomes, while emphasizing the need to balance surgical radicality with patient safety.

Methods

This narrative review was conducted to systematically identify clinical and anatomical factors contributing to surgical complexity in giant parasagittal and falcine meningiomas, based on published case reports and case series.

Eligibility criteria

The study followed the PICOS framework:

Population: Patients of any age diagnosed with parasagittal or falcine meningiomas ≥5 cm, with or without SSS invasion.

Intervention: Microsurgical resection, including GTR, near total, or subtotal resection (STR) approaches, with or without adjunctive measures such as sinus reconstruction, preoperative embolization, or radiotherapy.

Comparison: Cases were analyzed based on degree of sinus invasion (none, partial, complete), tumor location (anterior, middle, posterior third), patient age (pediatric vs. adult), histological grade (WHO I–III), and extent of resection.

Outcomes:

- Primary: Identification of factors associated with increased surgical difficulty, including sinus invasion, tumor location, patient age, etc.

- Secondary: Neurological recovery, extent of resection, recurrence, and surgical complications.

Study Design: Case reports and series with original surgical and outcome data.

Only full-text articles published in English were included.

Studies were excluded if tumors were <5 cm, located outside the parasagittal or falcine region, or lacked surgical or outcome details.

Search strategy

A structured search of PubMed, ScienceDirect, SpringerLink, and the Cochrane Library was conducted for articles published up to May 2025, using the following terms: "Falcine meningioma" OR "parasagittal meningioma") AND ("surgical resection" OR "Simpson grade") AND ("superior sagittal sinus" OR "SSS invasion") AND ("case report" OR "case series"). Relevant references from selected studies were also reviewed.

Data extraction and analysis

Two reviewers independently extracted data using a standardized form, collecting patient demographics, tumor features (size, location, SSS involvement, histology), surgical strategy, and clinical outcomes. Descriptive statistics were applied, and a structured comparison was used to explore associations between specific factors (e.g., venous anatomy, pediatric status, tumor site) and surgical complexity or outcomes.

Results

Study selection and identification

A total of 548 records were identified through a systematic literature search of four databases: PubMed (n=127), ScienceDirect (n=173), SpringerLink (n=130), and the Cochrane Library (n=148). After removing duplicates, the remaining articles were screened based on title, abstract, relevance to the predefined inclusion criteria, language (English), and full-text accessibility. Following full-text assessment, 22 studies, comprising 19 case reports [5, 7, 13–29] and 3 case series [6, 9, 30], met all eligibility criteria and were included in the final analysis.

Summary of findings

A total of 36 patients were included in the analysis (***Table 1***), comprising 19 males (52.8%) and 17 females

(47.2%). The majority were adults (n=32, 88.9%), with a mean age of 52.5±12.5 years, while four patients (11.1%) were children (mean age 5.75±3.8 years). The most common presenting symptoms were motor or sensory deficits, reported in 14 patients (38.9%), including weakness, hemiparesis, foot drop, and gait disturbances. Symptoms of raised intracranial pressure were present in 10 patients (27.8%), while seizures occurred in 9 cases (25%), including generalized, focal, and complex partial types. Cognitive or behavioral changes were reported in 4 patients (11.1%), such as memory impairment, aggression, or glossolalia.

The average tumor size was 7.69 × 5.80 × 5.56 cm, indicating a large lesion volume, primarily parasagittal (n=19, 52.8%) and falcine (n=16, 44.4%), with one patient (2.8%) exhibiting combined falcine–parasagittal involvement. Regarding tumor site within the SSS, the middle third was the most commonly affected region (n=14, 38.9%), followed by the anterior third (n=12, 33.3%). Multiple adjacent segments were also involved (anterior–middle: n=3, 8.3%; middle–posterior: n=1, 2.8%). Posterior third involvement was noted in 2 cases (5.6%). Overall, SSS invasion occurred in 22 patients (78.6%), with complete invasion in 18 (64.3%) and partial invasion in 4 (14.3%).

Gross total resection (GTR) was achieved in 28 patients (75.7%), including two cases who underwent simultaneous sinus reconstruction. Incomplete resection was reported in 4 cases (10.8%). Histopathologically, meningothelial meningioma was the most common subtype (n=12, 33.3%), followed by atypical (n=9, 25%), transitional (n=7, 19.4%), and malignant variants, including anaplastic and malignant meningiomas (n=2, 5.6%). Most tumors were WHO Grade I (n=19, 52.8%), with Grade II in 9 cases (25%) and Grade III in 2 (5.6%).

Postoperatively, 26 patients (72.2%) had favourable recovery, while 6 (16.7%) experienced residual neurological deficits (mild hemiparesis, seizures well controlled with anticonvulsants, apraxia, intermittent headaches, and sixth nerve palsy). Four patients (11.1%) who experienced tumor recurrence had poor outcomes (worsening of symptoms, metastases, progressive tumor enlargement, multiple tumors detected, and death). The median follow-up duration was 17.5 months (range 2–180 months), and the mean length of hospital stay was 10.77±8.36 days.

Table 1. Descriptive Analysis

Variable	Descriptive Data (n=36)
Gender	
Male	19 (51.4%)
Female	17 (45.9%)
Age Group	
Adults	32 (88.9%), 52.5±12.5
Children	4 (11.1%), 5.75±3.8
Presenting Symptoms	
Seizures	9 (25%)
ICP-related symptoms	10 (27.8%)
Motor/sensory deficits	14 (38.9%)
Cognitive/behavioral changes	4 (11.1%)
Tumor size (mean)	7.69 × 5.80 × 5.56
Tumor Location	
Falcine	16 (44.4%)
Parasagittal	19 (52.8%)
Falcine–Parasagittal	1 (2.8%)
Tumor Site (SSS thirds)	
Anterior third	12 (33.3%)
Middle third	14 (38.9%)
Posterior third	2 (5.6%)
Anterior-Middle	3 (8.3%)
Middle-Posterior	1 (2.8%)
SSS Invasion	
Complete	18 (64.3%)
Partial	4 (14.3%)
None	6 (21.4%)
Extent of Resection	
Gross Total Resection (GTR)	28 (75.7%)
Incomplete Resection	4 (10.8%)
GTR with sinus reconstruction	2 (5.4%)
Histopathological Subtype	
Meningothelial meningioma	12 (33.3%)
Transitional meningioma	7 (19.4%)
Atypical meningioma	9 (25%)
Anaplastic meningioma	1 (2.8%)
Malignant meningioma	1 (2.8%)
WHO Grade	
Grade I	19 (52.8%)
Grade II	9 (25%)
Grade III	2 (5.6%)
Postoperative Outcomes	
Good recovery	26 (72.2%)
Recovery with deficits	6 (26.7%)
Poor outcome / Recurrence	4 (11.1%)
Follow-up Duration (months)	17.50 (IQR 2-180)
Length of Hospital Stay (days)	10.77±8.36

Factors Contributing to Surgical Difficulty

Pediatric meningioma

The surgical management of giant parasagittal and falcine meningiomas is frequently complicated by a combination of factors, including patient age, vascular involvement, tumor location, and anatomical

subtype (***See Table 2 at the link https://theunj.org/article/view/338724/331688***). Pediatric patients, for instance, present unique challenges due to more aggressive tumor behaviour and a higher risk of intraoperative complications [5, 7, 21, 22]. In our review, four children (11.1%) were identified, with a mean age of 5.75±3.8 years; three had atypical and one had anaplastic meningioma. Li *et al*. reported a 2-year-old child with a 14.2 × 13.5 × 11.1 cm occipito-temporo-parietal tumor featuring necrosis, vascularity, and bone erosion. The patient underwent staged resection but experienced two episodes of hemorrhagic shock, including one with unrecordable intraoperative blood pressure; nonetheless, gross total resection was achieved, and the child remained recurrence-free at 5 years [5]. Similarly, Savateev *et al*. described a 10-year-old with an 11 × 8.5 cm parasagittal tumor extending intra- and extracranially with SSS invasion; initial surgery was aborted due to hemorrhage, and the tumor was removed during a second-stage operation, followed by complete recovery and adjuvant stereotactic radiotherapy [18]. Other cases, such as those reported by Honda and Doxtader, involved high-grade meningiomas with recurrence or metastasis despite surgical resection [21, 22]. These pediatric cases highlight the need for cautious, individualized, and often staged approaches as well as long-term postoperative surveillance.

Vascular complexity and middle third SSS involvement

Vascular factors, particularly SSS invasion, high tumor vascularity, and dependence on collateral venous pathways, pose significant challenges in resecting giant parasagittal and falcine meningiomas [7, 9, 26]. These challenges are especially pronounced when the tumor involves the middle third of the SSS, a region closely associated with the eloquent cortex and prominent bridging veins such as the rolandic and precentral veins [5]. In our review, nine cases (37.5%) demonstrated involvement of the middle third segment, resulting in SSS occlusion. Otani *et al*. (2018) utilized 3D computed tomography (CT) venography to visualize multiple rolandic veins near a 6 cm falcine tumor, enabling a gravity-assisted interhemispheric approach [9]. Similarly, Wang *et al*. (2022) described a large parasagittal meningioma infiltrating the middle third of the SSS, with CT venography revealing complete sinus occlusion and displacement of the right precentral vein [7]. Consequently, surgical strategies should prioritize the preservation of collateral venous pathways and employ patient positioning techniques that enhance cerebral venous drainage, thereby minimizing the risk of postoperative neurological deficits.

Several cases further illustrate the surgical impact of venous anatomy. In Bederson's 1995 report, partial SSS occlusion in an 8 cm parasagittal tumor led to significant sinus bleeding, requiring a staged resection [15]. In Kusdiansah's 2023 case, CT venography revealed complete SSS occlusion with compensatory diploic vein bypass. This finding led the surgical team to design an "L"-shaped craniotomy that preserved venous outflow, allowing for safe resection without compromising the bypass [28]. Rajagopal (2022) described a case with complete sinus blockage and prominent bridging vein networks, which necessitated an intrinsic resection strategy to avoid venous infarction [19]. Li and Gotohda each reported highly vascular tumors that resulted in intraoperative hemorrhagic shock; in Gotohda's case, prior embolization of arterial feeders made resection safer [5, 14]. Psaras *et al*. (2009) were only able to do subtotal resection of a middle-third SSS tumor due to dense sinus adherence and bleeding; tumor recurrence and lung metastasis developed 15 years later [27].

Falcine vs parasagittal meningioma

Finally, tumor location plays a key role in determining surgical complexity. Parasagittal meningiomas are generally more challenging to resect than falcine tumors due to higher rates of SSS invasion, peritumoral edema, and hyperostotic bone changes [16, 20, 22]. In this review, 18 cases (64.3%) of parasagittal meningiomas invaded the SSS, compared to just 3 cases (10.7%) of falcine tumors. Parasagittal tumors more frequently exhibited vasogenic edema, which complicates resection and recovery. For example, Walker *et al*. (2023) described a parasagittal tumor with extensive edema and intraoperative evidence of pial invasion [16]. Similarly, Bederson (1995) and Okunlola (2024) reported neurological decline associated with peritumoral edema and cystic changes [15, 20]. Hyperostosis further complicates surgery in parasagittal lesions. Rajagopal (2022) described hypervascular bone overlying a parasagittal tumor requiring a sinus-sparing approach [19]. Moreover, Savateev (2016) and Wang *et al*. (2016) noted cases where bony hyperostosis contributed to increased intracranial pressure, prompting decompressive craniectomy [6, 18]. Overall, these findings highlight parasagittal meningiomas are often more invasive and technically demanding than their falcine counterparts.

Discussion

Gross total resection (GTR) remains the primary surgical goal in the management of meningiomas due to its consistently superior outcomes in progression-free survival (PFS) and overall survival (OS), as demonstrated across multiple studies [31–34]. In our review, GTR was

achieved in 75.7% of patients, while STR was performed in 10.8%. Soyuer *et al*. (2004), reported significantly higher 5-year PFS rates in patients undergoing GTR compared to STR (77% vs. 52%, p=0.02) [35]. Similarly, Aizer *et al*. (2014) reported improved 5-year OS in patients with atypical and malignant meningiomas who underwent GTR [36]. Sun *et al*. (2015) also demonstrated superior PFS rates in favor of GTR [37]. In pediatric populations, Wach *et al*. (2025) reported significantly longer PFS and OS for GTR over STR based on pooled data from 20 studies (PFS: 113.8 vs. 40.1 months; OS: 602.9 vs. 173.8 months; both p<0.001) [31].

In this review, the extent of resection was recorded as described by the original authors. Most studies defined GTR as Simpson Grade I–III removal, consistent with evidence showing no significant difference in recurrence between these grades when modern microsurgical techniques are used [38]. In cases with SSS invasion or occlusion, GTR often referred to complete macroscopic removal of the extraluminal component with preservation or reconstruction of venous outflow. For example, Aguiar *et al*. (2022) achieved favorable outcomes following Simpson Grade II resection and sinus preservation, while Alzughaibi *et al*. (2024) and Aboud *et al*. (2021) reported complete excision of tumors invading occluded sinus segments, the latter with venous graft reconstruction. Consistent with this strategy, Sirko *et al*. (2022) and Kvasha & Spiridonov (2024) showed that tailoring the extent of resection to preoperative assessment of SSS patency and collateral venous outflow can increase completeness (Simpson Grade I–II) while lowering complications and subsequent tumor regrowth [40] [41].

Conversely, when safe sinus resection was not feasible, subtotal removal followed by observation or adjuvant radiotherapy was employed, as illustrated by Psaras *et al*. (2009) and Kusdiansah *et al*. (2023) [27,28]. Thus, the 28 cases labeled as GTR in this review should be interpreted within this context of "functional total resection," emphasizing maximal tumor removal while maintaining venous integrity. This approach reflects the current surgical philosophy that achieving a balance between radicality and preservation of venous drainage is crucial in the management of giant parasagittal and falcine meningiomas.

Despite its benefits, GTR is not always feasible, particularly in giant parasagittal or falcine meningiomas with high vascularity, SSS invasion, or proximity to eloquent cortex. For example, Savateev (2016) reported the need for staged resection due to intraoperative hemorrhage risk, resulting in a Simpson Grade IV resection [18]. Similarly, Li *et al*. (2016) described a successful two-stage GTR in a highly vascular pediatric tumor with bone erosion and mass effect [5]. These cases highlight that STR followed by delayed resection may be a safe and pragmatic alternative. In elderly patients, since the risk of recurrence may be unlikely within the patient's lifetime, and if the tumors are adjacent to critical structures, STR may be preferable. GTR may not confer significant survival benefits [42]. Studies by Psaras *et al*. (2009), Kusdiansah *et al*. (2023), and Karthigeyan *et al*. (2018) support STR with adjuvant radiotherapy or delayed GTR as effective strategies for long-term symptom control and favorable outcomes [27, 28, 30]. Therefore, while GTR should be pursued when safely achievable, STR remains a valid option to balance oncological control with surgical safety in selected cases.

Although tumor size often contributes to surgical complexity, our analysis suggests that biological behavior and tumor aggressiveness are more critical determinants. In our review, 72.2% of patients had favorable postoperative outcomes despite large tumor size, indicating that size alone is not a reliable predictor of surgical difficulty or outcome. Aggressive features —such as high vascularity, sinus invasion, and intraosseous extension—were more strongly associated with intraoperative challenges [5, 18, 26]. Pediatric patients, in particular, frequently presented with WHO grade II or III tumors requiring complex or staged resections. For instance, Savateev *et al*. (2016) described a 10-year-old with a large parasagittal meningioma invading both the SSS and the skull; although initially suspected to be grade I, the tumor was confirmed as atypical (grade II) during surgery [18]. The operation was halted due to life-threatening hemorrhage. Arivazhagan *et al*. (2008) and Tufan *et al*. also reported increased surgical risks and the need for staged operations in pediatric patients, primarily due to excessive bleeding [43, 44]. Lakhdar *et al*. (2010) identified radiographic signs—such as hyperostosis and intracranial hypertension that indicated aggressive tumor behavior, regardless of tumor size [45]. These findings underscore the need for further large-scale studies to clarify the association between tumor behavior and surgical complexity, particularly in high-risk populations.

Management of meningiomas involving the SSS, especially those affecting the middle third, remains controversial due to the complexity of venous anatomy and functional implications. Some authors including Aboud *et al*. (2021) and Sindou *et al*. (1997) advocate sinus reconstruction. They recommend resecting the invaded segment and restoring venous flow using autologous grafts when collateral drainage is insufficient [13, 46]. Sindou emphasized that reconstruction may help maintain venous circulation and prevent delayed complications even in completely occluded sinuses [15, 46]. Conversely, other studies challenge this approach. Wang *et al*. (2016) found that in cases of complete sinus

occlusion with adequate collateral flow, reconstruction may be unnecessary and it is associated with increased risks such as infection, prolonged operative time, and graft thrombosis. Similarly, Al-Mefty *et al*. also warned that reconstruction in well-collateralized sinuses could compromise critical cortical veins with limited benefit [6, 15]. In our review, SSS invasion was observed in 78.6% of cases, with complete occlusion in 64.3%, predominantly involving the middle third. While favorable outcomes following sinus reconstruction have been reported by Bederson (1995) and Aboud (2021), the decision to reconstruct should be individualized based on sinus patency, collateral circulation, anatomical location, and patient-specific factors [13, 15]. Reconstruction may be beneficial in select cases but is not universally required.

Surgical outcomes for giant parasagittal and falcine meningiomas are generally favorable, though complications and recurrences remain possible, especially in tumors with aggressive features or critical anatomical involvement. In our series, 72.2% of patients had favorable outcomes, while 16.7% experienced mild neurological deficits including hemiparesis, seizures, or cranial nerve palsies. Poor outcomes (11.1%) were mainly due to recurrence, progressive disease, or metastasis. Özsoy *et al*. highlighted the role of tumor location: among parasagittal meningiomas, GTR was achieved in seven patients, with six experiencing good recovery, two remaining unchanged, and two showing poor outcomes, including one fatality due to cerebral edema. In contrast, falcine meningiomas had more favorable results: seven out of eight underwent total resection, five experienced good recovery, and only one death occurred due to postoperative meningitis, with no recurrence reported [47].

Kalfas *et al*. reported that 87% of patients with parasagittal and falcine meningiomas experienced no complications postoperatively, with brain edema being the most common complication, although none required surgical intervention [32]. Similarly, Narayan *et al*. reported a 5% operative mortality rate in patients with large meningiomas (≥5 cm), while Yaşar *et al*. observed no deaths among patients with giant tumors who underwent Simpson grade I or II resections [4, 8].

This study presents a focused exploratory analysis of the surgical challenges associated with giant parasagittal and falcine meningiomas, emphasizing key factors such as sinus invasion, vascular complexity, and anatomical constraints. Synthesizing detailed case-level data offers practical insights that may inform surgical planning and guide future research. However, limitations include the heterogeneity and incompleteness of available reports, variability in surgical techniques, and short-term follow-up, all of which restrict the generalizability of the findings. Further large-scale studies are warranted to validate these observations and develop standardized management protocols.

Conclusion

Giant parasagittal and falcine meningiomas pose significant surgical challenges, primarily due to SSS invasion, vascular complexity, and high-grade pathology in pediatric cases. Parasagittal tumors, particularly with middle-third SSS involvement, are associated with greater technical difficulty and surgical risk. Despite these factors, gross total resection and favorable outcomes can be achieved in most cases. Optimal results depend on careful preoperative venous assessment and individualized surgical strategies that balance maximal tumor resection with preservation of critical venous structures.

Disclosure

Clinical trial number

Not applicable.

Competing interests

The authors declare that there is no conflict of interest regarding publication of this paper.

Funding

No funding is available

Authors' contributions

TAN and NA conceptualized the study, designed the protocol and methodology, conducted the literature search and article screening, and contributed to drafting the manuscript. FB, DWW, and FB2 assisted in drafting the manuscript, supervised the overall process, and validated the findings. All authors read and approved the final version of the manuscript.

Acknowledgments

We thank all contributors for their work in creating the paper.

Consent to Publish declaration

Not applicable.

References

1. Byard RW, Bourne AJ, Clark B, Hanieh A. Clinicopathological and radiological features of two cases of intraventricular meningioma in childhood. Pediatr Neurosci. 1989;15(5):260-4. doi: 10.1159/000120478
2. Casali C, Del Bene M, DiMeco F. Falcine meningiomas. Handb Clin Neurol. 2020;170:101-106. doi: 10.1016/B978-0-12-822198-3.00032-X
3. Black P, Kathiresan S, Chung W. Meningioma surgery in the elderly: a case-control study assessing morbidity and mortality. Acta Neurochir (Wien). 1998;140(10):1013-6; discussion 1016-7. doi: 10.1007/s007010050209
4. Narayan V, Bir SC, Mohammed N, Savardekar AR, Patra DP, Nanda A. Surgical Management of Giant Intracranial Meningioma: Operative Nuances, Challenges, and Outcome. World Neurosurg. 2018 Feb;110:e32-e41. doi: 10.1016/j.wneu.2017.09.184
5. Li J, Mzimbiri JM, Zhao J, Zhang Z, Liao X, Liu J. Surviving the Largest Atypical Parasagittal Meningioma in a 2-Year-

Old Child: A Case Report and a Brief Review of the Literature. World Neurosurg. 2016 Mar;87:662.e1-6. doi: 10.1016/j.wneu.2015.10.078
6. Wang X, Wu R, Zhang P, Zhang C, Song G, Gao Z. Superior Sagittal Sinus Obstruction by Giant Meningiomas: Is Total Removal Feasible? World Neurosurg. 2016 Oct;94:111-119. doi: 10.1016/j.wneu.2016.06.113
7. Wang H, Yang Z, You H, Song J. How I do it: the surgical resection of a middle third parasagittal meningioma with venous preservation strategy. Acta Neurochir (Wien). 2022 May;164(5):1385-1389. doi: 10.1007/s00701-022-05129-6
8. Yaşar S, Kırık A. Surgical Management of Giant Intracranial Meningiomas. Eurasian J Med. 2021 Jun;53(2):73-78. doi: 10.5152/eurasianjmed.2021.20155
9. Otani N, Wada K, Toyooka T, Mori K. Occipital Interhemispheric Approach for Surgical Removal of the Middle Third Falx Meningioma: Two Case Reports. Asian J Neurosurg. 2018 Jul-Sep;13(3):789-791. doi: 10.4103/ajns.AJNS_158_16
10. Bansal C, Shah H, Bora SK, Suri A. Middle third falcine meningiomas-surgical nuances for cortical venous preservation. Acta Neurochir (Wien). 2024 May 18;166(1):220. doi: 10.1007/s00701-024-06088-w
11. Luther E, Ramsay I, Berke C, Makhoul V, Lu V, Elarjani T, Burks J, Berry K, Eichberg DG, Di L, Mansour S, Echeverry N, Morell A, Ivan M, Komotar R. Widening the Operative Corridor-Evaluating the Transcortical Approach to Giant Falcine Meningiomas. World Neurosurg. 2024 May;185:e442-e450. doi: 10.1016/j.wneu.2024.02.046
12. Dudley RWR, Torok MR, Randall S, Béland B, Handler MH, Mulcahy-Levy JM, Liu AK, Hankinson TC. Pediatric versus adult meningioma: comparison of epidemiology, treatments, and outcomes using the Surveillance, Epidemiology, and End Results database. J Neurooncol. 2018 May;137(3):621-629. doi: 10.1007/s11060-018-2756-1
13. Aboud E, Tamer WA, Ibn Essayed W, Al-Mefty O. Resection of Giant Invasive Parasagittal Atypical Meningioma With a Venous Graft Reconstruction of the Sagittal Sinus: 2-Dimensional Operative Video. Oper Neurosurg. 2021 Sep 15;21(4):E332-E333. doi: 10.1093/ons/opab232
14. Gotohda K, Uchino A, Suzuki T, Mishima K, Homma T, Miyama Y, Baba Y. Acute subdural hematoma caused by hemorrhagic falx meningioma: A case report and review of the literature. Radiol Case Rep. 2024 Apr 24;19(7):2804-2811. doi: 10.1016/j.radcr.2024.03.056
15. Bederson JB, Eisenberg MB. Resection and replacement of the superior sagittal sinus for treatment of a parasagittal meningioma: technical case report. Neurosurgery. 1995 Nov;37(5):1015-8; discussion 1018-9. doi: 10.1227/00006123-199511000-00026
16. Walker SE, Kaoutzani L, Vale FL. Supplementary Motor Area Syndrome After Resection of a Dominant Hemisphere Parasagittal Meningioma: A Case Report. Neurosurg Pract. 2023 Oct 13;4(4):e00067. doi: 10.1227/neuprac.0000000000000067
17. Dimou S, Nehoff HL, Jackson S. Falcine meningioma masquerading as biliary colic - Case report and literature review. J Clin Neurosci. 2021 May;87:66-68. doi: 10.1016/j.jocn.2021.02.004
18. Savateev AN, Konovalov AN, Gorelyshev SK, Satanin LA, Khukhlaeva EA, Shishkina LV, Ozerova VI, Valiakhmetova EF, Medvedeva OA. A giant hyperostotic parasagittal meningioma in a child with neurofibromatosis type II (a case report and literature review). Zh Vopr Neirokhir Im N N Burdenko. 2016;80(6):66-73. English, Russian. doi: 10.17116/neiro201680666-73
19. Rajagopal M, Toms J, Graham RS. Meningioma with holo-sagittal sinus involvement treated successfully with intrinsic sinus surgery: illustrative case. J Neurosurg Case Lessons. 2022 Apr 18;3(16):CASE21710. doi: 10.3171/CASE21710
20. Okunlola AI, Ibijola AA, Babalola OF, Okunlola CK, Erinomo OO. Parasagittal cystic meningioma mimicking hemangioblastoma: A case report. Surg Neurol Int. 2021 Jul 27;12:368. doi: 10.25259/SNI_507_2021
21. Honda Y, Shirayama R, Morita H, Kusuhara K. Pulmonary and pleural metastasis of intracranial anaplastic meningioma in a 3-year-old boy: A case report. Mol Clin Oncol. 2017 Oct;7(4):633-636. doi: 10.3892/mco.2017.1375
22. Doxtader EE, Butts SC, Holsapple JW, Fuller CE. Aggressive pediatric meningioma with soft tissue and lymph node metastases: a case report. Pediatr Dev Pathol. 2009 May-Jun;12(3):244-8. doi: 10.2350/08-07-0501.1
23. Alzughaibi RA, Almuhammadi GA, Alasmari SS, Khoja MM, Almashni AA. Challenging Resection of Bilateral Parasagittal and Falcine Meningioma Involving Both Anterior Third and Middle Third of the Superior Sagittal Sinus: A Case Report and Literature Review. Cureus. 2024 Jul 18;16(7):e64865. doi: 10.7759/cureus.64865
24. Hassan M, Salman I, Salman A, Tofan S, Salman I. Massive cystic falcine meningioma presented with slight symptoms: a case report. Ann Med Surg (Lond). 2024 Apr 29;86(6):3766-3769. doi: 10.1097/MS9.0000000000002108
25. Sim SK, Khairul Aizad A, Lim SS, Wong A. Large falcine meningioma presented as treatment-resistant depression: A case report. Med J Malaysia. 2019 Feb;74(1):87-89.
26. Papadimitriou K, Rocca A, Dunet V, Daniel RT. Feeding artery aneurysms associated with large meningiomas: case report and review of the literature. Heliyon. 2020 May 28;6(5):e04071. doi: 10.1016/j.heliyon.2020.e04071
27. Psaras T, Pantazis G, Steger V, Meyermann R, Honegger J, Beschorner R. Benign meningioma developing late lung metastases: case report and review of the literature. Clin Neuropathol. 2009 Nov-Dec;28(6):453-9. doi: 10.5414/npp28453
28. Kusdiansah M, Benet A, Ota N. Adaptative Diploic Vein Bypass of the Superior Sagittal Sinus in a Large Falcine Meningioma. World Neurosurg. 2023 Jul;175:45-46. doi: 10.1016/j.wneu.2023.04.023
29. Mathuriya SN, Vasishta RK, Khandelwal N, Pathak A, Sharma BS, Khosla VK. Calcified falx meningioma. Neurol India. 2000 Sep;48(3):285-7.
30. Karthigeyan M, Rajasekhar R, Salunke P, Singh A. Modified unilateral approach for mid-third giant bifalcine meningiomas: resection using an oblique surgical trajectory and falx window. Acta Neurochir (Wien). 2019 Feb;161(2):327-332. doi: 10.1007/s00701-018-3770-y
31. Wach J, Vychopen M, Basaran AE, Tatagiba M, Goldbrunner R, Güresir E. Overall survival and progression-free survival in pediatric meningiomas: a systematic review and individual patient-level meta-analysis. J Neurooncol. 2025 Apr;172(2):289-305. doi: 10.1007/s11060-024-04917-7
32. Kalfas F, Scudieri C. Neurosurgical Management of Parasagittal and Falcine Meningiomas: Judicious Modern Optimization of the Results in a 100-Case Study. Asian J Neurosurg. 2019 Nov 25;14(4):1138-1143. doi: 10.4103/ajns.AJNS_245_18
33. Armocida D, Catapano A, Palmieri M, Arcidiacono UA, Pesce A, Cofano F, Picotti V, Salvati M, Garbossa D, D'Andrea G, Santoro A, Frati A. The Surgical Risk Factors of Giant Intracranial Meningiomas: A Multi-Centric Retrospective Analysis of Large Case Serie. Brain Sci. 2022 Jun 22;12(7):817. doi: 10.3390/brainsci12070817
34. Hua L, Wang D, Zhu H, Deng J, Luan S, Chen H, Sun S, Tang H, Xie Q, Wakimoto H, Gong Y. Long-term outcomes of multimodality management for parasagittal meningiomas. J Neurooncol. 2020 Apr;147(2):441-450. doi: 10.1007/s11060-020-03440-9
35. Soyuer S, Chang EL, Selek U, Shi W, Maor MH, DeMonte F. Radiotherapy after surgery for benign cerebral

meningioma. Radiother Oncol. 2004 Apr;71(1):85-90. doi: 10.1016/j.radonc.2004.01.006
36. Aizer AA, Arvold ND, Catalano P, Claus EB, Golby AJ, Johnson MD, Al-Mefty O, Wen PY, Reardon DA, Lee EQ, Nayak L, Rinne ML, Beroukhim R, Weiss SE, Ramkissoon SH, Abedalthagafi M, Santagata S, Dunn IF, Alexander BM. Adjuvant radiation therapy, local recurrence, and the need for salvage therapy in atypical meningioma. Neuro Oncol. 2014 Nov;16(11):1547-53. doi: 10.1093/neuonc/nou098
37. Sun SQ, Hawasli AH, Huang J, Chicoine MR, Kim AH. An evidence-based treatment algorithm for the management of WHO Grade II and III meningiomas. Neurosurg Focus. 2015 Mar;38(3):E3. doi: 10.3171/2015.1.FOCUS14757
38. Chotai S, Schwartz TH. The Simpson Grading: Is It Still Valid? Cancers (Basel). 2022 Apr 15;14(8):2007. doi: 10.3390/cancers14082007
39. Aguiar PHP, Dos Santos RRP, Marson FAL, Dezena RA, Rampazzo ACMR. What is the ideal grade of resection for parasagittal meningiomas with the invasion of superior sagittal sinus? Simpson I or Simpson II resection? A retrospective observational study. Surg Neurol Int. 2022 Sep 16;13:423. doi: 10.25259/SNI_436_2022
40. Sirko AH, Perepelytsia VA. Parasagittal meningiomas: surgical treatment outcomes. Ukr Neurosurg J. 2022Sep.29;28(3):33-42. doi: 10.25305/unj.259324
41. Kvasha MS, Spiridonov AV. Surgical treatment of meningiomas invading the superior sagittal sinus. Ukr Neurosurg J. 2024Dec.30;30(4):51-6. doi: 10.25305/unj.312398
42. Amoo M, Henry J, Farrell M, Javadpour M. Meningioma in the elderly. Neurooncol Adv. 2023 Jun 3;5(Suppl 1):i13-i25. doi: 10.1093/noajnl/vdac107
43. Arivazhagan A, Devi BI, Kolluri SV, Abraham RG, Sampath S, Chandramouli BA. Pediatric intracranial meningiomas--do they differ from their counterparts in adults? Pediatr Neurosurg. 2008;44(1):43-8. doi: 10.1159/000110661
44. Tufan K, Dogulu F, Kurt G, Emmez H, Ceviker N, Baykaner MK. Intracranial meningiomas of childhood and adolescence. Pediatr Neurosurg. 2005 Jan-Feb;41(1):1-7. doi: 10.1159/000084858
45. Lakhdar F, Arkha Y, El Ouahabi A, Melhaoui A, Rifi L, Derraz S, El Khamlichi A. Intracranial meningioma in children: different from adult forms? A series of 21 cases. Neurochirurgie. 2010 Aug;56(4):309-14. doi: 10.1016/j.neuchi.2010.05.008
46. Sindou M. Meningiomas invading the sagittal or transverse sinuses, resection with venous reconstruction. J Clin Neurosci. 2001 May;8 Suppl 1:8-11. doi: 10.1054/jocn.2001.0868
47. Özsoy KM, Ökten Aİ, Ateş T, Arslan A, Menekşe G, Çikili M, Güzel A. Intracranial benign giant meningiomas: a clinical analysis of 56 cases. Neurosurgery Quarterly. 2013 Feb 1;23(1):27-32. doi: 10.1097/WNQ.0b013e318266c501

Original article

Ukrainian Neurosurgical Journal. 2026;32(1):60-68
doi: 10.25305/unj.339497

Global research trends on seizure detection in critical care after decompressive craniectomy: A bibliometric analysis

Kuat Widodo, Saryono, Novita Anggraeni

Department of Nursing, Jenderal Soedirman University, Purwokerto, Indonesia

Received: 17 September 2025
Accepted: 03 November 2025

Address for correspondence: *Kuat Widodo, Departemen of Nursing, Jenderal Soedirman University, Jalan Prof. Dr. HR. Boenjamin 708, Purwokerto 53122, Indonesia, e-mail: kuat.widodo@mhs.unsoed.ac.id*

Background: Postoperative seizures are a recognized complication following decompressive craniectomy (DC); the global research landscape regarding seizure detection in this context remains insufficiently characterized. Bibliometric mapping provides insights into emerging trends and knowledge gaps.

Objective: This study aims to map and evaluate international research output on seizure detection in critically ill patients after decompressive craniectomy.

Methods: Relevant literature was collected from Scopus, PubMed, CrossRef, and Google Scholar using the terms 'decompressive craniectomy AND seizure AND detected' via the Publish or Perish software. Records were exported in RIS format and analysed with VOSviewer to generate keyword co-occurrence networks, cluster maps, and temporal trend visualizations.

Results: A total of 1,605 publications from 2015–2025 were analyzed. Annual research volume increased, particularly since 2018. The co-occurrence network analysis identified four thematic clusters: (1) clinical outcomes and prognosis, (2) surgical techniques and perioperative management, (3) intracranial pressure and monitoring strategies, and (4) seizure detection and critical neurological care. Overlay analysis revealed a gradual thematic shift toward seizure monitoring and electroencephalography EEG-based approaches in recent years, while density visualization confirmed that seizure detection remains an emerging but relatively underdeveloped research area. The most prolific contributor was identified with 126 publications.

Conclusion: Although publications on decompressive craniectomy have grown rapidly, seizure detection remains a relatively small but growing research topic. Increased focus on neurocritical monitoring indicates future opportunities for developing evidence-based protocols and collaborative studies in this field.

Keywords: *decompressive craniectomy; seizure detection; intensive care; bibliometric studies; VOSviewer*

Introduction

Decompressive craniectomy (DC) is a crucial surgical intervention often performed to reduce intracranial pressure in patients with severe brain injury, ischaemic or haemorrhagic stroke who experience refractory cerebral oedema [1-3]. Although DC can save lives by reducing herniation and improving cerebral perfusion, the procedure also places patients at risk of short-term and long-term neurological complications [4-6].

One of the most commonly reported complications is seizures. Seizures in post-DC patients not only worsen neurological dysfunction but are also associated with increased length of intensive care, morbidity, and mortality [7,8]. Therefore, early detection and monitoring of seizures in the critical care unit is an important aspect of postoperative management. The prevalence of post-craniotomy seizures varies, generally ranging from 3% to 30% in various studies, depending on the patient's condition and the type of surgical procedure performed [9, 10].

Clinical challenges surrounding seizure detection in the complex post-DC population: seizures can be clinical or subclinical (non-convulsive), and clinical signs are often masked by sedation, paralysis, or comorbid medical conditions, making clinical-based detection difficult. In this context continuous electroencephalography (cEEG) monitoring, automatic detection algorithms, multimodal monitoring including EEG, intracranial pressure, oximetry), and other non-invasive techniques play a crucial role [11-13].

However, the diversity of protocols, resource availability, variations in seizure definitions, and differences in reported outcomes make the consolidation of clinical knowledge and research challenging.

Although seizures are a common complication after severe brain injury, patients undergoing decompressive craniectomy represent a distinct subgroup due to their altered intracranial physiology and cortical exposure. This subgroup requires specific EEG monitoring approaches and postoperative management strategies, justifying the bibliometric focus on this population.

Over the past two decades, the literature on post-DC seizure detection has grown alongside advances in monitoring technology about portable EEG, machine

learning for EEG pattern detection and increased awareness of the importance of subclinical seizures [14-16]. In the present study, we employed bibliometric approach to describe research trends about seizure in post decompressive craniectomy patient based on numerous case studies such as case series, observational studies, and a number of narrative or systematic reviews.

The reasons for choosing bibliometric studies on this topic are based on several practical and scientific considerations. First, there has been no bibliometric study that systematically maps global trends in research on seizure detection in post-DC with outcomes in intensive care. Second, bibliometric research can also identify methodological trends, whether studies tend to be observational, experimental, or registry-based, thereby providing input for stronger study designs in the future. Third, the identification of international collaboration networks and funding sources can assist policymakers and researchers in designing collaboration strategies or resource allocation.

Given the complexity of clinical phenomena involved and the heterogeneity of the literature, bibliometric studies must be conducted with a clear scope regarding the range of publication years, databases and structured keywords. Analysis methods may involve basic quantitative metrics such as annual publication numbers, citations and H-index. Network analyses — such as author collaboration, citation collaboration, and bibliographic linking — as well as topic modelling or clustering using VOSviewer, CiteSpace, or other bibliometric tools, can be used to identify research trends and topic evolution over time.

Although the number of publications related to decompressive craniectomy has increased rapidly, research on the detection of post-DC seizures is still relatively limited, fragmented, and mostly in the form of observational studies or case reports. In addition, there has been no bibliometric analysis that specifically maps global trends, collaborations, and the direction of research development in this field.

Therefore, this study aims to present a bibliometric mapping of seizure detection in critically ill patients after decompressive craniectomy, thereby providing a foundation for future research development, clinical practice, and health policy.

Materials and methods

Study design

This study employed a bibliometric design to describe publication trends, author collaborations, and research topics related to seizure detection in patients after decompressive craniectomy in the last decades from 2015-2025.

Data sources and search strategy

Bibliographic data were collected from four main sources: Scopus, CrossRef, PubMed, and Google Scholar. Scopus was selected as the primary source due to its broad coverage and high indexing standards. CrossRef was used to obtain publication metadata including titles, authors, publication years, digital object identifiers (DOIs), journal names, and citations. PubMed was selected because it is relevant to the fields of medicine and critical care nursing, and provides peer-reviewed literature in the fields of neuroscience and intensive care. Google Scholar was used to supplement the literature search with a broader range of publications, including articles that may not be indexed in traditional databases. Data collection was carried out using the latest version of Publish or Perish software, which can extract publication metadata from these three sources in RIS format. The search strategy was formulated using a combination of the keywords 'decompressive craniectomy' AND 'seizures' AND 'detected' and complete Boolean operators such as "decompressive craniectomy" OR "craniectomy" AND "seizure" OR "epilepsy" OR "convulsion" AND "detection" OR "monitoring" OR 'EEG' OR "continuous EEG". The search was limited to the year range between 2015 and 2025, publication type must be research articles and reviews, in English and research procedure.

The search was restricted to the period from 2015-2025 in order to capture the post-digital monitoring era, during which continuous EEG and algorithmic seizure detection became more widespread in critical care and neurosurgical settings.

Data analysis

Vosviewer

The analysis was performed using the latest VOSviewer software (version 1.6.19) with the following steps: Descriptive bibliometric analysis: calculating the number of publications per year, journal distribution, citations, and H-index. Network analysis by Co-authorship: to map author and institutional collaborations, Co-citation: to identify the most influential references and Keyword co-occurrence: to find dominant research topics (research hotspots). Bibliometric map visualisation: created with VOSviewer, producing network visualisation, density visualisation, and temporal visualisation (overlay visualisation) maps to see developments.

PRISMA flowchart

Brief methodology used by researchers during processing. RIS parsing: each RIS file is separated per entry, then common tags are extracted. Duplicate removal prioritises DOI as the key and when DOI is unavailable, normalised titles are used. Records are filtered to include only publications between $2015 \leq$ year ≤ 2025. Prioritise relevance of titles, abstracts and keywords containing the terms decompressive craniectomy, craniectomy and craniotomy as well as terms related to seizures. Only documents with tags, journal indicators or articles included are retrieved. Each included record was manually screened to confirm that the population involved decompressive craniectomy or hemicraniectomy. Studies limited to closed-skull traumatic brain injury (TBI) without surgical decompression were excluded. Heuristic clinical trial method by searching for the phrases clinical trial, randomised, RCT, controlled trial, or tags containing Clinical Trial.

Results

Although 1,605 records were analysed for bibliometric mapping, only 13 met strict inclusion for detailed descriptive synthesis focusing specifically on

This article contains some figures that are displayed in color online but in black and white in the print edition.

EEG-based seizure detection following DC. This explains the apparent discrepancy between PRISMA and total bibliometric data (***Fig. 1***).

Base on mapping of research topic clusters, keywords related to decompressive craniectomy and seizure detection are distributed across several main clusters. The purple cluster focuses on seizures, detection, and neurocritical care representing research on post-operative seizure complications following craniectomy and both clinical and instrumental detection efforts. The green cluster is related to the terms management, review, craniotomy, acute subdural haematoma, and medical treatment emphasizing aspects of critical care management following DC. The blue cluster is dominated by the keywords including cranioplasty, intracranial hypertension, monitoring, and risk factors, reflecting research on postoperative intracranial pressure management and associated risks. The red cluster contains terms such as admission, Glasgow Coma Scale (GCS), discharge, mean age, outcome, and significant difference indicating a focus on patient characteristics, neurological assessment scores, and clinical outcomes. Notably, the keywords 'seizure' and 'detection' are located at the edge of the network, suggesting that these topics are still niche research area with limited connectivity compared to other major topics such as intracranial hypertension and postoperative management (***Fig. 2***).

The changes in research focus based on year of publication shows the distribution of research publication. Yellow indicates more recent research (2021–2022), while blue-violet denotes earlier research. Initial research predominantly focused on intracranial hypertension, cranioplasty, and management. In contrast, current trends (2021–2022) show an increased focus on admission characteristics, outcome measures (GOS, the Rankin scale), and seizure detection in critical care units. This indicates a shift in research from purely surgical aspects to neurological monitoring and patient outcomes, including seizure complications (***Fig. 3***).

Base on the research topic intensity and saturation level, the yellow areas indicate the most frequently occurring keywords and the focus of the research. The most prominent words are 'management', 'intracranial hypertension', and 'cranioplasty'. Meanwhile, the terms 'seizure', "detection", and 'neurocritical care', although appearing, are still in areas with lower intensity, indicating that literature related to seizure detection after decompressive craniectomy is still relatively limited compared to other topics (***Fig. 4***).

Description

Based on ***Figs. 2, 3 and 4***, research on seizure detection in patients after DC has begun to appear in the literature, but it is still marginalized compared to major themes such as intracranial hypertension management and post-operative outcomes. Recent trends show a

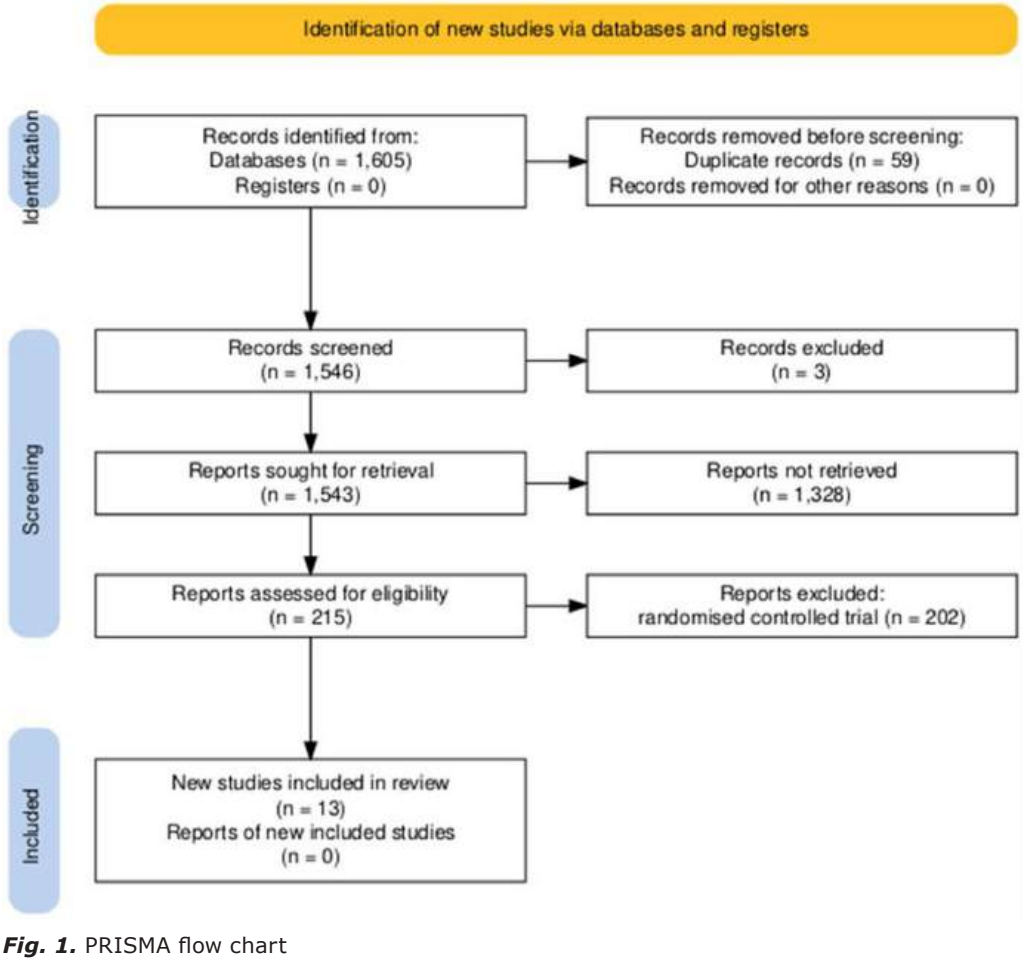

Fig. 1. PRISMA flow chart

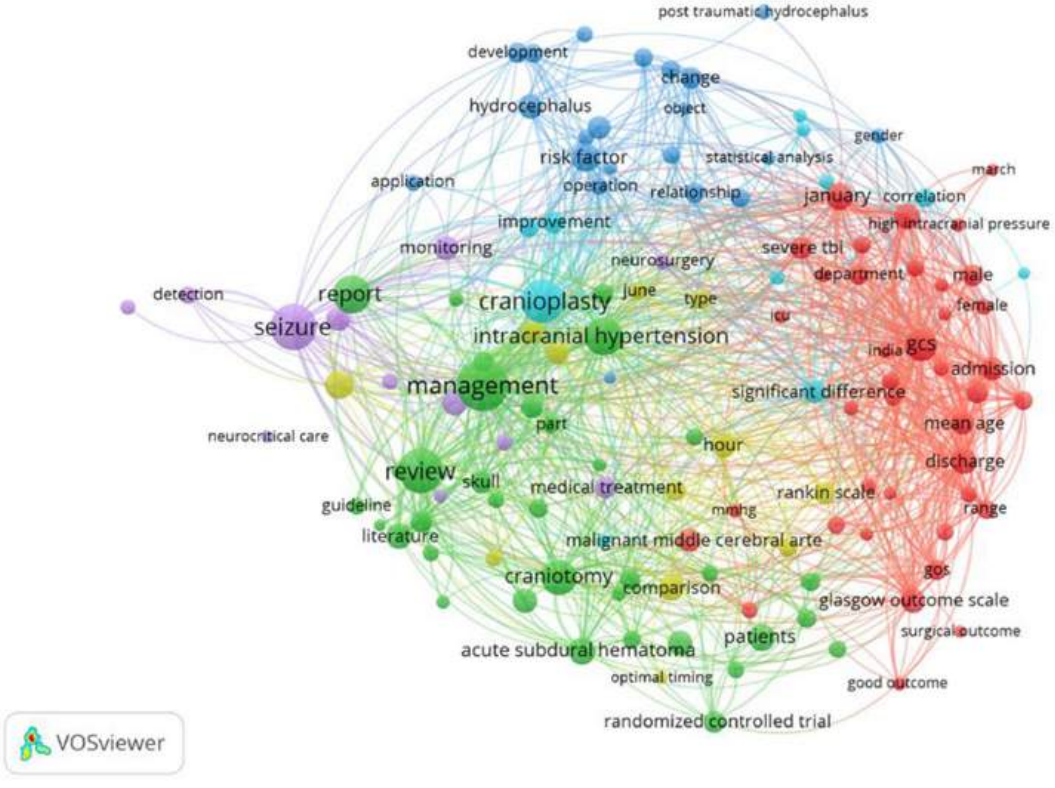

Fig. 2. Mapping of research topic clusters

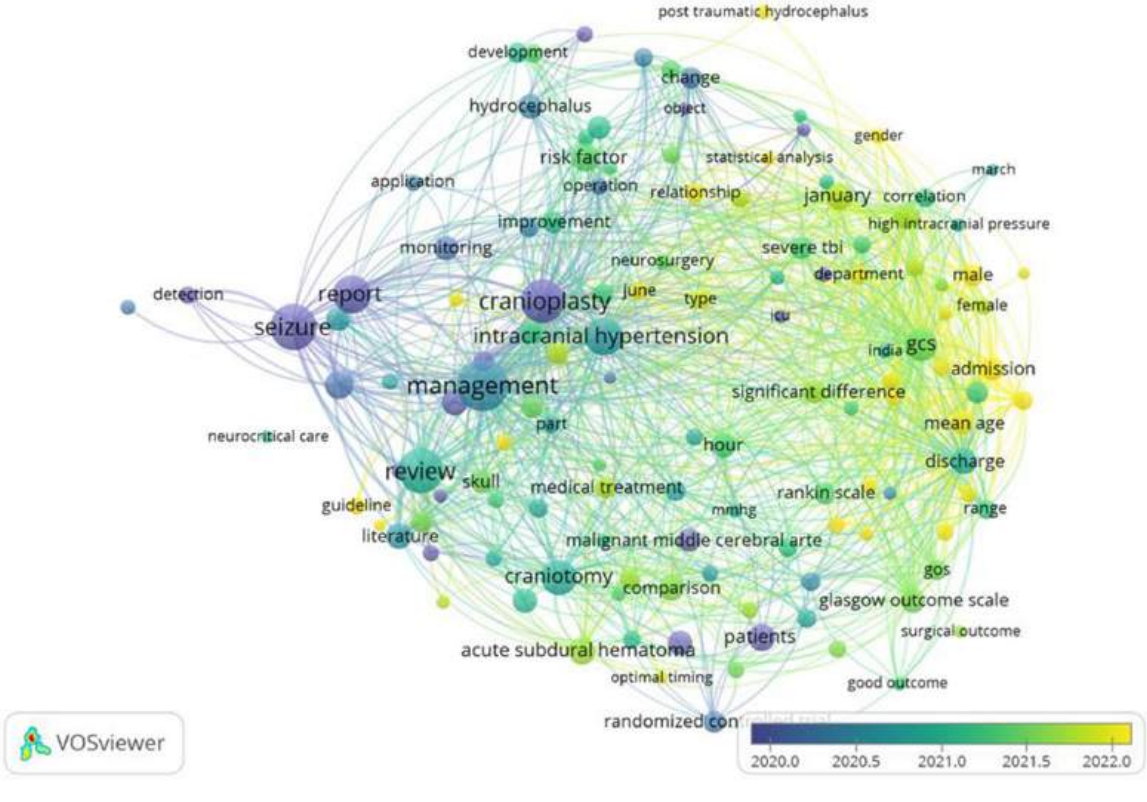

Fig. 3. Changes in research focus based on year of publication

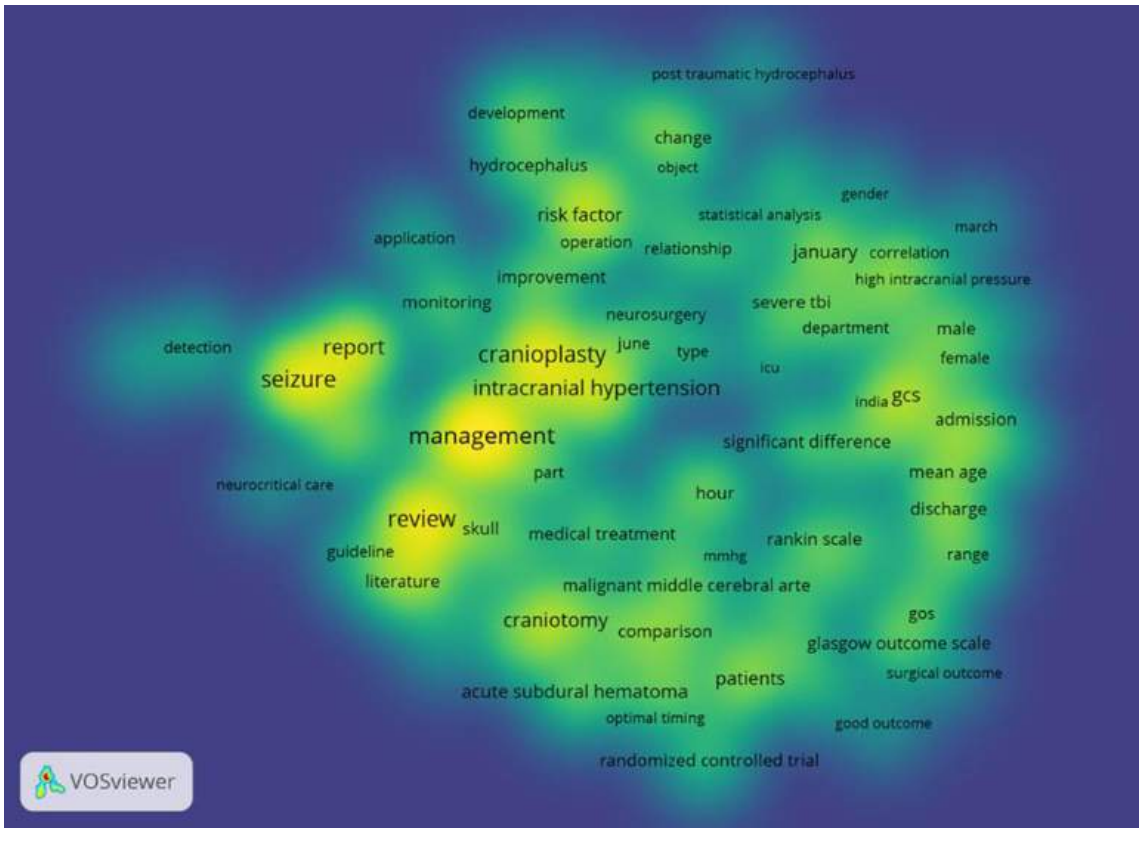

Fig. 4. Research topic intensity and saturation level

shift in focus towards neurological monitoring, patient outcomes, and post-surgical complications, including seizures. These developments highlight opportunities for further research with a continuous EEG monitoring approach, the use of artificial intelligence (AI) for automatic detection, and the relationship between subclinical seizures and long-term functional outcomes.

Discussion

Bibliometric analysis shows that publications on seizure detection in patients after decompressive craniectomy increased between 2015 and 2025. This trend illustrates the growing attention of clinicians and researchers to the problem of neurological complications in the form of seizures that can affect patient outcomes in critical care units. Studies on the use of continuous EEG in the ICU support these findings, as many critically ill patients experience subclinical seizures or non-convulsive status epilepticus that can only be detected with specialised monitoring [17]. Integrated bibliometric findings, covering author productivity, international contributions, methodological characteristics, instruments, and thematic grouping (***Tables 1–3***), provide a comprehensive overview of current research trends in decompressive craniectomy and seizure detection.

Publication patterns show a dominance of developed countries, such as the United States, Europe, and Japan, which have comprehensive neurocritical facilities as summarised in ***Table 3***. Conversely, contributions from developing countries remain limited due to constraints in resources, technology, and research funding. This pattern is consistent with bibliometrics on the topic of epilepsy, where the most numerous and influential publications originate from research centres in developed countries [18, 19].

Keyword analysis using VOSviewer reveals three main clusters: continuous EEG, seizure monitoring, and neurocritical outcome. These clusters emphasise that research is not only focused on seizure identification, but also on early detection efforts and their relationship with patient clinical outcomes as shown in ***Table 1 and 3***. This finding aligns with previous articles emphasising the importance of continuous EEG monitoring to detect non-convulsive seizures and their relationship with neurological outcomes [16, 20-22].

Compared with general TBI literature, publications focusing on decompressive craniectomy reveal distinct thematic patterns (***Table 1***), particularly cortical excitability and postoperative electrophysiology. While seizure risk is inherently linked to the primary brain injury, the DC procedure introduces secondary factors such as dural irritation and hemodynamic shifts which may modulate epileptogenesis. Therefore, bibliometric separation from the broader TBI population is justified to capture these unique research patterns.

The overlay map reveals a shift in research focus from descriptive studies to clinical trials assessing the effectiveness of detection methods, particularly continuous EEG. Whereas previous research mostly described phenomena, more recent publications explore new technologies, including the use of machine learning-based algorithms for automatic seizure detection [23-25].

EEG acquisition in post-craniectomy patients differs technically from conventional scalp EEG due to bone flap removal. The absence of skull attenuation enhances cortical potentials, possibly altering spectral power. Several studies place electrodes near the defect margins, whereas others employe intracranial or hybrid electrode arrays. Such heterogeneity in electrode configuration and montage contributes to methodological variation in seizure detection reports.

In terms of authors and institutions, it is evident that a number of highly productive researchers form centres of excellence in the field of neurocritical care as shown in ***Table 2 and 3***. However, international collaboration in publications remains relatively limited. This presents an opportunity to expand international collaboration to standardise seizure detection worldwide. A similar phenomenon is observed in epilepsy research, where global collaboration remains suboptimal [26-28].

Most publications appear in high-impact journals such as Neurocritical Care and the Journal of Clinical Neurophysiology. Related articles are also found in general neurology and intensive care journals, demonstrating the interdisciplinary nature of this research. One example is a publication in the Journal of Intensive Care highlighting non-convulsive seizures in intensive care unit (ICU) patients [17, 29, 30].

In terms of citations, articles discussing continuous EEG monitoring received the most attention. This is understandable given that subclinical seizures are often not identified through conventional methods. For example, research conducted in patients after brain tumour surgery have proved that non-convulsive seizures are more effectively detected using cEEG.

Temporally, publications increased sharply after 2020, coinciding with the development of bedside monitoring technology and increased clinical awareness of hidden seizures (***Table 2 and 3***). Additionally, there have been more clinical trials and research on new devices that enable real-time seizure detection using dual sensors such as accelerometers and oximeters [13, 16, 31].

However, limitations remain evident. Most publications are retrospective or based on a single research centre, resulting in insufficient external evidence. Multicentre studies with large populations and long-term observations are urgently needed to strengthen the scientific basis regarding the effectiveness of post-surgical seizure detection [32, 33].

Overall, these bibliometric findings confirm that the topic of post-decompressive craniectomy seizure detection is a rapidly developing and clinically important field. Future efforts should focus on enhancing international collaboration, conducting multicentre research, and the use of advanced, accessible technology, especially in developing countries. Evaluations of the effectiveness of detection methods should also consider aspects of sensitivity, specificity, and readiness for implementation in various healthcare settings.

Table 1. Mapping of keyword co-occurrence analysis produced several clusters

Cluster	Main topic	Keyword	Interpretation
Red	Clinical outcome	admission, GCS, discharge, outcome	Focus on the condition of patients admitted to the ICU and outcomes after discharge
Green	Management & Surgery	management, craniotomy, acute subdural hematoma	Management, craniotomy, acute subdural haematoma. Emphasises surgical aspects and critical care management
Blue	Intracranial Pressure	intracranial hypertension, monitoring, risk factor	Related to physiological complications after surgery
Purple	Seizures & Detection	seizure, detection, neurocritical care	Begins to highlight issues of clinical and subclinical seizure detection

Table 2. Mapping the most productive authors

No	Author	Number of publications	Description
1	Honeybul, Stephen	126	Numerous publications related to craniectomy & complications
2	Beucler, Nathan	10	Focus on patient outcomes
3	Kolias, Angelos G.	8	Neurosurgeon, active in DC research
4	Wettervik,Teodor Svedung	7	Focus on neurocritical care & monitoring
5	(others)	5–7	Researchers related to DC management

Table 3. Mapping country with high contributions

No	Country	Number of publications	Main focus	Register of bibliometric
1	United States	32	cEEG, post-craniectomy outcomes, ICU seizures	Highest citation dominance
2	Germany	15	Neurotrauma, detection of seizures after TBI and stroke	Central European collaboration
3	Japan	12	Neurosurgery, post-operative monitoring of brain tumours	Many single-center studies
4	China	11	Non-invasive detection, AI algorithms for seizure detection	Increasing trend since 2020
5	United Kingdom	10	Post-DC neurological prognosis, cEEG monitoring	Focus on clinical trials
6	South Korea	9	Brain trauma, post-DC outcomes with EEG	Active neurotrauma centers
7	Canada	7	Multicenter studies, neurocritical care guidelines	Collaboration with the US
8	Italy	6	Post-stroke and DC neurological outcomes	Focus on functional outcomes
9	France	6	Neurointensive monitoring, post-operative epilepsy	Mixed cohort & trial studies
10	India	5	Limited access to EEG, clinical focus on TBI	Few publications
11	Australia	4	Small ICU & post-brain trauma studies	International collaboration
12	Netherlands	3	Outcome & seizure prediction models	Computational focus
13	Spain	3	Neuroprognosis and post-operative epilepsy	ICU Based studies
14	Turkey	2	Case studies of DC and post-operative seizures	Limited publications
15	Other countries (misc.)	5	Sporadic studies (Sweden, Brazil, Egypt, Iran, Taiwan)	Minor contributions

Conclusion

Although research on decompressive craniectomy has advanced significantly over the past two decades, yet seizure detection remains an understudied area. Increased research in this area is crucial for improving clinical outcomes and guiding evidence-based practice in the critical care management of patients following decompressive craniectomy.

Future research directions

Given the number of studies related to early detection of post-DC seizures, further research is needed. This includes multicenter cohort studies to evaluate the incidence of seizures after DC, the application of advanced EEG techniques and digital biomarkers in seizure detection, and outcome-based studies linking seizure occurrence to functional recovery, clinical trials evaluating seizure monitoring interventions, and consensus guidelines that integrate seizure detection into the DC care pathway.

Declaration of interest

There is no conflict of interest in this study

Acknowledgements

The author would like to thank the Master's Programme in Nursing, Faculty of Health Science, Jenderal Soedirman University for supporting this study.

References

1. Honeybul S, Ho KM. Decompressive craniectomy--a narrative review and discussion. Aust Crit Care. 2014 May;27(2):85-91. doi: 10.1016/j.aucc.2013.06.001
2. Laurent D, Mohan A, Lucke-Wold B, Hoh B. Decompressive Hemicraniectomy and Suboccipital Craniectomy for Acute Ischemic Stroke. In: Ovbiagele B, Kim AS. Ischemic Stroke Therapeutics: A Comprehensive Guide. Springer International Publishing; 2024. P. 101-109. doi: 10.1007/978-3-031-49963-0
3. Mezue W, Ndubuisi C. Decompressive craniectomy in the management of traumatic brain injury: a review of

current practice. Open Access Surgery. 2015;8:73-83 https://doi.org/10.2147/OAS.S52742
4. Miller CA, Coughlin DJ, Bell R. Decompressive Craniectomy for Severe TBI. In: Ecklund J, Moores L, editors. Neurotrauma Management for the Severely Injured Polytrauma Patient. Springer International Publishing; 2017. P. 167-191 doi: 10.1007/978-3-319-40208-6_19
5. Pallesen LP, Barlinn K, Puetz V. Role of Decompressive Craniectomy in Ischemic Stroke. Front Neurol. 2019 Jan 9;9:1119. doi: 10.3389/fneur.2018.01119
6. Venturini S, Hutchinson P, Kolias AG. Decompressive Craniectomy in the Management of Traumatic Brain Injury. In: Honeybul S, Kolias AG, editors. Traumatic Brain Injury. Springer; 2021. P. 205-214. doi: 10.1007/978-3-030-78075-3_20
7. Gopalakrishnan MS, Shanbhag NC, Shukla DP, Konar SK, Bhat DI, Devi BI. Complications of Decompressive Craniectomy. Front Neurol. 2018 Nov 20;9:977. doi: 10.3389/fneur.2018.00977
8. Mraček J, Mork J, Dostal J, Tupy R, Mrackova J, Priban V. Complications Following Decompressive Craniectomy. J Neurol Surg A Cent Eur Neurosurg. 2021 Sep;82(5):437-445. doi: 10.1055/s-0040-1721001
9. Paquin-Lanthier G, Subramaniam S, Leong KW, Daniels A, Singh K, Takami H, Chowdhury T, Bernstein M, Venkatraghavan L. Risk Factors and Characteristics of Intraoperative Seizures During Awake Craniotomy: A Retrospective Cohort Study of 562 Consecutive Patients With a Space-occupying Brain Lesion. J Neurosurg Anesthesiol. 2023 Apr 1;35(2):194-200. doi: 10.1097/ANA.0000000000000798
10. Sueiras M, Thonon V, Santamarina E, Sánchez-Guerrero Á, Riveiro M, Poca MA, Quintana M, Gándara D, Sahuquillo J. Is Spreading Depolarization a Risk Factor for Late Epilepsy? A Prospective Study in Patients with Traumatic Brain Injury and Malignant Ischemic Stroke Undergoing Decompressive Craniectomy. Neurocrit Care. 2021 Jun;34(3):876-888. doi: 10.1007/s12028-020-01107-x
11. Desai M, Lewis C, Badjatia N. Multimodal Monitoring in Decompressive Craniectomy for Traumatic Brain Injury and Stroke. In: Aarabi B, Simard JM, editors. Decompressive Craniectomy. New York: Nova Science Publishers; 2018. P. 43–84.
12. Makarenko S, Griesdale DE, Gooderham P, Sekhon MS. Multimodal neuromonitoring for traumatic brain injury: A shift towards individualized therapy. J Clin Neurosci. 2016 Apr;26:8-13. doi: 10.1016/j.jocn.2015.05.065
13. Casault C, Couillard P, Kromm J, Rosenthal E, Kramer A, Brindley P. Multimodal brain monitoring following traumatic brain injury: A primer for intensive care practitioners. J Intensive Care Soc. 2022 May;23(2):191-202. doi: 10.1177/1751143720980273
14. Freund BE, Feyissa AM, Khan A, Middlebrooks EH, Grewal SS, Sabsevitz D, Sherman WJ, Quiñones-Hinojosa A, Tatum WO. Early Postoperative Seizures Following Awake Craniotomy and Functional Brain Mapping for Lesionectomy. World Neurosurg. 2024 Jan;181:e732-e742. doi: 10.1016/j.wneu.2023.10.119
15. Manzouri F, Duempelmann M, Heller S, Woias P, Schulze-Bonhage A. Patient-based feature optimization of a seizure detector for closed-loop stimulation. Brain Stimulation: Basic, Translational, and Clinical Research in Neuromodulation. 2019 Mar 1;12(2):411.
16. Nouboue C, Selfi S, Diab E, Chen S, Périn B, Szurhaj W. Assessment of an under-mattress sensor as a seizure detection tool in an adult epilepsy monitoring unit. Seizure. 2023 Feb;105:17-21. doi: 10.1016/j.seizure.2023.01.005
17. Kubota Y, Nakamoto H, Egawa S, Kawamata T. Continuous EEG monitoring in ICU. J Intensive Care. 2018 Jul 17;6:39. doi: 10.1186/s40560-018-0310-z
18. Huo Q, Luo X, Xu ZC, Yang XY. Machine learning applied to epilepsy: bibliometric and visual analysis from 2004 to 2023. Front Neurol. 2024 Apr 2;15:1374443. doi: 10.3389/fneur.2024.1374443
19. Schenck HE, Mangat HS. Towards Improved Organizational Governance of Neurotrauma Surveillance Comment on "Neurotrauma Surveillance in National Registries of Low- and Middle-Income Countries: A Scoping Review and Comparative Analysis of Data Dictionaries". Int J Health Policy Manag. 2023;12:7554. doi: 10.34172/ijhpm.2022.7554
20. Brondani R, Garcia de Almeida A, Abrahim Cherubini P, Mandelli Mota S, de Alencastro LC, Antunes ACM, Bianchin Muxfeldt M. High Risk of Seizures and Epilepsy after Decompressive Hemicraniectomy for Malignant Middle Cerebral Artery Stroke. Cerebrovasc Dis Extra. 2017;7(1):51-61. doi: 10.1159/000458730
21. Rowberry T, Kanthimathinathan HK, George F, Notghi L, Gupta R, Bill P, Wassmer E, Duncan HP, Morris KP, Scholefield BR. Implementation and Early Evaluation of a Quantitative Electroencephalography Program for Seizure Detection in the PICU. Pediatr Crit Care Med. 2020 Jun;21(6):543-549. doi: 10.1097/PCC.0000000000002278
22. Statsenko Y, Babushkin V, Talako T, Kurbatova T, Smetanina D, Simiyu GL, Habuza T, Ismail F, Almansoori TM, Gorkom KN, Szólics M, Hassan A, Ljubisavljevic M. Automatic Detection and Classification of Epileptic Seizures from EEG Data: Finding Optimal Acquisition Settings and Testing Interpretable Machine Learning Approach. Biomedicines. 2023 Aug 24;11(9):2370. doi: 10.3390/biomedicines11092370
23. Chawla D, Sharma E, Rajab N, Łajczak P, Silva YP, Baptista JM, Pomianoski BW, Ahmed AR, Majeed MW, de Sousa YG, Pinto ML, Sahin OK, Ibrahim MH, Guedes IHL, Chatterjee A, Barbosa RG, Fagundes W. Utilizing machine learning techniques for EEG assessment in the diagnosis of epileptic seizures in the brain: A systematic review and meta-analysis. Seizure. 2025 Mar;126:16-23. doi: 10.1016/j.seizure.2025.01.021
24. Vitt JR, Mainali S. Artificial Intelligence and Machine Learning Applications in Critically Ill Brain Injured Patients. Semin Neurol. 2024 Jun;44(3):342-356. doi: 10.1055/s-0044-1785504
25. Lamichhane B, Kim Y, Segarra S, Zhang G, Lhatoo S, Hampson J, Jiang X. Automated detection of activity onset after postictal generalized EEG suppression. BMC Med Inform Decis Mak. 2020 Dec 24;20(Suppl 12):327. doi: 10.1186/s12911-020-01307-7
26. Bakula DM, Junger KW, Guilfoyle SM, Mara CA, Modi AC. Key predictors of the need for a family-focused pediatric epilepsy adherence intervention. Epilepsia. 2022 Aug;63(8):2120-2129. doi: 10.1111/epi.17302
27. Mariajoseph FP, Chen Z, Sekhar P, Rewell SS, O'Brien TJ, Antonic-Baker A, Semple BD. Incidence and risk factors of posttraumatic epilepsy following pediatric traumatic brain injury: A systematic review and meta-analysis. Epilepsia. 2022 Nov;63(11):2802-2812. doi: 10.1111/epi.17398
28. Rosenthal ES. Seizures, Status Epilepticus, and Continuous EEG in the Intensive Care Unit. Continuum (Minneap Minn). 2021 Oct 1;27(5):1321-1343. doi: 10.1212/CON.0000000000001012
29. Limotai C, Jirasakuldej S, Wongwiangiunt S, Tumnark T, Suwanpakdee P, Wangponpattanasiri K, Rakchue P, Tungkasereerak C, Pleumpanupatand P, Tansuhaj P, et al. Efficacy of delivery of care with Tele-continuous EEG in critically ill patients: a multicenter randomized

controlled trial (Tele-cRCT study) study. Crit Care. 2025 Jan 7;29(1):15. doi: 10.1186/s13054-024-05246-x
30. Rubinos C, Alkhachroum A, Der-Nigoghossian C, Claassen J. Electroencephalogram Monitoring in Critical Care. Semin Neurol. 2020 Dec;40(6):675-680. doi: 10.1055/s-0040-1719073
31. Tagore S, Reche A, Paul P, Deshpande M. Electromyography: Processing, Muscles' Electric Signal Analysis, and Use in Myofunctional Orthodontics. Cureus. 2023 Dec 19;15(12):e50773. doi: 10.7759/cureus.50773
32. Karagianni MD, Brotis AG, Gatos C, Kalamatianos T, Vrettou C, Stranjalis G, Fountas KN. Neuromonitoring in Severe Traumatic Brain Injury: A Bibliometric Analysis. Neurocrit Care. 2022 Jun;36(3):1044-1052. doi: 10.1007/s12028-021-01428-5
33. Sconzo D, Wadhwa A, Balagurunath K, Berube M, Wetsel Z, Sakthiyendran NA, Penumaka A, Enriquez-Marulanda A, Ravina K, Binello E. Predictors of seizures in postoperative traumatic brain injury patients: A single center retrospective study. Clin Neurol Neurosurg. 2025 Oct;257:109116. doi: 10.1016/j.clineuro.2025.109116

Original article

Ukrainian Neurosurgical Journal. 2026;32(1):69-91
doi: 10.25305/unj.341693

Development and validation of a multilevel scale for quantitative assessment of mechanical exposure in traumatic spinal injuries

Oleksii S. Nekhlopochyn [1], Vadim V. Verbov [2], Ievgen V. Cheshuk [2], Milan V. Vorodi [2]

[1] Spine Surgery Department, Romodanov Neurosurgery Institute, Kyiv, Ukraine
[2] Restorative Neurosurgery Department, Romodanov Neurosurgery Institute, Kyiv, Ukraine

Received: 19 October 2025
Accepted: 14 November 2025

Address for correspondence:
Oleksii S. Nekhlopochyn, Spine Surgery Department, Romodanov Neurosurgery Institute, 32 Platona Maiborody st., Kyiv, 04050, Ukraine, e-mail: AlexeyNS@gmail.com

Objective: To develop, theoretically substantiate, and perform primary validation of a multilevel (0–10 points) scale for quantitative assessment of the intensity of external mechanical impact in traumatic spinal injuries.

Materials and methods: The study design followed the COSMIN (Consensus-based Standards for the Selection of Health Measurement Instruments) principles for developing and validating medical measurement tools, ensuring an adequate level of scientific validity and reproducibility. A literature review (PubMed, Scopus, Web of Science, 1990–2025) enabled the identification of threshold values and modifying factors, including patient body mass, the transmission coefficient of impulse ($T_{land)}$), and the effective deceleration distance (S_{land}). Two datasets were used for validation: 40 standardized clinical vignettes and 52 real cases of thoracolumbar junction trauma (T11–L2) with mandatory verification by computed tomography/magnetic resonance imaging. Construct and criterion validity, inter-rater reliability (ICC, κ), absolute reliability (SEM, MDC_{95}), diagnostic accuracy (ROC analysis), agreement level (Bland–Altman), and threshold stability were assessed.

Results: Based on comparative analysis of various approaches, the concept of "equivalent fall height" was proposed as a universal criterion of mechanical exposure in spinal trauma. An 11-level (0–10) quantitative scale and a spine-oriented derived metric were developed. Primary validation demonstrated high inter-rater agreement (ICC(2,1): 0.84 for the basic indicator and 0.79 for the spinal-oriented one; ICC(2,k): 0.95 and 0.92), acceptable absolute precision (SEM 0.80–0.95; MDC_{95} 2.2–2.6 points), and stable thresholds (discrepancies exceeding ±1 level occurred in <7% of cases). The metrics showed significant associations with vertebral body wedge deformity (r=0.58), spinal canal compromise (r=0.49), and ordinal injury severity by AO Spine (ρ=0.62; p<0.001). In logistic modeling, each additional 1 m in equivalent fall height nearly doubled the odds of burst/unstable injuries (OR=1.85; 95% CI 1.45–2.38). The diagnostic performance of the scale was confirmed (AUC=0.82) for identifying vertebral fractures (optimal threshold ≈1.3 m; sensitivity – 0.76; specificity – 0.72).

Conclusions: The proposed scale provides a quantitative, mass-neutral, and clinically interpretable measure of the "event severity," complements morphological classifications, enhances risk stratification, and can be applied for patient triage, diagnostic planning, and multicenter research.

Keywords: *spinal trauma; thoracolumbar junction; mechanical exposure; equivalent fall height; spinal-equivalent height; quantitative scale; measurement instrument validation; individualization.*

Introduction

Traumatic injuries of the spine constitute a heterogeneous group of conditions resulting from exposure to a wide spectrum of mechanical factors, ranging from low-energy events (e.g., falls from standing height) to high-energy mechanisms (falls from significant height, road traffic accidents (RTAs), sports-related and blast injuries) [1, 2]. According to population-based studies, the annual incidence of spinal trauma is 23–40 cases per 100,000 population, of which 15–20% are accompanied by neurological deficits of varying severity [2]. These estimates, however, require careful interpretation in light of methodological differences across studies and geographic regions.

Spinal injuries may arise from either direct or indirect mechanisms. Direct injury develops following the immediate application of force to the vertebral column (impact by a heavy object, gunshot or stab wounds, compression between massive objects) [3]. Such injuries are relatively uncommon and more

frequently limited to localized damage of the spinous and transverse processes or adjacent soft tissues. In contrast, the indirect mechanism—responsible for more than 90% of spinal injuries in peacetime—results from the transmission of external force to the body as a whole [1, 4]. This category includes falls of various types and RTAs, in which spinal damage occurs due to axial loading, flexion–rotation, or combined forces [3, 5–8].

In international clinical practice, fractures occurring under low-energy impact—defined as mechanical force that would not normally compromise bone integrity—are traditionally classified as fragility fractures (osteoporotic fractures) [9]. A classic example is a fall "from standing height or less" [10, 11]. This definition is reflected in World Health Organization (WHO) documents and is widely adopted in contemporary clinical guidelines [9, 12]. At the opposite end of the energy spectrum are high-energy mechanisms: in U.S. prehospital protocols, a fall in an adult from a height exceeding 20 feet (~6 m) has historically been regarded as a marker of high kinetic energy and increased risk of polytrauma [13]. More recent materials from the American College of Surgeons reference a lower threshold (>10 feet), underscoring the variability of cutoff values and the need for terminological standardization [14, 15].

Most widely used classification systems in vertebrology and traumatology focus on the characteristics of the injury outcome rather than on quantitative assessment of the intensity of external exposure [16]. For instance, the Abbreviated Injury Scale (AIS) is an anatomically based six-point system for grading injury severity by body region [17, 18], whereas the AO Spine Thoracolumbar Classification system categorizes thoracolumbar injuries according to morphological type (A, B, C), neurological status, and modifiers (including assessment of the integrity of the posterior ligamentous complex) [19–21]. These tools are indispensable for standardized injury description, risk stratification, and treatment planning; however, they do not provide a quantitative characterization of the "energy of the event" (mechanical exposure) preceding injury development [16].

In routine clinical practice, the mechanism of trauma is often described in simplified binary or qualitative terms ("low-/high-energy injury," "mild/severe"), which fail to reflect the continuous nature of mechanical exposure gradients and may lead to the loss of clinically relevant information [22, 23]. The absence of a standardized quantitative instrument complicates cohort comparisons and interpretation of research findings, and limits the potential for targeted preventive and rehabilitative strategies [24]. In this context, the development of a multilevel scale for the quantitative assessment of external mechanical impact intensity is warranted. Such a scale should be grounded in fundamental principles of mechanics (energy, impulse, acceleration) and be applicable in real-world clinical settings. A key methodological step is the introduction of a universal metric that enables different injury mechanisms to be translated into a unified energy scale, thereby standardizing the description of the "force of the event" for clinical communication and scientific analysis [5, 25].

Objective: To develop, theoretically substantiate, and conduct primary validation of a multilevel (0–10 points) scale for the quantitative assessment of the intensity of external mechanical impact in traumatic spinal injuries.

Materials and methods

The study design conforms to the principles of COSMIN (Consensus-based Standards for the Selection of Health Measurement Instruments) for the development and validation of measurement instruments in medicine, thereby ensuring an adequate level of scientific rigor and reproducibility of the obtained results [26, 27].

The literature search was conducted in two stages**.**

Stage 1 (analytical review of scales and terminology). The objective was to identify classification systems/scales, threshold values, and underlying principles used in clinical practice and guidelines that are necessary for formulating the conceptual framework of the proposed scale. Keywords: *AO Spine thoracolumbar classification, TLICS, Abbreviated Injury Scale, Injury Severity Score, spinal injury classification reliability, CDC field triage guidelines, mechanism of injury, fall height threshold, fall >10 ft, standing height or less, fragility fracture, osteoporotic vertebral fracture, mechanical exposure, energy of event, biomechanics of spinal injury.*

Stage 2 (collection of quantitative reference parameters). The objective was to determine threshold benchmarks for grading falls and to establish typical ranges/median values of parameters used in constructing the scale (collision scenarios, impulse transmission to the spine, effective stopping distance, environmental/surface modification factors). Keywords: *delta-v estimation, rollover, mass ratio, coefficient of restitution, impact angle, EDR, spine load transmission, landing biomechanics, knee flexion, energy absorption, feet-first, buttocks impact, supine impact, seat belt, airbag, torso kinematics, effective stopping distance, impact attenuation, concrete, asphalt, sand, snow, water entry, gym mat, tatami, HIC, g-max, fall from height, injury severity threshold adults, fragility fracture standing height.*

Databases and search parameters: PubMed/MEDLINE, Scopus, Web of Science; materials from AO Spine, the World Health Organization, and the International Osteoporosis Foundation. Language of publication: English; time frame: 1990–2025 (with no strict lower limit for fundamental biomechanical studies).

Screening was performed in stages by two independent reviewers (initially by titles and abstracts, followed by full-text assessment), with additional searches conducted through the reference lists of selected articles.

Datasets

Validation was performed using two complementary datasets:

Standardized clinical scenarios (vignettes) (n = 40) — synthetic clinical–biomechanical events uniformly covering the spectrum of mechanical exposure (including "adjacent" combinations of body position/surface/deceleration pathway), developed for independent expert assessment according to a standardized protocol.

This article contains some figures that are displayed in color online but in black and white in the print edition.

Real clinical cases (n = 52) — medical records of patients with sufficiently detailed descriptions of the injury mechanism, which, in the authors' judgment, allowed unambiguous reconstruction of the initial parameters required for calculations. In all cases, neuroimaging data (computed tomography (CT) and/or magnetic resonance imaging (MRI)) were available, enabling comparison of mechanical exposure values with morphological injury characteristics, determination of injury type according to the AO Spine classification, assessment of the degree of anterior wedge deformity, extent of spinal canal compromise, and integrity of the posterior ligamentous complex. Image analysis and measurements were performed using RadiAnt DICOM Viewer (Medixant, Poland; version 2023.1, license No. 1860F047).

For primary validation and reduction of interindividual variability, the sample included patients with injuries of the thoracolumbar junction (T11–L2).

Informed consent was obtained from all patients for data collection, processing, and publication of aggregated results in compliance with confidentiality standards. The data provided to experts were fully anonymized.

Sample size determination

To assess inter-rater reliability (intraclass correlation coefficient, ICC) in a design involving five experts, the study aimed to demonstrate an ICC of approximately 0.80 compared with a threshold value of 0.60, at α = 0.05 and statistical power of 0.80. The required sample size was estimated at 35–40 objects [28]. Accordingly, a set of 40 standardized vignettes was constructed, yielding 200 independent ratings (5 × 40), enabling test–retest assessment on a subsample of 10 vignettes [29] and improving the precision of the standard error of measurement (SEM) and the minimal detectable change at the 95% confidence level (MDC_{95}) [30, 31]. For clinical validation, 52 consecutive patients with complete datasets (detailed mechanism description plus CT/MRI data) were included. This sample size provides adequate power for key validity analyses (correlation coefficients r ≈ 0.5–0.6; known-groups comparisons with effect size d ≈ 1.1) [32–34] and acceptable precision for agreement analysis using the Bland–Altman method [35–37]. Receiver operating characteristic (ROC) analysis and regression modeling were considered secondary analyses, with correspondingly wider expected confidence intervals (CIs) [38,39].

Statistical analysis

Data were processed using descriptive and analytical statistical methods. Continuous variables are presented as mean ± SD or median [IQR], depending on distribution characteristics (normality assessed visually and using the Shapiro–Wilk test) [40, 41]. Construct and criterion validity were evaluated by correlation analysis with calculation of Pearson's (r) or Spearman's *(ρ)* coefficients, as appropriate [42, 43].

Predictive models. To assess the association between the proposed metrics and morphological injury severity according to the AO Spine classification, binary logistic regression was applied using a threshold of ≥A3, with estimation of odds ratios (ORs) and 95% CIs [44, 45]. As a sensitivity analysis for the ordinal outcome A1–A4, ordinal logistic regression was performed [46, 47]. Linearity of the logit was examined using the Box–Tidwell test [48] and restricted cubic splines [49, 50], while multicollinearity was assessed by the variance inflation factor (VIF) [51]. Discriminative performance was evaluated using ROC curves (AUC, with 95% CI) [52]. Sensitivity, specificity, the Youden index, and likelihood ratios (LR+, LR–) were calculated. Operational thresholds were selected by maximizing the Youden index, taking into account the intended purpose (screening vs. confirmation) [53].

The robustness of scale boundaries was examined through sensitivity analysis by varying threshold parameters by ±10–15% and recalculating results for alternative modifier scenarios [54, 55].

Known-groups validity. Comparisons were conducted for predefined clinically relevant groups [56]. Between-group differences were analyzed using the Mann–Whitney U test, with nonparametric effect sizes calculated as Cliff's δ [57] and/or Vargha–Delaney A [58]. Cohen's *d* was additionally reported (for reference), with robust interpretation in the presence of unequal variances [59].

Measurement reliability. Relative reliability was assessed through inter-rater agreement indices: ICC(2,1) (two-way random-effects model, absolute agreement, single measure) and ICC(2,k) (average measure) [60], as well as weighted κ with quadratic weights [61, 62]. Temporal stability was evaluated using a test–retest design in a subsample of cases [63]. Agreement between expert-based and algorithm-based calculations was assessed using the Bland–Altman method (mean bias and 95% limits of agreement) [64].

Absolute reliability. SEM and the MDC_{95} (MDC_{95} = 1.96 × √2 × SEM) were calculated [65]. For appropriate clinical interpretation, MDC was additionally expressed in continuous units: in meters for and in multiples of *g* for the spine-oriented metric (based on a reference stopping distance s_{ref} = 0.10 m), with level-specific (interval-specific) annotations indicating the ranges in which differences are clinically negligible or clinically meaningful [66].

All tests were two-sided. The threshold for statistical significance was set at $p < 0.05$ [67, 68].

Statistical analysis was performed using R version 4.5.1 (R Core Team) within RStudio IDE 2025.05.1+513 (Posit) [69].

Results

Definition of the criterion

The intensity of external mechanical impact during a traumatic event is defined as a quantitative characteristic of the force of the event preceding tissue damage [70, 71]. It is not identical to the severity of the resulting injury, which is determined using clinical outcome scales (e.g., the Abbreviated Injury Scale (AIS)) or morphological classifications (e.g., the AO Spine Thoracolumbar Classification) [72]. In contrast to AIS/AO classifications, which focus on anatomical and clinical consequences (type of disruption, instability, neurological status), the proposed criterion captures the mechanical exposure itself—that is, the physical quantity reflecting the amount of mechanical energy/impulse involved in the event [25].

As a universal physical metric, the "equivalent fall height" (h_{eq}) was selected [73, 74]. The underlying concept is that heterogeneous mechanisms (falls,

collisions, compression, blast effects) can, with certain assumptions, be translated onto a unified energy scale by equating them to a hypothetical fall from a given height in a uniform gravitational field. This metric is based on gravitational potential energy and enables comparison of events in terms of "energetically equivalent meters."

In selecting an appropriate physical metric (criterion) for assessing the degree of external mechanical impact on the spine, the following considerations were taken into account:

- first, falls from height represent the most common cause of traumatic spinal injuries. According to the Global Burden of Disease study, falls are the leading cause of vertebral trauma, accounting for 52.2% of spinal injuries and 63.0% of spinal cord injuries [75, 76]. Thus, more than half of traumatic events are attributable to falls, making a height-based scale the most relevant framework [77].

- second, the parameter "fall height" offers important practical advantages [13]. This criterion is intuitively understandable not only for specialists but also for patients and their relatives. A statement such as "a fall from the second floor" immediately conveys an impression of impact intensity [15, 78, 79]. Moreover, this parameter is readily obtainable from clinical documentation [80]. During history taking, patients or witnesses almost invariably refer to "a step and a fall" or "from a height of…," whereas quantitative data for RTAs (velocity), interpersonal violence (type of weapon), or compression injuries are often unavailable or difficult to interpret [81].

- third, falls encompass both the lower and upper limits of the mechanical action spectrum (low-energy and high-energy trauma). Consequently, they provide a broad and clinically relevant range of mechanical exposure [77].

- fourth, the approach is grounded in physical principles. The definition of h_{eq} in terms of fall height follows directly from the laws of mechanics (since potential energy $\Delta E = mgh$), thereby preserving maximal objectivity, avoiding subjective weighting coefficients in estimating impact force, and enabling quantitative comparison of diverse injury mechanisms within a unified physical scale [1, 15, 73].

Analysis of contemporary literature demonstrates that, when characterizing the severity of mechanical impact on the spine based on fall height, only two primary threshold benchmarks are effectively employed.

The first threshold is approximately 1 m. A fall from standing height (~1 m) or less is traditionally regarded as a low-energy mechanism, in which fractures indicate pathological bone fragility (osteoporotic fractures) [82, 83]. This definition is incorporated into recommendations of the World Health Organization and the International Osteoporosis Foundation and is widely applied in clinical practice for risk stratification and the initiation of secondary prevention [84–86].

The second threshold is 20 feet (~6 m). A fall in an adult from a height exceeding 20 feet has historically been recognized as a marker of severe mechanical impact in prehospital medical and trauma triage protocols (CDC, American College of Surgeons). This criterion is associated with a high probability of polytrauma and the need for transport to a specialized trauma center [87]. Although some contemporary guidelines discuss a lower universal threshold (>10 feet), 20 feet remains the most frequently cited "upper" benchmark of high-energy trauma.

Thus, in routine practice, only two quantified reference values are used when describing the mechanism of injury: ~1 m as the boundary of low-energy exposure and ~6 m as an indicator of high-energy trauma (***Fig. 1***). The intermediate range remains insufficiently formalized [15, 88, 89].

Intensity of overall external mechanical impact – fall scenario

To enhance the precision of stratifying the mechanical factor in traumatic spinal injuries, an 11-level scale for grading the intensity of external impact was developed based on our clinical experience and analysis of the literature [3, 5, 70, 90]. Unlike binary or simplified classifications, the proposed system is grounded in clinically verified threshold values [13, 15, 80] and encompasses the most typical fall scenarios, ensuring high clinical relevance and practical reproducibility [72, 88, 91]. The selected height thresholds are: 0; 0.1; 0.5; 0.75; 1; 2; 4; 6; 10; and 15 meters (***Table 1***).

The proposed scale is visually presented in ***Fig. 2*** (not to scale).

Intensity of overall external mechanical impact – RTA scenario

Determination of h_{eq} in RTAs. Since h_{eq} was adopted as the reference metric, for falls $h_{eq} = h$. For RTAs (the second most frequent cause of vertebral trauma), recalculation through Δv—the change in the victim's velocity at the moment of RTA—is required [5, 92, 93]. The fundamental concept is that h_{eq} represents the height of free fall that would generate the same kinetic energy as the described RTA [94]. Based on the principle of energy equivalence:

$$\frac{1}{2}m(\Delta v)^2 = mgh_{eq} \Rightarrow h_{eq} = \frac{(\Delta v)^2}{2g},$$

where g=9.81 m/s².

For practical purposes, if Δv is expressed in km/h:

$$h_{eq}\,[m] = \frac{(\Delta v[km/h])^2}{254}.$$

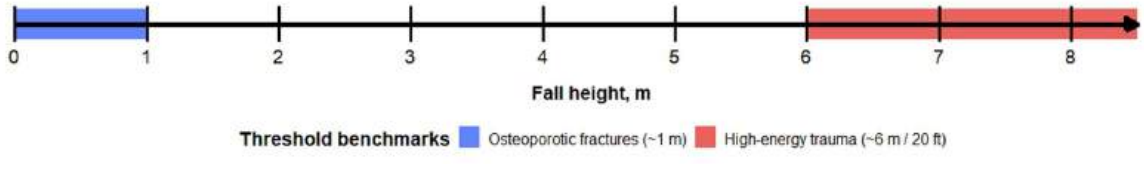

Fig. 1. Currently accepted scale for grading fall height in the context of spinal injury

Table 1. Height-based scale of mechanical exposure intensity (for clinical stratification)

Severity score	Height, m	Clinical scenario
0	0	Absence of external mechanical impact: spontaneous vertebral body compression in severe osteoporosis; fracture under minimal load in the setting of systemic/local bone pathology (tumor, infection, etc.)
1	0–0.1	Incomplete fall/stepwise level change ≤30 cm: stumbling on a flat surface with recovery of balance; partial "sliding" from a step/threshold; microtrauma during an awkward turn in confined space (domestic injury)
2	0.1–0.5	Fall from low furniture or architectural elements ~0.4–0.6 m (low stool, threshold, windowsill); fall from a low bed; in children—fall from a sofa/play surface of comparable height
3	0.50–0.75	Fall from sitting height: from a chair/bed (~0.6–0.7 m); fall during entry/exit from a bathtub; slip while attempting to reach an object from an upper shelf while standing on a seat
4	0.75–1.00	Fall from standing height (~0.8–1.0 m): slipping on ice/wet tiles; tripping over an obstacle (threshold, cable); syncopal fall in upright position; fall while ascending/descending stairs "skipping" a step
5	1–2	Fall from a ladder (2–3 rungs, ~1.5–2.0 m); from a first-floor balcony/platform (<3 m); occupational injury: fall while working on low scaffolding/loading platform; sports-related: fall from a low rock ledge
6	2–4	Fall from the roof of a single-story building (3–4 m), tree, warehouse rack; fall down a significant stair flight (≥6–8 steps); occupational: fall from a ramp/semitrailer
7	4–6	Fall from the second floor (~6 m); from an intermediate landing; fall into a shallow shaft; occupational: fall from an upper tier of construction scaffolding
8	6–10	Fall from the third floor (~9–10 m); from the roof of an industrial hangar/workshop; recreational/occupational fall due to safety failure (impact onto a horizontal surface)
9	10–15	Fall from the fourth–fifth floor (~13–15 m); from a communication mast, crane boom, high scaffolding; fall on a mountain route with impact against ledges/edges during descent
10	>15	Catastrophic fall: height >15 m (≥6th–7th floor); from a high-rise building/antenna mast; fall from a rock cornice/bridge in an urban or mountainous environment

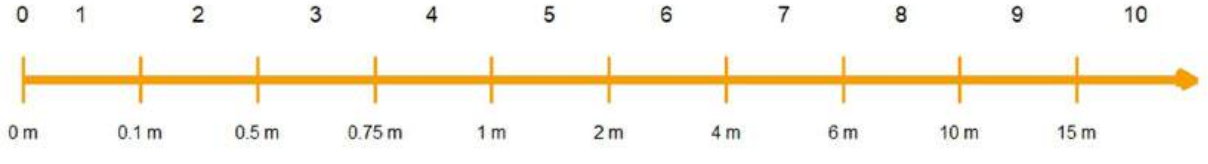

Fig. 2. Level scale (0–10) with boundaries defined by equivalent fall height (heq, m)

Objective limitations in applying this criterion.

First, accurate determination of *Δv* is currently feasible only when data from the vehicle's Event Data Recorder (EDR) (airbag control unit/telematics module) are available. This device records longitudinal and lateral changes in velocity, as well as their resultant value, during the first 0.3 seconds following impact. In the United States, the implementation and standardization of EDR are regulated by the National Highway Traffic Safety Administration (NHTSA), while in the European Union they are governed by Regulation (EU) 2019/2144, which mandated EDR installation in new vehicle models between 2022 and 2024 [95, 96]. Second, even when such equipment is formally present in the vehicle, these data are typically unavailable to the physician during hospital admission and primary assessment. Clinicians are therefore compelled to rely on information obtained from the patient or witnesses [97]. For this reason, indirect methods for estimating *Δv* in various types of RTAs are presented below.

As an example, we provide a detailed method for calculating *Δv* in the case of a collinear one-dimensional collision—that is, a scenario in which both vehicles move along the same straight line (rear-end or head-on collision) and impact occurs strictly along this axis [98].

Let m_1 and m_2 denote vehicle masses; v_1 and v_2 their pre-impact velocities (with signs defined along a single axis); v'_1 and v'_2 their post-impact velocities; and e the coefficient of restitution (typically for vehicles e ≈ 0.0–0.2; discussed in detail below). The derivation is based on the law of conservation of momentum:

$$m_1 v_1 + m_2 v_2 = m_1 v_1' + m_2 v_2',$$

and the restitution condition:

$$v_2' - v_1' = -e(v_2 - v_1)$$

Solving for the post-impact velocities:

$$v_1' = \frac{m_1 - em_2}{m_1 + m_2} v_1 + \frac{(1+e)m_2}{m_1 + m_2} v_2$$

$$v_2' = \frac{(1+e)m_1}{m_1+m_2} v_1 + \frac{m_2 - em_1}{m_1+m_2} v_2.$$

Since $\Delta v = v - v'$, for each vehicle:

$$\Delta v_1 = \frac{(1+e)m_2}{m_1+m_2}(v_1 - v_2),$$

$$\Delta v_2 = \frac{(1+e)m_1}{m_1+m_2}(v_2 - v_1).$$

These expressions demonstrate that each vehicle acquires a fraction of the relative velocity $V_{rel}=|v_1-v_2|$, proportional to the mass of the opposing vehicle. When the masses are equal, each vehicle experiences approximately $\Delta v \approx 0{,}5\,V_{rel}$. If one vehicle is substantially heavier ($m_2 \gg m_1$),the lighter vehicle "absorbs" nearly the entire relative velocity change ($\Delta v_1 \rightarrow (1+e)V_{rel}$), whereas the heavier vehicle undergoes minimal velocity change ($\Delta v_2 \approx 0$).

Since, in the above calculations, the coefficient of restitution is a parameter that is difficult to assess empirically, its brief characterization is provided below. In mechanics, e is defined as the ratio of the relative separation velocity to the relative approach velocity of colliding bodies along the line of impact [99, 100], i.e.:

$$e = \frac{v_2' - v_1'}{v_1 - v_2}.$$

Its values may be interpreted as follows:

$e=0$ — perfectly inelastic collision: after impact, the bodies move together as a single unit, and their common velocity v' is determined by the law of conservation of momentum [101];

$0<e<1$ — partially elastic collision: a portion of the relative velocity is preserved as "rebound" [102]

$e=1$ — perfectly elastic collision: kinetic energy is fully conserved (as in ideally rigid bodies, e.g., a billiard ball) [103, 104].

Vehicle bodies and bumpers are engineered to maximize energy absorption through plastic deformation during impact [105, 106]. Consequently, most motor vehicle collisions are predominantly plastic in nature. For this reason, the coefficient of restitution e in real-world RTAs is typically very small. Its value reflects only the fraction of energy retained in elastic deformation and subsequently released as a minor "rebound" effect.

In frontal collisions, e is generally within the range of 0.0–0.1, since nearly all energy is dissipated in structural crumpling [106]. In lateral impacts, the value is slightly higher (0.1–0.2), owing to a smaller programmed deformation zone and a relatively greater elastic response [107]. In low-speed rear-end collisions (bumper-to-bumper, parking scenarios), the coefficient may reach 0.2–0.3, as a greater proportion of elastic components is engaged and plastic deformation is limited. In impacts with rigid obstacles (e.g., a pole or a tree), e approaches zero [99, 107]. For collisions with Δv > 25 km/h, practical calculations conventionally assume e = 0, since the contribution of the elastic component becomes negligible.

To illustrate the practical application of the proposed calculation algorithm, several clinical examples are provided below.

Example 1. Passenger car A overtakes at a speed of v_1 = 90 km/h, while passenger car B approaches from the opposite direction at v_2 = 70 km/h. The collision is frontal and aligned with the direction of motion. Let m_1 = 1400 kg and m_2 = 1300 kg. Taking into account the impact severity, the coefficient of restitution is assumed to be e = 0. Accordingly, $V_{rel}=V_1+V_2=160$ km/h, $m_1+m_2=2700$ kg.

$$\Delta v_1 = \frac{m_2}{m_1+m_2}V_{rel} \approx 77\ km/h,$$

$$\Delta v_2 = \frac{m_1}{m_1+m_2}V_{rel} \approx 83\ km/h.$$

The equivalent fall height h_{eq} (based on Δv) is therefore:

$$h_{eq.1} \approx \frac{77^2}{254} \approx 23.4\ m,$$

$$h_{eq.2} \approx \frac{83^2}{254} \approx 27.1\ m,$$

For both affected vehicles, this corresponds to the maximum level of mechanical impact on the human body—10 points according to the proposed scale.

Example 2. Passenger car A, traveling at v_1 = 50 km/h, collides with passenger car B, which is stationary at a traffic light. In this case, the vehicle masses are assumed equal: $m_1=m_2=1400$ kg.

With e=0

$$\Delta v_1 = \Delta v_2 = \frac{1}{2}\,50 = 25\ km/h$$

$$h_{eq.1} = h_{eq.2}\ \frac{25^2}{254} \approx 2.46\ m,$$

which corresponds to 6 points on the proposed scale.

A logical objection to the use of the proposed methodology is the difficulty of accurately determining vehicle speed at the time of a RTA. However, in practical settings, drivers are generally able to provide an approximate estimate sufficient for primary stratification. To demonstrate the robustness of the conclusions with respect to plausible speed estimation error, several representative calculations based on Example 2 are presented below:

- 50 km/h→ Δv=25.0 km/h→ h_{eq}=2.46 m → 6 points;
- 55 km/h→ Δv=27.5 km/h→ h_{eq}=2.98 m → 6 points;
- 60 km/h→ Δv=30.0 km/h→ h_{eq}=3.54 m → 6 points.

These results demonstrate that moderate uncertainty in the initial speed does not alter the clinical assessment category. Furthermore, analysis indicates that, in calculating the equivalent fall height, small differences in vehicle mass (±100–200 kg) have a negligible effect on the resulting Δv and, consequently, do not influence classification according to the proposed scale. In clinical practice, such fine-grained precision is unnecessary. Of substantially greater importance is the vehicle class (e.g., subcompact car, sedan, SUV/crossover, minivan, truck, bus, articulated heavy truck), as inter-category differences are considerable and may significantly affect the distribution of impact severity between collision participants. Therefore, for stratification purposes, classification by vehicle type provides sufficient accuracy while preserving the practical applicability of the method. When vehicle masses are approximately equal, Δv equals one-half of the total closing speed, irrespective of the exact masses; thus, a coefficient of 0.5 is used in calculations.

Analogously to the section on colinear (1D) collisions, simplified coefficients for rapid estimation of Δ*v* in other types of RTAs were derived using methods of formal mechanics. These coefficients allow prompt estimation of the change in velocity of the injured vehicle—and subsequent calculation of h_{eq} —based solely on the speed of one participant and the collision configuration (***Table 2***).

When analyzing the table, particular attention should be paid to the rollover category of RTAs, which fundamentally differs from other scenarios in terms of Δ*v* determination. In this case, the change in velocity is not directly related to the frontal or lateral projection of the relative velocity but is determined by the characteristics of the vehicle's rotational motion and the number of body contacts with the surface [113]. A basic estimate is performed using the formula:

$$\Delta V_{roll} \approx k_{roll} \cdot V_0$$

where V_0 — is the velocity prior to the onset of rollover; k_{roll} — is a coefficient dependent on the number of rollovers/roof contacts, the rollover type, and the environmental conditions.

In the analysis of rollover RTAs, several methods are used to determine Δ*v*, two of which are considered the simplest and most effective. Both approaches are conceptually equivalent. It is recommended to apply the method that is easier to interpret based on the available documentation:

1. Quarter-turn (Nq) estimation method [114]. The assessment is based on the number of quarter-turns of the vehicle body (90° rotation = 1 quarter-turn):

Nq=1-2 – the vehicle comes to rest on its side or roof: k_{roll} ≈0.25–0.35;

Nq=3–4 – rollover over the roof or a complete 360° rotation: k_{roll} ≈0.35–0.50;

Nq ≥ 5 – multiple rollovers: k_{roll} ≈0.50–0.65.

2. Roof-impact count method (M, roof impacts) [115–117]. This method estimates the number of roof or pillar contacts with the road surface and is particularly convenient in cases of multiple rollovers:

$$k_{roll} \approx 0.2 + 0.08 \cdot M$$

where *M* is the number of contacts. In practice, k_{roll} does not exceed 0.65. To improve calculation accuracy, contextual adjustments are recommended depending on the specific conditions [113. 118]. In the analysis of rollover RTAs, the following scenarios are distinguished:

- "Tripped" rollover, initiated by an external obstacle (e.g., curb, ditch, soft shoulder) that "catches" the wheel and triggers rotation. Such scenarios are more likely to result in abrupt energy dissipation and a greater Δ*v*. In calculations: k_{roll} +0.03–0.05;

- "Untripped" rollover, occurring due to the vehicle's own dynamics (sharp maneuver, skidding, center-of-gravity displacement) without impact against an external obstacle. In these cases, Δ*v* is usually lower than in "tripped" scenarios; therefore, the coefficient is adjusted downward: k_{roll} –0.03…–0.05.

Additionally, terrain and surface conditions are taken into account: steep slope/embankment (k_{roll} =+0.03) hard road surface (asphalt) – k_{roll} –0.02…–0.03, soft surface (soil)– k_{roll} +0.02–0.03 [119]. Example. A vehicle was traveling on a rural road at approximately 70 km/h. During an overtaking maneuver, one wheel entered a soft unpaved shoulder. Loss of support caused a "tripped" rollover (a typical obstacle-initiated rollover), after which the vehicle overturned laterally, making two roof contacts with the surface.

Using the roof-impact method with M=2 k_{roll}≈0.36. Since the rollover was initiated by "tripping" on a soft soil edge, corrections of +0.04 ("tripped" mechanism) and +0.02 (soil surface) are applied, yielding a final: k_{roll} ≈0.42.

Thus,

$$\Delta v \approx (0.36 + 0.04 + 0.02) \cdot V_0 \approx 0.42 \cdot 70 \approx 29.4\, km/h$$

$$h_{eq} \approx \frac{29.4^2}{254} \approx 3.4\, m$$

The obtained value corresponds to level 6 on the proposed scale (interval 2–4 m).

Table 2. Coefficients for rapid estimation of Δv in various types of RTAs (assuming comparable vehicle masses) [107–112]

Type of RTA	Coefficient (k) for Δv	Comment
Colinear (frontal/ rear-end)	0.5	Each vehicle receives half of the relative velocity
Lateral impact	0.5	For the struck vehicle, Δv ≈ half of the normal velocity component
Oblique impact	0.25 – for 30⁰ 0.35 – for 45⁰ 0.43 – for 60⁰ 0.48 – for 75⁰	Δv depends on the contact angle
Sideswipe	0.05–0.20	With tangential contact, Δv is small; energy is dissipated in friction/sliding
Impact with rigid barrier	≈1	With e ≈ 0, Δv approximates the impact speed
Rollover	0.25–0.65	Δv estimated as a fraction of pre-rollover speed; depends on number of rotations
Multi-event collision	Maximum Δv	In multiple impacts, the largest Δv is used (based on EDR data or reconstruction)

The presented data demonstrate the feasibility of applying relatively simple methodologies for approximate assessment of the traumatic mechanical impact on the human body within two fundamental scenarios—fall from height and various types of RTAs. To accelerate and simplify information processing, eliminate the need for independent mathematical calculations, and account for multiple modifying factors, we developed a dedicated online calculator. Its structure, functional capabilities, and operating algorithms are described in the corresponding section of this article.

Assessment of mechanical impact on the spine

It is evident that h_{eq}, which reflects only the integrated magnitude of mechanical exposure, alone does not allow an adequate assessment of the impact on the spine [70]. Actual traumatic potential is determined by how the energy is converted into forces over the duration of deceleration and along the deceleration path, the geometry of its application to the body, and the proportion that mechanically affects the spinal column [1, 120]. Therefore, identical h_{eq} values can correspond to fundamentally different clinical outcomes [77, 121, 122]. For example, a fall from 1 m onto rigid concrete versus a thick mat, even with identical h_{eq}, results in markedly different loading and risk of injury [123].

Key additional factors influencing actual traumatic potential include the patient's body mass, the impulse transfer coefficient, and the effective deceleration distance [120, 124–126].

Patient body mass

The patient's body mass (m) is a fundamental parameter that determines the inertial properties of the system [127, 128]. For any traumatic event with a given Δv, and consequently a given equivalent height h_{eq}, mass linearly scales both the energy to be dissipated and the impulse that must be absorbed by supporting structures [129, 130].

According to the integral form of Newton's second law, the work of external forces required to bring the body to a complete stop equals its kinetic energy (E):

$$E = \frac{1}{2}m(\Delta v)^2 = mgh_{eq}.$$

At fixed V or h_{eq} the energy E is proportional to mass. Thus, a heavier body requires dissipation of a greater energy reserve at the same h_{eq}.

The impulse (J) that braking forces must provide is calculated as:

$$J = \int F(t)dt = m\Delta v$$

Impulse increases linearly with mass at a fixed Δv [131]. Accordingly, if the deceleration occurs over a fixed time (t), the average applied force is:

$$\bar{F} = \frac{J}{t} = \frac{m\Delta v}{t}$$

which also scales linearly with mass.

Closer to clinical practice, the relevant scenario is deceleration over a characteristic path (s), e.g., the thickness of a cushioning surface or the deformation depth of a structure. In this case, the average applied force can be calculated as:

$$\bar{F} = \frac{E}{s} = \frac{mgh_{eq}}{s},$$

which similarly reflects a linear dependence on mass under otherwise identical conditions [132, 133].

Thus, patient body mass is an independent modifying factor for traumatic potential. At fixed Δv or h_{eq}, it systematically increases the impulse and work required to stop the body, and consequently the average and peak loads transmitted to the spinal supporting structures [125]. For a correct interpretation of "event force," body mass should be considered at least descriptively, even if the metric used for assessment is mass-neutral [134].

Impulse transfer coefficient

The impulse transfer coefficient (T_{land}) is a dimensionless quantity that characterizes the fraction of mechanical energy from a traumatic event that reaches the spine [1, 135]. It reflects the effectiveness of "biomechanical filters" (joints, muscles, soft tissues) and protective systems (seat belts, airbags, seats) that dissipate or redistribute the impact [120, 136]. Accordingly, T_{land} determines the portion of the total mechanical exposure that is transformed into loading on the spinal column. While axial compression is most common, other components (shear or rotational) may dominate depending on the direction and resultant vector of the applied force [137].

The primary factors influencing T_{land} are the point of force application and contact geometry [126, 137, 138]. For instance, a fall onto the feet with deep knee flexion and active muscular engagement dissipates a significant portion of the impulse, yielding $T_{land} \approx 0.4–0.6$ [139, 140]. Conversely, a fall onto the buttocks or back results in minimal absorption, with T_{land} approaching 0.9–1.0, transferring almost the entire energy to the thoracolumbar spine [141]. In frontal RTAs, seat belts and airbags distribute the kinetic load across the chest and shoulder girdle, increasing the area and duration of energy absorption, thereby reducing direct impulse transfer to the spine [142, 143]. In the absence of restraints, impact against the steering wheel or dashboard occurs locally, with negligible damping, transmitting almost the entire load to the spinal column. In some cases (e.g., axial head impact), local impulse concentration may formally exceed 1, reflecting not "energy generation" but amplification of its effect on a limited spinal segment [144].

In clinical practice, T_{land} is estimated based on the injury scenario: which structures bear the main load, how much energy is absorbed along the transmission path, and what fraction reaches the spinal column [126, 141]. For calculations, a typical (average) coefficient value is used, while minimum and maximum limits are considered as a variability range.

Based on literature analysis, average T_{land} values with approximate ranges have been determined for main clinical scenarios (***Table 3***).

Table 3. Average impulse transfer coefficient values for the thoracolumbar spine in common clinical scenarios [1, 70, 120, 126, 135–154]

Brief description	Tland (min–typical–max)	Justification (concise)
Falls:		
Onto feet, deep absorption (deep squat)	0.40–0.55–0.65	Significant portion of the impulse is dissipated through knee and hip joint flexion and the musculoskeletal complex; no more than half of the energy reaches the spine
Onto feet, semi-flexed	0.60–0.70–0.80	Moderate energy filtering through joints and muscles; axial load fraction transmitted is higher than in deep absorption, but part of the impulse is absorbed
Onto feet, stiff/almost locked	0.80–0.90–0.95	Minimal joint cushioning; impulse is almost fully transmitted along the spinal axis, generating marked compression
Onto buttocks/pelvis	0.80–0.95–1.05	Limited cushioning by soft tissues of the pelvis; load is almost entirely transmitted to the lumbar spine. Local concentration (>1) may occur in some cases
Onto back	0.90–1.05–1.15	Impact over a broad surface with transmission through the rib-spine framework produces nearly complete axial loading; additional bending moment may occur
Onto side/pelvis	0.60–0.75–0.85	Significant portion of energy dissipated through lateral soft tissues and pelvic structure; axial component reduced
Onto hands/elbows/knees	0.40–0.60–0.70	Extremities act as shock absorbers, dissipating part of the energy; only 40–70% of impulse reaches the spine
Onto knees (with subsequent axial impact)	0.50–0.70–0.85	Primary filtering through knee flexion, followed by sharp transmission of residual energy along the axis; final fraction is variable
RTAs:		
Frontal, seatbelt + airbag	0.50–0.65–0.75	Seatbelt and airbag distribute load across the chest and shoulder girdle, prolonging contact duration and reducing the fraction of energy transmitted to the spine
Frontal, seatbelt only	0.60–0.75–0.85	Without an airbag, load distribution is less effective; impulse through the belt and chest is largely transmitted to the spine
Frontal, no restraint (dashboard/steering wheel)	0.85–0.95–1.00	Direct chest contact with steering wheel or panel; absence of cushioning structures leads to almost full impulse transfer to the spine
Side impact, with seatbelt	0.55–0.70–0.80	Belt restrains the torso and redistributes part of the energy; door and seat deformation further dissipate load
Side impact, no seatbelt	0.70–0.85–0.95	Rigid impact through lateral body surface; absence of controlled distribution increases transmitted fraction
Rollover, with seatbelt	0.90–1.00–1.10	Roof contact with head/shoulders generates axial load with minimal filtering; local concentration can increase transmission
Rollover, no seatbelt	0.90–1.05–1.15	Contact with rigid cabin elements or ground; impact geometry is variable, but direct, localized loading on the spine is more frequent

Note: For practical calculations, it is recommended to use the typical (average) Tland value, as it represents the most probable contact scenario. The "min" and "max" values are provided as references to assess the degree of variability and potential calculation error.

Effective deceleration distance

The effective deceleration distance (S_{land}) is defined as the actual path over which the velocity of the body (or the spine-relevant portion of it) is reduced following an impact [139, 150]. Unlike the "geometric" fall height, S_{land} encompasses all sources of system "compliance": support deformation (mats, soil, seats, airbags), soft tissue compression, joint flexion, as well as body sliding and rotation [129, 133]. A greater S_{land} distributes energy absorption more smoothly over time, resulting in lower average and peak spinal loads for the same event [154].

Factors influencing S_{land} include the point of force application and body posture (e.g., legs with flexed knees provide a long deceleration path, whereas landing on the buttocks or back yields a short path), surface properties (rigid asphalt offers minimal energy absorption, whereas soft surfaces, snow, or mats extend the deceleration distance), and passive safety elements in vehicles (seatbelts, pretensioners, airbags, seat and chassis deformation increase the effective path) [152] (***Tables 4 and 5***). Secondary movements are also important: sliding, rolling, and rotation reduce strictly axial compression on the spine, effectively increasing the deceleration distance [113, 118].

In clinical practice, the assessment is performed according to the scenario and context: body position at the moment of contact, surface or equipment type, and the nature of the injuries are analyzed, after which a realistic range of values is selected for calculations.

Proposed metrics for injury characterization

Based on the analysis of the described parameters and the principles of applied mechanics, a set of metrics has been proposed to formalize and quantitatively describe the mechanical impact on the spine.

Table 4. Effective deceleration distance values for selected typical clinical scenarios [131, 136, 139–150, 152–154]

Brief description	*Sland, m (min–typical –max)*	Mechanism
Falls:		
Onto feet, deep absorption (deep squat)	0.40–0.50–0.60	Knee and hip flexion, foot elasticity, posterior pelvic shift
Onto feet, semi-flexed	0.25–0.30–0.40	Partial knee flexion, joint elasticity, moderate absorption
Onto feet, stiff/almost locked	0.15–0.20–0.25	Minimal joint motion, abrupt impact transmission; short path
Onto buttocks/pelvis	0.02–0.04–0.06	Soft tissue compression, minimal sliding; very short path
Onto back	0.03–0.04–0.05	Deformation of back and chest soft tissues upon impact
Onto side/pelvis	0.06–0.08–0.10	Lateral soft tissue deformation and pelvic compression
Onto hands/elbows/knees (with load transfer)	0.10–0.15–0.20	Limb flexion, partial energy absorption by joints
Onto knees (with subsequent axial impact)	0.08–0.10–0.12	Soft tissue compression of the knees + joint flexion before spinal impact
RTAs:		
Frontal: seatbelt + airbag	0.20–0.30–0.40	Belt stretch, airbag compression, seat deformation
Frontal: seatbelt only	0.15–0.25–0.30	Belt elongation and seat deformation
Frontal: no seatbelt (dashboard/ steering wheel)	0.02–0.05–0.08	Near-instantaneous stop; extremely rigid contact
Side impact, with seatbelt	0.10–0.15–0.25	Door/seat deformation, torso sliding
Side impact, no seatbelt	0.05–0.10–0.15	Rigid contact; minimal controlled deformation
Rollover, with seatbelt	0.02–0.04–0.08	Roof contact with head/shoulders; limited deceleration path
Rollover, no seatbelt (contact with cabin/ground)	0.02–0.06–0.10	Rigid, variable geometry; short deceleration distance

Note: For practical calculations, it is recommended to use the typical (average) Sland value, as it represents the most probable contact scenario. The "min" and "max" values serve as references to estimate variability and potential calculation error.

Table 5. Modification factors for effective deceleration distance depending on environment, surface, and equipment [123, 155–168]

Parameter	Contribution to Sland, m (min– typical–max)
Asphalt/concrete/tiles	0.001–0.003–0.005
Wooden floor/linoleum	0.002–0.005–0.010
Sports mat 10–20 mm thick	0.01–0.02–0.03
Tatami mat 40–60 mm thick	0.03–0.05–0.07
Gymnastics mat 80–120 mm thick	0.08–0.12–0.18
Compacted soil/ground	0.005–0.015–0.030
Dry sand (beach)	0.10–0.20–0.30
Wet/compact sand	0.05–0.10–0.20
Packed snow	0.02–0.05–0.10
Loose snow (20–40 cm)	0.15–0.30–0.50
Water, entry "feet first"	0.50–1.00–1.50
Water, entry "flat"	0.05–0.10–0.20
Light clothing	0.002–0.005–0.010
Winter/multilayer clothing	0.01–0.02–0.03

Note: when modification factors are considered, the calculation uses the sum of the relevant components along the load path.

1. Mean "spinal" overload

The mean spinal overload ($\bar{g}_{spine}$) reflects the "stiffness" of the injurious event's impact on the spine and is expressed in multiples of gravitational acceleration (g). Unlike absolute force or energy parameters, ($\bar{g}_{spine}$) is independent of the patient's body mass and therefore provides a universal, comparable criterion across different clinical scenarios [169].

Formally, it is defined as:

$$\bar{g}_{spine} = \frac{h_{eq}}{s_{land}} * T_{land}.$$

For falls, $\bar{g}_{spine}$ is primarily determined by surface type and body position: minimal deceleration distance (e.g., falling on asphalt or concrete) results in high overloads, whereas soft ground, water, or mats increase the deceleration distance and reduce overload [133, 152, 170]. When falling on the feet, overload depends on the ability to absorb impact: the deeper the joint flexion, the longer S_{land} and the lower $\bar{g}_{spine}$.

In RTAs, the indicator depends on the effectiveness of passive safety systems. Seat belts and airbags increase the deceleration distance and duration, distribute the load over a larger area, and reduce the net overload [143, 170, 171]. In the absence of restraint systems or during contact with rigid cabin structures, deceleration distance is minimal, T_{land} approaches 1, and $\bar{g}_{spine}$ reaches maximum values.

The main advantage of $\bar{g}_{spine}$ is its comparability: the same value indicates the same "stiffness" of spinal loading regardless of the victim's body mass [169]. It is assumed that this metric correlates well with the probability of structural injuries and can serve as a key integrative criterion of biomechanical trauma.

2. Energy acting on the spine

The energy acting on the spine (E_{spine}) quantifies the absolute amount of mechanical energy absorbed by the spinal column. Unlike mass-neutral metrics, which reflect relative "stiffness" of impact, E_{spine} indicates the full energy budget that the spine must absorb:

$$E_{spine} = m\, g\, h_{eq}\, T_{land}$$

For falls, E_{spine} primarily depends on body mass and the biomechanical load path: when falling on the "feet", part of the energy is absorbed by joints and muscles, whereas when falling on the buttocks or head, nearly the entire impulse is transmitted along the spinal axis [158, 172, 173]. In RTAs, the energy reaching the spine depends on passenger mass and the force direction (through the chest or pelvis) [174]. Passive safety systems (belts, airbags) do not reduce E_{spine} but increase S_{land}, spreading the impulse over time and reducing peak loads [175, 176].

The advantage of this metric is its physical transparency: it is expressed in absolute energy units (J) and can be used for engineering and biomechanical calculations, as well as injury modeling. Its limitation is mass dependence: for the same h_{eq}, a heavier patient inevitably experiences a greater energy load on the spine [177].

Thus, E_{spine} should be considered a secondary parameter, important for analyzing the total energy component of an event and for biomechanical modeling, whereas mass-neutral metrics may be preferable for clinical comparison.

3. Mean force acting on the spine

The mean force acting on the spine ($\bar{F}_{spine}$) represents the averaged magnitude of the axial force transmitted to the spine during deceleration. Unlike mass-neutral parameters, F_{spine} directly depends on the patient's body mass and therefore characterizes the absolute force scale of the traumatic impact.

$$\bar{F}_{spine} = \frac{m\, g\, h_{eq}\, T_{land}}{S_{land}}$$

In falls, the magnitude of is determined by body mass and the type of contact: falling onto a rigid surface with minimal deceleration distance leads to extremely high mean forces [161, 162], whereas soft surfaces or the shock-absorbing properties of the joints substantially reduce them [155, 167]. In traffic collisions, the parameter depends on passenger body mass and the effectiveness of restraint systems [176]. Seat belts and airbags increase S_{land}, thereby reducing both mean and peak forces [178].

The advantage of this metric lies in its intuitive clarity: force expressed in newtons is readily interpretable for clinicians and engineers and can be directly compared with known strength limits of osseoligamentous structures [173]. Its limitations include dependence on body mass and the difficulty of accurately estimating S_{land}. Moreover, in real-world conditions, the peak force—rather than the mean force—may be most critical and may differ substantially from the averaged value [177].

Thus, $\bar{F}_{spine}$ may be regarded as an additional force descriptor useful for engineering and biomechanical applications, but not as a primary clinical indicator.

4. Spinal-equivalent height

The spinal-equivalent height (h_{spine}^{eff}) – is a recalculated (normalized) equivalent fall height that would produce the same mean axial load on the spinal column under reference deceleration conditions as the actual traumatic event under its specific posture and contact characteristics. This metric is mass-neutral and therefore enables valid case comparisons. The concept is to reduce heterogeneous injury mechanisms to a single, physically interpretable "height" scale specifically oriented to the spine, taking into account load transmission and contact "stiffness." Formally, it is defined as:

$$h_{spine}^{eff} = h_{eq}\, \frac{s_{ref}}{s_{land}}\, T_{land},$$

where s_{ref} – is the reference deceleration distance (0.10 m in the present study).

In clinical fall scenarios the magnitude of h_{spine}^{eff} naturally differentiates contact regimes. When landing on the feet, S_{land} is large due to multijoint shock absorption (knee and hip flexion, footwear elasticity), and part of the impulse and work is dissipated distal to the spine. This is reflected in a reduced transmission coefficient T_{land} (<1). Conversely, when falling onto the back or buttocks, the deceleration distance is markedly shorter (rigid contact, minimal support deformation), the axial impulse component is maximal, T_{land} increases, and for the same

h_{eq} a greater h_{spine}^{eff}, is obtained—indicating a locally "stiffer" impact on the thoracolumbar spine [172, 173]. In traffic collisions, the metric reflects the performance of passive safety systems: seat belts, pretensioners, and airbags do not alter the total energy budget of the event (mgh_{eq}), but they increase S_{land} (by extending torso deceleration distance and spreading the impulse over time), thereby reducing h_{spine}^{eff} [175, 176]. The geometry of the load path (through the torso) generally remains unchanged; thus, in first approximation, T_{lan} varies minimally.

Fixing the reference distance at s_{ref}=0.1 m standardizes the metric and ensures comparability across scenarios: h_{spine}^{eff} should be interpreted as the "height under standard conditions" energetically equivalent to the given event specifically for the spine. As noted above, the mean axial spinal overload in units of g is:

$$\bar{g}_{spine} = \frac{h_{eq}}{S_{land}} * T_{land} \Rightarrow \bar{g}_{spine} = \frac{h_{spine}^{eff}}{s_{ref}}.$$

In other words, h_{spine}^{eff} represents the mean spinal deceleration $\bar{g}_{spine}$ converted into "meters" relative to the selected s_{ref}, thereby preserving the physical relationship with deceleration dynamics while simultaneously providing an intuitive clinical interpretation [179]. The metric is mass-neutral and therefore suitable for population-based comparisons and for correlation with indicators of bone tissue quality.

The principal advantage of this parameter lies in the unification of event force description within a convenient "height-based" format while maintaining spine-specific clinical relevance. This facilitates risk stratification and cohort comparison, enables the direct conversion of h_{spine}^{eff} into categorical scores of the proposed (spine-oriented) scale for operational communication and statistical analysis, and allows its application in constructing quantitative associations with bone quality indicators—dual-energy X-ray absorptiometry (DXA), trabecular bone score (TBS), and computed tomography–derived density expressed in Hounsfield Units (CT-HU) [180, 181].

The limitations of the metric are related to the need for expert reconstruction of contact conditions: errors in the estimation of S_{land} and T_{land} are linearly propagated into the final result. Therefore, detailed documentation of injury circumstances substantially enhances the accuracy and effectiveness of the assessment.

Overall, h_{spine}^{eff} serves as a fundamental mass-neutral descriptor of mechanical exposure to the spine, integrating event geometry, posture, deceleration path, and the point of force application, thereby ensuring a physically valid and clinically meaningful evaluation of impact severity.

Development of the online calculator

To accelerate data processing, eliminate the need for constant reference to lookup tables, expand the range of applicable scenarios, and simplify coefficient adjustment for validation purposes, we developed a web-based calculator (***Fig. 3***).

The tool provides modular input based on typical scenarios ("Fall," "RTA"), automatically populating standard values and ranges for the parameters T_{land} and S_{land} depending on the selected body position and landing surface. In the case of RTAs, it additionally supplies rapid estimation coefficients for Δ*v* according to vehicle

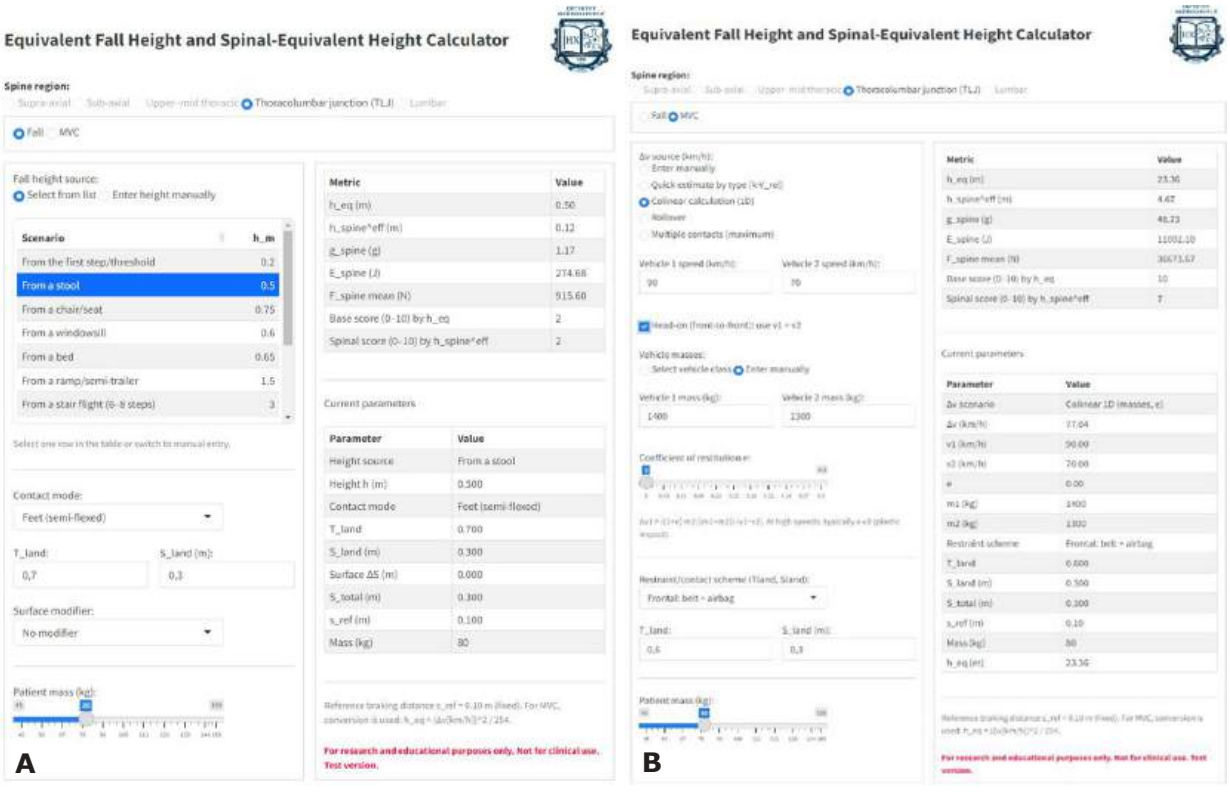

Fig. 3. Interface of the developed web calculator: A — fall; B — RTA

type and collision pattern. Users may retain the "default values" (in accordance with the embedded reference libraries) or manually override them; all modifications are instantly incorporated into the calculations.

The calculator is available at: www.spine.org.ua/scale.

Validation of the scale and derived metrics

The objective of the subsequent phase was to quantitatively evaluate the metric properties of the spine-oriented measure h_{spine}^{eff} and its derived indicators (baseline h_{eq}, $\bar{g}_{spine}$, E_{spine} and $\bar{F}_{spine}$), as well as the final composite scores (0–10) based on these parameters. The analysis included assessment of construct and criterion validity, relative and absolute reliability, agreement for continuous metrics, threshold stability, and known-groups validity.

Construct validity. Within the dataset of clinical and anamnestic variables used for verification, the metric h_{spine}^{eff} demonstrated the expected convergence with the integral measure of mechanical exposure: the correlation with baseline h_{eq} was 0.82 ($p < 0.001$), indicating that approximately 67% of the variance in h_{spine}^{eff} is explained by variability in event energy normalized to height. Associations with spinal injury morphology based on CT/MRI findings were also consistent with theoretical expectations: increasing h_{spine}^{eff} was accompanied by greater anterior wedge deformation ($r = 0.58$, $p < 0.001$; explained variance ≈34%) and a higher degree of spinal canal compromise ($r = 0.49$, $p < 0.001$; explained variance ≈24%). A monotonic relationship was identified with ordinal injury severity according to the AO Spine classification ($\rho = 0.62$, $p < 0.001$): progression from low-energy patterns (A1) to burst and complex types (A3/A4, B/C) was associated with increasing metric values.

In binary logistic regression for the threshold ≥A3, each additional 1 m was associated with a 1.85-fold increase in the odds ratio (OR) of sustaining burst/unstable injuries (95% CI 1.45–2.38, $p < 0.001$), after adjustment for age and sex. This finding is consistent with the biomechanical interpretation of the metric: an increase of 1 m in h_{spine}^{eff} nearly doubles the odds of injuries classified as ≥A3.

From a practical standpoint: if at $h_{spine}^{eff} = 0.8$ m the conditional probability of injury ≥A3 is approximately 20% (OR ≈0.25), then at 1.8 m (+1 m), the OR increases by a factor of 1.85 (≈0.46), and the probability rises to approximately 32%; with a 2 m increase, it approaches ≈46%. Assessment of logit linearity (Box–Tidwell test, restricted cubic splines) revealed no significant nonlinearity within the studied range and no evidence of multicollinearity.

The mass-neutral property, which is critically important for this metric, was confirmed by partial correlation with body weight: after controlling for mechanism and position, $r = 0.06$ ($p = 0.41$), indicating no statistically significant association. In contrast, the energy-dependent metric E_{spine} showed the expected strong correlation with body mass ($r = 0.74$, $p < 0.001$). These results support the theoretical interpretation of h_{spine}^{eff} as an indicator of external mechanical exposure to the spine rather than a surrogate marker of bone tissue strength.

Criterion validity. In the absence of external verified indicators (EDR, objective measurement of height), clinical outcomes based on neuroimaging findings served as the criterion. The ability of h_{spine}^{eff} to predict the presence of vertebral fracture was rated as "good" according to the Hosmer–Lemeshow criteria: the area under the ROC curve (AUC) was 0.82 (95% CI 0.73–0.90). For the detection of compression–burst injuries (A3/A4), the AUC was 0.78. An optimal threshold of approximately 1.3 m yielded a sensitivity of ≈0.76 and a specificity of ≈0.72 (based on the maximum Youden index). This corresponds to LR^{+}≈2.7 and LR^{-} ≈0.33, which clinically indicates a weak to borderline moderate increase in post-test probability with a positive result and a weak decrease with a negative result. Thus, the metric is useful as an adjunctive tool for risk stratification. For features of posterior ligamentous complex injury, discrimination was predictably lower due to more complex biomechanics: AUC = 0.74, with a threshold of approximately 2.4 m. In screening scenarios (where minimizing missed cases is critical), lowering the threshold below the optimum (favoring sensitivity) is advisable; in confirmatory contexts, raising the threshold above the optimum (favoring specificity) is appropriate. By definition, a single mechanical descriptor cannot account for the full extent of interindividual variability; however, the reported AUC values indicate practically meaningful diagnostic utility for risk stratification and severity ranking.

Additional robustness checks (restriction of analyses to cases with low uncertainty regarding T_{land} and S_{land}, analysis limited to thoroughly documented postures and contact surfaces, and bootstrap estimation of AUC) did not materially alter the conclusions. Model calibration (intercept/slope) remained satisfactory, with no evidence of systematic bias in clinically relevant threshold ranges. Collectively, construct and criterion validity consistently support that h_{spine}^{eff} is an informative indicator of "event severity" for the spine, useful for clinical communication, stratification, and research on associations with bone quality and therapeutic outcomes.

Relative reliability of measurements. Inter-rater agreement for the presented anamnestic cases (n = 40, 5 experts) was assessed using the intraclass correlation coefficient ICC (2.1) (two-way random-effects model, absolute agreement, single measure). For the baseline score calculated directly from h_{eq}, ICC was 0.84 (95% CI 0.77–0.89), corresponding to "good" agreement. For the spine-oriented score based on h_{spine}^{eff}, ICC was slightly lower at 0.79 (95% CI 0.71–0.86), also within the "good" reliability range.

When averaging the ratings of five experts (ICC(2,k)), agreement increased to 0.95 and 0.92 for h_{eq} and h_{spine}^{eff}, respectively, corresponding to an "excellent" level. The weighted κ coefficient with quadratic weights was 0.78 (h_{eq}) and 0.72 (h_{spine}^{eff}), indicating "substantial" agreement according to the scale of Landis & Koch.

Repeated assessment of a subsample of cases (test–retest, 10 cases, reassessment after ≥2 weeks) demonstrated high stability: ICC (2,1) was 0.90 (95% CI 0.83–0.95) for the baseline score and 0.85 (95% CI 0.76–0.92) for the spine-oriented score. The mean absolute difference between the first and repeated assessments

was 0.42 and 0.58 points, respectively, confirming high temporal reproducibility of the instrument.

Absolute reliability. To evaluate the precision of individual measurements, SEM and MDC_{95} were calculated.

$$SEM = SD\sqrt{1 - ICC},$$

where SD is the standard deviation of scores across the entire sample.

For the baseline score, SEM was 0.80 points; for the spine-oriented score, 0.95 points.

MDC_{95}, was calculated as

$$MDC_{95} = 1.96\sqrt{2}\,SEM,$$

yielding ≈2,2 і 2,6 points for h_{eq} and respectively.

These findings indicate that fluctuations of less than 2–3 points may be attributable to random variability. At the same time, the clinical relevance of such differences depends on the scale range: at lower levels (where intervals correspond to tens of centimeters), a change of 1–2 points is usually not meaningful, whereas at higher levels even a 1-point difference (corresponding to an increase in height by an order of meters or tens of meters) may reflect a substantial change in mechanical exposure. In general, exceeding the MDC_{95} threshold of approximately 2–3 points is highly likely to represent a statistically significant difference; however, its clinical interpretation should consider the scale level.

Thus, the scale demonstrates both high relative reliability (inter-rater agreement and temporal stability) and acceptable absolute precision (low SEM and MDC) (***Table 6***). This supports its use both for patient stratification based on a single measurement and for longitudinal monitoring, in which changes ≥MDC should be considered meaningful.

Agreement for continuous metrics. To assess agreement between the calculated metric values (based on expert ratings) and the reference algorithmic computations (online calculator based on author-derived values), Bland–Altman plots were constructed (***Fig. 4***).

Table 6. Indicators of relative and absolute reliability of the scale (40 cases, 5 experts)

Indicator	Baseline score (h_{eq})	Spine-oriented score (h_{spine}^{eff})	Interpretation
ICC (2.1) (inter-rater)	0.84 (95% CI 0.77–0.89)	0.79 (95% CI 0.71–0.86)	"Good" agreement (Koo & Li, 2016)
ICC (2.k) (mean of 5 experts)	0.95	0.92	"Excellent" agreement
Weighted κ	0.78	0.72	"Substantial" (Landis & Koch, 1977)
ICC (2.1) , test–retest	0.90 (95% CI 0.83–0.95)	0.85 (95% CI 0.76–0.92)	High stability
SEM, points	0.80	0.95	Standard error of measurement
MDC_95, points	2.2	2.6	Minimal detectable change

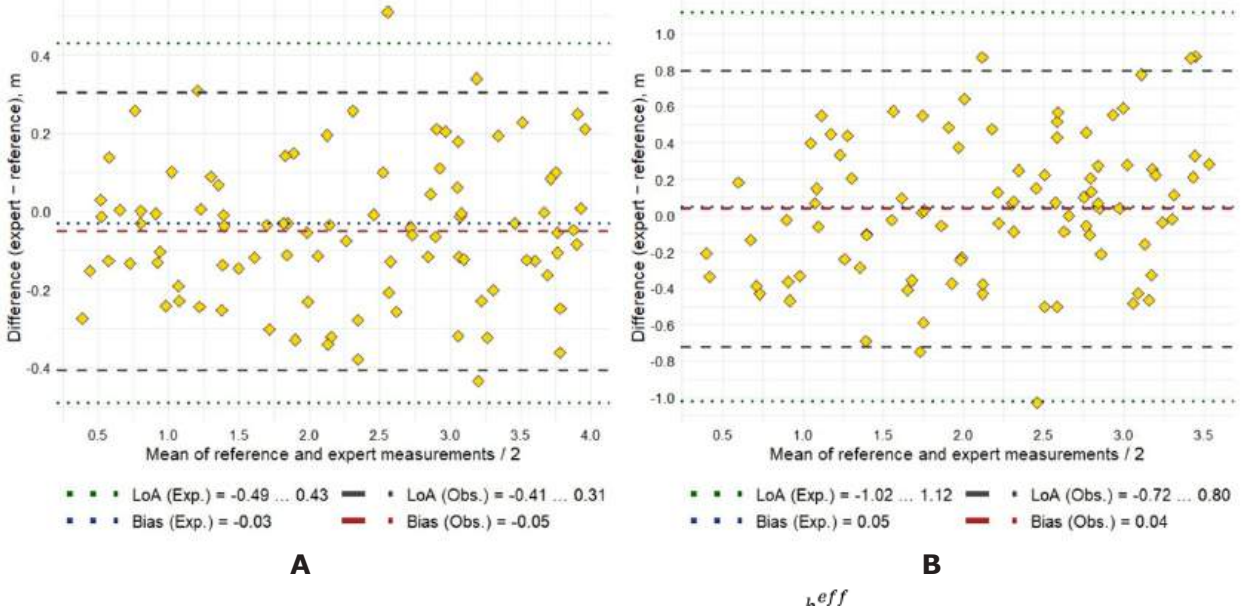

Fig. 4. Bland–Altman plots for the analyzed metrics: A – for heq; B – for h_{spine}^{eff}

For h_{eq} he mean bias was 0,03 m, with 95% limits of agreement (−0.49;0.43) m, for h_{spine}^{eff} − +0.05 m, with 95% limits of agreement (−1.02;1.12) m.

Thus, for the baseline metric h_{eq} near-complete concordance between expert-derived and reference estimates was observed, whereas for h_{spine}^{eff} the limits of agreement were wider. These findings reflect not methodological error but biomechanical uncertainty related to variability in the selection of the deceleration pathway and load-transfer coefficient. Analysis of heteroscedasticity demonstrated that dispersion did not increase at higher or lower metric levels, ensuring comparable precision across the entire range of analyzed values.

Threshold stability. To assess the robustness of score-based classification, a sensitivity analysis was conducted by varying threshold values by ±10–15%, as well as by recalculating scores under "minimal" and "maximal" S_{land} and T_{land} scenarios in the estimation of h_{spine}^{eff}.

For the baseline scale (based on h_{eq}) concordance of the assigned level was maintained in 77% of cases; disagreement by ±1 level occurred in 20%, and by more than ±1 level in only 3%.

For the spine-oriented scale (based on h_{spine}^{eff}) identical level assignment was observed in 62% of cases; a shift of ±1 level occurred in 31%, and of more than ±1 level in 7%.

The greatest sensitivity was noted in transitional scenarios (e.g., falling onto the knees with subsequent axial load transfer) and in landings on soft surfaces, where the potential ranges of S_{land} and T_{land} are broader. Nevertheless, even with parameter variation of 15%, discrepancies in most cases did not exceed one scale level, confirming the practical robustness of the instrument.

Known-groups validity. To evaluate discriminative ability, two clinically relevant groups were compared:

- fragility scenarios: patients ≥65 years old who sustained a fall from a height ≤1 m, typically associated with osteoporotic fractures.

- non-fragility scenarios: younger patients or those injured from falls >1 m and/or in RTAs.

The median h_{spine}^{eff} in the fragility group was 0.48 m (interquartile range 0.32–0.72), whereas in the non-fragility group it was 2.15 m (interquartile range 1.40–3.10). The differences were statistically significant ($p < 0.001$). Cohen's effect size was $d = 1.10$, corresponding to a large effect.

These findings confirm the clinical meaningfulness of the metric: low values of h_{spine}^{eff} are characteristic of low-energy osteoporotic fractures, whereas high values are typical of high-energy trauma requiring different management strategies and associated with a distinct therapeutic prognosis.

Discussion

Interpretation of results and clinical significance

Validation of the multilevel scale for quantitative assessment of external mechanical impact on the spine demonstrated its informativeness and consistency with the actual severity of injury. Higher values of the calculated indices—primarily h_{eq}, h_{spine}^{eff} and $\bar{g}_{spine}$ were statistically associated with more pronounced pathomorphological changes of the spine.

These findings further substantiate the clinical relevance of the metric: low h_{spine}^{eff} values are typical of low-energy osteoporotic fractures, whereas high values correspond to high-energy trauma requiring different therapeutic approaches and associated with different outcome expectations. Elevated h_{eq} and h_{spine}^{eff} were more frequently associated with severe structural damage, and increasing $\bar{g}_{spine}$ reflecting loads exceeding physiologically tolerable limits—was accompanied by a higher probability of severe injury (including categories corresponding to AIS ≥3). This concordance indicates that the scale effectively "captures" the physical "energy of the event" underlying injury severity.

A key advantage of the proposed approach is its quantitative and continuous nature. Instead of descriptive labels, the scale provides numerical values with direct physical interpretation: each increment in h_{eq}, h_{spine}^{eff} and $\bar{g}_{spine}$ corresponds to a real increase in injurious mechanical exposure rather than merely crossing an arbitrary threshold. This enhances clinical interpretability. For example, the conclusion that "the impact is equivalent to a fall from approximately 3 m" can be readily contextualized in terms of expected risk, while load values expressed in units of g are intuitively understood by practicing clinicians.

The results are consistent with clinical experience and epidemiological observations: more intense mechanical exposures (including falls from height and high-speed collisions) are predictably associated with more severe injuries [3, 182], whereas low-energy scenarios (e.g., "standing height or less") more often result in less extensive morphological damage [80, 183]. Importantly, the scale accurately describes the continuum of mechanical exposure: it can be applied to both high- and low-energy events, enabling risk ranking without an a priori assumption regarding the "dominant" mechanism [1, 88].

In practical terms, high values of h_{eq} and h_{spine}^{eff} serve as early indicators of potentially complex spinal injuries (even in the presence of minimal initial symptoms) [153, 184], whereas low values justify a more conservative diagnostic approach [185, 186]. Overall, the scale strengthens the causal link between event biomechanics and clinical outcome, thereby improving the accuracy of risk stratification and supporting evidence-based diagnostic and therapeutic decision-making [187, 188].

Comparison with existing classifications and scales

Abbreviated Injury Scale (AIS) The proposed quantitative approach differs substantially from traditional trauma severity scales. The Abbreviated Injury Scale (AIS) is a widely accepted instrument for grading injury severity based on anatomical damage [17, 18]. AIS assigns injuries scores from 1 (minor) to 6 (maximal, currently untreatable) according to the nature and location of the lesion. However, AIS represents a retrospective assessment—performed after patient evaluation—once specific injuries (fractures, ligament ruptures, spinal cord contusions, etc.) have been identified [153]. AIS neither measures nor describes the mechanism of injury [189]. Moreover, AIS encompasses injuries of the entire body rather than focusing

specifically on the spine; therefore, it inadequately reflects differences in external mechanical exposure. Two patients may receive the same AIS score—for example, AIS 3—although one sustained injury from a fall from height and the other from a high-speed RTA [190].

The scale proposed herein is oriented toward injury biomechanics, i.e., the characteristics of the external impact that caused the damage. It complements AIS by enabling assessment at the stage of mechanism evaluation, prior to definitive diagnosis. For example, knowing that h_{spine}^{eff}> ≈ 5 m allows one to anticipate a high probability of serious spinal injury, even in the absence of obvious signs at initial examination. Thus, the scale functions as a prognostic tool [88]. Similarly, a high h_{eq} value may raise suspicion of injuries to both the musculoskeletal system and internal organs. In contrast, severity according to AIS (e.g., AIS ≥3, typically indicative of serious trauma) is determined only after the injury itself has been documented [191]. Accordingly, the proposed scale does not replace AIS but rather complements the trauma assessment system: AIS ranks severity by consequence, whereas the present scale ranks it by causal factor (impact energy). The integration of both approaches enables a more comprehensive characterization and prognosis of trauma.

Classifications of spinal injuries. Existing classification systems (e.g., AO Spine, TLICS) are primarily oriented toward injury morphology and clinical consequences [19, 192, 193], without providing a quantitative assessment of mechanical exposure [3, 194]. The contemporary international AO Spine Classification System, developed under the auspices of the AO Foundation and partially derived from the Magerl system, categorizes injuries by type (A – compression, B – distraction, C – rotational/ translational injuries), supplemented by neurological status and clinical modifiers, including the condition of the posterior ligamentous complex [195–197]. Its principal strength lies in its comprehensiveness and high reproducibility for guiding management decisions [198]. However, two injuries with the same AO code may result from fundamentally different magnitudes and directions of external load.

The proposed scale quantitatively characterizes the "force of the event" prior to the anatomical outcome, thereby complementing morphological systems. Clinically, this allows the conventional diagnostic formulation (e.g., "AO Spine A3") to be supplemented with the level of mechanical exposure (e.g., "equivalent to a fall from ≈4 m" or the numerical values of h_{eq}, h_{spine}^{eff} and $\bar{g}_{spine}$. Such an approach enhances the prognostic and communicative value of case descriptions: the morphological system specifies what is injured, whereas the quantitative scale indicates the energy/rigidity of the impact that produced the injury [199, 200]. An additional advantage is the mass-neutral and physically interpretable nature of the indicators, which reduces subjectivity and enables valid comparisons across patients and cohorts.

CDC Field Triage Guidelines. In emergency medicine, decisions regarding transport to a trauma center have traditionally relied on mechanism-of-injury criteria [88]. The U.S. National CDC Field Triage Guidelines (developed by the Centers for Disease Control and Prevention in collaboration with the American College of Surgeons) identify several "high-risk mechanisms." For example, an adult fall from >6 m (20 feet) is considered indicative of a high risk of severe trauma and constitutes a criterion for transport to a specialized trauma center [201, 202]. Other "dangerous mechanisms" include significant vehicle deformation (intrusion >30 cm), partial or complete ejection from the vehicle, death of the passenger in the same vehicle, and high-speed motorcycle crashes [5, 199]. The principal advantage of this approach lies in its simplicity and rapid applicability: paramedics can make prompt decisions even when vital signs remain stable [185, 203].

However, the limitations of a threshold-based scheme are evident. Mechanism severity is a continuous variable: the difference between 5.9 m and 6.1 m is negligible, while the threshold itself is conventional [80]. Outcomes are influenced by modifiers that are typically not explicitly incorporated, such as surface type and stiffness, posture/contact geometry, deceleration duration, and the performance of passive safety systems [133, 137, 152]. Consequently, clinical paradoxes arise: a formally "low-energy" event may result in severe injury, whereas a "threshold" event may not [204,205]. This is particularly relevant in vulnerable populations. In older adults, even a fall from standing height may lead to severe cervical injury [82, 183]. Reviews addressing medical triage have also documented substantial rates of under-triage and over-triage, reflecting inevitable information loss when a continuous variable is dichotomized [88].

The proposed quantitative scale complements field triage rules without attempting to replace them. Instead of a binary "threshold exceeded/not exceeded" approach, it provides a graded assessment of mechanical exposure (e.g., h_{eq} 4, 6, or 8 m) and incorporates key modifiers (surface/posture/ S_{land}), such that two falls "from the same height" yield different values when the "rigidity" of contact is fundamentally different. Such integration allows risk differentiation within a given category, potentially reducing both underdiagnosis and unnecessary over-triage. The evolution of medical triage is increasingly oriented toward objective data and telemetry (vehicle parameters/event data recorder, EDR) [171]. In this context, numerical indicators such as (h_{eq}) can be naturally incorporated into EMS algorithms as an additional standardized, evidence-based parameter supporting individualized decision-making [149, 206].

The practical application of the scale lies in its role as a complement—not a substitute—for morphological classifications (e.g., AO Spine, AIS). Quantitative assessment of mechanical exposure is particularly valuable during prehospital triage and patient routing (risk prediction of complex injuries; justification for transport to a trauma center), in planning the scope of imaging, and in multicenter research for standardizing the description of "event severity." In the in-hospital setting, treatment decisions are based primarily on injury morphology and patient status, whereas the scale provides a quantitative context of the mechanism, thereby enhancing communication and risk stratification.

Limitations

This study represents the initial (pilot) stage of scale development and validation. For active implementation in healthcare practice, further calibration of the proposed

indices and expansion of clinical scenarios are required. In particular, external multicenter validation of thresholds and coefficients underlying the calculations is necessary (refinement of T_{land} and S_{land}, the selected reference s_{ref}, and the boundaries of the 0–10 categories). Additional accumulation and analysis of cases with "atypical" mechanics (sliding/oblique contacts, multi-impulse events, compression injuries, blast trauma, multistage falls) are also warranted. Furthermore, the impact of integrating the scale into clinical and organizational decision-making (scope of imaging, patient routing, choice of fixation strategy) on clinical outcomes and resource utilization should be evaluated.

The proposed indicators were optimized for the thoracolumbar junction (T11–L2) as the region most vulnerable to indirect axial loading. Regional adaptation is required for other spinal segments. For example, in the cervical spine, consideration of "head-first" and diving scenarios, as well as whiplash components, is necessary. Overall, this entails the development of segment-specific scenario libraries and recalibration of coefficients accounting for anatomical and biomechanical differences.

Conclusions

The proposed scale represents a mechanistically grounded, mass-neutral, and quantitatively interpretable descriptor of mechanical exposure that complements morphological classifications and is suitable for standardizing trauma description. For clinical implementation, multicenter external validation, refinement of parameters (including calibration of T_{land}, S_{land} and threshold values), and expansion of scenario coverage with consideration of segment-specific biomechanics are required.The technological trajectory involves integration with EMR/EMS systems, utilization of telemetry (EDR, wearable IMU), and automated calculators; the scientific direction includes integration with multibody models and bone quality parameters to develop hybrid risk models.

In light of current clinical and organizational trends (mechanism-oriented triage, harmonization of classifications, and individualization of care), the scale has potential for incorporation into diagnostic and routing protocols, educational modules, and healthcare analytics frameworks. Its implementation may contribute to establishing a unified "language" for quantitative assessment of "event severity," improving data comparability and potentially enhancing the quality of risk stratification and clinical outcomes in spinal trauma.

Acknowledgments

The authors express their gratitude to the experts for their participation in the evaluation of clinical materials, discussion of key methodological decisions, and contributions to the refinement of the proposed scale.

Disclosure

Conflict of interest

The authors declare no conflict of interest.

Informed consent

Informed consent was obtained from each patient.

Funding

The study received no external funding.

References

1. Roberts SB, Tsirikos AI. Biomechanics of the spine and the implications for spinal injuries. Orthopaedics and Trauma. 2024;38(5):258-263. doi: 10.1016/j.mporth.2024.07.001
2. Zileli M, Sharif S, Fornari M. Incidence and Epidemiology of Thoracolumbar Spine Fractures: WFNS Spine Committee Recommendations. Neurospine. 2021;18(4):704-712. doi: 10.14245/ns.2142418.209
3. Iencean SM. Classification of spinal injuries based on the essential traumatic spinal mechanisms. Spinal Cord. 2003;41(7):385-396. doi: 10.1038/sj.sc.3101468
4. Zhaoli M, Hengrui Z, Feiyue L, Hui L, Fei D, Tong L, et al. A Retrospective Epidemiological Study of Patients Hospitalized with Spinal Cord Injury in Dalian Port Hospital from 2017 to 2019. International Journal of Chinese Medicine. 2020;4(4). doi: 10.11648/j.ijcm.20200404.14
5. Kent R, Cormier J, McMurry TL, Johan Ivarsson B, Funk J, Hartka T, Sochor M. Spinal injury rates and specific causation in motor vehicle collisions. Accid Anal Prev. 2023;186:107047. doi: 10.1016/j.aap.2023.107047
6. Neyaz O, Kanaujia V, Yadav RK, Sarkar B, Azam MQ, Kandwal P. Epidemiology of Traumatic Spinal Cord Injury in the Himalayan Range and Sub-Himalayan region: A Retrospective Hospital Data-Based Study. Ann Rehabil Med. 2024;48(1):86-93. doi: 10.5535/arm.23107
7. Wang ZM, Zou P, Yang JS, Liu TT, Song LL, Lu Y, et al. Epidemiological characteristics of spinal cord injury in Northwest China: a single hospital-based study. J Orthop Surg Res. 2020;15(1):214. doi: 10.1186/s13018-020-01729-z
8. Beausejour MH, Wagnac E, Arnoux PJ, Thiong JM, Petit Y. Numerical Investigation of Spinal Cord Injury After Flexion-Distraction Injuries at the Cervical Spine. J Biomech Eng. 2022;144(1). doi: 10.1115/1.4052003
9. Whittier DE, Bevers M, Geusens P, van den Bergh JP, Gabel L. Characterizing Bone Phenotypes Related to Skeletal Fragility Using Advanced Medical Imaging. Curr Osteoporos Rep. 2023;21(6):685-697. doi: 10.1007/s11914-023-00830-6
10. An N, Lin JS, Fei Q. Beijing Friendship Hospital Osteoporosis Self-Assessment Tool for Elderly Male (BFH-OSTM) vs Fracture Risk Assessment Tool (FRAX) for identifying painful new osteoporotic vertebral fractures in older Chinese men: a cross-sectional study. BMC Musculoskelet Disord. 2021;22(1):596. doi: 10.1186/s12891-021-04476-2
11. Ihama F, Pandyan A, Roffe C. Assessment of fracture risk tools in care home residents: a multi-centre observational pilot study. Eur Geriatr Med. 2021;12(1):79-89. doi: 10.1007/s41999-020-00383-2
12. Gibbs JC, MacIntyre NJ, Ponzano M, Templeton JA, Thabane L, Papaioannou A, Giangregorio LM. Exercise for improving outcomes after osteoporotic vertebral fracture. Cochrane Database Syst Rev. 2019;7(7):CD008618. doi: 10.1002/14651858.CD008618.pub3
13. Nau C, Leiblein M, Verboket RD, Horauf JA, Sturm R, Marzi I, Stormann P. Falls from Great Heights: Risk to Sustain Severe Thoracic and Pelvic Injuries Increases with Height of the Fall. J Clin Med. 2021;10(11). doi: 10.3390/jcm10112307
14. Gross C, Menard J, Mull J, Diaz-Zuniga Y, Skarupa D, Crandall M. Assessing Fall Mortality by Field-Relevant Categories at an Urban Level I Trauma Center. J Surg Res. 2024;300:279-286. doi: 10.1016/j.jss.2024.04.008
15. Fujii M, Shirakawa T, Nakamura M, Baba M, Hitosugi M. Factors influencing the injury severity score and the probability of survival in patients who fell from height. Sci Rep. 2021;11(1):15561. doi: 10.1038/s41598-021-95226-w
16. Costachescu B, Popescu CE, Iliescu BF. Analysis of the Classification Systems for Thoracolumbar Fractures in Adults and Their Evolution and Impact on Clinical Management. J Clin Med. 2022;11(9). doi: 10.3390/jcm11092498
17. Gennarelli TA, Wodzin E. AIS 2005: a contemporary injury scale. Injury. 2006;37(12):1083-1091. doi: 10.1016/j.injury.2006.07.009
18. Sahin T, Batin S. A descriptive study of orthopaedic injuries due to parachute jumping in soldiers. BMC Emerg Med. 2020;20(1):58. doi: 10.1186/s12873-020-00354-7

19. Bajamal AH, Permana KR, Faris M, Zileli M, Peev NA. Classification and Radiological Diagnosis of Thoracolumbar Spine Fractures: WFNS Spine Committee Recommendations. Neurospine. 2021;18(4):656-666. doi: 10.14245/ns.2142650.325
20. Hwang Z, Abdalla M, Ajayi B, Bernard J, Bishop T, Lui DF. Thoracolumbar spine trauma: a guide for the FRCS examination. Eur J Orthop Surg Traumatol. 2023;33(6):2655-2661. doi: 10.1007/s00590-022-03430-9
21. Vu C, Gendelberg D. Classifications in Brief: AO Thoracolumbar Classification System. Clin Orthop Relat Res. 2020;478(2):434-440. doi: 10.1097/CORR.0000000000001086
22. Jeanmougin T, Cole E, Duceau B, Raux M, James A. Heterogeneity in defining multiple trauma: a systematic review of randomized controlled trials. Crit Care. 2023;27(1):363. doi: 10.1186/s13054-023-04637-w
23. Donnelly NA, Brent L, Hickey P, Masterson S, Deasy C, Moloney J, et al. Substantial heterogeneity in trauma triage tool characteristic operationalization for identification of major trauma: a hybrid systematic review. Eur J Trauma Emerg Surg. 2025;51(1):74. doi: 10.1007/s00068-024-02694-6
24. Wohlgemut JM, Marsden MER, Stoner RS, Pisirir E, Kyrimi E, Grier G, et al. Diagnostic accuracy of clinical examination to identify life- and limb-threatening injuries in trauma patients. Scand J Trauma Resusc Emerg Med. 2023;31(1):18. doi: 10.1186/s13049-023-01083-z
25. Xiong T, Luo Q, Chen Q, Shi L, Duan A, Liu S, Li K. Development of a repetitive traumatic brain injury risk function based on real-world accident reconstruction and wavelet packet energy analysis. Front Bioeng Biotechnol. 2025;13:1548265. doi: 10.3389/fbioe.2025.1548265
26. Mokkink LB, Prinsen CA, Bouter LM, Vet HC, Terwee CB. The COnsensus-based Standards for the selection of health Measurement INstruments (COSMIN) and how to select an outcome measurement instrument. Braz J Phys Ther. 2016;20(2):105-113. doi: 10.1590/bjpt-rbf.2014.0143
27. Swan K, Speyer R, Scharitzer M, Farneti D, Brown T, Woisard V, Cordier R. Measuring what matters in healthcare: a practical guide to psychometric principles and instrument development. Front Psychol. 2023;14:1225850. doi: 10.3389/fpsyg.2023.1225850
28. Mokkink LB, de Vet H, Diemeer S, Eekhout I. Sample size recommendations for studies on reliability and measurement error: an online application based on simulation studies. Health Services and Outcomes Research Methodology. 2022;23(3):241-265. doi: 10.1007/s10742-022-00293-9
29. Lewis CC, Klasnja P, Lyon AR, Powell BJ, Lengnick-Hall R, Buchanan G, et al. The mechanics of implementation strategies and measures: advancing the study of implementation mechanisms. Implement Sci Commun. 2022;3(1):114. doi: 10.1186/s43058-022-00358-3
30. Galhardas L, Raimundo A, Marmeleira J. Test-retest reliability of upper-limb proprioception and balance tests in older nursing home residents. Arch Gerontol Geriatr. 2020;89:104079. doi: 10.1016/j.archger.2020.104079
31. Hage R, Detrembleur C, Dierick F, Brismee JM, Roussel N, Pitance L. Sensorimotor performance in acute-subacute non-specific neck pain: a non-randomized prospective clinical trial with intervention. BMC Musculoskelet Disord. 2021;22(1):1017. doi: 10.1186/s12891-021-04876-4
32. Gatsonis C, Sampson AR. Multiple correlation: exact power and sample size calculations. Psychol Bull. 1989;106(3):516-524. doi: 10.1037/0033-2909.106.3.516
33. Hattie J, Cooksey RW. Procedures for Assessing the Validities of Tests Using the "Known-Groups" Method. Applied Psychological Measurement. 1984;8(3):295-305. doi: 10.1177/014662168400800306
34. Kalcev G, Barbov I, Kotevska PI, Preti A, Carta MG. Biological Rhythms in People from North Macedonia with Bipolar Disorder: Application of the Macedonian Biological Rhythms Interview of Assessment in Neuropsychiatry (BRIAN). The Open Psychology Journal. 2022;15(1). doi: 10.2174/18743501-v15-e2208301
35. Hiraishi M, Tanioka K, Shimokawa T. Concordance rate of a four-quadrant plot for repeated measurements. BMC Med Res Methodol. 2021;21(1):270. doi: 10.1186/s12874-021-01461-0
36. Jan SL, Shieh G. The Bland-Altman range of agreement: Exact interval procedure and sample size determination. Comput Biol Med. 2018;100:247-252. doi: 10.1016/j.compbiomed.2018.06.020
37. Taffe P, Zuppinger C, Burger GM, Nussle SG. The Bland-Altman method should not be used when one of the two measurement methods has negligible measurement errors. PLoS One. 2022;17(12):e0278915. doi: 10.1371/journal.pone.0278915
38. Bansal A, Heagerty PJ. A comparison of landmark methods and time-dependent ROC methods to evaluate the time-varying performance of prognostic markers for survival outcomes. Diagn Progn Res. 2019;3:14. doi: 10.1186/s41512-019-0057-6
39. Seshan VE, Gonen M, Begg CB. Comparing ROC curves derived from regression models. Stat Med. 2013;32(9):1483-1493. doi: 10.1002/sim.5648
40. Ruxton GD, Wilkinson DM, Neuhäuser M. Advice on testing the null hypothesis that a sample is drawn from a normal distribution. Animal Behaviour. 2015;107:249-252. doi: 10.1016/j.anbehav.2015.07.006
41. Shapiro SS, Wilk MB. An analysis of variance test for normality (complete samples). Biometrika. 1965;52(3-4):591-611. doi: 10.1093/biomet/52.3-4.591
42. Bahariniya S, Ezatiasar M, Madadizadeh F. A Brief Review of the Types of Validity and Reliability of scales in Medical Research. Journal of Community Health Research. 2021. doi: 10.18502/jchr.v10i2.6582
43. de Winter JC, Gosling SD, Potter J. Comparing the Pearson and Spearman correlation coefficients across distributions and sample sizes: A tutorial using simulations and empirical data. Psychol Methods. 2016;21(3):273-290. doi: 10.1037/met0000079
44. Schober P, Vetter TR. Logistic Regression in Medical Research. Anesth Analg. 2021;132(2):365-366. doi: 10.1213/ANE.0000000000005247
45. Zabor EC, Reddy CA, Tendulkar RD, Patil S. Logistic Regression in Clinical Studies. Int J Radiat Oncol Biol Phys. 2022;112(2):271-277. doi: 10.1016/j.ijrobp.2021.08.007
46. Abreu MN, Siqueira AL, Cardoso CS, Caiaffa WT. Ordinal logistic regression models: application in quality of life studies. Cad Saude Publica. 2008;24 Suppl 4:s581-591. doi: 10.1590/s0102-311x2008001600010
47. Guzman-Castillo M, Brailsford S, Luke M, Smith H. A tutorial on selecting and interpreting predictive models for ordinal health-related outcomes. Health Services and Outcomes Research Methodology. 2015;15(3-4):223-240. doi: 10.1007/s10742-015-0140-6
48. Zeng G. A graphic and tabular variable deduction method in logistic regression. Communications in Statistics - Theory and Methods. 2020;51(16):5412-5427. doi: 10.1080/03610926.2020.1839499
49. Discacciati A, Palazzolo MG, Park JG, Melloni GEM, Murphy SA, Bellavia A. Estimating and presenting non-linear associations with restricted cubic splines. Int J Epidemiol. 2025;54(4). doi: 10.1093/ije/dyaf088
50. Schuster NA, Rijnhart JJM, Twisk JWR, Heymans MW. Modeling non-linear relationships in epidemiological data: The application and interpretation of spline models. Front Epidemiol. 2022;2:975380. doi: 10.3389/fepid.2022.975380
51. Shrestha N. Detecting Multicollinearity in Regression Analysis. American Journal of Applied Mathematics and Statistics. 2020;8(2):39-42. doi: 10.12691/ajams-8-2-1
52. Corbacioglu SK, Aksel G. Receiver operating characteristic curve analysis in diagnostic accuracy studies: A guide to interpreting the area under the curve value. Turk J Emerg Med. 2023;23(4):195-198. doi: 10.4103/tjem.tjem_182_23
53. Ruopp MD, Perkins NJ, Whitcomb BW, Schisterman EF. Youden Index and optimal cut-point estimated from observations affected by a lower limit of detection. Biom J. 2008;50(3):419-430. doi: 10.1002/bimj.200710415
54. Paiva JRB, Pacheco VMG, Barbosa PS, Almeida FR, Wainer GA, Gomes FA, et al. Complexity measure based on sensitivity analysis applied to an intensive care unit system. Scientific Reports. 2023;13(1):14602. doi: 10.1038/s41598-023-40149-x

55. den Boon S, Jit M, Brisson M, Medley G, Beutels P, White R, et al. Guidelines for multi-model comparisons of the impact of infectious disease interventions. BMC Medicine. 2019;17(1):163. doi: 10.1186/s12916-019-1403-9
56. Kien C, Schultes MT, Szelag M, Schoberberger R, Gartlehner G. German language questionnaires for assessing implementation constructs and outcomes of psychosocial and health-related interventions: a systematic review. Implement Sci. 2018;13(1):150. doi: 10.1186/s13012-018-0837-3
57. Williams ZJ, Failla MD, Davis SL, Heflin BH, Okitondo CD, Moore DJ, Cascio CJ. Thermal Perceptual Thresholds are typical in Autism Spectrum Disorder but Strongly Related to Intra-individual Response Variability. Sci Rep. 2019;9(1):12595. doi: 10.1038/s41598-019-49103-2
58. Vargha A, Delaney HD. A Critique and Improvement of the CL Common Language Effect Size Statistics of McGraw and Wong. Journal of Educational and Behavioral Statistics. 2000;25(2):101-132. doi: 10.3102/10769986025002101
59. Panjeh S, Nordahl-Hansen A, Cogo-Moreira H. Establishing new cutoffs for Cohen's d: An application using known effect sizes from trials for improving sleep quality on composite mental health. Int J Methods Psychiatr Res. 2023;32(3):e1969. doi: 10.1002/mpr.1969. PMID: 37186318
60. Bobak CA, Barr PJ, O'Malley AJ. Estimation of an inter-rater intra-class correlation coefficient that overcomes common assumption violations in the assessment of health measurement scales. BMC Med Res Methodol. 2018;18(1):93. doi: 10.1186/s12874-018-0550-6
61. Kvalseth TO. An Alternative Interpretation of the Linearly Weighted Kappa Coefficients for Ordinal Data. Psychometrika. 2018. doi: 10.1007/s11336-018-9621-1
62. Mitani AA, Freer PE, Nelson KP. Summary measures of agreement and association between many raters' ordinal classifications. Ann Epidemiol. 2017;27(10):677-685 e674. doi: 10.1016/j.annepidem.2017.09.001
63. Polit DF. Getting serious about test-retest reliability: a critique of retest research and some recommendations. Qual Life Res. 2014;23(6):1713-1720. doi: 10.1007/s11136-014-0632-9
64. Bland JM, Altman DG. Measuring agreement in method comparison studies. Stat Methods Med Res. 1999;8(2):135-160. doi: 10.1177/096228029900800204
65. Chan PY, Mohd Ripin Z, Abdul Halim S, Kamarudin MI, Ng KS, Eow GB, et al. Biomechanical System Versus Observational Rating Scale for Parkinson's Disease Tremor Assessment. Sci Rep. 2019;9(1):8117. doi: 10.1038/s41598-019-44142-1
66. Stratford PW, Riddle DL. When minimal detectable change exceeds a diagnostic test-based threshold change value for an outcome measure: resolving the conflict. Phys Ther. 2012;92(10):1338-1347. doi: 10.2522/ptj.20120002
67. Bonovas S, Piovani D. On p-Values and Statistical Significance. J Clin Med. 2023;12(3). doi: 10.3390/jcm12030900
68. Sharma H. Statistical significance or clinical significance? A researcher's dilemma for appropriate interpretation of research results. Saudi J Anaesth. 2021;15(4):431-434. doi: 10.4103/sja.sja_158_21
69. Gonzalvez M, Munoz-Hernandez C. R programming environment in wildlife: Are Veterinary Sciences at the same level than other research areas? Res Vet Sci. 2024;166:105079. doi: 10.1016/j.rvsc.2023.105079
70. Ivancevic VG. New Mechanics of Spinal Injury. International Journal of Applied Mechanics. 2012;01(02):387-401. doi: 10.1142/s1758825109000174
71. LaPlaca MC, Simon CM, Prado GR, Cullen DK. CNS injury biomechanics and experimental models. Prog Brain Res. 2007;161:13-26. doi: 10.1016/S0079-6123(06)61002-9
72. Teresinski G, Milaszkiewicz A, Cywka T. An analysis of the relationship between bodily injury severity and fall height in victims of fatal falls from height. Arch Med Sadowej Kryminol. 2016;66(3):133-140. doi: 10.5114/amsik.2016.66397
73. Casali MB, Blandino A, Grignaschi S, Florio EM, Travaini G, Genovese UR. The pathological diagnosis of the height of fatal falls: A mathematical approach. Forensic Sci Int. 2019;302:109883. doi: 10.1016/j.forsciint.2019.109883
74. Petrone N, Cognolato M, McNeil JA, Hubbard M. Designing, building, measuring, and testing a constant equivalent fall height terrain park jump. Sports Engineering. 2017;20(4):283-292. doi: 10.1007/s12283-017-0253-y
75. Liu C, Xu T, Xia W, Xu S, Zhu Z, Zhou M, Liu H. Incidence, prevalence, and causes of spinal injuries in China, 1990-2019: Findings from the Global Burden of Disease Study 2019. Chin Med J (Engl). 2024;137(6):704-710. doi: 10.1097/CM9.0000000000003045
76. Lu Y, Shang Z, Zhang W, Pang M, Hu X, Dai Y, et al. Global incidence and characteristics of spinal cord injury since 2000-2021: a systematic review and meta-analysis. BMC Med. 2024;22(1):285. doi: 10.1186/s12916-024-03514-9
77. Gnanaprakash G, Peddireddy S, Kanna RM, Shetty AP, Rajasekaran S. Spinal Injuries Due to Falls from Height. Indian Spine Journal. 2024;7(2):168-174. doi: 10.4103/isj.isj_75_23
78. Goodacre S, Than M, Goyder EC, Joseph AP. Can the distance fallen predict serious injury after a fall from a height? J Trauma. 1999;46(6):1055-1058. doi: 10.1097/00005373-199906000-00014
79. Palacio C, Darwish M, Acosta M, Bautista R, Hovorka M, Chen C, Hovorka J. Incidence of fall-from-height injuries and predictive factors for severity. J Osteopath Med. 2025;125(5):229-236. doi: 10.1515/jom-2024-0158
80. Zhang ZR, Wu Y, Wang FY, Wang WJ. Traumatic spinal cord injury caused by low falls and high falls: a comparative study. J Orthop Surg Res. 2021;16(1):222. doi: 10.1186/s13018-021-02379-5
81. Koch M, Lunde LK, Gjulem T, Knardahl S, Veiersted KB. Validity of Questionnaire and Representativeness of Objective Methods for Measurements of Mechanical Exposures in Construction and Health Care Work. PLoS One. 2016;11(9):e0162881. doi: 10.1371/journal.pone.0162881
82. Bruggink C, van de Ree CLP, van Ditshuizen J, Polinder-Bos HA, Oner FC, Reijman M, Rutges J. Increased incidence of traumatic spinal injury in patients aged 65 years and older in the Netherlands. Eur Spine J. 2024;33(10):3677-3684. doi: 10.1007/s00586-024-08310-w
83. Wang F, Sun R, Zhang SD, Wu XT. Comparison of thoracolumbar versus non-thoracolumbar osteoporotic vertebral compression fractures in risk factors, vertebral compression degree and pre-hospital back pain. J Orthop Surg Res. 2023;18(1):643. doi: 10.1186/s13018-023-04140-6
84. Bodmer NS, Hauselmann HJ, Frey D, Aeberli D, Bachmann LM. Expert consensus on relevant risk predictors for the occurrence of osteoporotic fractures in specific clinical subgroups - Delphi survey. BMC Rheumatol. 2019;3:50. doi: 10.1186/s41927-019-0099-y
85. Kanis JA, McCloskey EV, Harvey NC, Cooper C, Rizzoli R, Dawson-Hughes B, et al. Intervention thresholds and diagnostic thresholds in the management of osteoporosis. Aging Clin Exp Res. 2022;34(12):3155-3157. doi: 10.1007/s40520-022-02216-7
86. Wool NK, Wilson S, Chong ACM, Dart BR. Bone Health Improvement Protocol. Kansas Journal of Medicine. 2017;10(3):62-66. doi: 10.17161/kjm.v10i3.8659
87. McCoy CE, Chakravarthy B, Lotfipour S. Guidelines for Field Triage of Injured Patients: In conjunction with the Morbidity and Mortality Weekly Report published by the Center for Disease Control and Prevention. West J Emerg Med. 2013;14(1):69-76. doi: 10.5811/westjem.2013.1.15981
88. Haske D, Lefering R, Stock JP, Kreinest M, TraumaRegister DGU. Epidemiology and predictors of traumatic spine injury in severely injured patients: implications for emergency procedures. Eur J Trauma Emerg Surg. 2022;48(3):1975-1983. doi: 10.1007/s00068-020-01515-w
89. Braken P, Amsler F, Gross T. Simple modification of trauma mechanism alarm criteria published for the TraumaNetwork DGU((R)) may significantly improve overtriage - a cross sectional study. Scand J Trauma Resusc Emerg Med. 2018;26(1):32. doi: 10.1186/s13049-018-0498-x
90. Basiratzadeh S, Hakimjavadi R, Baddour N, Michalowski W, Viktor H, Wai E, et al. A data-driven approach to categorize patients with traumatic spinal cord injury: cluster analysis of a multicentre database. Front Neurol. 2023;14:1263291.

doi: 10.3389/fneur.2023.1263291
91. Yokogawa N, Kato S, Sasagawa T, Hayashi H, Tsuchiya H, Ando K, et al. Differences in clinical characteristics of cervical spine injuries in older adults by external causes: a multicenter study of 1512 cases. Sci Rep. 2022;12(1):15867. doi: 10.1038/s41598-022-19789-y
92. Wu Y, Zhang Z, Wang F, Wang W. Current status of traumatic spinal cord injury caused by traffic accident in Northern China. Sci Rep. 2022;12(1):13892. doi: 10.1038/s41598-022-16930-9
93. Yuan H, Guo Q, Zhang Z, Ou L, Wang H, Yu H, Xiang L. Sex, age, role and geographic differences in traumatic spinal fractures caused by motor vehicle collisions: a multicentre retrospective study. Sci Rep. 2023;13(1):3712. doi: 10.1038/s41598-023-30982-5
94. Breitlauch P, Erbsmehl CT, van Ratingen M, Mallada JL, Sandner V, Ferson N, Urban M. A novel method for the automated simulation of various vehicle collisions to estimate crash severity. Traffic Inj Prev. 2023;24(sup1):S116-S123. doi: 10.1080/15389588.2022.2159761
95. Pinter K, Szalay Z, Vida G. Road Accident Reconstruction Using On-board Data, Especially Focusing on the Applicability in Case of Autonomous Vehicles. Periodica Polytechnica Transportation Engineering. 2020;49(2):139-145. doi: 10.3311/PPtr.13469
96. Vida G, Török Á. Effects of developing data recording technologies on the reliability of accident reconstruction and liability determination. European Transport Research Review. 2025;17(1). doi: 10.1186/s12544-025-00727-8
97. Bastien C, Wellings R, Burnett B. An evidence based method to calculate pedestrian crossing speeds in vehicle collisions (PCSC). Accid Anal Prev. 2018;118:66-76. doi: 10.1016/j.aap.2018.05.020
98. Ogura A. Analyzing collisions in classical mechanics using mass–momentum diagrams. European Journal of Physics. 2017;38(5):055001. doi: 10.1088/1361-6404/aa750b
99. Chatterjee A, James G, Brogliato B. Approximate coefficient of restitution for nonlinear viscoelastic contact with external load. Granular Matter. 2022;24(4). doi: 10.1007/s10035-022-01284-w
100. Meyer N, Wagemann EL, Jackstadt A, Seifried R. Material and particle size sensitivity analysis on coefficient of restitution in low-velocity normal impacts. Computational Particle Mechanics. 2022;9(6):1293-1308. doi: 10.1007/s40571-022-00471-z
101. Seifried R, Schiehlen W, Eberhard P. Numerical and experimental evaluation of the coefficient of restitution for repeated impacts. International Journal of Impact Engineering. 2005;32(1-4):508-524. doi: 10.1016/j.ijimpeng.2005.01.001
102. Green I. The prediction of the coefficient of restitution between impacting spheres and finite thickness plates undergoing elastoplastic deformations and wave propagation. Nonlinear Dynamics. 2022;109(4):2443-2458. doi: 10.1007/s11071-022-07522-3
103. Higham JE, Shepley P, Shahnam M. Measuring the coefficient of restitution for all six degrees of freedom. Granular Matter. 2019;21(2). doi: 10.1007/s10035-019-0871-0
104. Hunt KH, Crossley FRE. Coefficient of Restitution Interpreted as Damping in Vibroimpact. Journal of Applied Mechanics. 1975;42(2):440-445. doi: 10.1115/1.3423596
105. Reyes A, Børvik T. Quasi-static behaviour of crash components with steel skins and polymer foam cores. Materials Today Communications. 2018;17:541-553. doi: 10.1016/j.mtcomm.2018.09.015
106. Wang D, Zhang J, Wang S, Hu L. Frontal Vehicular Crash Energy Management Using Analytical Model in Multiple Conditions. Sustainability. 2022;14(24). doi: 10.3390/su142416913
107. Gidlewski M, Prochowski L, Jemioł L, Żardecki D. The process of front-to-side collision of motor vehicles in terms of energy balance. Nonlinear Dynamics. 2018;97(3):1877-1893. doi: 10.1007/s11071-018-4688-x
108. Brach RM, Brach RM, Pongetti K. Analysis of High-Speed Sideswipe Collisions Using Data from Small Overlap Tests. SAE International Journal of Transportation Safety. 2014;02(1):86-99. doi: 10.4271/2014-01-0469
109. Davison TM, Collins GS. Complex Crater Formation by Oblique Impacts on the Earth and Moon. Geophysical Research Letters. 2022;49(21). doi: 10.1029/2022gl101117
110. Li S, Anis M, Lord D, Zhang H, Zhou Y, Ye X. Beyond 1D and oversimplified kinematics: A generic analytical framework for surrogate safety measures. Accid Anal Prev. 2024;204:107649. doi: 10.1016/j.aap.2024.107649
111. Statler TS, Raducan SD, Barnouin OS, DeCoster ME, Chesley SR, Barbee B, et al. After DART: Using the First Full-scale Test of a Kinetic Impactor to Inform a Future Planetary Defense Mission. The Planetary Science Journal. 2022;3(10). doi: 10.3847/PSJ/ac94c1
112. Stickle AM, DeCoster ME, Burger C, Caldwell WK, Graninger D, Kumamoto KM, et al. Effects of Impact and Target Parameters on the Results of a Kinetic Impactor: Predictions for the Double Asteroid Redirection Test (DART) Mission. The Planetary Science Journal. 2022;3(11). doi: 10.3847/PSJ/ac91cc
113. Ataei M, Khajepour A, Jeon S. A general rollover index for tripped and un-tripped rollovers on flat and sloped roads. Proceedings of the Institution of Mechanical Engineers, Part D: Journal of Automobile Engineering. 2017;233(2):304-316. doi: 10.1177/0954407017743345
114. Viano DC, Parenteau CS, Edwards ML. Rollover injury: effects of near- and far-seating position, belt use, and number of quarter rolls. Traffic Inj Prev. 2007;8(4):382-392. doi: 10.1080/15389580701583379
115. Dobbertin KM, Freeman MD, Lambert WE, Lasarev MR, Kohles SS. The relationship between vehicle roof crush and head, neck and spine injury in rollover crashes. Accid Anal Prev. 2013;58:46-52. doi: 10.1016/j.aap.2013.04.020
116. Freeman MD, Dobbertin K, Kohles SS, Uhrenholt L, Eriksson A. Serious head and neck injury as a predictor of occupant position in fatal rollover crashes. Forensic Sci Int. 2012;222(1-3):228-233. doi: 10.1016/j.forsciint.2012.06.003
117. Heller MF, Newberry WN, Smedley JE, Eswaran SK, Croteau JJ, Carhart MR. Occupant Kinematics and Injury Mechanisms During Rollover in a High Strength-to-Weight Ratio Vehicle. SAE International Journal of Passenger Cars - Mechanical Systems. 2010;03(1):450-466. doi: 10.4271/2010-01-0516
118. Kazemian AH, Fooladi M, Darijani H. Rollover Index for the Diagnosis of Tripped and Untripped Rollovers. Latin American Journal of Solids and Structures. 2017;14(11):1979-1999. doi: 10.1590/1679-78253576
119. Ikhsan N, Saifizul A, Ramli R. The Effect of Vehicle and Road Conditions on Rollover of Commercial Heavy Vehicles during Cornering: A Simulation Approach. Sustainability. 2021;13(11). doi: 10.3390/su13116337
120. El-Rich M, Arnoux PJ, Wagnac E, Brunet C, Aubin CE. Finite element investigation of the loading rate effect on the spinal load-sharing changes under impact conditions. J Biomech. 2009;42(9):1252-1262. doi: 10.1016/j.jbiomech.2009.03.036
121. Davidson PL, Wilson SJ, Wilson BD, Chalmers DJ. An approach to modeling impact energy absorption by surfaces. J Appl Biomech. 2009;25(4):351-359. doi: 10.1123/jab.25.4.351
122. Shimizu T, Yoshitani K. Impact-reduction effect of tatami floor mat made of nonwoven fabric for head injuries in fall accidents. Journal of Building Engineering. 2019;24. doi: 10.1016/j.jobe.2019.02.020
123. Wei W, Evin M, Bailly N, Arnoux PJ. Biomechanical evaluation of Back injuries during typical snowboarding backward falls. Scand J Med Sci Sports. 2023;33(3):224-234. doi: 10.1111/sms.14254
124. Mattucci S, Speidel J, Liu J, Kwon BK, Tetzlaff W, Oxland TR. Basic biomechanics of spinal cord injury - How injuries happen in people and how animal models have informed our understanding. Clin Biomech (Bristol). 2019;64:58-68. doi: 10.1016/j.clinbiomech.2018.03.020
125. Rao RD, Delbar K, Yoganandan N. Body Morphology and Its Associations With Thoracolumbar Trauma Sustained in Motor Vehicle Collisions. J Am Acad Orthop Surg. 2015;23(12):769-777. doi: 10.5435/JAAOS-D-15-00277
126. Yoganandan N, Moore J, DeVogel N, Pintar F, Banerjee A, Baisden J, et al. Human lumbar spinal column injury

criteria from vertical loading at the base: Applications to military environments. J Mech Behav Biomed Mater. 2020;105:103690. doi: 10.1016/j.jmbbm.2020.103690
127. Bose D, Crandall JR, Untaroiu CD, Maslen EH. Influence of pre-collision occupant parameters on injury outcome in a frontal collision. Accid Anal Prev. 2010;42(4):1398-1407. doi: 10.1016/j.aap.2010.03.004
128. Kimpara H, Lee JB, Yang KH, King AI. Effects of body weight, height, and rib cage area moment of inertia on blunt chest impact response. Traffic Inj Prev. 2010;11(2):207-214. doi: 10.1080/15389580903554863
129. Khorasani-Zavareh D, Bigdeli M, Saadat S, Mohammadi R. Kinetic energy management in road traffic injury prevention: a call for action. J Inj Violence Res. 2015;7(1):36-37. doi: 10.5249/jivr.v7i1.458
130. Palanca M, Perilli E, Martelli S. Body Anthropometry and Bone Strength Conjointly Determine the Risk of Hip Fracture in a Sideways Fall. Ann Biomed Eng. 2021;49(5):1380-1390. doi: 10.1007/s10439-020-02682-y
131. Rostro-González H, Puigoriol-Forcada JM, Pérez-Peña A, Menacho J, Garcia-Granada A-A. Optimizing crash box design to meet injury criteria: a protocol for accurate simulation and material selection. Structural and Multidisciplinary Optimization. 2024;67(8). doi: 10.1007/s00158-024-03855-2
132. Bahlsen A, Nigg BM. Influence of Attached Masses on Impact Forces and Running Style in Heel-Toe Running. International Journal of Sport Biomechanics. 1987;3(3):264-275. doi: 10.1123/ijsb.3.3.264
133. Bhan S, Levine IC, Laing AC. Energy absorption during impact on the proximal femur is affected by body mass index and flooring surface. J Biomech. 2014;47(10):2391-2397. doi: 10.1016/j.jbiomech.2014.04.026
134. Somasundaram K, Humm JR, Yoganandan N, Hauschild H, Driesslein K, Pintar FA. Obese Occupant Response in Reclined and Upright Seated Postures in Frontal Impacts. Stapp Car Crash J. 2022;66:31-68. doi: 10.4271/2022-22-0002
135. Raj N, Krishnapillai S. An improved spinal injury parameter model for underbody impulsive loading scenarios. Int J Numer Method Biomed Eng. 2020;36(3):e3307. doi: 10.1002/cnm.3307
136. Ferenczi MA, Bershitsky SY, Koubassova NA, Kopylova GV, Fernandez M, Narayanan T, Tsaturyan AK. Why muscle is an efficient shock absorber. PLoS One. 2014;9(1):e85739. doi: 10.1371/journal.pone.0085739
137. Cutlan R, Khokhar M, Shammout N, Shah AS, Frazer L, Yoganandan N, et al. Lumbar Spine Orientation Affects Compressive Fracture Outcome. Ann Biomed Eng. 2024. doi: 10.1007/s10439-024-03604-y
138. Yoganandan N, Moore J, Pintar FA, Banerjee A, DeVogel N, Zhang J. Role of disc area and trabecular bone density on lumbar spinal column fracture risk curves under vertical impact. J Biomech. 2018;72:90-98. doi: 10.1016/j.jbiomech.2018.02.030
139. Schwarze M, Hurschler C, Welke B. Force, impulse and energy during falling with and without knee protection: an in-vitro study. Sci Rep. 2019;9(1):10336. doi: 10.1038/s41598-019-46880-8
140. Tamura A, Akasaka K, Otsudo T. Energy Absorption Strategies in the Lower Extremities during Double-Leg Landings in Knee Valgus Alignment. Applied Sciences. 2020;10(23). doi: 10.3390/app10238742
141. Ivancic PC. Biomechanics of Thoracolumbar Burst and Chance-Type Fractures during Fall from Height. Global Spine J. 2014;4(3):161-168. doi: 10.1055/s-0034-1381729
142. Amiri S, Naserkhaki S, Parnianpour M. Assessment of lumbar spinal disc injury in frontal crashes. Comput Biol Med. 2020;123:103846. doi: 10.1016/j.compbiomed.2020.103846
143. Pachocki L, Daszkiewicz K, Luczkiewicz P, Witkowski W. Biomechanics of Lumbar Spine Injury in Road Barrier Collision-Finite Element Study. Front Bioeng Biotechnol. 2021;9:760498. doi: 10.3389/fbioe.2021.760498
144. Ivancic PC. Cervical spine instability following axial compression injury: a biomechanical study. Orthop Traumatol Surg Res. 2014;100(1):127-133. doi: 10.1016/j.otsr.2013.10.015
145. Hajiaghamemar M, Seidi M, Ferguson JR, Caccese V. Measurement of Head Impact Due to Standing Fall in Adults Using Anthropomorphic Test Dummies. Ann Biomed Eng. 2015;43(9):2143-2152. doi: 10.1007/s10439-015-1255-1
146. Ivancic PC. Instabilité du rachis cervical par traumatisme en compression axiale : une étude biomécanique. Revue de Chirurgie Orthopédique et Traumatologique. 2014;100(1). doi: 10.1016/j.rcot.2013.10.091
147. Li L, Baur M, Baldwin K, Kuehn T, Zhu Q, Herman D, Dai B. Falling as a strategy to decrease knee loading during landings: Implications for ACL injury prevention. J Biomech. 2020;109:109906. doi: 10.1016/j.jbiomech.2020.109906
148. Li M, Zhang D, Liu Q, Zhang T. Driver Injury from Vehicle Side Impacts When Automatic Emergency Braking and Active Seat Belts Are Used. Sensors (Basel). 2023;23(13). doi: 10.3390/s23135821
149. Mishra E, Mroz K, Pipkorn B, Lubbe N. Effects of Automated Emergency Braking and Seatbelt Pre-Pretensioning on Occupant Injury Risks in High-Severity Frontal Crashes. Frontiers in Future Transportation. 2022;3. doi: 10.3389/ffutr.2022.883951
150. Tamura A, Akasaka K, Otsudo T. Contribution of Lower Extremity Joints on Energy Absorption during Soft Landing. Int J Environ Res Public Health. 2021;18(10). doi: 10.3390/ijerph18105130
151. Van Toen C, Melnyk AD, Street J, Oxland TR, Cripton PA. The effect of lateral eccentricity on failure loads, kinematics, and canal occlusions of the cervical spine in axial loading. J Biomech. 2014;47(5):1164-1172. doi: 10.1016/j.jbiomech.2013.12.001
152. Van Toen C, Sran MM, Robinovitch SN, Cripton PA. Transmission of force in the lumbosacral spine during backward falls. Spine (Phila Pa 1976). 2012;37(9):E519-527. doi: 10.1097/BRS.0b013e31823ecae0
153. Whyte T, Melnyk AD, Van Toen C, Yamamoto S, Street J, Oxland TR, Cripton PA. A neck compression injury criterion incorporating lateral eccentricity. Sci Rep. 2020;10(1):7114. doi: 10.1038/s41598-020-63974-w
154. Yeow CH, Lee PV, Goh JC. Effect of landing height on frontal plane kinematics, kinetics and energy dissipation at lower extremity joints. J Biomech. 2009;42(12):1967-1973. doi: 10.1016/j.jbiomech.2009.05.017
155. Giatsis G, Panoutsakopoulos V, Kollias IA. Drop Jumping on Sand Is Characterized by Lower Power, Higher Rate of Force Development and Larger Knee Joint Range of Motion. J Funct Morphol Kinesiol. 2022;7(1). doi: 10.3390/jfmk7010017
156. Harris DA, Spears IR. The effect of rugby shoulder padding on peak impact force attenuation. Br J Sports Med. 2010;44(3):200-203. doi: 10.1136/bjsm.2008.047449
157. Jung S. Water entry and exit in nature: review. Interface Focus. 2025;15(2):20240055. doi: 10.1098/rsfs.2024.0055
158. Kerdok AE, Biewener AA, McMahon TA, Weyand PG, Herr HM. Energetics and mechanics of human running on surfaces of different stiffnesses. J Appl Physiol (1985). 2002;92(2):469-478. doi: 10.1152/japplphysiol.01164.2000
159. Lachance CC, Jurkowski MP, Dymarz AC, Robinovitch SN, Feldman F, Laing AC, Mackey DC. Compliant flooring to prevent fall-related injuries in older adults: A scoping review of biomechanical efficacy, clinical effectiveness, cost-effectiveness, and workplace safety. PLoS One. 2017;12(2):e0171652. doi: 10.1371/journal.pone.0171652
160. Laforest S, Robitaille Y, Dorval D, Lesage D, Pless B. Severity of fall injuries on sand or grass in playgrounds. J Epidemiol Community Health. 2000;54(6):475-477. doi: 10.1136/jech.54.6.475
161. Laing AC, Robinovitch SN. Low stiffness floors can attenuate fall-related femoral impact forces by up to 50% without substantially impairing balance in older women. Accid Anal Prev. 2009;41(3):642-650. doi: 10.1016/j.aap.2009.03.001
162. Laing AC, Tootoonchi I, Hulme PA, Robinovitch SN. Effect of compliant flooring on impact force during falls on the hip. J Orthop Res. 2006;24(7):1405-1411. doi: 10.1002/jor.20172
163. Mackey DC, Lachance CC, Wang PT, Feldman F, Laing AC, Leung PM, et al. The Flooring for Injury Prevention (FLIP) Study of compliant flooring for the prevention of fall-related injuries in long-term care: A randomized trial. PLoS Med. 2019;16(6):e1002843. doi: 10.1371/journal.pmed.1002843

164. Nakanishi T, Hitosugi M, Murayama H, Takeda A, Motozawa Y, Ogino M, Koyama K. Biomechanical Analysis of Serious Neck Injuries Resulting from Judo. Healthcare (Basel). 2021;9(2). doi: 10.3390/healthcare9020214
165. Qu H, Zhang S, Sorochan JC, Weinhandl JT, Thoms AW, Dickson KH. Effects of synthetic turf and shock pad on impact attenuation related biomechanics during drop landing. Sports Biomech. 2022;21(6):748-760. doi: 10.1080/14763141.2019.1690570
166. Tessutti V, Ribeiro AP, Trombini-Souza F, Sacco IC. Attenuation of foot pressure during running on four different surfaces: asphalt, concrete, rubber, and natural grass. J Sports Sci. 2012;30(14):1545-1550. doi: 10.1080/02640414.2012.713975
167. Tomin M, Kossa A, Berezvai S, Kmetty Á. Investigating the impact behavior of wrestling mats via finite element simulation and falling weight impact tests. Polymer Testing. 2022;108. doi: 10.1016/j.polymertesting.2022.107521
168. Wardiningsih W, Troynikov O. An evaluation of force attenuation, comfort properties and density of materials for hip protective pads. Journal of Engineered Fibers and Fabrics. 2019;14. doi: 10.1177/1558925019853955
169. Schafer R, Trompeter K, Fett D, Heinrich K, Funken J, Willwacher S, et al. The mechanical loading of the spine in physical activities. Eur Spine J. 2023;32(9):2991-3001. doi: 10.1007/s00586-023-07733-1
170. Huang Q, Kleiven S. Finite Element Analysis of Energy-Absorbing Floors for Reducing Head Injury Risk during Fall Accidents. Applied Sciences. 2023;13(24). doi: 10.3390/app132413260
171. Mishra E, Lubbe N. Assessing injury risks of reclined occupants in a frontal crash preceded by braking with varied seatbelt designs using the SAFER Human Body Model. Traffic Inj Prev. 2024;25(3):445-453. doi: 10.1080/15389588.2024.2318414
172. Harper DJ, McBurnie AJ, Santos TD, Eriksrud O, Evans M, Cohen DD, et al. Biomechanical and Neuromuscular Performance Requirements of Horizontal Deceleration: A Review with Implications for Random Intermittent Multi-Directional Sports. Sports Med. 2022;52(10):2321-2354. doi: 10.1007/s40279-022-01693-0
173. Stemper BD, Chirvi S, Doan N, Baisden JL, Maiman DJ, Curry WH, et al. Biomechanical tolerance of whole lumbar spines in straightened posture subjected to axial acceleration. J Orthop Res. 2018;36(6):1747-1756. doi: 10.1002/jor.23826
174. Chastain K, Gepner B, Moreau D, Koerber B, Forman J, Hallman J, Kerrigan J. Effect of axial compression on stiffness and deformation of human lumbar spine in flexion-extension. Traffic Inj Prev. 2023;24(sup1):S55-S61. doi: 10.1080/15389588.2023.2198627
175. Gabauer DJ, Gabler HC. The effects of airbags and seatbelts on occupant injury in longitudinal barrier crashes. J Safety Res. 2010;41(1):9-15. doi: 10.1016/j.jsr.2009.10.006
176. Soica A, Gheorghe C. A Review of Seatbelt Technologies and Their Role in Vehicle Safety. Applied Sciences. 2025;15(10). doi: 10.3390/app15105303
177. Pintar FA, Yoganandan N, Myers T, Elhagediab A, Sances A, Jr. Biomechanical properties of human lumbar spine ligaments. J Biomech. 1992;25(11):1351-1356. doi: 10.1016/0021-9290(92)90290-h
178. Sequeira GJ, Brandmeier T. Evaluation and characterization of crash-pulses for head-on collisions with varying overlap crash scenarios. Transportation Research Procedia. 2020;48:1306-1315. doi: 10.1016/j.trpro.2020.08.156
179. King AI, Yang KH. Research in biomechanics of occupant protection. J Trauma. 1995;38(4):570-576. doi: 10.1097/00005373-199504000-00017
180. Hans D, Goertzen AL, Krieg MA, Leslie WD. Bone microarchitecture assessed by TBS predicts osteoporotic fractures independent of bone density: the Manitoba study. J Bone Miner Res. 2011;26(11):2762-2769. doi: 10.1002/jbmr.499
181. Schreiber JJ, Anderson PA, Rosas HG, Buchholz AL, Au AG. Hounsfield units for assessing bone mineral density and strength: a tool for osteoporosis management. J Bone Joint Surg Am. 2011;93(11):1057-1063. doi: 10.2106/jbjs.J.00160
182. Wang TY, Park C, Zhang H, Rahimpour S, Murphy KR, Goodwin CR, et al. Management of Acute Traumatic Spinal Cord Injury: A Review of the Literature. Front Surg. 2021;8:698736. doi: 10.3389/fsurg.2021.698736
183. Grabel ZJ, Lunati MP, Segal DN, Kukowski NR, Yoon ST, Jain A. Thoracolumbar spinal fractures associated with ground level falls in the elderly: An analysis of 254,486 emergency department visits. J Clin Orthop Trauma. 2020;11(5):916-920. doi: 10.1016/j.jcot.2020.04.009
184. Chen S, Li G, Li F, Wang G, Wang Q. A dynamic nomogram for predicting the probability of irreversible neurological dysfunction after cervical spinal cord injury: research based on clinical features and MRI data. BMC Musculoskelet Disord. 2023;24(1):459. doi: 10.1186/s12891-023-06570-z
185. Kreinest M, Gliwitzky B, Schuler S, Grutzner PA, Munzberg M. Development of a new Emergency Medicine Spinal Immobilization Protocol for trauma patients and a test of applicability by German emergency care providers. Scand J Trauma Resusc Emerg Med. 2016;24:71. doi: 10.1186/s13049-016-0267-7
186. Maschmann C, Jeppesen E, Rubin MA, Barfod C. New clinical guidelines on the spinal stabilisation of adult trauma patients - consensus and evidence based. Scand J Trauma Resusc Emerg Med. 2019;27(1):77. doi: 10.1186/s13049-019-0655-x
187. Mohammad Ismail A, Forssten MP, Hildebrand F, Sarani B, Ioannidis I, Cao Y, et al. Cardiac risk stratification and adverse outcomes in surgically managed patients with isolated traumatic spine injuries. Eur J Trauma Emerg Surg. 2024;50(2):523-530. doi: 10.1007/s00068-023-02413-7
188. Dao QA, Nguyen VS, Dang VQ, Tran PC, Le DTS. Diagnostic accuracy and clinical utility of mTLICS versus TLICS and TL AOSIS in stratifying three-tier treatment for thoracolumbar injuries: focus on intermediate score range. BMC Musculoskelet Disord. 2025;26(1):824. doi: 10.1186/s12891-025-09124-7/
189. Loftis KL, Price J, Gillich PJ. Evolution of the Abbreviated Injury Scale: 1990-2015. Traffic Inj Prev. 2018;19(sup2):S109-S113. doi: 10.1080/15389588.2018.1512747
190. van Wessem KJP, Niemeyer MJS, Leenen LPH. Polytrauma patients with severe cervical spine injuries are different than with severe TBI despite similar AIS scores. Sci Rep. 2022;12(1):21538. doi: 10.1038/s41598-022-25809-8
191. Germanetti F, Fiumarella D, Belingardi G, Scattina A. Injury Criteria for Vehicle Safety Assessment: A Review with a Focus Using Human Body Models. Vehicles. 2022;4(4):1080-1095. doi: 10.3390/vehicles4040057
192. Lee JY, Vaccaro AR, Lim MR, Oner FC, Hulbert RJ, Hedlund R, et al. Thoracolumbar injury classification and severity score: a new paradigm for the treatment of thoracolumbar spine trauma. J Orthop Sci. 2005;10(6):671-675. doi: 10.1007/s00776-005-0956-y
193. Patel AA, Vaccaro AR. Thoracolumbar spine trauma classification. J Am Acad Orthop Surg. 2010;18(2):63-71. doi: 10.5435/00124635-201002000-00001
194. Fradet L, Petit Y, Wagnac E, Aubin CE, Arnoux PJ. Biomechanics of thoracolumbar junction vertebral fractures from various kinematic conditions. Med Biol Eng Comput. 2014;52(1):87-94. doi: 10.1007/s11517-013-1124-8
195. Karamian BA, Schroeder GD, Lambrechts MJ, Canseco JA, Oner C, Vialle E, et al. An international validation of the AO spine subaxial injury classification system. Eur Spine J. 2023;32(1):46-54. doi: 10.1007/s00586-022-07467-6
196. Schnake KJ, Schroeder GD, Vaccaro AR, Oner C. AOSpine Classification Systems (Subaxial, Thoracolumbar). J Orthop Trauma. 2017;31 Suppl 4:S14-S23. doi: 10.1097/BOT.0000000000000947
197. Vaccaro AR, Oner C, Kepler CK, Dvorak M, Schnake K, Bellabarba C, et al. AOSpine thoracolumbar spine injury classification system: fracture description, neurological status, and key modifiers. Spine (Phila Pa 1976). 2013;38(23):2028-2037. doi: 10.1097/BRS.0b013e3182a8a381
198. Schroeder GD, Karamian BA, Canseco JA, Vialle LR, Kandziora F, Benneker LM, et al. Validation of the AO Spine Sacral Classification System: Reliability Among Surgeons Worldwide. J Orthop Trauma. 2021;35(12):e496-e501. doi: 10.1097/BOT.0000000000002110

199. Bak AB, Moghaddamjou A, Malvea A, Fehlings MG. Impact of Mechanism of Injury on Long-term Neurological Outcomes of Cervical Sensorimotor Complete Acute Traumatic Spinal Cord Injury. Neurospine. 2022;19(4):1049-1056. doi: 10.14245/ns.2244518.259
200. Goulet J, Richard-Denis A, Petit Y, Diotalevi L, Mac-Thiong JM. Morphological features of thoracolumbar burst fractures associated with neurological outcome in thoracolumbar traumatic spinal cord injury. Eur Spine J. 2020;29(10):2505-2512. doi: 10.1007/s00586-020-06420-9
201. Newgard CD, Fischer PE, Gestring M, Michaels HN, Jurkovich GJ, Lerner EB, Fallat ME, Delbridge TR, Brown JB, Bulger EM; Writing Group for the 2021 National Expert Panel on Field Triage. National guideline for the field triage of injured patients: Recommendations of the National Expert Panel on Field Triage, 2021. J Trauma Acute Care Surg. 2022 Aug 1;93(2):e49-e60. doi: 10.1097/TA.0000000000003627
202. Lokerman RD, van Rein EAJ, Waalwijk JF, van der Sluijs R, Houwert RM, Lansink KWW, et al. Accuracy of Prehospital Triage of Adult Patients With Traumatic Injuries Following Implementation of a Trauma Triage Intervention. JAMA Network Open. 2023;6(4):e236805-e236805. doi: 10.1001/jamanetworkopen.2023.6805
203. Geduld C, Muller H, Saunders CJ. Factors which affect the application and implementation of a spinal motion restriction protocol by prehospital providers in a low resource setting: A scoping review. Afr J Emerg Med. 2022;12(4):393-405. doi: 10.1016/j.afjem.2022.08.005
204. caravantes R, Quezada A, Jimenez L. Low-energy trauma causing multiple cervical fracture: a case report. MOJ Surgery. 2024;12(3):117-119. doi: 10.15406/mojs.2024.12.00276
205. Freeman MD, Croft AC, Nicodemus CN, Centeno CJ, Elkins WL. Significant spinal injury resulting from low-level accelerations: a case series of roller coaster injuries. Arch Phys Med Rehabil. 2005;86(11):2126-2130. doi: 10.1016/j.apmr.2005.05.017
206. Yoganandan N, Stemper BD, Baisden JL, Pintar FA, Paskoff GR, Shender BS. Effects of acceleration level on lumbar spine injuries in military populations. Spine J. 2015;15(6):1318-1324. doi: 10.1016/j.spinee.2013.07.486

Original article

Ukrainian Neurosurgical Journal. 2026;32(1):92-98
doi: 10.25305/unj.337777

Comparative efficacy of progesterone and vitamin D in improving functional outcomes after traumatic brain injury

Kenzie Ongko Wijaya [1], Nunki Puspita Utomo [2], Muhammad Andika Wibisono [1], Endro Basuki Sadjiman [2]

[1] Neurosurgery Department, Rumah Sakit Umum Daerah Wates, Yogyakarta, Indonesia
[2] Neurosurgery Department, Bethesda Hospital Yogyakarta, Indonesia

Received: 20 August 2025
Accepted: 17 November 2025

Address for correspondence: *Kenzie Ongko Wijaya, Neurosurgery Department, Rumah Sakit Umum Daerah Wates, Jl. Tentara Pelajar No.Km. 1 No. 5, Area Sawah, Beji, Kec. Wates, Kabupaten Kulon Progo, Daerah Istimewa Yogyakarta 55651, Indonesia, email: kenzieow7@gmail.com*

Background: Traumatic brain injury (TBI) remains a major clinical challenge in neurosurgery due to its heterogeneous pathophysiology and the limited availability of effective pharmacological interventions. Progesterone and vitamin D have demonstrated neuroprotective and anti-inflammatory properties in preclinical models; however, their translational efficacy in clinical trials remains inconclusive. Clarifying their therapeutic roles may help inform adjunctive strategies in the acute management of neurotrauma.

Objectives: To assess the neuroprotective effects of progesterone and vitamin D in enhancing functional recovery following moderate to severe TBI, and to compare the clinical efficacy of these agents based on standardized neurological outcome measures derived from randomized controlled trials (RCTs).

Methods: A systematic review and meta-analysis were conducted in accordance with the PRISMA guidelines. Randomized controlled trials (RCTs) were identified through searches of PubMed, EMBASE, Web of Science, and the Cochrane Library, comparing progesterone and/or vitamin D with placebo in patients with traumatic brain injury (TBI). Studies reporting Glasgow Outcome Scale–Extended (GOS-E) outcomes were included. Standardized mean differences (SMDs) with 95% confidence intervals (CIs) were calculated using Review Manager version 5.4. Study quality and heterogeneity were assessed.

Results: Six RCTs were included: three progesterone trials (n = 1,426) and three vitamin D trials (n = 192). Progesterone showed no significant improvement in functional outcomes compared with placebo (SMD = −0.07; 95% CI: −0.32 to 0.19; p = 0.60; I^2 = 58%). Vitamin D demonstrated a non-significant trend toward improved outcomes (SMD = 0.37; 95% CI: −0.27 to 1.02; p = 0.26; I^2 = 78%). Variability in trial design, timing of intervention, and baseline vitamin D deficiency status may have influenced the observed effects.

Conclusions: Although neither agent showed standalone efficacy, their safety and complementary mechanisms suggest promise for combinatorial or biomarker-guided approaches. This meta-analysis highlights the need for early, precision-targeted, and stratified neuroprotective trials in TBI care.

Keywords: *traumatic brain injury (TBI); progesterone; vitamin D; functional outcome*

Introduction

Traumatic brain injury (TBI) remains a significant global health concern, contributing to substantial morbidity, long-term disability, and mortality, particularly among young adults [1]. The pathophysiology of TBI is complex, involving both immediate primary injury and subsequent secondary cascades including neuroinflammation, oxidative stress, excitotoxicity, mitochondrial dysfunction, and apoptosis [2]. Current therapeutic strategies are predominantly supportive, and despite decades of research, effective pharmacologic interventions that significantly improve neurological outcomes remain elusive.

Progesterone, a neurosteroid with pleiotropic neuroprotective properties, has garnered attention for its potential to modulate secondary brain injury. Experimental studies have demonstrated its anti-inflammatory, anti-apoptotic, and neurodegenerative effects [3]. Several randomized controlled trials (RCTs) have evaluated progesterone administration following TBI; however, results regarding its efficacy in improving functional recovery have been inconsistent. [4]. Vitamin D, traditionally known for its role in calcium homeostasis, has emerged as a neuroimmunomodulator with potential therapeutic implications in central nervous system injuries. It exerts neuroprotective effects through regulation of neurotrophic factors, attenuation of oxidative damage, and modulation of immune responses [5]. Preclinical studies and early-phase clinical trials have suggested a beneficial role of vitamin D in TBI, though robust evidence from randomized trials remains limited [6]. The Glasgow Outcome Scale–Extended

(GOS-E) is a validated and widely used measure of functional recovery following TBI. As a standardized outcome scale, it facilitates comparison across studies and enables evaluation of treatment efficacy based on meaningful improvements in neurological function and disability status [7].

Given the increasing interest in hormone-based and vitamin-based neuroprotective therapies, this meta-analysis aims to systematically compare the efficacy of progesterone and vitamin D in improving functional outcomes in patients with TBI, as assessed by GOS-E scores, using data from randomized controlled trials. By synthesizing available evidence, this study seeks to provide clarity on their comparative therapeutic value and guide future clinical decision-making.

Materials and methods

Search strategy

A comprehensive literature search was conducted in PubMed, EMBASE, Web of Science, and the Cochrane Library to identify studies published from 2005 to March 2025. The search strategy combined Medical Subject Headings (MeSH) and free-text terms, including "Traumatic Brain Injury" OR "TBI," "Progesterone," "Vitamin D," and "Randomized Controlled Trial," using Boolean operators and synonyms to maximize sensitivity. Reference lists of relevant studies and prior systematic reviews were manually screened to identify additional eligible trials.

Study selection

Eligible studies were randomized controlled trials published in English with a placebo-controlled design, enrolling patients with clinically confirmed moderate to severe traumatic brain injury. TBI diagnosis was established based on clinical assessment and/or neuroimaging, such as CT or MRI. Trials were required to report at least one functional outcome, with the GOS-E prioritized as the primary endpoint, and to include sufficient follow-up to evaluate functional recovery. Studies were included only if key intervention details—including dosage, route of administration, and timing relative to injury—were clearly reported. Studies with significant methodological limitations, non-randomized designs, non-clinical populations, or incomplete outcome reporting were excluded.

Data extraction

Data extraction was independently performed by two reviewers using a standardized form, with discrepancies resolved through discussion or consultation with a third reviewer. Extracted data included study characteristics, intervention details, patient demographics, and baseline functional status where available. Timing of therapy initiation relative to the injury phase was recorded, categorized as acute (≤24 hours), subacute (1–7 days), or chronic (>7 days), as this factor can influence treatment response. The primary outcome of interest was functional recovery assessed by GOS-E, while secondary outcomes included neurological improvement and safety endpoints, such as treatment-related adverse events, discontinuations, and total dropouts. When standard deviations were not directly reported, they were derived from standard errors, confidence intervals, t-values, or p-values using established conversion methods.

Statistical analysis

Meta-analysis was performed using Review Manager (RevMan) version 5.4. Continuous outcomes, particularly GOS-E scores, were synthesized using mean differences or standardized mean differences with 95% confidence intervals. Statistical heterogeneity was assessed using Cochran's Q test and quantified with the I^2 statistic, with I^2 values greater than 50% or $p<0.10$ considered indicative of substantial heterogeneity. Planned subgroup analyses explored the influence of intervention timing, TBI severity, and type of neuroprotective agent on functional outcomes.

Results

Literature search findings

The search strategy yielded 36 citations in PubMed, EMBASE, Web of Science, and the Cochrane Library of Systematic Reviews. ***Fig. 1*** shows the results of the literature search and study selection. A total of 32 potentially relevant articles were identified in the initial search; however, only six studies met the inclusion criteria and were included in the meta-analysis. Of these, three progesterone trials (Wright *et al*., 2007; Wright *et al*., 2014; Skolnick *et al*., 2014), and three vitamin D trials (Sharma *et al*., 2020; Shafiei *et al*., 2022; Intiso *et al*., 2024) were included in the review. The design and population characteristics of the progesterone and vitamin D tests are shown in ***Table 1 and 2***.

Effects and adverse events of progesterone intervention

A total of three RCTs comprising 1,426 patients (742 in the progesterone group and 684 in the placebo group) were included in the meta-analysis. All studies assessed the efficacy of intravenous progesterone in patients with moderate to severe TBI, with follow-up periods ranging from 30 days to 6 months.

The pooled analysis of SMD revealed no statistically significant improvement in neurological outcomes with progesterone therapy compared to placebo (SMD=–0.07; 95% CI: –0.32 to 0.19; p=0.60). Subgroup analysis showed mixed results across studies. Wright *et al*. (2014) reported a slight benefit in the placebo group (SMD=–0.35; 95% CI: –0.68 to –0.02), whereas Skolnick *et al*. (2014) found no significant difference (SMD=0.00; 95% CI: –0.11 to 0.12), and Wright *et al*. (2007) favored progesterone, albeit not significantly (SMD=0.17; 95% CI: –0.29 to 0.64). The heterogeneity was moderate (I^2=58%, p=0.09), suggesting variability in study designs or populations.

Baseline characteristics were generally similar across studies, with the mean age of participants around 35 years and a predominance of male patients (71% to 78.5%). Progesterone dosing protocols were consistent, utilizing a loading dose of 0.71 mg/kg followed by maintenance infusions ranging from 11 to 119 hours. Notably, only Wright *et al*. (2007) reported a statistically significant reduction in 30-day mortality (13% vs. 30.4% in placebo), while the other two trials did not demonstrate significant clinical benefit in long-term functional outcomes (***Fig. 2***).

Adverse events were reported across all trials, with the largest number observed in Skolnick *et al*. (2014) study (n=4,025). Dropout rates ranged from 3.9% to

15.5%, and very few adverse events directly led to participant withdrawal (0–3 cases per study).

Effects and adverse events of vitamin D intervention

Three RCTs comprising 192 patients (98 in the vitamin D group and 94 in the placebo group) were included in this meta-analysis to evaluate the effects of vitamin D supplementation on neurological recovery in moderate to severe TBI patients.

The pooled SMD favored vitamin D over placebo, but the effect was not statistically significant (SMD=0.37; 95% CI: –0.27 to 1.02; p=0.26). Individual studies showed variable outcomes. Sharma *et al*. (2020) reported a significant improvement in the GOS-E scores at 14 days in the vitamin D group (mean 4.80 vs. 2.21, p<0.0001), while Shafiei *et al*. (2022) also demonstrated a statistically significant higher proportion of favorable outcomes at 3 months (p=0.03). In contrast, Intiso *et al*. (2024) found no significant difference in GOS-E scores between groups.

There was a high degree of heterogeneity among the included studies (I^2=78%, p=0.01), which may be attributed to differences in dosing regimens, patient ages, and follow-up durations. Intiso *et al*. (2024) used a bolus plus maintenance approach, while the other two studies administered single high-dose oral regimens (***Fig. 3***).

Baseline characteristics showed comparable TBI severity across studies. However, patient age varied, with the Intiso *et al*. cohort having a markedly higher mean age (57.5 years) compared to others (~36 years). The male proportion was similar (58.3%–71.4%).

No adverse events or dropouts due to treatment were reported in any of the included trials.

Participant demographics

Across the included studies, male participants constituted the majority, with proportions ranging from 58.3% to 78.5%. Female representation was consistently low, highlighting a clear gender imbalance in both progesterone and vitamin D trials for traumatic brain injury. This limited inclusion of women may affect the generalizability of study findings, as sex-based differences in injury response, hormonal influences, and recovery trajectories are well-documented in TBI research. Future clinical trials should aim for more balanced recruitment or sex-stratified analyses to ensure outcomes are applicable to a broader patient population.

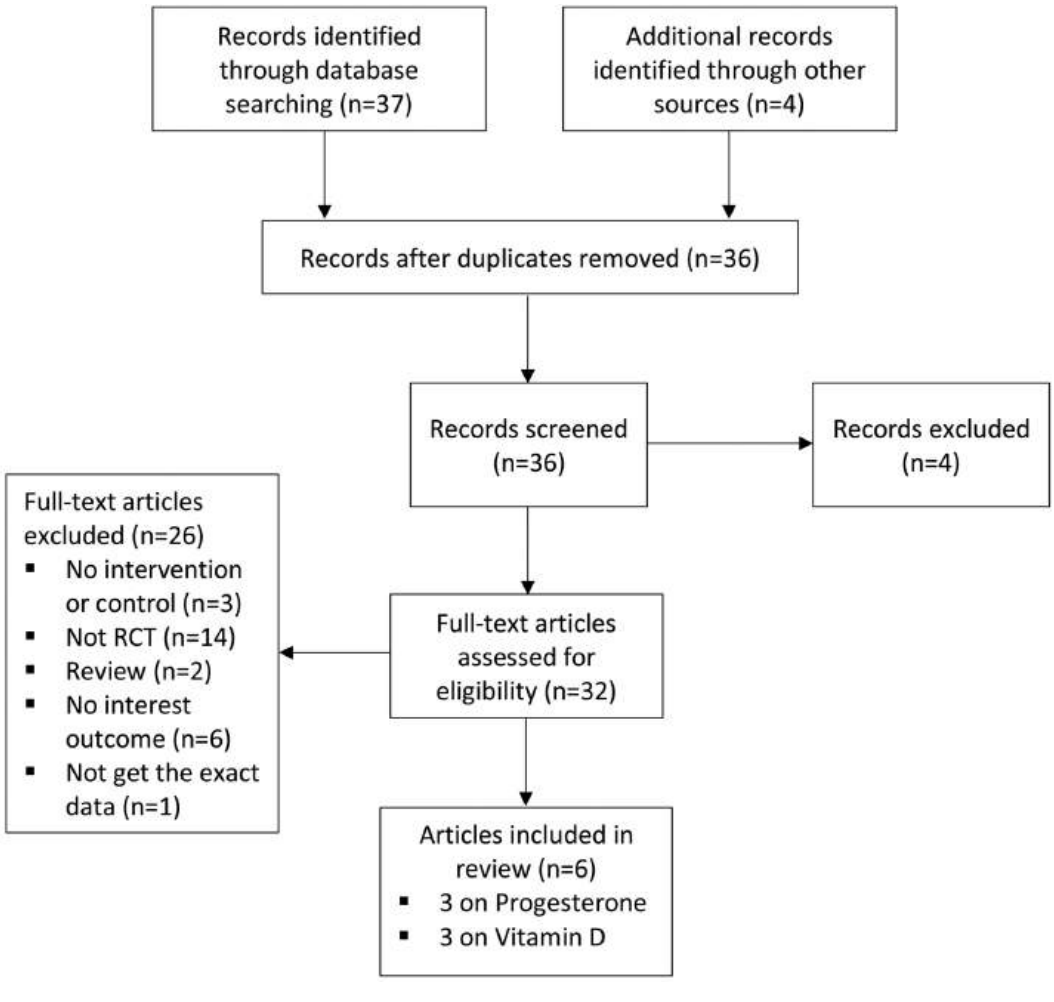

Fig. 1. Flowchart describing the approach used to identify all eligible studies of meta-analysis

Table 1. Baseline characteristics of studies included in the meta-analysis, by Progesterone intervention.

Study	Country	Dose (number of patients)	Male (%)	Mean age (SD)	TBI severity	Drug dosing regimen	Duration (weeks)	Results	Dropout rate (%)	Adverse events leading to dropout (n)	Total adverse events (n)
Wright *et al.*, 2007	USA	0.71 mg/kg loading, then 0.5 mg/kg/h (77)	71	35.3 (14.3)	Moderate to severe	IV infusion: 0.71 mg/kg over 1 h, 0.5 mg/kg/h for 11 h, followed by five 12-h infusions	1	Lower 30-day mortality in progesterone group (13% vs 30.4%)	3.9	0	21 types reported (exact number not provided)
Wright *et al.*, 2014	USA	0.71 mg/kg loading, then 0.5 mg/kg/h (442)	74.5	35.2 (15.7)	Moderate to severe	IV infusion: 0.71 mg/kg over 1 h, 0.5 mg/kg/h for 71 h, tapered over 24 h	2	No significant improvement vs placebo	15.5	3	278
Skolnick *et al.*, 2014	21 countries	0.71 mg/kg loading, then 0.5 mg/kg/h for 119 h (591)	78.5	35 (20.7)	Severe	IV infusion: 0.71 mg/kg/h × 1 h, then 0.5 mg/ kg/h × 119 h (total 120 h)	1	No significant benefit vs placebo in GOS at 6 months (OR 0.96, $p>0.05$)	4.9	1	4025

Notes. TBI (Traumatic Brain Injury), GOS-E (Glasgow Outcome Scale Extended) (range 1–8, higher scores indicate better outcome), IU (International Units), SD (Standard Deviation).

Table 2. Baseline characteristics of studies included in the meta-analysis, by Vitamin D intervention.

Study	Country	Dose (number of patients)	Male (%)	Age (SD)	TBI severity	Drug dosing regimen	Duration (weeks)	Results	Dropout rate (%)	Adverse events leading to dropout (n)	Total adverse events (n
Sharma *et al.*, 2020	India	Oral 120,000 IU (n=20)	71.4	36.4 (16.4)	Moderate to severe	Single oral dose	2	Higher GOS-E at 14 days (4.80 vs 2.21 in control, $p<0.0001$)	0	0	0
Shafiei *et al.*, 2022	Iran	Oral 150,000 IU (n=42)	71.4	36.76 (16.12)	Moderate to severe	Single oral dose	12	Higher GOS-E at 3 months: 62.8% favorable vs 49.7% (placebo), $p=0.03$	0	0	0
Intiso *et al.*, 2024	Italy	Oral 50,000 IU once + 1,000 IU/day (36)	58.3	57.5 (14.9)	Severe	Oral (bolus + maintenance)	8	GOS-E: no significant difference	0	0	0

Notes. TBI (Traumatic Brain Injury), GOS-E (Glasgow Outcome Scale Extended) (range 1–8, higher scores indicate better outcome), IU (International Units), SD (Standard Deviation)

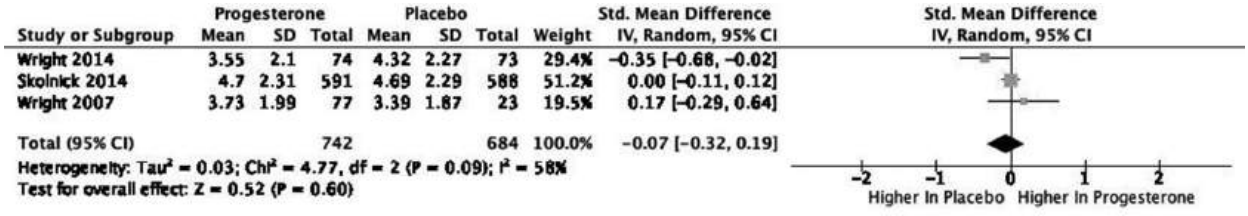

Fig. 2. Functional outcomes based on Glasgow Outcome Scale–Extended (GOS-E) scores in traumatic brain injury patients receiving progesterone treatment

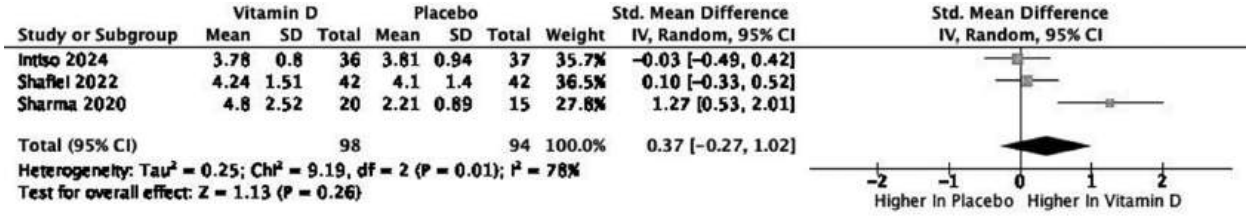

Fig. 3. Functional outcomes based on Glasgow Outcome Scale–Extended (GOS-E) scores in traumatic brain injury patients receiving vitamin D treatment

Discussion

The meta-analysis highlights the challenges of translating the preclinical neuroprotective mechanisms of progesterone and vitamin D into clinically meaningful functional improvements after moderate to severe TBI. While both agents demonstrate biological plausibility, their efficacy remains inconsistent in human trials, underscoring the complexity of TBI pathophysiology and the limitations of monotherapy approaches.

Despite robust preclinical evidence of progesterone's anti-inflammatory and anti-apoptotic effects, pooled data from three RCTs (n=1,426) revealed no significant improvement in GOS-E scores (SMD=−0.07; p=0.60). This finding aligns with the failures of Phase III trials, where delays in treatment initiation (often >6 hours post-injury) and heterogeneous injury patterns may have blunted therapeutic effects [8]. Notably, one trial reported a mortality reduction (13.6% vs. 30.4% in controls), but this did not correlate with long-term functional recovery. The moderate heterogeneity (I^2=58%) across studies suggests variability in dosing regimens or patient stratification, emphasizing the need for precision in trial design [9].

Vitamin D supplementation showed a non-significant trend toward improved outcomes (SMD=0.37; p=0.26), with high heterogeneity (I^2=78%) likely reflecting divergent protocols (e.g., single high-dose vs. maintenance regimens). Preclinical models suggest a role in modulating oxidative stress and neurotrophic factors, but clinical translation is hampered by small sample sizes (n=192 total) and inconsistent reporting of baseline deficiency status—a critical confounder given vitamin D's pleiotropic mechanisms. Age-related metabolic differences may further explain null findings in older cohorts [10].

Notably, a network meta-analysis identified the combination of progesterone and vitamin D as superior to either agent alone, with higher rates of favorable outcomes and reduced mortality [11]. Preclinical data support this synergy; in rodent models, progesterone combined with low-dose vitamin D enhanced spatial memory preservation and astrocyte activation compared to monotherapy (p<0.05) [12]. Vitamin D deficiency has been shown to blunt progesterone's efficacy, suggesting metabolic interdependence. These findings align with the hypothesis that TBI's multifactorial pathology demands multitarget therapies. For instance, progesterone mitigates edema, while vitamin D addresses chronic inflammation and oxidative stress—a dual approach that may counteract secondary injury cascades more effectively [13].

The neutral efficacy findings for progesterone and vitamin D as standalone therapies do not negate their potential utility in optimized regimens. First, progesterone's neuroprotective effects appear critically time-dependent, with preclinical models demonstrating maximal benefit when administered within ≤2 hours post-injury. This contrasts with clinical trials where treatment initiation often exceeded 6 hours—a delay that may explain the diminished therapeutic effects [14]. Incorporating real-time biomarkers such as S100B or glial fibrillary acidic protein (GFAP) could help identify patients within this narrow therapeutic window. [15]. Second, patient stratification based on injury phenotype (e.g., diffuse axonal injury) or baseline vitamin D status might enhance responsiveness, though current trials lack such precision in enrollment [16]. Finally, both agents exhibit excellent safety profiles, positioning them as viable adjuncts to rehabilitation or emerging neuroprotectants in multimodal strategies.

This analysis has several constraints: the small number of vitamin D trials (n=3) limits statistical power; heterogeneity in GOS-E assessment timelines, ranging from 30 days to 6 months complicates outcome comparisons; and incomplete reporting of baseline vitamin D status obscures deficiency-driven treatment effects. Future research should prioritize Phase III trials evaluating progesterone and vitamin D in combination,

leveraging their complementary mechanisms (e.g., progesterone's acute anti-inflammatory effects paired with vitamin D's chronic anti-inflammatory properties). Integrating biomarkers to guide treatment timing and patient selection could enhance precision, while expanding cohorts to include pediatric and geriatric populations—groups with high vitamin D deficiency rates and distinct neuroplasticity profiles—may clarify context-specific efficacy.

A critical limitation of the included trials is the disproportionate male representation, with male participants comprising 58–79% of enrolled cohorts. This underrepresentation of women limits the generalizability of findings, as sex-based differences in neuroinflammation, hormonal responses, and recovery trajectories are increasingly recognized in TBI research. Future trials should adopt sex-stratified enrollment and analyses to determine whether therapeutic responses differ by gender, particularly given progesterone's hormonal interactions and the variable prevalence of vitamin D deficiency across sexes.

Another consideration is potential publication bias. The small number of vitamin D studies and the predominance of neutral-to-negative progesterone trials increase the risk that positive preclinical findings are preferentially published, while underreporting of null or adverse results in early-phase studies could skew the perceived therapeutic promise. Formal assessment using funnel plots or Egger's regression was not feasible given the limited number of included trials, but this bias may inflate the apparent consistency between animal models and selected human studies. Addressing publication bias will require prospective trial registration, rigorous reporting of all outcomes, and the inclusion of unpublished data in future meta-analyses.

Conclusion

Based on the meta-analysis of randomized controlled trials, current evidence does not demonstrate a statistically significant improvement in functional outcomes, as measured by the GOS-E, with either progesterone or vitamin D supplementation in patients with moderate to severe TBI. While progesterone showed no overall benefit, vitamin D exhibited a trend toward improved neurological recovery, though this finding was not statistically significant. The limitations of the existing studies, including small sample sizes and high heterogeneity, highlight the need for larger, well-designed clinical trials to further investigate the therapeutic potential of vitamin D, particularly in combination with other neuroprotective strategies.

Author contributions

Conceptualization, K.O.W. and N.P.U.; Methodology, K.O.W.; Formal Analysis, M.A.W.; Writing—Original Draft Preparation, K.O.W.; Writing—Review & Editing, E.B.S. and N.P.U.; Visualization, M.A.W.; Supervision, E.B.S. All authors have read and agreed to the published version of the manuscript.

Disclosure

Funding

This research received no external funding.

Institutional review board statement

Not applicable.

Informed consent statement

Not applicable.

Data availability statement

All the data supporting the findings of this study are available in the included publications referenced in this meta-analysis.

Conflict of interest

The authors declare no conflict of interest and accept the terms and conditions.

References

1. Lele AV. Traumatic Brain Injury in Different Age Groups. J Clin Med. 2022 Nov 14;11(22):6739. doi: 10.3390/jcm11226739
2. Freire MAM, Rocha GS, Bittencourt LO, Falcao D, Lima RR, Cavalcanti JRLP. Cellular and Molecular Pathophysiology of Traumatic Brain Injury: What Have We Learned So Far? Biology (Basel). 2023 Aug 17;12(8):1139. doi: 10.3390/biology12081139
3. Zhou Z, Li Y, Peng R, Shi M, Gao W, Lei P, Zhang J. Progesterone induces neuroprotection associated with immune/inflammatory modulation in experimental traumatic brain injury. Neuroreport. 2024 Apr 3;35(6):352-360. doi: 10.1097/WNR.0000000000002013
4. Xiao G, Wei J, Yan W, Wang W, Lu Z. Improved outcomes from the administration of progesterone for patients with acute severe traumatic brain injury: a randomized controlled trial. Crit Care. 2008;12(2):R61. doi: 10.1186/cc6887
5. Jiang H, Yang X, Wang Y, Zhou C. Vitamin D Protects against Traumatic Brain Injury via Modulating TLR4/MyD88/NF-κB Pathway-Mediated Microglial Polarization and Neuroinflammation. Biomed Res Int. 2022 Jul 15;2022:3363036. doi: 10.1155/2022/3363036
6. Sharma S, Kumar A, Choudhary A, Sharma S, Khurana L, Sharma N, Kumar V, Bisht A. Neuroprotective Role of Oral Vitamin D Supplementation on Consciousness and Inflammatory Biomarkers in Determining Severity Outcome in Acute Traumatic Brain Injury Patients: A Double-Blind Randomized Clinical Trial. Clin Drug Investig. 2020 Apr;40(4):327-334. doi: 10.1007/s40261-020-00896-5
7. Hudak AM, Caesar RR, Frol AB, Krueger K, Harper CR, Temkin NR, Dikmen SS, Carlile M, Madden C, Diaz-Arrastia R. Functional outcome scales in traumatic brain injury: a comparison of the Glasgow Outcome Scale (Extended) and the Functional Status Examination. J Neurotrauma. 2005 Nov;22(11):1319-26. doi: 10.1089/neu.2005.22.1319
8. Stein DG. Embracing failure: What the Phase III progesterone studies can teach about TBI clinical trials. Brain Inj. 2015;29(11):1259-72. doi: 10.3109/02699052.2015.1065344
9. Stein DG. Is progesterone a worthy candidate as a novel therapy for traumatic brain injury? Dialogues Clin Neurosci. 2011;13(3):352-9. doi: 10.31887/DCNS.2011.13.2/dstein
10. Rebelos E, Tentolouris N, Jude E. The Role of Vitamin D in Health and Disease: A Narrative Review on the Mechanisms Linking Vitamin D with Disease and the Effects of Supplementation. Drugs. 2023 Jun;83(8):665-685. doi: 10.1007/s40265-023-01875-8
11. Aminmansour B, Nikbakht H, Ghorbani A, Rezvani M, Rahmani P, Torkashvand M, Nourian M, Moradi M. Comparison of the administration of progesterone versus progesterone and vitamin D in improvement of outcomes in patients with traumatic brain injury: A randomized clinical trial with placebo group. Adv Biomed Res. 2012;1:58. doi: 10.4103/2277-9175.100176
12. Hua F, Reiss JI, Tang H, Wang J, Fowler X, Sayeed I, Stein DG. Progesterone and low-dose vitamin D hormone treatment enhances sparing of memory following traumatic

brain injury. Horm Behav. 2012 Apr;61(4):642-51. doi: 10.1016/j.yhbeh.2012.02.017
13. Cekic M, Cutler SM, VanLandingham JW, Stein DG. Vitamin D deficiency reduces the benefits of progesterone treatment after brain injury in aged rats. Neurobiol Aging. 2011 May;32(5):864-74. doi: 10.1016/j.neurobiolaging.2009.04.017
14. Gibson CL, Gray LJ, Bath PM, Murphy SP. Progesterone for the treatment of experimental brain injury; a systematic review. Brain. 2008 Feb;131(Pt 2):318-28. doi: 10.1093/brain/awm183
15. Abdelhak A, Foschi M, Abu-Rumeileh S, Yue JK, D'Anna L, Huss A, Oeckl P, Ludolph AC, Kuhle J, Petzold A, Manley GT, Green AJ, Otto M, Tumani H. Blood GFAP as an emerging biomarker in brain and spinal cord disorders. Nat Rev Neurol. 2022 Mar;18(3):158-172. doi: 10.1038/s41582-021-00616-3
16. Soltani Z, Shahrokhi N, Karamouzian S, Khaksari M, Mofid B, Nakhaee N, Reihani H. Does progesterone improve outcome in diffuse axonal injury? Brain Inj. 2017;31(1):16-23. doi: 10.1080/02699052.2016.1213421

Original article

Ukrainian Neurosurgical Journal. 2026;32(1):99-105
doi: 10.25305/unj.342454

Artificial Intelligence algorithms for decision-making in thrombolysis and thrombectomy

Dmytro V. Shchehlov [1], Mykola B. Vyval [1], Stanislav V. Konotopchyk [1], Vladyslav O. Svyrydyiuk [2], Daryna L. Tarasenko[3], Victoria O. Liubysh [4], Victoria D. Savosik [5]

[1] Department of Endovascular Neuroradiology, State Institution "Scientific and Practical Center of Endovascular Neuroradiology of the National Academy of Medical Sciences of Ukraine", Kyiv, Ukraine
[2] Department of Neuroanatomy, Lithuanian University of Health Sciences, Kaunas, Lithuania
[3] Department of Medical Psychology, Psychosomatic Medicine and Psychotherapy, O.O. Bogomolets National Medical University, Kyiv, Ukraine
[4] Department 15, Clinical Institution for Psychiatric Care "Psychiatry", Kyiv, Ukraine
[5] Department of Biochemistry, Educational and Scientific Center "Institute of Biology and Medicine" of Taras Shevchenko National University of Kyiv, Kyiv, Ukraine

Received: 29 October 2025
Accepted: 27 November 2025

Address for correspondence*: Mykola B. Vyval, Scientific and Practical Center of Endovascular Neuroradiology, 32 Platona Maiborody st., Kyiv, 04050, Ukraine, e-mail: vyval_mukola@ukr.net*

Acute ischemic stroke is a medical emergency in which every minute of delay results in irreversible loss of brain tissue. The main treatment modalities—intravenous thrombolysis and endovascular thrombectomy—have strict time windows and depend critically on the accuracy of neuroimaging. Conventional image interpretation requires substantial clinical expertise, is time-consuming, and is subject to interobserver variability. Modern artificial intelligence (AI) algorithms open new opportunities for the automated detection of vascular occlusions, assessment of ischemic core volume, and generation of real-time treatment recommendations. The application of these algorithms can significantly reduce the time from patient admission to the initiation of reperfusion therapy, improve the accuracy of patient selection, and standardize clinical decision-making.

Objective: To summarize current evidence on the role of AI algorithms in decision-making for thrombolysis and thrombectomy and to assess their potential to improve the speed and accuracy of patient selection.

Materials and methods: A literature review (2015–2025) was conducted using the PubMed, Scopus, Web of Science, and Google Scholar databases with the keywords "artificial intelligence," "machine learning," "deep learning," "stroke," "thrombolysis," and "thrombectomy" to synthesize contemporary data on the use of AI algorithms in clinical decision-making for acute ischemic stroke. Clinical studies, reviews, and protocols describing the application of AI in neuroimaging, prognostication, and patient stratification were analyzed.

Results: Deep learning algorithms (e.g., Viz.ai, e-ASPECTS) enable automated processing of computed tomography and magnetic resonance imaging, rapidly identifying ischemic lesions and vascular occlusions. This reduces the time from diagnosis to treatment by 15–37 minutes, improves the reproducibility of assessments, and optimizes patient selection for reperfusion therapy. Models integrating clinical and neuroimaging data demonstrate superior predictive accuracy and allow consideration of individual patient characteristics.

Conclusions: Artificial intelligence is becoming an integral tool in stroke management by providing rapid, standardized, and objective data analysis. Its implementation reduces "door-to-needle" and "door-to-puncture" times, improves treatment outcomes, and decreases disability. The synergy between clinicians and AI heralds a new era of personalized stroke therapy aimed at preserving brain tissue and saving patients' lives.

Keywords*: ischemic stroke; thrombolysis; thrombectomy; artificial intelligence; machine learning.*

Acute ischemic stroke is a critical medical condition in which every minute of delay results in the loss of viable brain tissue. In the absence of reperfusion, a patient with a large cerebral artery occlusion loses approximately 1.9 million neurons per minute [1]. This phenomenon, commonly referred to as "time is brain", underscores the decisive importance of time in achieving successful treatment outcomes. The mainstay therapeutic approaches remain intravenous thrombolysis (administration of a thrombolytic agent) and endovascular thrombectomy (mechanical removal of the thrombus), both of which have clearly defined time windows and are based on the assessment of clinical data and neuroimaging findings [1]. Modern artificial intelligence (AI) algorithms open new opportunities for the automated detection of vascular occlusions, estimation of ischemic lesion volume, and real-time generation of treatment recommendations. Their implementation can substantially reduce the time from patient admission to the initiation of reperfusion therapy, improve the accuracy of patient selection, and standardize clinical decision-making.

Objective: To summarize current evidence on the role of AI algorithms in decision-making regarding thrombolysis and thrombectomy, and to evaluate their potential to improve the speed and accuracy of patient selection.

Materials and methods

This study is a narrative literature review aimed at synthesizing contemporary data on the use of AI algorithms for clinical decision-making in acute ischemic stroke. Literature searches were conducted in PubMed, Scopus, Web of Science, and Google Scholar databases covering the period from 2015 to 2025. The following keywords and their combinations were used: "artificial intelligence," "machine learning," "deep learning," "stroke," "thrombolysis," "thrombectomy," and "clinical decision support." Original studies, systematic reviews, meta-analyses, as well as clinical protocols and technical reports addressing the role of AI in neuroimaging assessment, outcome prediction, or determination of indications for thrombolysis and/or thrombectomy were analyzed.

Artificial intelligence in stroke neuroimaging

Neuroimaging is a key step in the evaluation of patients with stroke, as it allows confirmation of the ischemic nature of the event, identification of vessel occlusion, and assessment of the extent of brain injury. Contemporary AI algorithms are increasingly used for the automated analysis of computed tomography (CT), magnetic resonance imaging (MRI), and angiographic images. Convolutional neural networks are capable of detecting large vessel occlusion (LVO) on CT angiography with speed and accuracy comparable to those of expert radiologists [11]. Commercial software solutions, such as Viz.ai LVO, have demonstrated high specificity (95–97%) for detecting occlusion of the internal carotid artery or the proximal segment of the middle cerebral artery, although sensitivity remains moderate (78–82%) [2]. Importantly, the negative predictive value of such systems approaches 99%, indicating that only isolated cases are missed [2]. Automated LVO detection enables immediate notification of the stroke team about the presence of a thrombus, even while the patient is being transported to the hospital, thereby saving valuable time. For example, a multicenter study reported that implementation of automated occlusion alert software reduced the time from CT acquisition to initiation of thrombectomy by approximately 11 minutes on average [3], which was associated with nearly a 60% reduction in in-hospital mortality [3]. In addition to thrombus detection, AI can quantitatively assess the volume of ischemic brain injury. Algorithms for automated calculation of the Alberta Stroke Program Early CT Score (ASPECTS) analyze non-contrast CT images to identify early ischemic changes. The e-ASPECTS software has been shown to improve interobserver agreement among clinicians. According to published data, the use of e-ASPECTS increased the accuracy of ASPECTS assessment by neurologists from approximately 72% to 78%, while Cohen's kappa agreement improved from 0.60 to 0.65 ($p = 0.013$) [4]. Thus, AI reduces variability between different specialists and brings the performance of less experienced physicians closer to that of expert neuroradiologists [4].

More accurate and standardized assessment of infarct volume (ischemic core) is critical for treatment strategy selection. For instance, a very low ASPECTS score (indicating a large infarct) is a contraindication to early thrombectomy. Automated software packages such as RAPID analyze CT or MR perfusion data to calculate the volume of the ischemic core and the penumbra (hypoperfused tissue). These tools allow rapid (<5 minutes) generation of brain perfusion maps and calculation of mismatch parameters (core–penumbra discrepancy) [5]. Consequently, in extended time windows (beyond 6 hours from stroke onset), AI-based applications such as RAPID help identify patients with viable penumbral tissue who may be candidates for late endovascular intervention. The implementation of automated perfusion analysis was critical in clinical trials that expanded the indications for thrombectomy up to 24 hours in selected patients (e.g., the DAWN and DEFUSE 3 trials). In these studies, treatment decisions were made based on rapid software-based measurement of infarct and penumbra volumes [5].

AI also enables the use of telemedicine and real-time interaction in stroke care. In settings where a neurologist or radiologist is unavailable (e.g., primary stroke centers), algorithms can automatically analyze imaging data and transmit the results to specialists at a comprehensive stroke center. Systems such as Viz.ai send push notifications with annotated images highlighting the site of occlusion directly to physicians' smartphones, thereby facilitating and accelerating multidisciplinary consultation. Studies have shown that activation of such algorithms reduced interhospital transfer time from regional hospitals to comprehensive centers by approximately 37 minutes (from 141 to 104 minutes, $p = 0.04$) compared with the pre-implementation period [6]. In another center in the United Kingdom, the introduction of a comprehensive AI solution (e-Stroke by Brainomix) reduced the average door-in–door-out time (from admission to onward transfer) from 141 to 79 minutes (a reduction of 62 minutes, $p < 0.001$). This improvement was associated with a substantial increase in the proportion of patients undergoing thrombectomy and achieving functional independence (modified Rankin Scale score 0–2 in 48% with AI versus 16% without AI, $p = 0.04$) [7]. These findings indicate that integration of AI into "stroke network workflows" improves logistics and clinical outcomes.

Decision-making algorithms for thrombolysis

Intravenous thrombolysis (administration of recombinant tissue plasminogen activator) is an effective treatment for ischemic stroke when performed within the first 4.5 hours after symptom onset. Determining eligibility for thrombolysis requires assessment of the "therapeutic time window" and identification of contraindications, such as intracranial hemorrhage or a large established infarct volume. Artificial intelligence (AI) can assist in addressing both tasks. First, based on clinical data and neuroimaging, algorithms can estimate the actual time window and the condition of brain tissue. For example, in strokes with an unknown time of onset ("wake-up" strokes), the decision to administer thrombolysis may be made if MRI demonstrates a small diffusion-restricted lesion without a corresponding FLAIR signal, indicating a recent stroke. Automated software

can interpret such MRI findings or CT perfusion studies and recommend treatment for patients with a substantial penumbral zone and a small infarct core, even when the standard time threshold has been exceeded [5]. This approach underlies extended treatment protocols. For instance, the EXTEND trial demonstrated the efficacy of thrombolysis up to 9 hours after symptom onset in patients selected on the basis of perfusion imaging.

Second, AI enables rapid detection of contraindications to thrombolytic therapy. The most critical contraindication is the presence of intracerebral hemorrhage on CT. Neural networks trained on thousands of CT scans have demonstrated sensitivities of approximately 82–93% for the detection of acute hemorrhage, comparable to the accuracy of experienced radiologists. In one study, a deep learning algorithm outperformed medical interns in hemorrhage detection sensitivity (0.82 vs. ~0.70) while maintaining a specificity of approximately 0.90 [8]. Thus, AI systems can promptly identify hemorrhagic changes on imaging and prevent inappropriate thrombolysis. Another important contraindication is a large infarct volume, defined as involvement of more than one third of the middle cerebral artery territory. As noted above, automated tools (e.g., ASPECTS analyzers and infarct segmentation software based on perfusion maps) provide standardized assessments of lesion size. This is particularly valuable in emergency settings, where clinicians under time pressure may overlook subtle imaging features, whereas AI performs parallel analysis and highlights signs of extensive infarction or mass effect due to edema [6–8].

Beyond immediate assessment, AI algorithms can also predict the risk of thrombolysis-related complications. One of the most serious complications is symptomatic intracranial hemorrhage (sICH) following thrombolytic therapy, which occurs in 2–5% of cases and markedly worsens prognosis. Using large stroke databases, machine learning models have been developed that integrate clinical variables (age, blood glucose level, blood pressure, National Institutes of Health Stroke Scale [NIHSS] score) and neuroimaging findings to estimate the probability of hemorrhage prior to thrombolysis. According to a multicenter study published in 2023 involving approximately 9,000 cases, the area under the ROC curve (AUC) of the best-performing ML model reached ~0.87 for predicting the risk of symptomatic hemorrhage [9], substantially outperforming traditional prognostic scales. The authors recommended the neural network model with the highest accuracy as a decision-support tool, enabling clinicians to weigh the predicted risks and benefits of thrombolysis for individual patients [9]. Although an AI-based risk estimate does not constitute a formal contraindication, prior knowledge of a high hemorrhagic risk may prompt clinicians to adjust subsequent management, such as stricter blood pressure control or avoidance of aggressive interventions after thrombolysis.

In summary, AI algorithms function as an "electronic assistant" during patient selection for thrombolysis, simultaneously screening imaging for hemorrhage, estimating infarct volume, and providing prognostic insights. This approach accelerates decision-making and enhances its evidentiary basis, reducing the impact of human factors in high-stress clinical settings.

Decision-making algorithms for thrombectomy

Mechanical thrombectomy for occlusion of proximal cerebral arteries (e.g., the internal carotid artery, the M1 segment of the middle cerebral artery) can dramatically improve stroke outcomes when performed in a timely manner. Current guidelines define clear indications: the presence of large vessel occlusion (LVO) causing neurological deficit within 6 hours from symptom onset constitutes an unconditional indication for thrombectomy; in the 6–24-hour time window, the procedure is recommended for patients selected on the basis of advanced imaging demonstrating a small infarct core and a large penumbral region [5]. Artificial intelligence (AI) plays a crucial role at all stages of this decision-making process.

Algorithms for LVO detection on angiographic images help prevent missed occlusions, which is particularly important in cases with atypical or subtle findings. Studies have shown that the Viz.ai LVO system correctly identifies approximately 81% of internal carotid or proximal middle cerebral artery occlusions, while also providing negative results in 99% of cases without occlusion [11]. Although false-positive alerts do occur, a specificity exceeding 95% indicates that the vast majority of LVO notifications are reliable. Moreover, contemporary software versions can classify the exact location of the occlusion, for example, distinguishing thrombi in M_{2-} segments or in the basilar artery, which is diagnostically more challenging. Consequently, neurosurgeons or interventional radiologists receive not only an alert regarding the presence of a thrombus but also precise information on its localization, allowing advance planning of the interventional strategy [11].

AI systems also assess the status of collateral circulation—the network of alternative pathways that partially supply blood to the ischemic territory. Good collateral circulation is associated with slower infarct progression and more favorable outcomes after thrombectomy. Automated collateral assessment on CT angiography (e.g., the e-CTA module within the e-Stroke system) can quantitatively rank distal vessel opacification beyond the site of occlusion [10]. In a 2024 study involving 97 patients, AI-based analysis classified 58.8% of patients as having "good" collaterals. The presence of good collateral circulation was associated with a statistically significant reduction in the risk of death or severe disability by hospital discharge (odds ratio 0.27, $p = 0.003$). Accordingly, the AI-derived collateral index is considered an important biomarker: patients with favorable collateral status may remain candidates for intervention even at later time points after stroke onset, whereas poor collaterals are associated with a lower likelihood of benefit [10]. Automation not only saves time but also provides a more objective assessment than visual grading by clinicians, which is often characterized by substantial interobserver variability.

AI algorithms further support the identification of candidates for thrombectomy in the late time window (>6 hours). As noted above, software such as RAPID rapidly quantifies infarct core volume (using diffusion-weighted MRI or CT cerebral blood flow maps) and hypoperfused tissue volume (using Tmax maps). A small core combined with a large penumbra constitutes

a mismatch profile, in which thrombectomy may be beneficial even 9, 12, or 16 hours after stroke onset. Automated algorithms calculate the penumbra-to-core ratio and determine whether the patient meets criteria analogous to those used in the DAWN and DEFUSE trials. In an Indian study employing RAPID, volumetric results and mismatch ratios were obtained within 5 minutes for each patient. Three patients treated beyond the conventional 6-hour window achieved good functional outcomes at 3 months [5]. Owing to such technologies, indications for thrombectomy have been expanded. In 2018, the American Heart Association/American Stroke Association recommended mechanical thrombectomy up to 16 or 24 hours in patients selected using perfusion-based screening [1]. AI thus represents an integral component of this screening process, ensuring both speed and standardization across centers.

An additional important application of AI is outcome prediction after thrombectomy. Not all patients achieve comparable recovery even after successful vessel recanalization, as outcomes depend on age, comorbidities, infarct size, ischemia duration, and other factors. Machine learning models can use early clinical and imaging data, often within the first 24 hours, to predict whether a patient will achieve functional independence at 3 months (modified Rankin Scale [mRS] 0–2).

A large study based on the German Stroke Registry recently reported the development of a neural network trained on 7,485 thrombectomy cases [12]. The model analyzed 30 variables (including age, NIHSS score at admission and at 24 hours, use of thrombolysis, infarct volume, and presence of hemorrhage) to identify key prognostic factors. After optimization, only seven predictors were sufficient for accurate model performance, achieving an AUC of approximately 0.90 for predicting favorable outcomes. By comparison, neurologists' prognostic accuracy on the second hospital day is typically substantially lower. This model provides clinicians with an individualized probability of recovery and may support planning of rehabilitation, communication with patients' families, and therapeutic decision-making (e.g., consideration of more aggressive management in patients with an unfavorable prognosis). Notably, the authors designed the model to be interpretable, indicating which factors most strongly influenced the predicted outcome for a given patient (for example, very high NIHSS scores and intracranial hemorrhage worsen prognosis, whereas younger age and absence of prior stroke improve it) [12]. Such transparency enhances clinicians' trust in AI-based tools and facilitates their integration into clinical reasoning.

Integration of algorithms into clinical practice

The implementation of artificial intelligence (AI) in stroke care systems is occurring gradually. Decision-support systems are being developed that integrate with hospital Picture Archiving and Communication Systems (PACS) and image-sharing networks. This is particularly relevant within the "hub-and-spoke" model commonly used in stroke services, where AI can serve as a critical link enabling rapid patient triage and routing. Software solutions such as Viz.ai or e-Stroke automatically transmit imaging analysis results between hospitals, reducing delays associated with awaiting radiology reports and conducting telephone consultations. Many centers have reported reductions in door-to-needle and door-to-groin times following the adoption of these tools. According to a randomized cluster trial, the mean time from hospital admission to arterial puncture for thrombectomy was reduced by 11.2 minutes through automated occlusion detection and team-wide notification via a secure messaging platform [3]. Another study demonstrated a reduction in interhospital transfer time of approximately 37 minutes when Viz.ai software was installed at spoke hospitals compared with centers without the system ($p = 0.04$) [6]. In a UK center, implementation of the e-Stroke platform resulted in a 62-minute reduction in door-in–door-out time [7]. These time savings translate into preservation of a greater volume of viable brain tissue and enable a larger proportion of patients to receive appropriate treatment. Following the introduction of AI-based LVO analysis, a reduction in mortality among stroke patients was observed (13% vs. 31%, $p < 0.001$), although functional outcomes at 90 days did not differ significantly [3]. It is plausible that faster care prevented some fatal complications (e.g., earlier thrombectomy reducing the risk of hemorrhagic transformation or cerebral edema), even though no significant differences in neurological deficit were detected.

The integration of AI into clinical practice requires organizational adaptations, including the establishment of protocols governing human–algorithm interaction. Telemedicine consultants (neurologists, neurosurgeons) must have real-time access to AI-generated analyses. These systems are often accompanied by mobile applications that allow physicians to review image series with AI-annotated regions (ischemic core, collateral circulation, occlusion) on their smartphones while off-site and to promptly provide recommendations regarding thrombolysis or patient transfer. In the United States, such applications have already been certified by the Food and Drug Administration (FDA) as medical software devices. In a large hospital network (Atrium Health, USA), implementation of Viz.ai enabled the establishment of a unified "code stroke" protocol: when stroke is suspected, CT angiography is automatically uploaded to a cloud-based service, where AI screens for vessel occlusion; if detected, all members of the stroke team receive an alert with the relevant images. This capability is particularly valuable in smaller hospitals lacking 24/7 neuroradiology coverage. The algorithm addresses this gap by performing rapid image screening without the need to wait for an expert radiological opinion [2]. While the final clinical decision always remains with the physician, AI provides more comprehensive information more rapidly than previously available. Within telemedicine-based care models, AI also contributes to reducing unnecessary activations of tertiary teams (e.g., avoiding false nighttime mobilization of angiography teams when no LVO is present), as preliminary AI-based filtering can prevent unwarranted escalations.

Challenges and limitations

Despite substantial progress, the implementation of artificial intelligence (AI) in stroke medicine faces several important challenges. The first concerns the reliability and validity of algorithms across different populations and clinical settings. Deep learning models

are often trained on data from a single region or even a single center. When applied in other hospitals, their performance may decline because of differences in scanners, imaging protocols, or patient characteristics [13]. For example, a model trained predominantly on a Caucasian population may exhibit reduced accuracy in Asian populations with distinct risk profiles (certain vasculopathies, such as moyamoya disease, are prevalent in Asian countries but rare in Western populations) [14]. Similarly, an algorithm trained on MRI slices with 1-mm thickness may lose sensitivity when applied to images with 5-mm slice thickness. Therefore, extensive multicenter validation is required before widespread deployment. Developers are gradually addressing this issue by incorporating data from multiple countries into training datasets, adapting algorithms to different acquisition parameters, and conducting post-marketing surveillance to monitor AI performance after deployment in new environments and to retrain models when necessary [13].

The second major challenge relates to transparency and explainability. Most contemporary AI models function as "black boxes," producing outputs (e.g., "occlusion present" or "ASPECTS = 7") without clarifying how these conclusions were reached [15]. Such opacity can undermine clinicians' trust. Physicians are accustomed to understanding the rationale underlying a diagnosis, for example, by directly visualizing hemorrhage on imaging. If an AI system indicates the presence of hemorrhage without highlighting its location or if the features are not readily apparent to the human eye, clinicians may question the result and spend additional time verifying it. Consequently, a "trust deficit" represents a significant barrier to AI adoption. For high-risk decisions—such as withholding thrombolysis or proceeding with surgery—clinicians are reluctant to rely on algorithmic recommendations without a clear explanation [13]. This has led to growing interest in Explainable AI (EAI), which aims to make model decisions interpretable. Techniques such as Gradient-Weighted Class Activation Mapping (grad-CAM) can highlight image regions that contributed most to the model's output, thereby indicating where features of occlusion were detected [16]. Another approach involves developing more interpretable models that output clinically meaningful parameters (e.g., penumbral volume in milliliters, collateral indices) rather than abstract probabilities. Insufficient interpretability is now formally recognized as a factor that reduces trust and delays the integration of AI into medical practice [17].

A third aspect involves legal and ethical issues of responsibility. When a physician makes a decision, accountability is clearly defined. However, when an algorithm contributes to the decision-making process, responsibility becomes less straightforward: who is liable if the AI system makes an error and the patient is harmed? Formally, the physician remains responsible for treatment decisions. Nevertheless, if the clinician followed an algorithmic recommendation, an ethical dilemma arises. Developers and vendors of AI systems are also stakeholders—should they bear partial responsibility for algorithmic errors? These questions remain insufficiently addressed within current regulatory frameworks [18]. Experts emphasize the need for clear boundaries, including transparent logging of AI actions, decision audit trails, and the ability to audit algorithms to identify the causes of errors. In addition, issues of informed consent emerge: should patients be informed that AI contributed to clinical decision-making, and should they consent to such an "assistive" mode of care? At present, this is rarely implemented explicitly in routine practice, but debate continues. Conversely, if an algorithm detects signs of stroke earlier than a physician and the clinician ignores the alert, does responsibility lie with the physician for disregarding the signal? Legal practice will likely evolve in parallel with the expanding use of AI [13].

The fourth challenge concerns validation and certification. For an algorithm to achieve widespread adoption, it must undergo clinical evaluation and demonstrate stable accuracy and tangible benefit. Health authorities and regulatory agencies (e.g., the U.S. Food and Drug Administration [FDA] and the European Medicines Agency [EMA]) impose increasingly stringent requirements on AI tools. Evidence from "real-world" data, comparisons with physician performance, and proof that algorithm use improves clinical outcomes are required. For systems that provide treatment recommendations, the threshold is even higher, as such tools effectively become part of the clinical decision itself rather than a supplementary imaging analysis. To date, most AI systems in stroke care have been approved as diagnostic decision-support tools, meaning they inform but do not replace clinical judgment. For example, e-ASPECTS and Viz LVO have been authorized in this category. Consequently, physicians must verify AI outputs before acting upon them [2,4]. Strict accuracy requirements also raise questions regarding sensitivity and specificity. If an algorithm misses even a small percentage of occlusions (approximately 18% are reportedly missed) [2], is this acceptable, given that a missed patient may lose the opportunity for treatment? Conversely, excessive sensitivity at the expense of specificity may lead to frequent false alarms and unnecessary mobilization of teams. Achieving an appropriate balance and defining acceptable thresholds are therefore critical technical and ethical considerations prior to implementation.

The fifth challenge relates to staff training. The adoption of new technologies requires education of physicians and nurses. Clear interfaces and protocols must be developed, specifying who reviews AI outputs, how results are documented, and how discrepancies between AI assessments and clinician judgment should be managed. Clinicians need to understand the limitations of AI, including scenarios in which errors are more likely. This represents a new category of clinical technology that necessitates formal training through courses and workshops. Some clinicians, particularly from older generations, may be skeptical or distrustful of algorithms. Providing robust evidence of benefit and training in appropriate interpretation of AI results are therefore essential. A culture of collaboration between clinicians and AI is required, in which the algorithm is viewed not as a competitor or a threat to professional authority but as a tool analogous to a new type of medical equipment [13, 18].

Finally, ethical considerations and bias must not be overlooked. AI algorithms are human-designed systems and may inadvertently inherit biases present in the underlying data. For instance, a model trained predominantly on male patients may perform less accurately in women. If training data are drawn mainly from urban hospitals, the algorithm may underestimate issues relevant to patients from rural settings. It is the responsibility of developers and clinicians to identify such biases and mitigate them through dataset optimization and appropriate corrective adjustments. From an ethical standpoint, AI use should remain patient-centered: patients are entitled to high-quality care with or without AI assistance, and technologies should be implemented to improve outcomes rather than for novelty or promotional purposes [18].

Future perspectives

The prospects for the application of artificial intelligence (AI) in cerebrovascular medicine are exceptionally broad. One promising direction is the integration of AI algorithms with biomarkers and clinical scales to generate comprehensive prognostic assessments. For example, future models may incorporate not only imaging data but also genetic markers, coagulation parameters, and results of neuropsychological testing. This approach aligns with the concept of personalized medicine, in which therapeutic decisions are tailored to the individual patient. In the coming years, rapid blood assays for biomarkers of ischemic injury may become routine at hospital admission for stroke, with AI systems integrating these data with neuroimaging to more accurately estimate time since stroke onset or predict the likelihood of successful thrombectomy. Active research is ongoing to identify such biomarkers and to develop multifactorial predictive models [19].

Another promising area involves generative models and the simulation of clinical scenarios. Generative Adversarial Networks (GANs) are being used to create synthetic medical images that can augment training datasets [20]. In the context of stroke, this approach enables the "generation" of thousands of virtual CT scans with diverse ischemic patterns, thereby improving algorithm performance even in rare or atypical cases. Generative models may also be capable of predicting infarct evolution; for instance, based on an initial scan, they could simulate how brain tissue might appear after 6 hours without treatment. Such tools could inform therapeutic decision-making: if a model predicts rapid infarct expansion in the absence of intervention, this would support a more aggressive treatment strategy. The application of large language models (LLMs) opens an additional avenue, including improved clinical documentation and support for clinical reasoning [21]. In the future, clinicians may describe a patient's situation in natural language, and an AI system integrated with clinical knowledge bases could suggest treatment options based on the latest guidelines and evidence, adapted to the patient's specific parameters. In stroke care, this could be particularly valuable in nonstandard scenarios, such as ischemic stroke in the setting of recent surgery, where AI assistance could help assess thrombolysis-related risks [22].

From a health system perspective, future developments may include unified platforms for comprehensive stroke care, encompassing the entire patient journey from emergency medical services activation to rehabilitation. AI could provide continuous support across all stages: in the prehospital phase, assisting in stroke recognition based on symptoms (with existing prototypes already analyzing speech, facial movements, and coordination via smartphones); during hospitalization, interpreting CT or MRI scans and proposing treatment strategies; and after discharge, monitoring recovery through wearable devices that assess speech, gait, and cognitive exercises, while alerting clinicians to deviations or complications. In this way, AI may become embedded within the stroke care continuum, strengthening each component of care delivery [23]. Naturally, all these perspectives must be rigorously evaluated for safety and effectiveness; nevertheless, the overall trend is clear—AI is becoming an integral part of the evolution of stroke care. It is not an exaggeration to state that a new era in stroke treatment is emerging. AI integrated into stroke management has the potential to raise the standard of care by enabling faster, more accurate, and more personalized therapy. The gradual, evidence-based implementation of these technologies may in the near future substantially reduce the societal burden of stroke by lowering mortality and disability rates, improving patients' quality of life, and optimizing the use of healthcare resources. This represents a compelling example of how innovation at the intersection of information technology and medicine can directly benefit clinical practice by achieving the highest goal—saving human brain tissue and lives.

Conclusions

A clear transition is currently underway from experimental AI developments in stroke medicine to their implementation in real-world clinical practice. AI algorithms do not replace neurologists or neurosurgeons; rather, they serve as powerful tools that augment clinical expertise. At the diagnostic stage, AI provides speed (image analysis within minutes) and objectivity (standardized assessment of lesion volume, vessel occlusion, and related parameters). In decision-making for thrombolysis and thrombectomy, algorithms help exclude unsuitable candidates—thereby avoiding unnecessary or potentially harmful interventions—and identify patients who may benefit from aggressive treatment, even when such potential is not readily apparent to the human eye. The clinical impact of these technologies is reflected in improved patient outcomes: more individuals spared from severe disability, reduced stroke-related mortality, and faster return to active life. Notably, centers that have implemented AI solutions have achieved substantial reductions in key time metrics (e.g., "door-to-needle" and "door-to-puncture" times), with each minute saved potentially preserving millions of neurons.

However, AI implementation must proceed gradually and responsibly. Barriers must be addressed, ranging from technical challenges (data harmonization, cybersecurity) to human factors (user training, trust building). AI models should be sufficiently transparent to allow clinicians to explain decisions to patients. Physicians must maintain critical thinking and use AI as a "second opinion" or coordination tool that provides

insights, while the final therapeutic decision remains with the clinician. The greatest potential lies in the synergy between human expertise and AI.

Disclosures

Conflict of interest

The authors declare no conflicts of interest.

Funding

This study received no external financial support.

References

1. Powers WJ, Rabinstein AA, Ackerson T, Adeoye OM, Bambakidis NC, Becker K, Biller J, Brown M, Demaerschalk BM, Hoh B, Jauch EC, Kidwell CS, Leslie-Mazwi TM, Ovbiagele B, Scott PA, Sheth KN, Southerland AM, Summers DV, Tirschwell DL; American Heart Association Stroke Council. 2018 Guidelines for the Early Management of Patients With Acute Ischemic Stroke: A Guideline for Healthcare Professionals From the American Heart Association/American Stroke Association. Stroke. 2018 Mar;49(3):e46-e110. doi: 10.1161/STR.0000000000000158
2. Karamchandani RR, Helms AM, Satyanarayana S, Yang H, Clemente JD, Defilipp G, Strong D, Rhoten JB, Asimos AW. Automated detection of intracranial large vessel occlusions using Viz.ai software: Experience in a large, integrated stroke network. Brain Behav. 2023 Jan;13(1):e2808. doi: 10.1002/brb3.2808
3. Martinez-Gutierrez JC, Kim Y, Salazar-Marioni S, Tariq MB, Abdelkhaleq R, Niktabe A, Ballekere AN, Iyyangar AS, Le M, Azeem H, Miller CC, Tyson JE, Shaw S, Smith P, Cowan M, Gonzales I, McCullough LD, Barreto AD, Giancardo L, Sheth SA. Automated Large Vessel Occlusion Detection Software and Thrombectomy Treatment Times: A Cluster Randomized Clinical Trial. JAMA Neurol. 2023 Nov 1;80(11):1182-1190. doi: 10.1001/jamaneurol.2023.3206
4. Kobeissi H, Kallmes DF, Benson J, Nagelschneider A, Madhavan A, Messina SA, Schwartz K, Campeau N, Carr CM, Nasr DM, Braksick S, Scharf EL, Klaas J, Woodhead ZVJ, Harston G, Briggs J, Joly O, Gerry S, Kuhn AL, Kostas AA, Nael K, AbdalKader M, Kadirvel R, Brinjikji W. Impact of e-ASPECTS software on the performance of physicians compared to a consensus ground truth: a multi-reader, multi-case study. Front Neurol. 2023 Sep 7;14:1221255. doi: 10.3389/fneur.2023.1221255
5. Vyas D, Bohra V, Karan V, Huded V. Rapid Processing of Perfusion and Diffusion for Ischemic Strokes in the Extended Time Window: An Indian Experience. Ann Indian Acad Neurol. 2019 Jan-Mar;22(1):96-99. doi: 10.4103/aian.AIAN_142_18
6. Field NC, Entezami P, Boulos AS, Dalfino J, Paul AR. Artificial intelligence improves transfer times and ischemic stroke workflow metrics. Interv Neuroradiol. 2023 Oct 17:15910199231209080. doi: 10.1177/15910199231209080
7. Nagaratnam K, Neuhaus A, Briggs JH, Ford GA, Woodhead ZVJ, Maharjan D, Harston G. Artificial intelligence-based decision support software to improve the efficacy of acute stroke pathway in the NHS: an observational study. Front Neurol. 2024 Jan 18;14:1329643. doi: 10.3389/fneur.2023.1329643
8. Angkurawaranon S, Sanorsieng N, Unsrisong K, Inkeaw P, Sripan P, Khumrin P, Angkurawaranon C, Vaniyapong T, Chitapanarux I. A comparison of performance between a deep learning model with residents for localization and classification of intracranial hemorrhage. Sci Rep. 2023 Jun 20;13(1):9975. doi: 10.1038/s41598-023-37114-z
9. Wen R, Wang M, Bian W, Zhu H, Xiao Y, He Q, Wang Y, Liu X, Shi Y, Hong Z, Xu B. Machine learning-based prediction of symptomatic intracerebral hemorrhage after intravenous thrombolysis for stroke: a large multicenter study. Front Neurol. 2023 Oct 20;14:1247492. doi: 10.3389/fneur.2023.1247492
10. Scavasine VC, Stoliar GA, Teixeira BCA, Zétola VHF, Lange MC. Automated evaluation of collateral circulation for outcome prediction in acute ischemic stroke. J Stroke Cerebrovasc Dis. 2024 Apr;33(4):107584. doi: 10.1016/j.jstrokecerebrovasdis.2024.107584
11. Yahav-Dovrat A, Saban M, Merhav G, Lankri I, Abergel E, Eran A, Tanne D, Nogueira RG, Sivan-Hoffmann R. Evaluation of Artificial Intelligence-Powered Identification of Large-Vessel Occlusions in a Comprehensive Stroke Center. AJNR Am J Neuroradiol. 2021 Jan;42(2):247-254. doi: 10.3174/ajnr.A6923
12. Shirvani O, Warnat-Herresthal S, Savchuk I, Bode FJ, Nitsch L, Stösser S, Ebrahimi T, von Danwitz N, Asperger H, Layer J, Meissner J, Thielscher C, Dorn F, Lehnen N, Schultze JL, Petzold GC, Weller JM; GSR-ET Investigators. Machine learning models for outcome prediction in thrombectomy for large anterior vessel occlusion. Ann Clin Transl Neurol. 2024 Oct;11(10):2696-2706. doi: 10.1002/acn3.52185
13. Park S. Rethinking Clinical AI Applications in Stroke – Pitfalls, Misconceptions, and Directions for Responsible Use. J Neurosonol Neuroimag. 2025;17(1):1–10. doi: 10.31728/jnn.2025.00171
14. Kim JS. Moyamoya Disease: Epidemiology, Clinical Features, and Diagnosis. J Stroke. 2016 Jan;18(1):2-11. doi: 10.5853/jos.2015.01627
15. Heo J. Application of Artificial Intelligence in Acute Ischemic Stroke: A Scoping Review. Neurointervention. 2024 Mar;20(1):4-14. doi: 10.5469/neuroint.2025.00052
16. Zhang H, Ogasawara K. Grad-CAM-Based Explainable Artificial Intelligence Related to Medical Text Processing. Bioengineering (Basel). 2023 Sep 10;10(9):1070. doi: 10.3390/bioengineering10091070
17. Kelly CJ, Karthikesalingam A, Suleyman M, Corrado G, King D. Key challenges for delivering clinical impact with artificial intelligence. BMC Med. 2019 Oct 29;17(1):195. doi: 10.1186/s12916-019-1426-2
18. Weiner EB, Dankwa-Mullan I, Nelson WA, Hassanpour S. Ethical challenges and evolving strategies in the integration of artificial intelligence into clinical practice. PLOS Digit Health. 2025 Apr 8;4(4):e0000810. doi: 10.1371/journal.pdig.0000810
19. Agripnidis T, Ayobi A, Quenet S, Chaibi Y, Avare C, Jacquier A, Girard N, Hak JF, Reyre A, Brun G, El Ahmadi AA. Performance of an artificial intelligence tool for multi-step acute stroke imaging: A multicenter diagnostic study. Eur J Radiol Open. 2025 Aug 29;15:100678. doi: 10.1016/j.ejro.2025.100678
20. Ivanenko M, Wanta D, Smolik WT, Wróblewski P, Midura M. Generative-Adversarial-Network-Based Image Reconstruction for the Capacitively Coupled Electrical Impedance Tomography of Stroke. Life (Basel). 2024 Mar 21;14(3):419. doi: 10.3390/life14030419
21. Owens D, Nguyen DQ, Dohopolski M, Rousseau JF, Peterson ED, Navar AM. Accuracy of Large Language Models to Identify Stroke Subtypes Within Unstructured Electronic Health Record Data. Stroke. 2025 Oct;56(10):2966-2975. doi: 10.1161/STROKEAHA.125.051993
22. Qiang S, Zhang H, Liao Y, Zhang Y, Gu Y, Wang Y, Xu Z, Shi H, Han N, Yu H. Application of Large Language Models in Stroke Rehabilitation Health Education: 2-Phase Study. J Med Internet Res. 2025 Jul 22;27:e73226. doi: 10.2196/73226
23. Alhakeem A, Chaurasia B, Khan MM. Revolutionizing stroke prediction: a systematic review of AI-powered wearable technologies for early detection of stroke. Neurosurg Rev. 2025 May 29;48(1):458. doi: 10.1007/s10143-025-03629-4

Original article

Ukrainian Neurosurgical Journal. 2026;32(1):106-112
doi: 10.25305/unj.341960

Comparison of microdiscectomy and microdiscectomy with cage interbody fusion in lumbar–sacral disc herniation

Ievgenii I. Slynko, Roman V. Chamata

Spinal Department, Romodanov Neurosurgery Institute, Kyiv, Ukraine

Received: 23 October 2025
Accepted: 17 January 2026

Address for correspondence: *Roman V. Chamata, Spinal Department, Romodanov Neurosurgery Institute, 32 Platon Mayboroda St., Kyiv, Ukraine, 04050, e-mail: chamataroman@gmail.com*

Objective: To optimize the selection of surgical treatment strategy for patients with lumbar and lumbosacral disc herniation by performing a comparative analysis of the outcomes of microdiscectomy and microdiscectomy with interbody cage fusion in order to improve treatment results.

Materials and methods: The study included 200 patients with lumbar and lumbosacral disc herniation treated at the Romodanov Neurosurgery Institute of the National Academy of Medical Sciences of Ukraine between 2015 and 2022. Neurological status was assessed based on the severity of pain syndrome, the presence of segmental instability was determined. Magnetic resonance imaging, computed tomography, and radiographic findings were evaluated. The following surgical techniques were used: microdiscectomy for lumbar and lumbosacral disc herniation.

Results: Microdiscectomy with interbody cage fusion eliminated manifestations of instability and provided more effective stabilization of the lumbosacral spine compared with microdiscectomy alone. The recurrence rate of disc herniation after microdiscectomy with cage fusion lower (3%) compared with microdiscectomy alone (9%). In the group treated with microdiscectomy and cage fusion, a more pronounced reduction in pain intensity (–82%) and a greater decrease in the Oswestry Disability Index (–81%) were observed, indicating higher effectiveness of the stabilization technique. According to the Macnab and Prolo scales, excellent and good outcomes were recorded more frequently in the microdiscectomy with cage fusion group than in the microdiscectomy group (91% vs 78% and 91% vs. 77%, respectively). The Wilcoxon test confirmed a high level of within-group improvement ($p<0.001$), while the t-test demonstrated statistically significant differences between the groups.

Conclusions: The lumbosacral segment with an implanted cage is more stable and withstands greater mechanical loads during motion, reduces the recurrence rate of disc herniation, and decreases pain severity. Microdiscectomy with interbody cage fusion may be considered in carefully selected patients with signs of segmental instability as an approach that combines decompression and stabilization and is associated with better long-term clinical outcomes.

Keywords: *lumbar–sacral disc herniation; microdiscectomy; microdiscectomy with cage interbody fusion*

Introduction

According to statistical data, herniation localized in the lumbosacral region of the spine occurs most frequently. Such herniations are among the leading causes of chronic pain syndrome and temporary disability [1, 2]. In the majority of cases (59%), intervertebral disc herniations affecting the lumbar and sacral nerve roots are located at the L4–L5 level (with compression of the L5 nerve root). The second most common level is L5–S1 (with compression of the S1 nerve root), accounting for 30% of cases [3, 4].

The gold standard for surgical treatment of lumbosacral disc herniation is microdiscectomy (microsurgical removal of the herniated intervertebral disc). The main advantage of this method is the ability to remove herniations of any density, location, and size, including cases associated with spinal canal stenosis and sequestrated intervertebral disc herniation [5]. However, this technique does not prevent the development of recurrent herniation or instability of the lumbosacral spine, which may necessitate repeat surgical intervention [6, 7]. Thus, the choice of the optimal surgical strategy (microdiscectomy alone versus microdiscectomy combined with interbody fusion using a cage) remains a relevant clinical issue.

Aim: to optimize the selection of surgical treatment strategy for patients with lumbosacral disc herniation through a comparative analysis of outcomes following microdiscectomy and microdiscectomy combined with interbody cage fusion, with the goal of improving treatment results.

Materials and methods

Study participants

The study included 200 patients with lumbosacral disc herniation who were treated at the A.P. Romodanov Institute of Neurosurgery of the National Academy of Medical Sciences of Ukraine between 2015 and 2022.

Written informed consent for participation in the study and for publication of the data was obtained from all patients.

The study protocol was approved by the Ethics and Bioethics Committee of the A.P. Romodanov Institute of Neurosurgery of the National Academy of Medical Sciences of Ukraine (Minutes No. 3, dated November 24, 2022).

Inclusion criteria:

1. Patient age 19–70 years.
2. Presence of L4–L5 or L5–S1 intervertebral disc herniation confirmed by magnetic resonance imaging (MRI).
3. No prior stabilization surgery in the lumbar spine.
4. Duration of clinical symptoms of at least 6 weeks with ineffective conservative treatment.
5. Written informed consent to participate in the study.

Exclusion criteria:

1. Multisegmental involvement (>1 spinal level).
2. Traumatic, infectious, or neoplastic lesions of the spine.
3. Severe comorbid conditions increasing surgical risk.
4. Pregnancy or inability to undergo postoperative rehabilitation.

Group characteristics

All patients underwent surgical treatment for lumbosacral disc herniation. Of these, 100 patients underwent microdiscectomy, while the remaining patients underwent microdiscectomy combined with interbody fusion using cages.

Indications for microdiscectomy (MD):

1. Presence of clinical symptoms of nerve root compression (lumboischialgia-type pain syndrome, positive nerve tension signs).
2. Presence of L4–L5 or L5–S1 intervertebral disc herniation confirmed by MRI.
3. Absence of signs of advanced degeneration of adjacent structures (Modic type 0–I, without significant loss of disc height).
4. Ineffectiveness of conservative treatment for 6–8 weeks.
5. Stability of the motion segment on functional radiographs (displacement <3 mm, angular deformation <10°).

Thus, microdiscectomy was predominantly performed in patients with isolated disc herniation without structural instability.

Microdiscectomy combined with interbody cage fusion (MD + Cage) was applied in patients with discogenic pathology accompanied by structural or biomechanical segmental instability, in whom decompression alone was insufficient to stabilize the spine and prevent herniation recurrence.

Main indications for microdiscectomy with interbody cage fusion:

1. Disc herniation combined with radiographic signs of segmental instability (vertebral body displacement >3 mm or pathological mobility >10° on functional studies).
2. Modic type II changes on MRI (signs of endoplastic degeneration, cystic remodeling, or fibrosis).
3. Recurrent disc herniation after prior discectomy.
4. Marked loss of disc height (>50%) or post-discectomy segmental deformity.
5. Clinical manifestations of mechanical pain relieved in unloading positions (a sign of motion segment instability).

Thus, microdiscectomy with interbody fusion using a cage was performed in patients for whom decompression alone was insufficient to stabilize the spinal segment and prevent recurrence.

Contraindications to microdiscectomy:

1. Severe somatic condition (grade III–IV cardiac, respiratory, or renal failure).
2. Systemic infections, febrile conditions, coagulopathies, or use of anticoagulants without the possibility of temporary discontinuation.
3. Mental disorders that preclude adequate postoperative rehabilitation.
4. Spinal segment instability (displacement>3 mm, pathological mobility >10°).
5. Significant loss of disc height with collapse of the vertebral bodies.
6. Severe degenerative changes (cystic–fibrotic alterations, Modic type II–III changes).

Contraindications to microdiscectomy with interbody fusion using a cage:

1. Severe osteoporosis that prevents stable cage implantation.
2. Active infectious spondylodiscitis.
3. Anatomical inaccessibility of the surgical approach (congenital anomalies, cicatricial–adhesive changes after multiple surgeries).
4. Pronounced grade III spinal segment instability (displacement >6 mm, pathological mobility >15°), which constitutes an indication for spinal fusion.

Study design

A comparative study was conducted involving two groups of patients who underwent microdiscectomy and microdiscectomy with cage fixation, respectively. The analysis focused on the surgical techniques, the recurrence rate following both types of procedures, and neurological outcomes in the early and long-term postoperative periods. Based on the obtained results, indications for the use of these surgical methods and corresponding clinical recommendations were developed.

All patients underwent neurological assessment, including evaluation of pain syndrome manifestations, pain intensity measured using the Visual Analog Scale (VAS), functional status assessed by the Oswestry Disability Index (ODI), the Macnab Scale (***Table 1***), and the Prolo functional–economic outcome scale (***Table 2***). In addition, recurrence rates were recorded. The surgical techniques applied included microdiscectomy and microdiscectomy of lumbosacral disc herniations with interbody fusion using cages at the L4–L5 or L5–S1 levels. The posterior interlaminar approach at the L4–L5 or L5–S1 level was predominantly used; in isolated cases with a narrow interlaminar space, a microscopic transforaminal lumbar interbody fusion (TLIF) approach was employed. Titanium or PEEK (polyetheretherketone) cages manufactured by "Medtronic" or "Novo Spine" were used. The cages were of "banana" and "bullet" shapes, with the size selected individually based on the intraoperative height of the intervertebral disc space. The space inside and around the cage was not filled with autologous bone graft material. No additional fixation

was applied. In the comparison group, only the stand-alone cage technique was used.

Among the main preoperative complaints, low back pain radiating to the lower limb, inability to walk for prolonged periods, and difficulty maintaining an upright position predominated. Foot paresis was observed in 12.5% of patients, while pelvic dysfunction was identified in 4.2%.

Analysis of patient distribution by age groups demonstrated that intervertebral disc herniation was most frequently diagnosed in patients aged 41–50 years (***Table 3***). The distribution of lumbosacral intervertebral disc herniations by spinal level was as follows: L4–L5 — 108 cases (54%) and L5–S1 — 92 cases (46%).

In the late postoperative period (12 months after surgery), patients completed a questionnaire-based assessment.

1. Subjective pain perception was evaluated using the VAS, represented by a 100-mm horizontal line, where 0 mm corresponds to the complete absence of pain and 100 mm indicates the maximum imaginable pain. Patients marked the level of pain intensity, and the distance from the zero point to the mark was measured in millimeters.

For analytical purposes, VAS scores were conditionally categorized into the following pain intensity levels:

- 0 mm — no pain;
- 1–20 mm — mild pain;
- 21–60 mm — moderate pain;
- 61–100 mm — severe pain.

For ease of clinical interpretation, VAS results were also presented on a 0–10 point scale, equivalent to the 0–100 mm range.

2. Oswestry Disability Index (ODI).

The Oswestry Disability Index (ODI) questionnaire (***Table 4***) is a validated instrument for the quantitative assessment of disability associated with degenerative spinal disorders. In the present study, ODI version 2.0

Table 1. Macnab scale [13]

Rating	Outcome characteristics
Excellent	Complete relief of pain; the patient has returned to normal daily activities and work
Good	Occasional mild pain that does not limit daily activities; the patient is able to work in the same position;
Fair	Persistent pain, but significantly reduced compared with the preoperative level; activity is partially limited, and the patient must change to less physically demanding work
Poor	No improvement or worsening of pain compared with the preoperative condition; the patient is unable to work

*Note.** Patient-reported assessment of treatment outcomes.

Table 2. Prolo functional–economic outcome scale [11]

1. Economic scale (E)	
Score	**Description**
1	The patient is unable to work and is completely disabled
2	Work capacity is partially preserved; the patient performs light or part-time work
3	The patient is able to work with limitations (change of profession or working conditions)
4	The patient works in the previous occupation with minor limitations
5	Full work capacity; return to previous professional activity
2. Functional scale (F)	
Score	**Description**
1	Severe pain; constant need for analgesics
2	Moderate pain; significant limitation of daily activities
3	Intermittent pain; partial limitation of activity
4	Mild pain; preservation of everyday activity
5	No pain; normal physical activity without limitations
Interpretation of the total score (E + F)	
Total score	**Outcome assessment**
9–10	Excellent
7–8	Good
5–6	Fair
<5	Poor

Note. * Designed for comprehensive assessment of the patient's functional and economic status after surgical treatment of lumbar spine pathology. The scale consists of two subscales: economic (E) and functional (F). Each subscale is scored from 1 to 5 points, with a maximum total score of 10 points.

Table 3. Patient distribution by age groups

Age groups, years	Number of patients	
	Abs.	%
19–30	25	12,5
31–40	51	25,5
41–50	53	26,5
51–60	49	24,5
61–70	22	11,0
Total	200	100,0

Table 4. Interpretation of ODI scores [12]

Level of disability	ODI%	Interpretation
Minimal disability	0–20	Patient is able to perform most activities of daily living
Moderate disability	21–40	Reduced activity level, predominantly due to pain
Severe disability	41–60	Significant limitation of work capacity
Crippling disability	61–80	Substantial functional limitations
Bed-bound state/ complete immobility	81–100	The patient is unable to work

[8] was used. This version comprises 10 items, each scored from 0 to 5 points. Initial scoring was performed in accordance with the questionnaire structure, after which the results were converted into percentages. This approach corresponds to the widely accepted method for interpreting ODI scores and enables standardized comparison with data reported in the literature.

The total ODI score (0–50) was converted into a percentage disability score using the following formula: ODI% = (Obtained score: 50) ×100.

Statistical analysis

Statistical data processing was performed using the Statistica 6.0 software package. Differences between the groups for all primary indicators (VAS, ODI, ΔVAS, ΔODI) were assessed using Welch's t-test, a statistical method for comparing the means of two independent samples that does not assume equality of variances. This test represents a more robust adaptation of Student's t-test, particularly when variances between samples differ substantially or when sample sizes are small.

Changes over time in quantitative dependent variables within each group were evaluated using the nonparametric Wilcoxon signed-rank test. Differences were considered statistically significant at $p < 0.05$.

Results

According to the assessment of pain intensity using the VAS, the mean pain level in the MD group decreased by 5.3 points (corresponding to approximately 63.1% reduction), whereas in the MD + Cage group the decrease amounted to 7.1 points (82.6%). Thus, patients who underwent MD + Cage demonstrated a more pronounced postoperative reduction in pain, as well as a lower recurrence rate of intervertebral disc herniation (***Table 5***).

Prior to surgical treatment, the mean ODI values were high in both groups, indicating substantial functional limitation among patients (***Table 6***). At 12 months, a significant decrease in ODI was observed in both groups, with more pronounced improvement in the MD + Cage group.

The relative improvement in functional status was 61% in the MD group and 81% in the MD + Cage group, suggesting greater effectiveness of the combined surgical approach using cages in reducing disability as measured by the ODI.

A comparison of functional treatment outcomes according to the Macnab scale was performed (***Table 7***). The obtained data indicate better functional outcomes in the MD + Cage group, reflected by a higher proportion of excellent results and a lower proportion of fair and poor outcomes.

Evaluation using the Prolo functional–economic outcome scale was conducted across four categories depending on the degree of return to work, presence of pain syndrome, and functional limitations (***Table 8***). The results demonstrate more favorable functional and economic outcomes in the MD + Cage group, characterized by a higher proportion of excellent results and a lower proportion of fair and poor outcomes.

The application of the Wilcoxon signed-rank test demonstrated statistically significant improvement in both pain syndrome (VAS) and functional status (ODI) in both groups ($p < 0.001$). The magnitude of the effect was high ($r = 0.79–0.88$), indicating clinically significant postoperative improvement, with a more pronounced effect observed in the MD + Cage group (***Table 9***).

Table 5. Dynamics of pain syndrome and recurrence rate

Group	Mean VAS score (points)		Reduction, %	Recurrence rate, %
	before treatment	at 12 months		
MD	8,4	3,1	63,1	9 (9 out of 100)
MD + Cage	8,6	1,5	82,6	3 (3 out of 100)

Table 6. Dynamics of ODI, %

Indicator	MD (n=100)	MD+Cage (n=100)	Improvement
ODI before surgery	62	64	—
ODI at 12 months	24	12	—
Δ (reduction)	38	52	61/81

Table 7. Functional outcomes according to the Macnab scale, %

Outcome category	MD (n=100)	MD+Cage (n=100)
Excellent	46	63
Good	32	28
Fair	14	7
Poor	8	2
Total	100	100

Table 8. Assessment according to the Prolo functional–economic outcome scale

Outcome category	Description	MD (n=100)	MD+Cage (n=100)
Excellent (9–10 points)	Complete return to work, absence of pain	42 %	61 %
Good (7–8 points)	Mild pain, preservation of most functions, return to work achieved	35 %	30 %
Fair (5–6 points)	Moderate residual symptoms, partial work limitation	15 %	7 %
Poor (≤4 points)	Persistent disability, loss of working capacity	8 %	2 %
Total	—	100 %	100 %

Table 9. Results of the Wilcoxon signed-rank test

Group	Indicator	n	W (Statistics)	p-value	Effect size (r)	Interpretation
MD	VAS (before–after)	100	0	<0,001*	0,82	Significant reduction in pain
	ODI (before–after)	100	120	<0,001*	0,79	Improvement in functional status
MD+Cage	VAS(before–after)	100	0	<0,001*	0,88	Marked reduction in pain
	ODI (before–after)	100	45	<0,001*	0,84	Substantial functional improvement

Discussion

The obtained results confirm that both surgical methods—conventional microdiscectomy and microdiscectomy with cage-assisted interbody fusion—provide significant reduction of pain syndrome and improvement in functional status in patients with lumbosacral intervertebral disc herniation.

Postoperative reduction in VAS scores in the MD group averaged −63% (from 8.4 to 3.1 points), whereas in the MD + Cage group it reached −82% (from 8.6 to 1.5 points). The ODI decreased from 62% to 24% and from 64% to 12%, respectively, indicating more pronounced functional recovery with the use of cages.

Analysis according to the Macnab and Prolo scales demonstrated the superiority of microdiscectomy with cage-assisted interbody fusion:

- 91% of patients achieved "Excellent" or "Good" outcomes on the Macnab scale compared with 78% after conventional microdiscectomy;

- According to the Prolo scale, favorable outcomes were observed in 91% of patients in the MD + Cage group and in 77% in the MD group.

The recurrence rate in the MD group was 9%, whereas in the MD + Cage group it was only 3%, indicating improved segmental stability following interbody fixation.

A statistically significant difference ($p < 0.001$) between the groups was established using Welch's t-test for all primary indicators (VAS, ODI, ΔVAS, ΔODI).

Within-group analysis using the Wilcoxon signed-rank test (pre–post comparison) confirmed the high effectiveness of both methods ($p < 0.001$), with a larger effect size ($r = 0.84–0.88$) observed in patients who underwent microdiscectomy with cage-assisted interbody fusion.

The study groups were not entirely homogeneous in terms of clinical and radiological characteristics. Given the heterogeneity of disc pathology, achieving complete homogeneity between the study and comparison groups is practically impossible. In the microdiscectomy with interbody fusion group, signs of segmental instability and Modic type II changes were more frequently observed, which determined the indications for stabilization surgical techniques. To minimize the impact of this heterogeneity on the study results, a multivariate statistical analysis was performed, along with within-group dynamic comparisons (pre–post), ensuring an appropriate evaluation of the effectiveness of each investigated treatment method despite the lack of complete group homogeneity.

Based on the obtained results, the indications for microdiscectomy may include:

- the presence of clinical symptoms of nerve root compression (lumbosciatic pain syndrome, positive tension signs);

- the presence of L4–L5 or L5–S1 intervertebral disc herniation confirmed by MRI;

- absence of pronounced degeneration of adjacent structures (Modic type 0–I changes, without significant loss of disc height);

- ineffectiveness of conservative treatment for 6–8 weeks;

- stability of the motion segment on functional radiographs (displacement <3 mm, angular deformation <10°).

Thus, microdiscectomy is indicated for patients with predominantly isolated disc herniation without structural instability, whereas microdiscectomy with interbody cage fusion is indicated for patients with discogenic lesions accompanied by structural or biomechanical instability of the segment, when nerve root decompression alone is insufficient to stabilize the spine and prevent recurrence. These include the following conditions:

- disc herniation combined with radiological signs of segmental instability (vertebral body displacement >3 mm or pathological mobility >10° on functional testing);

- Modic type II changes on MRI (signs of endoplastic degeneration, cystic remodeling, or fibrosis);

- recurrent disc herniation after previous discectomy;

- significant loss of disc height (>50%) or post-discectomy segmental deformity;

- clinical manifestations of mechanical pain relieved in an unloading position (a sign of motion segment instability).

Our findings are consistent with the literature and confirm the effectiveness and safety of interbody cage application in lumbosacral disc herniation.

According to F. Lei *et al*. (2023) [9], the use of stabilization procedures for recurrent intervertebral disc herniation in carefully selected patients is associated with a lower recurrence rate compared with repeat discectomy.

Similar conclusions regarding the acceptable safety profile of interbody cages, provided appropriate patient selection and adherence to surgical technique, were reported by R.J. Mobbs *et al*. (2015) [10].

Therefore, the use of an interbody cage may be considered a safe and effective component of surgical treatment in selected clinical situations, which is consistent with the results of our study. In cases where MRI and dynamic radiographs demonstrate segmental instability or Modic type II changes, microdiscectomy with cage-assisted interbody fusion appears justified as a more stabilizing technique that provides a more durable functional outcome.

Conclusions

1. Both surgical techniques—microdiscectomy and microdiscectomy with cage-assisted interbody fusion—provide statistically significant improvement in pain and functional status in patients with lumbosacral disc herniation.

2. The recurrence rate after microdiscectomy with cage-assisted interbody fusion is significantly lower (3%) compared with microdiscectomy alone (9%).

3. The microdiscectomy with cage-assisted interbody fusion group demonstrated a more pronounced reduction in pain (−82%) and a greater decrease in ODI (−81%), indicating higher effectiveness of the stabilization technique.

4. According to the Macnab and Prolo scales, excellent and good outcomes were observed more frequently in the microdiscectomy with cage-assisted interbody fusion group (91% vs 78% and 91% vs 77%, respectively).

5. The Wilcoxon signed-rank test confirmed a high level of within-group improvement ($p < 0.001$), while the t-test demonstrated a statistically significant difference between the groups.

6. Microdiscectomy with cage-assisted interbody fusion may be considered for carefully selected patients with signs of segmental instability as an approach combining decompression and stabilization, characterized by superior long-term clinical outcomes.

Disclosure

Conflict of interest

The authors declare no conflict of interest.

Informed consent

Informed consent was obtained from each patient.

Ethical standards

All procedures performed in studies involving human participants were conducted in accordance with the ethical standards of the institutional and national research committee and with the 1964 Declaration of Helsinki and its subsequent amendments or comparable ethical standards.

Funding

The study received no external funding.

References

1. Weinstein JN, Tosteson TD, Lurie JD, Tosteson AN, Hanscom B, Skinner JS, Abdu WA, Hilibrand AS, Boden SD, Deyo RA. Surgical vs nonoperative treatment for lumbar disk herniation: the Spine Patient Outcomes Research Trial (SPORT): a randomized trial. JAMA. 2006 Nov 22;296(20):2441-50. doi: 10.1001/jama.296.20.2441
2. Deyo RA, Mirza SK. CLINICAL PRACTICE. Herniated Lumbar Intervertebral Disk. N Engl J Med. 2016 May 5;374(18):1763-72. doi: 10.1056/NEJMcp1512658
3. Peul WC, van Houwelingen HC, van den Hout WB, Brand R, Eekhof JA, Tans JT, Thomeer RT, Koes BW; Leiden-The Hague Spine Intervention Prognostic Study Group. Surgery versus prolonged conservative treatment for sciatica. N Engl J Med. 2007 May 31;356(22):2245-56. doi: 10.1056/NEJMoa064039
4. Hoang R, Song J, Tiao J, Ngan A, Hoang T, J Corvi J, K Namiri N, Chaudhary S, K Cho S, C Hecht A, Essig D, Virk S, D Katz A. Patient Factors Associated with Recurrent Herniation and Revision Surgery following Lumbar Microdiscectomy. Spine Surg Relat Res. 2024 Oct 5;9(2):244-250. doi: 10.22603/ssrr.2024-0148
5. Caspar W, Campbell B, Barbier DD, Kretschmmer R, Gotfried Y. The Caspar microsurgical discectomy and comparison with a conventional standard lumbar disc procedure. Neurosurgery. 1991 Jan;28(1):78-86; discussion 86-7. doi: 10.1097/00006123-199101000-00013
6. Ebeling U, Kalbarcyk H, Reulen HJ. Microsurgical reoperation following lumbar disc surgery. Timing, surgical findings, and outcome in 92 patients. J Neurosurg. 1989 Mar;70(3):397-404. doi: 10.3171/jns.1989.70.3.0397
7. McGirt MJ, Ambrossi GL, Datoo G, Sciubba DM, Witham TF, Wolinsky JP, Gokaslan ZL, Bydon A. Recurrent disc herniation and long-term back pain after primary lumbar discectomy: review of outcomes reported for limited versus aggressive disc removal. Neurosurgery. 2009 Feb;64(2):338-44; discussion 344-5. doi: 10.1227/01.NEU.0000337574.58662.E2
8. Fairbank JC, Pynsent PB. The Oswestry Disability Index. Spine (Phila Pa 1976). 2000 Nov 15;25(22):2940-52; discussion 2952. doi: 10.1097/00007632-200011150-00017
9. Lei F, Yanfang L, Shangxing W, Weihao Y, Wei L, Jing T. Spinal Fusion Versus Repeat Discectomy for Recurrent Lumbar Disc Herniation: A Systematic Review and Meta-Analysis. World Neurosurg. 2023 May;173:126-135.e5. doi: 10.1016/j.wneu.2022.12.091
10. Mobbs RJ, Phan K, Malham G, Seex K, Rao PJ. Lumbar interbody fusion: techniques, indications and comparison of interbody fusion options including PLIF, TLIF, MI-TLIF, OLIF/ATP, LLIF and ALIF. J Spine Surg. 2015 Dec;1(1):2-18. doi: 10.3978/j.issn.2414-469X.2015.10.05
11. Prolo DJ, Oklund SA, Butcher M. Toward uniformity in evaluating results of lumbar spine operations. A paradigm applied to posterior lumbar interbody fusions. Spine (Phila Pa 1976). 1986 Jul-Aug;11(6):601-6. doi: 10.1097/00007632-198607000-00012
12. Fairbank JC, Pynsent PB. The Oswestry Disability Index. Spine (Phila Pa 1976). 2000 Nov 15;25(22):2940-52; discussion 2952. doi: 10.1097/00007632-200011150-00017
13. Ahn Y, Lee U, Kim WK, Keum HJ. Five-year outcomes and predictive factors of transforaminal full-endoscopic lumbar discectomy. Medicine (Baltimore). 2018 Nov;97(48):e13454. doi: 10.1097/MD.0000000000013454

Original article

Ukrainian Neurosurgical Journal. 2026;32(1):113-125
doi: 10.25305/unj.344539

The quality of life of patients with vestibular schwannoma assessed using cross-cultural adapted and validated PANQOL and Mayo VSQOL questionnaires in comparison

Mykola V. Yehorov [1], Vasyl V. Shust [1], Oleg M. Borysenko [2], Volodymyr O. Fedirko [1]

[1] Subtentorial Neurooncology Department, Romodanov Neurosurgery Institute, Kyiv, Ukraine
[2] Department of Ear Microsurgery and Otoneurosurgery, O.S. Kolomyichenko Institute of Otolaryngology of National Academy of Medical Science of Ukraine, Kyiv, Ukraine

Received: 24 November 2025
Accepted: 22 December 2025

Address for correspondence: *Mykola V. Yehorov, Subtentorial Neurooncology Department, Romodanov Neurosurgery Institute, 32 Platona Maiborody st., Kyiv, 04050, Ukraine, e-mail: neiron25@ukr.net*

Introduction: Vestibular schwannoma (VS) adversely affects patients' functional status and quality of life (QoL). Disease-specific questionnaires, such as PANQOL and Mayo VSQOL, provide a more sensitive assessment of disease progression and treatment outcomes compared with general instruments. Modern microsurgical techniques aim to preserve facial and cochlear nerve function, which directly influences postoperative QoL.

Objective: To evaluate the QoL of patients with VS using the Ukrainian versions of PANQOL and Mayo VSQOL questionnaires and to validate them according to COSMIN standards.

Materials and methods: The prospective study included 190 patients with VS, divided into three groups: Group I (n=64) — traditional microsurgery (2001–2016); Group II (n=57) — modern microsurgical techniques (2017–2024); Group III (n=69) — observation ("wait-and-scan"). QoL was assessed using PANQOL, Mayo VSQOL, SF-36, QLQ-C30, and BN20 questionnaires. Correlation analysis was performed; statistical significance was set at $p<0.05$.

Results: Mayo VSQOL scores were significantly higher in Group II compared with Group I in the domains of balance (+33.3%), tinnitus/pain (+36.4%), emotional well-being (+43.1%), memory (+58.4%), and total score (+32.2%). Comparison with Group III also confirmed the advantage of surgical treatment, particularly in emotional well-being and memory (+44.3%). PANQOL demonstrated the greatest improvement in the "Face" domain (+35.6%), while changes in other domains were not statistically significant. Significant correlations were found between PANQOL and Mayo VSQOL results with SF-36, QLQ-C30, and BN20, confirming their validity. Internal consistency was high (PANQOL α=0.75–0.93 preoperatively; α=0.81–0.90 postoperatively; Mayo α=0.763–0.938 preoperatively; α=0.858–0.937 postoperatively). Test–retest reliability (ICC) ranged from 0.60–0.91 for PANQOL and 0.778–0.953 for Mayo. Mayo VSQOL demonstrated higher responsiveness to clinical changes (Cohen's d=2.11; SRM=1.74) compared with PANQOL (Cohen's d=0.87; SRM=0.75).

Conclusions: PANQOL and Mayo VSQOL are reliable instruments for assessing QoL in patients with VS. Mayo VSQOL demonstrated higher sensitivity, while PANQOL showed stable correlation with general QoL scales. The use of modern microsurgical techniques substantially improves postoperative QoL in VS patients.

Keywords: *vestibular schwannoma; quality of life; PANQOL; Mayo VSQOL; treatment outcomes*

Background

Over the past three decades, the diagnosis and treatment of sporadic vestibular schwannomas (VS) have changed significantly. Widespread magnetic resonance imaging (MRI) availability has increased the detection of incidental tumors, while radiosurgery and the "wait-and-scan" strategy have been increasingly used for small, clinically inactive lesions. These changes shifted the focus from purely morphological and neurosurgical endpoints (resection completeness, survival) to broader concepts of "treatment success," including functional outcomes and patient-reported QoL [1–6].

In VS clinical studies general questionnaires such as SF-36, EORTC QLQ-C30 have long been used. They effectively assess general health but poorly capture VS-specific problems such as hearing loss, tinnitus, balance disorders, anxiety, or social/occupational impacts [5, 7-10]. Over the last 15 years, there has been growing interest in validating disease-specific scales: PANQOL (Penn Acoustic Neuroma QoL) and the newer Mayo VSQOL Index. These scales correlate better with clinical symptoms and provide sensitive criteria for comparing treatment strategies [1–3, 7–11].

PANQOL was developed and validated specifically for patients with acoustic/vestibular schwannomas. It

has good psychometric properties including internal consistency, test-retest reliability and demonstrated correlation with clinical indicators. Translations into Italian, Spanish, Hindi, and other languages have confirmed its stability across cultures, making it suitable for multicenter and long-term cohort studies [3, 9, 12-16].

Mayo VSQOL is a newer 40-item tool designed for a comprehensive assessment of VS impact and treatment on QoL, including employment, treatment satisfaction, and side effects. Initial validation showed excellent psychometric properties and the ability to detect differences between treatment groups. However, further independent validation and comparative studies with PANQOL and general instruments are needed [2, 4, 7].

Recent studies comparing PANQOL and Mayo VSQOL, as well as their correlation with general scales (QLQ-C30/BN20, SF-36), show that disease-specific instruments are more sensitive to VS-related symptoms including hearing, balance, face and emotional state. General scales correlate with overall QoL but may "smooth out" differences between treatment strategies. Using both disease-specific and general tools provides the most complete assessment of the overall and symptom-specific impact of VS and its treatment [1, 2, 4, 5, 7–11, 17].

Prospective studies using PANQOL have tracked QoL dynamics in patients undergoing different strategies including observation, radiosurgery, microsurgery. Differences in disease-specific QoL between strategies are often minimal in the long term, while early postoperative periods show more pronounced differences [4, 18-22]. Modern microsurgery with intraoperative neuromonitoring and nerve-sparing techniques can achieve favorable long-term functional outcomes and improve certain QoL domains. However, results must be interpreted in the context of patient age, tumor size, preoperative hearing status, comorbidities, and individual expectations [5, 17, 23].

Ukrainian data show later diagnosis with a predominance of large tumors (Koos grades III–IV), affecting treatment choice and functional outcomes [1]. Ukrainian versions of PANQOL and Mayo VSQOL questionnaires have undergone cross-cultural adaptation, pilot testing, with most items demonstrating good comprehensibility (<1% required clarification) [1]. However, multi-center registries and long-term follow-up (>5 years) are necessary to evaluate outcomes and treatment impact on QoL patients with VS in Ukraine [1, 2, 5, 17].

Despite the use of PANQOL and Mayo VSQOL, several questions remain open: standardized translation and cross-cultural adaptation and validation, optimal combination of specific and general instruments in routine practice, determination of clinically meaningful minimal changes for each questionnaire, commonly agreed and accepted criteria of VS surgical removal radicality as well as the impact of socioeconomic and professional factors on subjective quality of life. Therefore, large-scale prospective studies are needed to determine which strategies provide better long-term quality of life in different patient subgroups. In this context, the cross-cultural adaptation, validation and comparative use of PANQOL and Mayo VSQOL are particularly important for developing optimal treatment strategies and enhancing patient-centered care in Ukraine and wherever [2, 4, 10, 15, 17].

The cross-cultural adaptation and validation PANQOL and Mayo VSQOL in Ukraine and comparing them with QLQ-C30/BN20 and SF-36 is not only a methodological need but also clinically relevant: only localized, sensitive instruments allow treatment strategies to be adjusted according to patient priorities such as hearing preservation, facial nerve function, balance, return to work, etc.) and justify choices between early microsurgery, observation, or primary radiosurgery within a specific social-medical context [1, 2, 5, 17, 18, 23]. The present study combines cross-cultural adaptation and validation with analysis of clinical outcomes using contemporary microsurgical techniques and aims to provide evidence to optimize local treatment protocols and improve QoL for patients with VS in Ukraine [1].

Materials and methods

Study participants

A total of 373 patients with VS were under dynamic observation at the Kolomyichenko Institute of Otolaryngology, National Academy of Medical Sciences of Ukraine. The present study was conducted at the Subtentorial Neuro-oncology Department of the Romodanov Neurosurgery Institute and included patients treated or followed between 2001 and 2024.

Quality-of-life (QoL) assessment was completed in 190 patients. Patients were evaluated during inpatient treatment, outpatient follow-up visits, telephone interviews, as well as postal or electronic surveys. Postoperative QoL assessment was performed no earlier than 6 months after surgery.

Inclusion criteria

Patients were eligible for inclusion if they met all of the following criteria:

- unilateral sporadic vestibular schwannoma;
- preoperative MRI or contrast-enhanced CT confirming the diagnosis;
- histopathological verification (for surgically treated patients);
- age ≥ 18 years;
- written informed consent;
- completed PANQOL and/or Mayo VSQOL questionnaires.

Exclusion criteria

Patients were excluded from the study if they had:

- neurofibromatosis type II;
- absence of imaging or histopathological confirmation of vestibular schwannoma;
- incomplete questionnaire data;
- Bell's palsy during follow-up;
- age < 18 years.

Group characteristics

Based on treatment strategy and time period, patients were divided into three groups:

Group I – 64 patients who underwent microsurgical removal of VS using conventional microsurgical techniques between 2001 and 2016;

Group II – 57 patients treated with updated contemporary microsurgical techniques between 2017 and 2024;

Group III – 69 patients managed using a "wait-and-scan" observation strategy without surgical intervention.

The mean follow-up duration was 159.44 months (median 136 months) in Group I and 49.52 months (median 60 months) in Group II.

The follow-up period in Group III ranged from 6 months to 18 years.

Response rates were as follows: Group I – PANQOL (61 patients), Mayo VSQOL (64 patients), BN20/QLQ-C30/SF-36 (64 patients); Group II – PANQOL (57 patients), Mayo VSQOL (56 patients), BN20/QLQ-C30/SF-36 (57 patients); Group III – PANQOL and Mayo VSQOL (69 patients), BN20/QLQ-C30/SF-36 (44 patients).

Comparative analysis of the domains "Hearing," "Balance," "Pain," and "Face" between PANQOL and Mayo VSQOL was performed across the three groups, along with analyses of BN20, QLQ-C30, and SF-36 scores between Groups I–II and II–III. Comparative analysis between Groups I and III was not performed because outdated surgical techniques were associated with different indications for surgery, levels of functional risk, and standards for outcome assessment.

Study design

This study employed a retrospective comparative cohort design and was aimed at assessing quality of life in patients with VS using both disease-specific and generic QoL instruments.

The study combined cross-cultural adaptation and validation of the Ukrainian versions of the PANQOL and Mayo VSQOL questionnaires with a comparative analysis of QoL outcomes according to the selected treatment strategy: conventional microsurgery, contemporary microsurgical techniques, or active surveillance using a "wait-and-scan" approach.

In addition, patients completed the EORTC QLQ-C30, EORTC QLQ-BN20, and SF-36 questionnaires. Comparative analyses were performed between Groups I and II and between Groups II and III, with evaluation of specific functional domains (hearing, balance, pain, facial nerve function) as well as overall composite QoL scores.

Cross-cultural adaptation and validation of the PANQOL and Mayo VSQOL [1] questionnaires were conducted in accordance with international recommendations and COSMIN guidelines [24, 25]. Official permission for the translation and use of the Mayo VSQOL questionnaire in Ukraine was obtained from the developers of the original instrument.

Statistical analysis

Statistical analysis was performed using the Deducer package (Java GUI for R, GNU license) [26]. Continuous variables were analyzed using descriptive statistics. Differences were considered statistically significant at $p < 0.05$.

Internal consistency of questionnaire domains was assessed using Cronbach's α. Test–retest reliability was evaluated using the intraclass correlation coefficient (ICC) based on paired observations with an interval of 2–14 days. Responsiveness to clinically meaningful changes was assessed using Effect Size (Cohen's d) and Standardized Response Mean (SRM).

Postoperative hearing outcomes were classified according to the Gardner–Robertson hearing scale [27]. Facial nerve function was evaluated using the House–Brackmann grading system. Correlation and regression analyses were applied to assess the relationships between disease-specific and general QoL instruments.

Results

Adaptation and validation of questionnaires

A standardized multi-step cross-cultural adaptation and validation of the PANQOL and Mayo VSQOL questionnaires was conducted in accordance with international guidelines [24, 25, 28]. Three neurosurgeons independently translated the scale into Ukrainian. A professional Ukrainian philologist from Taras Shevchenko National University of Kyiv compiled three texts into one. The back translation was performed by two native English speakers residing in Canada and the United Kingdom. The reconciled version was subsequently reviewed by a linguist and a methodology expert from Taras Shevchenko National University of Kyiv. Pilot testing in 30 patients confirmed high comprehensibility, with less than 1% of items requiring clarification. The back-translated version demonstrated 96% semantic equivalence with the originals, meeting the recommended validation criteria [28]. The final Ukrainian version of the Mayo VSQOL questionnaire was approved by the original developers, Carlson ML and Lohse CM, and accepted as the official localized version [1].

To assess QoL in Ukrainian patients with VS and validate the PANQOL and Mayo VSQOL scales, a study was conducted using PANQOL, Mayo VSQOL Index, BN20, QLQ-C30, and SF-36 questionnaires (***Tables 1-7***). The observation period spanned 2001–2024 and included patients treated at the Subtentorial Neuro-oncology Department, as well as outpatients followed in the Ear Microsurgery and Oto-neurosurgery Department of the Kolomyichenko Institute of Otolaryngology after diagnosis verification. Patients with tumor progression (increase in VS size to T3 according to Hannover classification or higher on follow-up imaging) were referred for surgical treatment at the Neurosurgery Institute.

A total of 1,183 statistical cards and 829 medical records from the Institutes archive was reviewed. For the survey, 244 patients were possible to reach, and fully completed questionnaires were received from 190 individuals. Comparative analysis of QoL measures using validated scales (PANQOL, Mayo VSQOL, BN20, QLQ-C30, SF-36) revealed significant differences between the three study groups (see ***Tables 1–7***).

A total of 373 patients were under dynamic observation at the Kolomyichenko Otolaryngology Institute of the National Academy of Medical Sciences of Ukraine, of whom 110 (29.5%) subsequently underwent surgical removal of VS due to symptom progression or a progressive disease course, and 24 (6.4%) received radiotherapy (RT). QoL data were obtained for 10 patients who remained under "wait-and-scan" management. Patients who underwent surgery following "wait-and-scan," either in our department or at the Kolomyichenko Institute, were evaluated according to the department where the surgery was performed.

Comparative analysis of Groups I and II

According to the PANQOL scale, patients in Group II showed improvement across all domains compared to Group I, except for the "Anxiety" domain. The most pronounced positive changes were observed in the following domains: Pain, which increased from 42.2 to 50.4 (+19.5%, mean comparison criterion 0.905); Facial function, from 45.1 to 61.1 (+35.6%, 1.968); Overall health, from 45.7 to 52.9 (+15.7%, 1.222); and the Total

Table 1. Correlation between Groups I, II, and III according to the PANQOL and Mayo VSQOL scales with the BN20 and QLQ-C30 scales, as well as correlation between QLQ-C30 and BN20

Correlation of Group I on the PANQOL and Mayo scales with the BN20 and QLQ-C30 scales, and correlation between QLQ-C30 and BN20			
	Parameter	**Parameter**	**Correlation coefficient**
1	PANQOL total score	QLQ C30	0,635
2	PANQOL total score	BN20	0,635
3	Mayo total score	QLQ C30	-0,126
4	Mayo total score	BN20	-0,133
5	QLQ C30	BN20	0,816
Correlation of Group II scores on the PANQOL and Mayo scales with the BN20 and QLQ-C30 scales			
1	PANQOL total score	QLQ C30	0,596
2	PANQOL total score	BN20	0,629
3	Mayo total score	QLQ C30	0,586
4	Mayo total score	BN20	0,501
Correlation of Group III scores on the PANQOL and Mayo scales with the BN20 and QLQ-C30 scales			
1	PANQOL total score	QLQ C30	0,663
2	PANQOL total score	BN20	0,743
3	Mayo total score	QLQ C30	0,155
4	Mayo total score	BN20	0,093

Table 2. Comparison of Groups I and II based on the PANQOL scale

№	**Parameter**	**Divergence Coefficient**	**Mean Value Group I**	**Mean Value Group II**	**Increase of Group II over I, % of Mean**	**Mean Comparison Criterion**	**Direction of Shift in Group II vs I**
1	Hearing	0,118	46	49,7	8%	0,582	+
2	Balance	0,089	48,4	50,3	4%	0,259	+
3	Anxiety	0,145	63,2	62,6	-1%	-0,085	-
4	Energy	0,161	48,4	49,6	2,3%	0,165	+
5	Pain	0,197	42,2	50,4	19,5%	0,905	+
6	Face	0,292	45,1	61,1	35,6%	1,968	+
7	Overall Health	0,146	45,7	52,9	15,7%	1,222	+
8	Total Score	0,174	48,4	53,8	11,1%	0,964	+

Table 3. Comparison of Groups I and II based on the Mayo VSQOL

№	**Parameter**	**Divergence Coefficient**	**Mean Value Group I**	**Mean Value Group II**	**Increase of Group II over I, % of Mean**	**Mean Comparison Criterion**	**Direction of Shift in Group II vs I**
1	Domain I (Hearing problems)	0,19	49	57,1	16,5%	1,09	+
2	Domain II (Dizziness and balance disorders)	0,35	46,7	62,3	33,3%	1,872	+
3	Domain III (Pain, discomfort, and ear noise)	0,397	46,7	65,8	36,4%	2,191	+
4	Domain IV (Face or eye problems)	0,128	50,3	55	9,4%	0,668	+
5	Domain V (Impact on physical, emotional, and social well-being)	0,35	47,8	68,4	43,1%	2,532	+
6	Domain VI (Cognitive and memory difficulties)	0,432	43,3	68,5	58,4%	2,858	+
7	Domain VII (Satisfaction or regret)	0,19	47,9	49	2,2%	0,126	+
8	Domains I–VI (average)	0,652	47,3	62,5	32,2%	2,243	+

Table 4. Comparison of Group I and II according to the QLQ-C30, BN20 and SF-36

№	Parameter	Divergence Coefficient	Mean Value Group I	Mean Value Group II	Increase of Group II over I, % of Mean	Mean Comparison Criterion	Direction of Shift in Group II vs I
1	QLQ C30	0,19	65,5	72	9,9%	1,252	+
2	BN20	0,208	67	72,5	8,1%	1,027	+
3	Overall Physical Health Score (SF-36)	0,353	31	34,2	10,3%	0,958	+
4	Overall Mental Health Score (SF-36)	0,261	47,6	49,7	4,4%	0,435	+
5	SF-36 Total score	0,359	39,3	41,9	6,7%	0,706	+

Table 5. Distribution comparison characteristics of Group II and III based on the PANQOL scale

№	Parameter	Divergence Coefficient	Mean Value Group III	Mean Value Group II	Increase of Group II over III, % of Mean	Mean Comparison Criterion	Direction of Shift in Group II vs III
1	Hearing	0,224	42,3	49,7	17,4	1,19	+
2	Balance	0,186	48,9	50,3	2,9	0,182	+
3	Anxiety	0,17	56,3	62,6	11,1	0,883	+
4	Energy	0,141	46,9	49,6	5,8	0,388	+
5	Pain	0,114	43,1	50,4	17	0,855	+
6	Face	0,143	66,8	61,1	-8,5	-0,733	-
7	Overall Health	0,158	52,3	52,9	0,6	0,051	+
8	Total Score	0,824	51	53,8	5,6	0,511	+

Table 6. Distribution comparison characteristics of Group II and III based on the MAYO VSQOL scale

№	Parameter	Divergence Coefficient	Mean Value Group III	Mean Value Group II	Increase of Group II over III, % of Mean	Mean Comparison Criterion	Direction of Shift in Group II vs III
1	Domain I (Hearing problems)	0,203	48,2	57,1	18,6	1,06	+
2	Domain II (Dizziness and balance disorders)	0,276	47,3	62,3	31,5	1,699	+
3	Domain III (Pain, discomfort, and ear noise)	0,231	46,8	63,8	36,2	2,174	+
4	Domain IV (Face or eye problems)	0,175	47,7	55	15,3	0,95	+
5	Domain V (Impact on physical, emotional, and social well-being)	0,328	46	68,4	48,7	2,743	+
6	Domain VI (Cognitive and memory difficulties)	0,32	46,5	68,5	47,5	2,453	+
7	Domain VII (Satisfaction or regret)	0,157	43,6	49	12,5	0,608	+
8	Domains I–VI (average)	0,317	47,2	62,5	32,5	2,142	+

Table 7. Comparison of Group II and III according to the QLQ-C30, BN20 and SF-36

№	Parameter	Divergence Coefficient	Mean Value Group III	Mean Value Group II	Increase of Group II over III, % of Mean	Mean Comparison Criterion	Direction of Shift in Group II vs III
1	QLQ C30	0,187	67,5	72	6,7	0,901	+
2	BN20	0,126	67,5	72,5	7,4	0,916	+
3	Overall Physical Health Score (SF-36)	0,263	30,8	34,2	10,9	1,123	+
4	Overall Mental Health Score (SF-36)	0,172	43,8	49,7	13,4	1,495	+
5	SF-36 Total score	0,19	37,3	41,9	12,3	1,517	+

score, from 48.4 to 53.8 (+11.1%, 0.964). In contrast, the "Anxiety" domain showed a minimal decrease (–1%). Statistically significant improvements ($p<0.05$) were noted specifically in the domains of Pain, Facial function, Overall health, and the Total score (see ***Table 2***).

Assessment using the Mayo VSQOL scale also demonstrated systematic improvement in Group II compared to Group I across all domains. The most notable and statistically significant changes were observed in: Domain I ("Hearing problems"), from 49 to 57.1 (+16.5%, mean comparison criterion 1.09); Domain II ("Dizziness and balance disturbances"), from 46.7 to 62.3 (+33.3%, –1.872); Domain III ("Pain, discomfort, and tinnitus"), from 46.7 to 65.8 (+36.4%, 2.191); Domain V ("Impact on physical, emotional, and social well-being"), from 47.8 to 68.4 (+43.1%, 2.532); Domain VI ("Cognitive difficulties and memory"), from 43.3 to 68.5 (+58.4%, 2.858). Additionally, the mean total score on the Mayo scale significantly increased from 47.3 to 62.5 (+32.2%, 2.243). For these measures, the null hypothesis of equal population means was rejected with $p=0.001$, confirming the high statistical significance of the results (see ***Table 3***).

Comparison of BN20, QLQ-C30, and SF-36 scores showed a consistent shift in Group II toward improvement of QoL relative to Group I. The most pronounced differences were observed for BN20 (from 67 to 72.5, +8.1%, mean comparison criterion 1.027) and QLQ-C30 (from 65.5 to 72, +9.9%, 1.252), with statistically significant results ($p<0.05$). Regarding SF-36, improvement in overall physical health in Group II nearly reached statistical significance (mean comparison criterion = 0.958, $p=0.06$), indicating a trend toward a positive effect of the enhanced microsurgical techniques on patients' QoL (see ***Table 4***).

Comparative analysis of Groups II and III

QoL assessment in patients with VS using PANQOL, Mayo VSQOL, BN20, QLQ-C30, and SF-36 instruments demonstrated statistically significant improvement in Group II (operated on from 2017) compared to the observation group (Group III).

According to the PANQOL scale (see Table 5), Group II showed improvement in most domains compared to the observation group. The mean score for the Hearing domain increased from 42.3 to 49.7 (+17.4%), which was statistically significant (mean comparison criterion = 1.19, positive shift). Improvements were also observed in the Balance domain from 48.9 to 50.3 (+2.9%, 0.182), Anxiety from 56.3 to 62.6 (+11.1%, 0.883), Energy from 46.9 to 49.6 (+5.8%, 0.388), Pain from 43.1 to 50.4 (+17%, 0.855), and Overall health from 52.3 to 52.9 (+0.6%, 0.051). The only domain showing a slight decrease was Facial function (from 66.8 to 61.1, –8.5%, –0.733), reflecting the prolonged recovery of facial nerve function, which typically requires more than six months postoperatively. The total PANQOL score increased from 51.0 to 53.8 (+5.6%, 0.511).

Mayo VSQOL analysis (Table 6) also revealed statistically significant improvement in Group II. All domains showed increased mean scores, with significant improvement in six domains: Domain I (Hearing problems) – from 48.2 to 57.1 (+18.6%, mean comparison criterion –1.06); Domain II (Dizziness and balance disturbances) – from 47.3 to 62.3 (+31.5%, 1.699); Domain III (Pain, discomfort, and tinnitus) – from 46.8 to 63.8 (+36.2%, 2.174); Domain V (Impact on physical, emotional, and social well-being) – from 46.0 to 68.4 (+48.7%, 2.743); Domain VI (Cognitive difficulties and memory) – from 46.5 to 68.5 (+47.5%, 2.453); Total Mayo VSQOL score – from 47.2 to 62.5 (+32.5%, 2.142); Domains IV (Facial or eye problems) and VII (Satisfaction or regret) also showed positive trends; however, these changes did not reach statistical significance.

Regarding QLQ-C30, BN20, and SF-36, Group II demonstrated improvement compared to Group III (Table 7). Mean QLQ-C30 scores increased from 67.5 to 72 (+6.7%, mean comparison criterion =0.901), and BN20 scores increased from 67.5 to 72.5 (+7.4%, 0.916). Overall physical health on SF-36 increased from 30.8 to 34.2 (+10.9%, 1.123), mental health from 43.8 to 49.7 (+13.4%, 1.495), and the total SF-36 score from 37.3 to 41.9 (+12.3%, 1.517).

Clinical status evaluation between groups: facial and cochlear nerve function

Facial nerve function was assessed using the House-Brackmann (HB) scale in the early postoperative period, with distribution as follows: Group 1: HB I was observed in 24 patients (5%), II – 30 (6.3%), III – 67 (14.1%),

IV – 102 (21.6%), V – 149 (31.5%), VI – 102 (21.5%); Group 2: HB I was recorded in 132 patients (37.2%), II – 77 (21.7%), III – 95 (26.8%), IV – 37 (10.4%), V – 11 (3.1%), VI – 3 (0.8%) ($p<0.001$, χ^2 test).

Intraoperative identification and preservation of the cochlear nerve were not performed in Group 1. In Group 2, such attempts were made in patients with functional hearing preoperatively. Among 93 identified patients, anatomical preservation of the cochlear nerve was achieved in 49 (52.7%). Postoperative hearing outcomes in these patients were classified according to the Gardner–Robertson (GR) scale as follows: GR-I in 21 patients (42.9%), GR-II – 12 (24.5%), GR-III – 16 (32.6%).

Correlation analysis

Correlation analysis showed a moderate to high positive relationship between total PANQOL and Mayo VSQOL scores and QLQ-C30 and BN20 scores in Group II: PANQOL and QLQ-C30 – r = 0.596, PANQOL and BN20 – r = 0.629, Mayo and QLQ-C30 – r = 0.586, Mayo and BN20 – r = 0.501, confirming consistency of QoL assessment across different scales (see ***Table 1***).

Correlation analysis and multiple correlation coefficient assessment were used to compare the consistency of PANQOL and Mayo VSQOL questionnaires with the validated SF-36 scale across the three groups of patients with VS.

Group I: Correlation between PANQOL and physical health – r = 0.651; mental health – r = 0.532; SF-36 total score – r = 0.611. Mayo VSQOL: physical health – r = 0.188; mental health – r = 0.129; SF-36 total score – r = 0.163. Multiple regression: PANQOL (physical health β = 0.623; mental health β = 0.035), Mayo (physical health β = 0.189).

Group II: Correlation between PANQOL and physical health – r = 0.495; mental health – r = 0.397; SF-36 total score – r = 0.503. Mayo VSQOL: physical health – r = 0.477; mental health – r = 0.451; SF-36 total score – r = 0.532. Multiple regression: PANQOL (physical health β = 0.527), Mayo (physical health β = 0.539).

Group III: Correlation between PANQOL and physical health – r = 0.716; mental health – r = 0.613; SF-36 total score – r = 0.748. Mayo VSQOL: physical health – r = 0.208; mental health – r = –0.182; SF-36 total score – r = –0.007. Multiple regression: PANQOL (physical health β = 0.753), Mayo (physical health β = 0.414).

Overall, PANQOL consistently demonstrated moderate to high concordance with SF-36 across all three groups, confirming its ability to reflect both physical and psycho-emotional status of patients. In contrast, Mayo VSQOL showed weak or minimal correlation with SF-36, particularly in Group III, indicating limited sensitivity of this scale for evaluating overall physical and mental health. Multiple regression confirmed that the main predictor of total PANQOL score is physical health, while the contribution of mental health is minimal. For Mayo, the contribution of physical health in regression was significantly lower, consistent with the observed correlation coefficients.

Comparison of corresponding domains between PANQOL and Mayo VSQOL

Analysis of correlations between corresponding domains of the PANQOL and Mayo VSQOL questionnaires in Group II patients revealed only weak positive correlations: Hearing – r = 0.395, Balance – r = 0.405, Pain – r = 0.440, Face – r = 0.470. In Group III, the strength of correlations was even lower: Hearing – r = 0.262, Balance – r = 0.117, Pain – r = 0.181, Face – r = 0.080. These results indicate that direct comparison of individual domains between the two questionnaires has limited clinical significance, as the content and structure of the respective questions partially differ. It is more appropriate to use each questionnaire as an independent tool for assessing the QoL or to compare their total scores, which demonstrates better concordance between the scales.

Test–retest reliability, internal consistency, and responsiveness

The internal consistency of the Ukrainian versions of PANQOL and Mayo VSQOL questionnaires was evaluated using Cronbach's α for each domain in pre- and postoperative samples. The ICC was interpreted according to commonly accepted categories: Cronbach's α < 0.50 – poor/unacceptable reliability; 0.50–0.59 – weak; 0.60–0.69 – moderate/acceptable; 0.70–0.79 – acceptable/satisfactory; 0.80–0.89 – high; ≥ 0.90 – excellent [29].

The preoperative sample for PANQOL included 154 patients. Cronbach's α values ranged from 0.75 to 0.93 across domains I, II, III, V, and VI, indicating acceptable to excellent internal consistency. Domain IV consisted of a single item and was not analyzed. Domain VII showed low consistency (α = 0.38), typical for two-item scales. The overall Cronbach's α for PANQOL in the preoperative sample was 0.91, confirming high internal consistency for the entire scale. Postoperatively (199 patients), domain-specific α values remained stable (0.75–0.90 for domains I, II, III, V, and VI), while domain VII improved slightly (α = 0.48) but remained below the acceptable threshold due to the limited number of items. The overall Cronbach's α after surgery was 0.92, demonstrating stability and reliability of the scale postoperatively (***Table 8***).

The preoperative sample for Mayo VSQOL included 105 patients, with α values ranging from 0.763 to 0.938, indicating high internal consistency. In the postoperative sample (177 patients), the overall Cronbach's α for all 40 items was 0.953, reflecting excellent internal consistency. Domain-specific α values ranged from 0.858 to 0.937, demonstrating high to very high reliability of the measured constructs after surgery (***Table 9***).

Test–retest reliability of the Ukrainian versions of PANQOL and Mayo VSQOL was evaluated to determine the temporal stability of the scales. All domains of PANQOL and Mayo VSQOL are presented as interval scales; therefore, reliability was assessed using the ICC, in accordance with COSMIN recommendations [24,26]. ICC interpretation followed widely accepted categories: <0.50 – poor; 0.50–0.75 – moderate; 0.75–0.90 – good; >0.90 – excellent reliability. The test–retest interval ranged from 2 to 14 days, in line with guidelines.

For PANQOL analysis, 33 paired observations were included. ICC values across domains ranged from 0.60 to 0.91. The highest stability was observed in Domain VI (ICC = 0.91), indicating excellent reliability. Domains II, III, IV, and V demonstrated good to high reliability (ICC = 0.72–0.84). Domains I and VII showed moderate

reliability (ICC = 0.60–0.65), corresponding to an acceptable level according to COSMIN [25, 26]. Overall, all PANQOL domains had ICC > 0.60, indicating sufficient and clinically acceptable stability of the questionnaire during repeated administration (***Table 10***).

For the Mayo VSQOL test–retest analysis, 31 patients were included. ICC values for all domains ranged from 0.778 to 0.953, corresponding to good or excellent reliability according to conventional criteria. The highest stability was observed in Domains II (ICC = 0.942) and III (ICC = 0.953), indicating exceptional reproducibility during repeated completion. Pearson's correlation coefficients were also high (r = 0.872–0.975), further confirming the reliability of results (***Table 11***).

The responsiveness of the Ukrainian versions of the PANQOL and Mayo VSQOL questionnaires was evaluated to determine their ability to detect clinically meaningful postoperative changes. Responsiveness was assessed using two commonly accepted indicators — Effect Size (Cohen's d) and Standardized Response Mean (SRM), calculated based on paired pre- and postoperative observations. The interpretation followed established thresholds: <0.20 — negligible; 0.20–0.49 — small; 0.50–0.79 — moderate; ≥0.80 — large effect.

A total of 30 paired PANQOL patient observations in Group II were analyzed. All PANQOL domains demonstrated improvement after surgery. Cohen's d ranged from 0.52 to 1.09, indicating moderate to large responsiveness. The highest responsiveness was observed in Domain VI (Energy/Vitality) with Cohen's d = 1.09 and SRM = 0.81, reflecting a substantial improvement in overall well-being and functional vitality. The total PANQOL score also showed a large effect (Cohen's d = 0.87; SRM = 0.75), confirming the high sensitivity of the scale in detecting overall changes in quality of life after treatment. Domains I, II, III, V and VII demonstrated moderate responsiveness, whereas Domain IV (Headache) showed the lowest yet still clinically meaningful effect (Cohen's d = 0.52), corresponding to a small–moderate effect (***Table 12***).

For the Mayo VSQOL, 31 paired observations in Group II were included. All domains demonstrated clinically meaningful changes, with Cohen's d values ranging from 0.31 to 2.11. The greatest responsiveness was observed in Domain V, where Cohen's d = 2.11 and SRM = 1.74, indicating an exceptionally large effect. High responsiveness was also demonstrated in domains VI (Cohen's d = 1.33; SRM = 1.36) and VII (Cohen's d = 1.12; SRM = 0.94), reflecting substantial improvements in social functioning, emotional status, and treatment satisfaction. The total Mayo VSQOL score demonstrated a large effect (Cohen's d = 1.17; SRM = 1.11), confirming high overall responsiveness of the scale. Domains I–IV showed small to moderate effects (Cohen's d = 0.31–0.63), which is typical for physical or functional aspects of QoL (***Table 13***).

Table 8. Internal consistency (Cronbach's α) of the PANQOL domains before and after surgery

Domain	Preoperative α	Postoperative α	Interpretation
I. Hearing	0.75	0.75	Acceptable internal consistency at both time points
II. Balance	0.93	0.90	Excellent and consistently high reliability
III. Face	0.79	0.81	Good consistency, no deterioration
IV. Headache	—	—	α not computed (single item domain)
V. Anxiety / Stress	0.81	0.83	Good reliability both pre- and postoperatively
VI. Energy / Vitality	0.87	0.87	Very good and stable reliability
VII. Isolation / Cognition	0.38	0.48	Low (expected for a 2-item domain), slight improvement postoperatively

Table 9. Internal consistency (Cronbach's α) of the MAYO VSQOL domains before and after surgery

Domain	Preoperative α	Postoperative α	Interpretation
I	0.867	0.858	Very good
II	0.931	0.905	Excellent
III	0.873	0.875	Very good
IV	0.763	0.864	Acceptable / good
V	0.938	0.937	Excellent
VI	0.925	0.913	Excellent
VII	0.886	0.894	Very good

Table 10. Test–retest reliability of PANQOL domains (n = 33 paired observations)

PANQOL Domain	ICC	Interpretation
I	0.65	Moderate
II	0.84	High
III	0.75	Good
IV	0.82	High
V	0.72	Good
VI	0.91	Excellent
VII	0.60	Moderate

Table 11. Test–retest reliability of Mayo VSQOL domains (n = 31 paired observations)

Domain	Pearson r	ICC	Interpretation
I	0.896	0.889	Good
II	0.961	0.942	Excellent
III	0.975	0.953	Excellent
IV	0.884	0.858	Good
V	0.872	0.778	Good
VI	0.944	0.860	Good
VII	0.930	0.893	Good

Table 12. Responsiveness of PANQOL domains (n = 30 paired observations)

Domain	Δ (post–pre)	Cohen's d	SRM	Interpretation
I. Hearing	+16.00	0.60	0.55	Moderate effect
II. Balance	+17.17	0.65	0.47	Moderate (d), small–moderate (SRM)
III. Face	+14.67	0.54	0.53	Moderate effect
IV. Headache	+15.00	0.52	0.49	Small–moderate effect
V. Anxiety/Stress	+16.25	0.76	0.59	Moderate–large effect
VI. Energy/Vitality	+24.50	1.09	0.81	Large effect
VII. Isolation/Cognition	+12.50	0.58	0.53	Moderate effect
Total PANQOL	+16.58	0.87	0.75	Large effect

Table 13. Responsiveness of Mayo VSQOL domains (n = 31 paired observations)

Domain	Δ (post–pre)	Cohen's d	SRM	Interpretation
I	+10.17	0.41	0.40	Small–moderate effect
II	+16.82	0.63	0.58	Moderate effect
III	+11.33	0.45	0.37	Small–moderate effect
IV	+7.00	0.31	0.37	Small effect
V	+29.36	2.11	1.74	Very large effect
VI	+22.58	1.33	1.36	Large effect
VII	+18.81	1.12	0.94	Large effect
Total Mayo	+16.58	1.17	1.11	Large effect

Both scales demonstrated adequate ability to detect clinically important postoperative changes; however, their sensitivity profiles differed: PANQOL provided more uniform responsiveness across domains and was particularly sensitive to changes in energy/vitality and overall quality of life. In contrast, Mayo VSQOL showed markedly higher responsiveness in social and emotional domains and in the total score, with Cohen's d exceeding 1.0 in three domains.

Discriminant Validity

The discriminant validity of the Ukrainian versions of PANQOL and Mayo VSQOL was assessed based on their ability to differentiate patients with objectively different clinical outcomes. Patients were stratified according to the extent of tumor resection, facial nerve (FN) function assessed by HB scale in the early postoperative period, and cochlear nerve preservation and hearing outcomes. In Group 1 (traditional microsurgery, 2001–2016), FN function was distributed as follows: HB I – 24 (5%), II – 30 (6.3%), III – 67 (14.1%), IV – 102 (21.6%), V – 149 (31.5%), VI – 102 (21.5%). In Group 2 (modern microsurgical techniques, 2017–2024), significantly better outcomes were observed: HB I – 132 (37.2%), II – 77 (21.7%), III – 95 (26.8%), IV – 37 (10.4%), V – 11 (3.1%), VI – 3 (0.8%) ($p < 0.001$). Cochlear nerve preservation and postoperative hearing further demonstrated the discriminant ability of the questionnaires. In Group 2, among 93 patients with functional preoperative hearing, the cochlear nerve was anatomically preserved in 49 (52.7%), with postoperative hearing graded as GR-I in 42.9%, GR-II in 24.5%, and GR-III in 32.6%. Cochlear nerve preservation was not performed in Group 1.

Both PANQOL and Mayo VSQOL effectively reflected these clinical differences, confirming the questionnaires' ability to discriminate clinically distinct subgroups and demonstrating adequate discriminant validity.

Discussion

We performed cross-cultural adaptation and validation of the PANQOL and Mayo VSQOL questionnaires for Ukrainian-speaking patients. To the best of our knowledge, for the first time, apart from the authors of Mayo VSQOL, a comparative analysis of these questionnaires and cross-cultural adaptation and validation of the Mayo VSQOL scale was conducted outside the USA.

The study results confirmed that the Ukrainian versions of PANQOL and Mayo VSQOL demonstrate high internal consistency, adequate test–retest reliability, and sensitivity to clinically meaningful postoperative changes. Internal consistency of PANQOL was high across most domains, whereas Domain VII (Isolation/Cognition) showed lower α values due to the limited number of items, which is typical for short domains. Similarly, Mayo VSQOL exhibited high α values in all domains postoperatively, reflecting the reliability of the measured constructs.

Test–retest analysis indicated that both questionnaires were stable upon repeated administration, with ICCs >0.75 in most domains and exceeding 0.90 in some, corresponding to high to excellent reliability.

Responsiveness analysis demonstrated that PANQOL provides a more uniform detection of clinically meaningful changes, particularly in domains related to energy and overall well-being, while Mayo VSQOL showed exceptionally high responsiveness in social–emotional domains and in the total score. For more precise assessment of responsiveness, a larger sample size than 30 patients and a longer postoperative follow-up period may be required. These findings support the practical utility of both scale for evaluating quality of life in patients after microsurgical removal of vestibular schwannoma and highlight different sensitivity profiles, which may inform the choice of tool depending on research or clinical objectives.

In this study, we assessed and compared patients with vestibular schwannomas who underwent surgical treatment or were managed using the "wait-and-scan" strategy. However, for a comprehensive evaluation of the quality of life of all VS patients, it would be also necessary to include groups treated with radiation or combined (surgical and radiation) modalities. Unfortunately, this was not possible due to the lack of feedback from these patient categories, as well as whole amount included into research (244 from 829) largely as a result of the people migration during war in Ukraine.

Our study demonstrated that the PANQOL and Mayo VSQOL questionnaires provide complementary information on the quality of life of patients with VS.

PANQOL showed a stable moderate-to-high correlation with total SF-36, QLQ-C30, and BN20 scores across all three groups, confirming its reliability for comprehensive assessment in both physical and mental health. For example: In Group I, the correlation coefficients were $r = 0.635$ with QLQ-C30 and $r = 0.635$ with BN20; In Group II, $r = 0.596$ with QLQ-C30 and $r = 0.629$ with BN20; In Group III, $r = 0.663$ with QLQ-C30 and $r = 0.743$ with BN20. These data indicate that PANQOL provides consistent and reliable quality-of-life assessment across different patient groups. Mayo VSQOL, on the other hand, showed a moderate correlation with SF-36, QLQ-C30, and BN20 only in Group II ($r = 0.586$ with QLQ-C30 and $r = 0.501$ with BN20) but demonstrated higher sensitivity to intergroup differences, particularly when comparing Group I vs. II and Group II vs. III. This suggests that Mayo VSQOL more effectively reflects clinical differences between patients undergoing different treatment modalities, even if its correlation with total SF-36 scores is lower.

Therefore, PANQOL can be used for comprehensive assessment of physical and mental health, whereas Mayo VSQOL is more suitable for sensitive detection of clinical differences between treatment groups. Direct comparisons of corresponding domains showed only weak correlations, indicating that each questionnaire should be used as an independent tool or that only total scores should be compared. Although further investigation is advisable to spend on more material for precise comparison.

Comparative analysis of Groups II and III demonstrated a statistically significant improvement after surgery in several domains. The "Anxiety" domain showed a mild decrease only when comparing Groups I and II, while between Groups II and III it remained

relatively stable, though without statistical significance. In our opinion, this trend may be influenced by the timing of the study in Ukraine during the wartime period (2022–2024).

When comparing Groups II and III, not all patients completed the items within the "Satisfaction or Regret" domain, as some questions were applicable only to individuals who had undergone active treatment (surgery or radiation). Additionally, some patients did not fully understand that the "wait-and-scan" strategy constitutes an independent management approach. Therefore, including this domain for patients managed with the "wait-and-scan" strategy may be methodologically inappropriate unless accompanied by additional clarification regarding this treatment modality.

For comprehensive validation, PANQOL and Mayo VSQOL should be compared to other scales; however, the total number of items in all of these questionnaires including BN20, QLQ-C30, and SF-36 reaches 152. Continuous completion of all instruments takes 20–60 minutes, requiring many patients to take breaks. Fatigue and cognitive load may affect the accuracy of responses and overall perception of questions. Practical experience showed that PANQOL can be self-administered by patients, whereas Mayo VSQOL requires explanations, comfortable conditions, and greater attention to each question. Despite or due to the greater complexity and duration, Mayo VSQOL demonstrates increased sensitivity to intergroup differences compared with other assessment tools, making it effective for detailed evaluation of treatment impact on QoL.

The use of the Mayo VSQOL, developed by Carlson *et al*. (2022) [2], demonstrates a contemporary approach to assessing disease-specific quality of life in patients with VS, taking into account hearing, balance, cognitive impairments, anxiety, and psychosocial adaptation. The authors emphasized high internal consistency (Cronbach's $\alpha > 0.80$ for most domains), adequate test–retest reliability, and confirmed construct validity of the instrument [2]. In our study, the adapted Ukrainian version demonstrated similar psychometric properties, confirming its effectiveness and validity for use in clinical practice and research in Ukraine. To further enhance the reliability and generalizability of the results, analysis on a larger patient cohort is warranted, considering potential cultural and socio-economic factors that may influence patients' perception of QoL.

Conclusion

1. PANQOL demonstrates a stable moderate-to-high correlation with total SF-36, QLQ-C30, and BN20 scores across all three groups of vestibular schwannoma patients treated by: Group I - traditional microsurgery (2001–2016); Group II – contemporary modern microsurgical techniques (2017–2024); and Group III – observation ("wait and scan"), confirming its adequacy for comprehensive assessment of physical and mental health.

2. Mayo VSQOL shows a moderate correlation with SF-36, QLQ-C30, and BN20 only in Group II, but demonstrates higher sensitivity to intergroup differences, making it effective for detecting clinical differences between patients undergoing different treatment modalities.

3. Direct comparison of corresponding domains between PANQOL and Mayo VSQOL is of limited clinical value; it is more appropriate to compare total scores or treat the questionnaires as independent instruments.

4. PANQOL is convenient for self-administration by patients, whereas Mayo VSQOL requires explanations and a comfortable setting but shows higher sensitivity to differences between treatment groups.

5. Updated microsurgical techniques (2017–2024) provide a statistically significant improvement in quality of life for patients with VS compared with traditional methods and "wait and scan"/observation.

6. The Ukrainian versions of PANQOL and Mayo VSQOL demonstrated high reliability, stability, and sensitivity to clinically meaningful postoperative changes. PANQOL showed more uniform responsiveness across domains, particularly for energy and overall well-being, while Mayo VSQOL was especially sensitive in social–emotional domains and the total score.

7. The Ukrainian versions of PANQOL and Mayo VSQOL demonstrated adequate discriminant validity, effectively distinguishing patients with different facial nerve outcomes, extent of tumor resection, and cochlear nerve preservation. Higher quality-of-life scores were reported in patients with better clinical outcomes, confirming the scale sensitivity to meaningful clinical differences.

8. The cross-cultural adaptation and validation of the PANQOL and Mayo VSQOL questionnaires were successfully completed. However, further statistical analysis on a larger patient cohort is required to confirm their reliability and generalizability.

Disclosure

Conflict of interest

The authors declare no conflict of interest.

Funding

The study was conducted as part of a research project (R&D) funded by the institution, project number 2 dated 14.04.2021. No additional sponsorship or financial support was received.

Informed consent

Written informed consent was obtained from all patients who participated in the study and/or whose images or clinical data were used in the publication.

Ethical approval

The study was conducted in accordance with the Declaration of Helsinki (2013) and the current legislation of Ukraine. The protocol was approved by the Ethics Committee of SI «Romodanov Neurosurgery Institute of NAMS of Ukraine» (Minutes No. 2, 14.04.2021).

Use of artificial intelligence

Individual sections of the text were edited, translated and grammar-checked using ChatGPT (OpenAI, San Francisco, USA). All statements were verified by the authors.

Author contributions

All authors equally contributed to study conception, data collection and analysis, manuscript drafting and revision, and approved the final version of the manuscript.

References

1. Fedirko VO, Yehorov MV, Chuvashova OY, Malysheva TA, Borysenko OM, Shust VV, Tsiurupa DM, Onishchenko PM, Rozumenko AV, Kruchok IV, Lisianyi AO. Vestibular schwannomas: implementation of PANQOL and Mayo VSQOL Index scales in Ukraine and justification of treatment strategy with preservation of quality of life (problem analysis, own experience, discussion points). Ukr Neurosurg J. 2024;30(2):20–35. doi: 10.25305/unj.299185.
2. Carlson ML, Lohse CM, Link MJ, Tombers NM, McCaslin DL, Saoji AA, Hutchins M, Yost KJ. Development and validation of a new disease-specific quality of life instrument for sporadic vestibular schwannoma: the Mayo Clinic Vestibular Schwannoma Quality of Life Index. J Neurosurg. 2022 Sep 2;138(4):981-991. doi: 10.3171/2022.7.JNS221104. PMID: 36057121.
3. Pattankar S, Churi O, Misra BK. Validation of the Penn Acoustic Neuroma Quality of Life (PANQOL) Scale for Hindi-Speaking Patients Recently Diagnosed with Vestibular Schwannoma. Neurol India. 2022 May-Jun;70(3):978-982. doi: 10.4103/0028-3886.349775. PMID: 35864628.
4. Carlson ML, Barnes JH, Nassiri A, Patel NS, Tombers NM, Lohse CM, Van Gompel JJ, Neff BA, Driscoll CLW, Link MJ. Prospective Study of Disease-Specific Quality-of-Life in Sporadic Vestibular Schwannoma Comparing Observation, Radiosurgery, and Microsurgery. Otol Neurotol. 2021 Feb 1;42(2):e199-e208. doi: 10.1097/MAO.0000000000002863. PMID: 33177408.
5. Carlson ML, Tveiten ØV, Driscoll CL, Goplen FK, Neff BA, Pollock BE, Tombers NM, Lund-Johansen M, Link MJ. What drives quality of life in patients with sporadic vestibular schwannoma? Laryngoscope. 2015 Jul;125(7):1697-702. doi: 10.1002/lary.25110. PMID: 25546382.
6. Stangerup SE, Tos M, Thomsen J, Caye-Thomasen P. True incidence of vestibular schwannoma? Neurosurgery. 2010 Nov;67(5):1335-40; discussion 1340. doi: 10.1227/NEU.0b013e3181f22660. PMID: 20871439.
7. Apa E, Maccarrone F, Gherpelli C, Sacchetto L, Monzani D, Palma S, Nocini R. Italian validation of the Penn Acoustic Neuroma Quality of Life Scale (PANQOL-It). Acta Otorhinolaryngol Ital. 2023 Apr;43(2):130-139. doi: 10.14639/0392-100X-N2263. PMID: 37099437; PMCID: PMC10132483.
8. Di Perna G, De Marco R, Baldassarre BM, Lo Bue E, Cofano F, Zeppa P, Ceroni L, Penner F, Melcarne A, Garbossa D, Lanotte MM, Zenga F. Facial nerve outcome score: a new score to predict long-term facial nerve function after vestibular schwannoma surgery. Front Oncol. 2023 Jun 12;13:1153662. doi: 10.3389/fonc.2023.1153662. PMID: 37377918; PMCID: PMC10291180.
9. Wiegand DA, Fickel V. Acoustic neuroma--the patient's perspective: subjective assessment of symptoms, diagnosis, therapy, and outcome in 541 patients. Laryngoscope. 1989 Feb;99(2):179-87. doi: 10.1288/00005537-198902000-00010. PMID: 2913427.
10. Bieńkowska K, Kostecka B, Kokoszka A. Quality-of-life assessment instruments for patients with vestibular schwannoma: A systematic review. Braz J Otorhinolaryngol. 2025 May-Jun;91(3):101585. doi: 10.1016/j.bjorl.2025.101585. PMID: 40120480; PMCID: PMC11982967.
11. Glaas MF, Schäfer R, Jansen P, Franz M, Stenin I, Klenzner T, Schipper J, Eysel-Gosepath K, Kristin J. Quality of Life After Translabyrinthine Vestibular Schwannoma Resection-Reliability of the German PANQOL Questionnaire. Otol Neurotol. 2018 Jul;39(6):e481-e488. doi: 10.1097/MAO.0000000000001819. PMID: 29889791.
12. Bender M, Tatagiba M, Gharabaghi A. Quality of Life After Vestibular Schwannoma Surgery: A Question of Perspective. Front Oncol. 2022 Feb 11;11:770789. doi: 10.3389/fonc.2021.770789. PMID: 35223451; PMCID: PMC8873590.
13. Tufarelli D, Meli A, Alesii A, De Angelis E, Badaracco C, Falcioni M, Sanna M. Quality of life after acoustic neuroma surgery. Otol Neurotol. 2006 Apr;27(3):403-9. doi: 10.1097/00129492-200604000-00018. PMID: 16639281.
14. Nishiyama T, Oishi N, Kojima T, Kasuya K, Noguchi M, Ishikawa T, Hosoya M, Ogawa K. Validation and multidimensional analysis of the japanese penn acoustic neuroma quality-of-life scale. Laryngoscope. 2020 Dec;130(12):2885-2890. doi: 10.1002/lary.28488. PMID: 31922264.
15. van Leeuwen BM, Herruer JM, Putter H, Jansen JC, van der Mey AG, Kaptein AA. Validating the Penn Acoustic Neuroma Quality Of Life Scale in a sample of Dutch patients recently diagnosed with vestibular schwannoma. Otol Neurotol. 2013 Jul;34(5):952-7. doi: 10.1097/MAO.0b013e31828bb2bb. PMID: 23714709.
16. Kristin J, Glaas MF, Stenin I, Albrecht A, Klenzner T, Schipper J, Eysel-Gosepath K. Multistep translation and cultural adaptation of the Penn acoustic neuroma quality-of-life scale for German-speaking patients. Acta Neurochir (Wien). 2017 Nov;159(11):2161-2168. doi: 10.1007/s00701-017-3304-z. PMID: 28861705.
17. Neve OM, Jansen JC, Koot RW, Ridder M, Paul G van Benthem P, Stiggelbout AM, Hensen EF. Long-Term Quality of Life of Vestibular Schwannoma Patients: A Longitudinal Analysis. Otolaryngol Head Neck Surg. 2023 Feb;168(2):210-217. doi: 10.1177/01945998221088565. PMID: 35349360.
18. Marinelli JP, Lohse CM, Link MJ, Carlson ML. Quality of Life in Sporadic Vestibular Schwannoma. Otolaryngol Clin North Am. 2023 Jun;56(3):577-586. doi: 10.1016/j.otc.2023.02.016. PMID: 37019770.
19. Helal A, Carlson ML, Link MJ. Management of vestibular schwannoma in the elderly. Handb Clin Neurol. 2025;212:325-332. doi:10.1016/B978-0-12-824534-7.00025-1. PMID:41052854.
20. Fuentealba-Bassaletti C, Neve OM, van Esch BF, Jansen JC, Koot RW, van Benthem PPG, Hensen EF. Vestibular Complaints Impact on the Long-Term Quality of Life of Vestibular Schwannoma Patients. Otol Neurotol. 2023 Feb 1;44(2):161-167. doi: 10.1097/MAO.0000000000003773. PMID: 36624597; PMCID: PMC9835658.
21. Bambakidis E, Mowry S, Amin-Hanjani S. A Scoping Review on Vestibulopathy After Microsurgical Resection of Vestibular Schwannoma-The Forgotten Symptom. Neurosurg Pract. 2024 Aug 28;5(4):e00107. doi: 10.1227/neuprac.0000000000000107. PMID: 39959543; PMCID: PMC11810020.
22. Betchen SA, Walsh J, Post KD. Self-assessed quality of life after acoustic neuroma surgery. J Neurosurg. 2003 Nov;99(5):818-23. doi: 10.3171/jns.2003.99.5.0818. PMID: 14609159.
23. Machetanz K, Lee L, Wang SS, Tatagiba M, Naros G. Trading mental and physical health in vestibular schwannoma treatment decision. Front Oncol. 2023 Jun 26;13:1152833. doi: 10.3389/fonc.2023.1152833. PMID: 37434979; PMCID: PMC10332305.
24. Sharif-Nia H, Sánchez-Teruel D, Sivarajan Froelicher E, Hejazi S, Hosseini L, Khoshnavay Fomani F, Moshtagh M, Mollaei F, Goudarzian AH, Babaei A. Connor-Davidson Resilience Scale: a systematic review psychometrics properties using the COSMIN. Ann Med Surg (Lond). 2024 Mar 27;86(5):2976-2991. doi: 10.1097/MS9.0000000000001968. PMID: 38694299; PMCID: PMC11060289.
25. Mokkink LB, Elsman EBM, Terwee CB. COSMIN guideline for systematic reviews of patient-reported outcome measures version 2.0. Qual Life Res. 2024 Nov;33(11):2929-2939. doi: 10.1007/s11136-024-03761-6. PMID: 39198348; PMCID:

PMC11541334.
26. Fellows I. Deducer: A data analysis GUI for R. Version 0.7-9. https://cran.r-project.org/package=Deducer
27. Casazza GC, Bowers CA, Gurgel RK. Hearing Outcomes Reporting in Lateral Skull Base Surgery. J Neurol Surg B Skull Base. 2019 Apr;80(2):120-124. doi: 10.1055/s-0038-1676371. PMID: 30931218; PMCID: PMC6438792.
28. Beaton DE, Bombardier C, Guillemin F, Ferraz MB. Guidelines for the process of cross-cultural adaptation of self-report measures. Spine (Phila Pa 1976). 2000 Dec 15;25(24):3186-91. doi: 10.1097/00007632-200012150-00014. PMID: 11124735.
29. Taber K.S. The Use of Cronbach's Alpha When Developing and Reporting Research Instruments in Science Education. Res Sci Educ. 2018;48:1273–1296 (2018). doi: 10.1007/s11165-016-9602-2

Case report

Ukrainian Neurosurgical Journal. 2026;32(1):126-128
doi: 10.25305/unj.340623

Bifid median nerve: case report

Irakli B. Goginava [1], Giorgi Murvelashvili [2], Mikheil A. Shavgulidze [3], Mariia V. Riezunenko [4], Giorgi L. Giorgidze [5]

[1] Department of Pelvic Fractures Surgery, West Georgia Medical Center, Kutaisi, Georgia
[2] Orthopedics and Traumatology Department, Medical Center Medina, Batumi, Georgia
[3] High Franconia Clinics, Münchberg, Germany
[4] Department of Traumatology and Orthopedics, West Georgia Medical Center, Kutaisi, Georgia
[5] Department of Neurology, West Georgia Medical Center, Kutaisi, Georgia

Received: 03 October 2025
Accepted: 27 October 2025

Address for correspondence*:*
Irakli Borisovich Goginava, Department of Pelvic Fractures Surgery, West Georgia Medical Center, Javakhishvili str., 83a, Kutaisi, 4600, Georgia, e-mail: igoginava@evex.ge

In the article a rare case of abnormal anatomical structure of the median nerve in a patient with carpal tunnel syndrome is described: a high bifurcation of the median nerve.

A 67-year-old woman complained of periodic intense nocturnal pain and numbness of 1-3 fingers of her left hand. During clinical examination Phalen's wrist flexion and wrist extension tests, Hoffmann-Tinel, postural provocation, median nerve compression, and the "tourniquet" tests were positive. Allen's test was negative. There was no atrophy of the thenar muscles, the strength of palmar abduction of the thumb was comparable to that of the right hand. Sensitivity of the fingers was unchanged. Based on the history and clinical examination, a diagnosis of idiopathic carpal tunnel syndrome of the left hand was made. Open carpal tunnel release, mesoepineurolysis of the median nerve, and tenosynovectomy were performed. Intraoperatively, it was found that from the proximal edge of the wound, the trunk of the median nerve was split into two parts, which were reconnected in the area of the exit from the carpal tunnel, forming a "loop" like structure. An hourglass deformity was also noted on both branches of the median nerve. The radial branch of the split nerve was visually thicker than the ulnar branch. Postoperatively, pain and numbness of 1-3 fingers resolved completely.

The median nerve bifurcation is extremely difficult to detect preoperatively. In the case of a traumatic complete anatomical injury to the median nerve, one should make sure that this structural anomaly is absent, and if there is a bifurcation of the nerve, an extended revision should be performed and a suture should be placed on both damaged branches.

During surgical treatment of carpal tunnel syndrome, it is advisable to check whether the bifurcated nerve runs through a single canal rather than two separate canals. In the latter case, it is necessary to influence both canals during operative or conservative treatment.

Keywords: *abnormal anatomical structure; high bifid median nerve; carpal tunnel syndrome*

Introduction

The anatomical structure of the median nerve in the forearm and hand has been extensively described in numerous studies. However, various anomalies in the structure of the nerve are of particular theoretical and practical interest. One such anomaly is high bifurcation—the splitting of the median nerve at the level of the forearm and carpal tunnel. In foreign literature, descriptions of this anomaly, especially clinical cases, are quite rare [1]. Only one publication has been found in the available Ukrainian-language scientific literature [2], and none have been found in national medical publications.

The aim of this study is to familiarize readers of the journal with a rare anomaly in the anatomical structure of the median nerve and to describe the features of diagnosis and treatment of carpal tunnel syndrome in combination with median nerve bifurcation.

Case presentation

A 67-year-old woman was admitted with complaints of periodic, predominantly nocturnal, intense pain and numbness in 1-3 fingers of her left hand. At night, her condition improved only by lowering the hand, rubbing it, and shaking it (the "flick" sign). These complaints began 4 years ago, and her condition gradually worsened. She did not seek treatment. During the clinical examination, Phalen's wrist flexion and wrist extension tests, Hoffmann-Tinel test from the median nerve projection site on the forearm, the postural provocation test, median nerve compression, and the "tourniquet" tests were positive. Allen's test was negative. There was no atrophy of the thenar muscles, and the strength of the palmar abduction of the thumb was comparable to that of the right hand. Sensitivity in the fingers was unchanged. Based on the medical history and clinical examination, a diagnosis of idiopathic carpal tunnel

syndrome of the left hand was made and surgical treatment was indicated.

Surgery was performed under local anesthesia using the WALANT technique with a 1% lidocaine solution [3]. A C-shaped skin incision was made, extending to the lower third of the forearm. The flexor retinaculum was completely dissected longitudinally over the grooved probe inserted into the carpal tunnel. Mesoepineurolysis of the median nerve was subsequently performed. It was found that, starting from the proximal edge of the wound, the trunk of the median nerve was split into two parts, which rejoined in the area of the exit from the carpal tunnel, forming a so-called "loop" (***Fig. 1***).

An hourglass deformity was also noted on both branches of the median nerve. The radial branch of the split nerve was visually thicker than the ulnar branch. Due to severe finger flexor tenosynovitis, a tenosynovectomy was performed. The edges of the flexor retinaculum were excised. Sutures were applied to the skin. The postoperative period proceeded without complications.

Three months after the operation, the patient reported complete resolution of pain and numbness in the fingers of the operated hand.

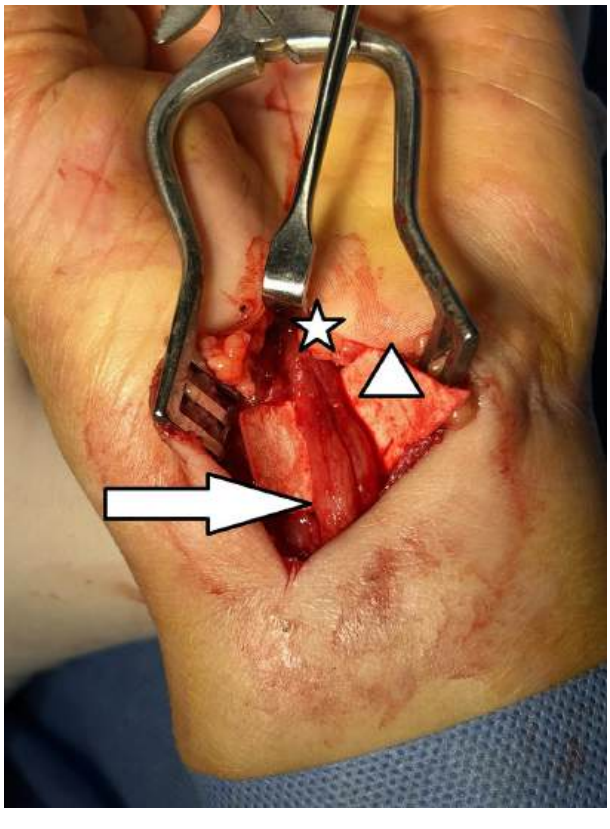

Fig. 1. High bifurcation of the median nerve (arrow – bifurcated median nerve; triangle – hourglass deformity of the median nerve; asterisk – "loop" of the median nerve)

Discussion

According to normal anatomy, the median nerve in the lower third of the forearm looks like a single trunk. In this form, it enters the carpal tunnel distally together with the flexor tendons of I-V fingers and, in the area of the distal edge of the flexor retinaculum, splits into six motor branches to the thenar muscles, two radial lumbrical muscles, and sensory branches to I-III fingers and the radial surface of the ring finger [4]. Most practicing surgeons are guided precisely by this normal anatomy of the median nerve during operations on the forearm and hand**.** However, upon closer examination of the anatomy of the nerve, many features can be noted that quite often affect the outcomes of surgical interventions. The scientific literature describes variants of the unusual structure and location of the branches of the median nerve in the area immediately adjacent to the carpal tunnel and in the area where it exits, including extraligamentous location of the recurrent motor branch (standard location), transligamentous, supraligamentous, and subligamentous locations; accessory recurrent motor branches; and the origin of the recurrent motor branch from the volar or volar-medial surface of the median nerve trunk, etc. [4, 5, 6]. Variants of bifurcation or even trifurcation of the median nerve at the level of the lower third of the forearm are also presented [7].

During surgery for carpal tunnel syndrome, we incidentally encountered a bifurcation of the median nerve in the lower third of the forearm and hand corresponding to a high bifurcation of the median nerve of group 3A according to the Lanz classification. This variant is characterized by bifurcation of the median nerve trunk proximal to the carpal tunnel, with or without a connecting branch, in the absence of a persistent median artery and lumbrical muscles originating in the carpal tunnel region [8]. High bifurcation of the median nerve was first described in scientific medical literature by I. Kessler [9].

The clinical picture in the patient described above did not differ from that observed in many other patients we operated on with carpal tunnel syndrome. Therefore, it is practically impossible to suspect the presence of high bifurcation of the median nerve in advance. In rare cases of persistent median artery thrombosis, which sometimes occurs with bifurcation of the median nerve, the clinical picture of carpal tunnel syndrome may be altered and include sudden numbness and paresthesia in the fingers innervated by the median nerve, as well as pain and swelling in the volar surface of the wrist joint [10, 11].

Another important feature of the abnormal anatomical structure of the median nerve is that the two branches of the nerve can run in separate cylindrical canals formed by the fibers of the flexor retinaculum [1]. Therefore, during operative or conservative treatment it is necessary to influence both canals.

Conclusion

We describe a case of unusual anatomical structure of the median nerve in the lower third of the forearm and carpal tunnel, specifically a high bifurcation of the median nerve. It is necessary to

be aware of the existence of such an anomaly in order to avoid negative treatment outcomes. In the case of traumatic complete anatomical injury to the median nerve, one should make sure that this structural anomaly is absent, and if there is a bifurcation of the nerve, an extended revision should be performed and a suture should be placed on both damaged branches.

During surgical treatment of carpal tunnel syndrome, it is advisable to check that the bifurcated nerve runs through a single canal**,** rather than two separate canals. In the latter case, it is necessary to influence both canals during operative or conservative treatment.

Disclosure

Conflict of interest statement

The authors declare that there is no conflict of interest.

Funding

The research had no sponsor support.

Informed consent

The patient gave written consent for this report to be published and for information about the nature of her illness to be posted online.

References

1. Kamat AS, Woon K. Unusually high bifurcation of the median nerve resulting in two separate cylindrical compartments within the transverse carpal ligament: a case report. International Journal of Anatomical Variations. 2014;7:24-26. https://www.pulsus.com/scholarly-articles/unusually-high-bifurcation-of-the-median-nerve-resulting-in-two-separate-cylindrical-compartments-within-the-transverse.pdf
2. Goloborod'ko S. High bifurcation of the median nerve at carpal tunnel syndrome: case study. Orthopaedics, Traumatology and Prosthetics. 2020;(2):89-91. doi: 10.15674/0030-59872020289-91
3. Lalonde D, Martin A. Epinephrine in local anesthesia in finger and hand surgery: the case for wide-awake anesthesia. J Am Acad Orthop Surg. 2013 Aug;21(8):443-7. doi: 10.5435/JAAOS-21-08-443
4. Demircay E, Civelek E, Cansever T, Kabatas S, Yilmaz C. Anatomic variations of the median nerve in the carpal tunnel: a brief review of the literature. Turk Neurosurg. 2011;21(3):388-96. doi: 10.5137/1019-5149.JTN.3073-10.1
5. Bakhshi Kashi M, Behnejad M, Loghman AH, Zamani-Badi T, Nikzad H. Study of median nerve variations and its clinical implications at the distal art of upper limb: a review. Anatomical Sciences Journal. 2022;19(1):1-10. http://anatomyjournal.ir/article-1-189-en.html
6. Osiak K, Elnazir P, Walocha JA, Pasternak A. Carpal tunnel syndrome: state-of-the-art review. Folia Morphol. 2022;81(4):851–862. doi: 10.5603/FM.a2021.0121
7. Duymus M, Yilmaz O, Ulasli AM, Asal N, Kosar U. Coexistence of trifid and bifid median nerve in a patient with bilateral carpal tunnel syndrome. Turk Neurosurg. 2013;23(5):685-7. doi: 10.5137/1019-5149.JTN.6565-12.0
8. Neumann M, Suchomlinov A. Pilot Cadaveric Study of Anatomical Variations of the Median Nerve at the Wrist in the Lithuanian Population. Cureus. 2023 May 21;15(5):e39282. doi: 10.7759/cureus.39282
9. Kessler I. Unusual distribution of the median nerve at the wrist. A case report. Clin Orthop Rel Res. 1969 Nov-Dec;67:124–126. doi: 10.1097/00003086-196911000-00019
10. Akgun AS, Ertan G, Ulus S. Acute carpal tunnel syndrome caused by thrombosed persistent median artery associated with bifurcated median nerve in a pregnant woman. BMJ Case Rep.2017 Sep 19;2017:bcr2017221446.doi: 10.1136/bcr-2017-221446
11. Miyashima Y, Gotani H, Okamoto K, Yagi H, Tanaka Y. Median nerve neuropathy caused by persistent median artery thrombosis. Plast Reconstr Surg Glob Open. 2023 Apr 10;11(4):e4916. doi: 10.1097/GOX.0000000000004916